

**NASA Technical Memorandum 84508**

NASA-TM-84508 19820021437

THE FEASIBILITY OF A HIGH-ALTITUDE  
AIRCRAFT PLATFORM WITH CONSIDERATION  
OF TECHNOLOGICAL AND SOCIETAL  
CONSTRAINTS

FOR REFERENCE

NOT TO BE TAKEN FROM THIS ROOM

ERNALD B. GRAVES

JUNE 1982

LIBRARY COPY

JUL 1 1982

LANGLEY RESEARCH CENTER  
LIBRARY, NASA  
HAMPTON, VIRGINIA



National Aeronautics and  
Space Administration

Langley Research Center  
Hampton, Virginia 23665



ENTER:

2 1 1 RN/NASA-TM-84508

DISPLAY 02/6/1

82N29313\*\* ISSUE 20 PAGE 2788 CATEGORY 5 RPT#: NASA-TM-84508 NAS

1.15:84508 82/06/00 250 PAGES UNCLASSIFIED DOCUMENT

UTTL: The feasibility of a high-altitude aircraft platform with consideration of technological and societal constraints TLSP: Thesis - Kansas Univ.

AUTH: A/GRAVES, E. B.

CORP: National Aeronautics and Space Administration, Langley Research Center, Hampton, Va. AVAIL.NTIS SAP: NC A15/MF A01

MAJS: /\*AIRCRAFT FUELS/\*AIRSHIPS/\*MICROWAVE TRANSMISSION/\*NUCLEAR PROPULSION/\* REMOTELY PILOTED VEHICLES/\*SOLAR POWERED AIRCRAFT

MINS: / AIRCRAFT CONSTRUCTION MATERIALS/ FEASIBILITY ANALYSIS/ FLIGHT ALTITUDE/ METEOROLOGICAL PARAMETERS

ABA: S.L.





## PREFACE

This document contains the results of a study to determine the feasibility of remotely piloted, relatively stationary flight at very high altitudes, using current technologies. The project was used to fulfill part of the requirements for the Doctor of Engineering Degree for Ernald B. Graves, an in absentia graduate student at the University of Kansas.



## TABLE OF CONTENTS

	Page
Preface . . . . .	i
Table of Contents . . . . .	iii
List of Symbols . . . . .	xi
List of Acronyms . . . . .	xv
 CHAPTER 1 - SUMMARY . . . . .	 1
CHAPTER 2 - INTRODUCTION . . . . .	3
2.1 Background . . . . .	4
2.1.1 SRI HAAP Feasibility Study . . . . .	4
2.1.2 BCL HAAP Applications Study . . . . .	6
2.1.3 BCL HAAP User Definition Study . . . . .	6
2.1.4 Other HAAP-Related Studies . . . . .	7
2.1.4.1 The Hufnagel Report . . . . .	8
2.1.5 Summary of Proposed HAAP Applications . . . . .	9
2.2 Project Purpose and Objectives . . . . .	10
2.3 Project Approach . . . . .	11
CHAPTER 3 - THE OPERATIONAL ENVIRONMENT . . . . .	13
3.1 Winds . . . . .	14
3.2 Temperatures . . . . .	18
3.3 Environmental Parameter Summary . . . . .	19

	Page
CHAPTER 4 - SOLAR-VOLTAIC POWER TECHNOLOGY . . . . .	21
4.1 Global Interest . . . . .	21
4.2 The Sun and Its Energy . . . . .	22
4.3 The Solar Cell . . . . .	25
4.3.1 Arrays . . . . .	28
4.4 Technology Status . . . . .	29
CHAPTER 5 - MICROWAVE POWER TECHNOLOGY . . . . .	33
5.1 Technology Background . . . . .	33
5.2 Microwave Power Transmission, Reception, and Conversion . . . . .	36
5.3 The Rectenna . . . . .	39
5.4 Technology Status . . . . .	42
CHAPTER 6 - ALTERNATE POWER TECHNOLOGIES . . . . .	46
6.1 Laser Power Technology . . . . .	46
6.2 Nuclear Power Technology . . . . .	50
6.3 Solar-Thermal Power Technology . . . . .	56
CHAPTER 7 - SELECTED FLIGHT SYSTEMS TECHNOLOGIES . . . . .	60
7.1 Energy Storage Systems . . . . .	60
7.1.1 Batteries . . . . .	60
7.1.2 Fuel Cells . . . . .	64
7.1.3 Flywheels . . . . .	68
7.1.4 Summary . . . . .	72
7.2 Electric Motors . . . . .	74
7.3 Power Processing . . . . .	76

	Page
CHAPTER 8 - AERODYNAMIC CONSIDERATIONS . . . . .	79
8.1 Blimp . . . . .	79
8.2 Airplane . . . . .	84
8.3 Propellers . . . . .	93
CHAPTER 9 - MATERIALS, STRUCTURES, AND PAYLOADS . . . . .	95
9.1 Materials and Structures . . . . .	95
9.2 Payloads . . . . .	96
CHAPTER 10 - ANALYSIS CONSIDERATIONS . . . . .	97
10.1 HAAP Design Philosophy . . . . .	97
10.1.1 Solar-Powered Concepts . . . . .	97
10.1.2 Microwave-Powered Concepts . . . . .	99
10.1.3 Blimps . . . . .	99
10.1.4 Airplanes . . . . .	100
10.2 Computer Codes . . . . .	101
10.3 HAAP Power System Schematic . . . . .	106
10.4 HAAP Concept Energy Requirements . . . . .	107
10.5 Summary of System Parameters . . . . .	108
CHAPTER 11 - HAAP BLIMP FEASIBILITY AND ANALYSIS . . . . .	112
11.1 Solar-Powered Concept . . . . .	113
11.1.1 Parametric Variations . . . . .	117
11.1.1.1 Maximum Airspeed . . . . .	117
11.1.1.2 Drag Coefficient . . . . .	119
11.1.1.3 Propeller Efficiency . . . . .	121
11.1.1.4 Solar Cell Efficiency . . . . .	122

	Page
11.1.1.5 Incident Solar Power . . . . .	123
11.1.1.6 Fuel Cell Weight . . . . .	124
11.1.1.7 Structural Weight Fraction . . . . .	125
11.1.1.8 Payload Weight . . . . .	126
11.1.1.9 Helium Gas Fraction . . . . .	127
11.1.1.10 Superpressure . . . . .	128
11.1.1.11 Advanced Technology Solar-Powered HAAP Blimp . . . . .	129
11.1.2 General Remarks . . . . .	130
11.2 Microwave-Powered Concept . . . . .	131
11.2.1 Parametric Variations . . . . .	134
11.2.1.1 Drag Coefficient . . . . .	134
11.2.1.2 Propeller Efficiency . . . . .	135
11.2.1.3 Rectenna Efficiency . . . . .	136
11.2.1.4 Incident Microwave Power . . . . .	137
11.2.1.5 Structural Weight Fraction . . . . .	138
11.2.1.6 Payload Weight . . . . .	139
11.2.1.7 Helium Gas Fraction . . . . .	140
11.2.1.8 Superpressure . . . . .	140
11.2.2 General Remarks . . . . .	141
11.3 Nuclear-Powered Concept . . . . .	141
CHAPTER 12 - HAAP AIRPLANE FEASIBILITY AND ANALYSIS . . . . .	144
12.1 Solar-Powered Concept . . . . .	145

	Page
12.1.1 Parametric Variations . . . . .	148
12.1.1.1 Design Airspeed . . . . .	149
12.1.1.2 Maximum Operating Lift Coefficient . .	150
12.1.1.3 Profile Drag Coefficient . . . . .	151
12.1.1.4 Propeller Efficiency . . . . .	152
12.1.1.5 Solar Cell Efficiency . . . . .	153
12.1.1.6 Incident Solar Power . . . . .	154
12.1.1.7 Fuel Cell Weight . . . . .	155
12.1.1.8 Structural Weight-Wing Area Ratio . .	156
12.1.1.9 Payload Weight . . . . .	157
12.1.1.10 Aspect Ratio . . . . .	157
12.1.1.11 Oswald's Airplane Efficiency Factor . . . . .	158
12.1.2 General Remarks . . . . .	159
12.2 Microwave-Powered Concept . . . . .	160
12.2.1 Parametric Variations . . . . .	162
12.2.1.1 Maximum Operating Lift Coefficient . .	163
12.2.1.2 Profile Drag Coefficient . . . . .	164
12.2.1.3 Propeller Efficiency . . . . .	165
12.2.1.4 Rectenna Efficiency . . . . .	166
12.2.1.5 Incident Microwave Power . . . . .	167
12.2.1.6 Structural Weight-Wing Area Ratio . .	168
12.2.1.7 Payload Weight . . . . .	168

	Page
12.2.1.8 Aspect Ratio . . . . .	169
12.2.1.9 Oswald's Airplane Efficiency Factor . . . . .	170
12.2.2 General Remarks . . . . .	170
12.3 Nuclear-Powered Concept . . . . .	171
CHAPTER 13 - LAUNCH CONSIDERATIONS . . . . .	174
13.1 Blimps . . . . .	174
13.2 Airplanes . . . . .	178
13.2.1 Solar-Powered . . . . .	178
13.2.2 Microwave-Powered . . . . .	180
13.2.3 Nuclear-Powered . . . . .	182
13.2.4 General Remarks . . . . .	182
CHAPTER 14 - SOCIETAL CONSTRAINTS . . . . .	184
14.1 HAAP Airspace . . . . .	184
14.2 HAAP Propulsion Methods . . . . .	185
14.2.1 Solar Power . . . . .	185
14.2.2 Microwave Power . . . . .	185
14.2.2.1 Controversial Issues . . . . .	186
14.2.2.1.1 Safety Standards . . . . .	186
14.2.2.1.2 Environmental Effects . . . . .	188
14.2.2.2 Public Perception . . . . .	190
14.2.2.3 Microwave Transmission Station . . . . .	192
14.2.3 Nuclear Power . . . . .	195
14.3 General Remarks . . . . .	198



	Page
CHAPTER 15 - CONCLUSIONS . . . . .	199
15.1 Solar-Powered HAAP Concepts . . . . .	199
15.2 Microwave-Powered HAAP Concepts . . . . .	200
15.3 Nuclear-Powered HAAP Concepts . . . . .	201
BIBLIOGRAPHY AND REFERENCE LIST . . . . .	202
APPENDIX A - COMPUTER PROGRAM LISTINGS . . . . .	213
A.1 Blimp . . . . .	213
A.2 Airplane . . . . .	223
APPENDIX B - LIST OF CONSULTANTS . . . . .	232
B.1 Solar Power Technology . . . . .	232
B.2 Microwave Power Technology . . . . .	233
B.3 Alternate Power Technologies . . . . .	233
B.4 Flight Systems Technologies . . . . .	233
B.5 Aerodynamics . . . . .	235
B.6 Systems Integration . . . . .	235
B.7 Societal Constraints . . . . .	236



# LIST OF SYMBOLS

A	aspect ratio, $\frac{b^2}{S_{ref}}$
Ag	silver
A <sub>r</sub>	area of receiving antenna
A <sub>t</sub>	area of transmitting antenna
b	wing span
c	constant (14,543.9 gm/slug)
Cd	cadmium
CO <sub>2</sub>	carbon dioxide
C <sub>D</sub>	total drag coefficient
C <sub>L</sub>	total lift coefficient
C <sub>D,h</sub>	blimp hull drag coefficient
C <sub>D,0</sub>	profile drag coefficient
C <sub>D,S</sub>	static drag coefficient
C <sub>Ld</sub>	dynamic lift coefficient
C <sub>L,max</sub>	maximum lift coefficient
C <sub>L,max op</sub>	maximum operating lift coefficient
C <sub>L,opt</sub>	lift coefficient at minimum power
C <sub>d</sub>	airfoil drag coefficient
C <sub>l</sub>	airfoil lift coefficient
D	drag
d	propeller diameter
$\bar{D}$	distance between A <sub>t</sub> and A <sub>r</sub>
d-c	direct current
E	daily energy requirement

e	Oswald's airplane efficiency factor
GaAs	gallium arsenide
hp	horsepower
H <sub>2</sub>	hydrogen
J	advance ratio $\left(J = \frac{v}{nd}\right)$
L	total lift
L <sub>d</sub>	dynamic lift
Li	lithium
ℓ	characteristic length
m	molecular weight of lifting gas
n	propeller rotational speed
Ni	nickel
O <sub>2</sub>	oxygen
P	power density
P <sub>a</sub>	ambient pressure
P <sub>M</sub>	power delivered by motor
P <sub>min</sub>	minimum pressure
P <sub>off</sub>	number of hours daily that power is provided by energy storage system
R	universal gas constant
R <sub>n</sub>	Reynolds number, $R_n = \frac{v\ell}{\eta}$
S, S <sub>ref</sub>	reference planform area
Si	silicon
T	thrust
t	time
T <sub>a</sub>	ambient temperature

$T_{\min}$	minimum temperature
$T_{\max}$	maximum temperature
$V$	volume
$v$	airspeed
$W$	weight
$\Delta P_{\max}$	maximum superpressure
$\Delta P_{\min}$	minimum superpressure
$\Delta T$	superheat, degrees
$\lambda$	wavelength
$\mu$	micron ( $1 \mu = 3.2808 \times 10^{-6} \text{ ft}$ )
$\rho_a$	ambient density
$\tau$	$= \sqrt{\frac{A_t A_r}{\lambda \bar{D}}}$
$\eta$	kinematic viscosity
$\eta_{es}$	energy storage efficiency
$\eta_m$	motor efficiency
$\eta_p$	propeller efficiency
$\eta_{pp}$	power processing efficiency



## LIST OF ACRONYMS

BCL	Battelle Columbus Laboratories
DE	Doctor of Engineering
FAA	Federal Aviation Administration
HAAP	High-Altitude Aircraft Platform
HASPA	high-altitude superpressured powered aerostat
NASA	National Aeronautics and Space Administration
NTS	Navigation Technology Satellite
RTG	radioisotope thermoelectric generator
SNAP	systems for nuclear auxiliary power
SPAR	space power advanced reactor
SPS	solar power satellite
SRI	Stanford Research Institute
U.S.	United States





## CHAPTER 1

### SUMMARY

This study has been conducted to determine the feasibility of a remotely piloted, High-Altitude Aircraft Platform (HAAP) which would perform year-around missions over the United States. Technologies anticipated to be available within the next 5 to 7 years were used in analyzing solar-, microwave-, and nuclear-powered concepts. Both blimps and airplanes were considered for carrying a nominal 100-pound payload requiring 1000 watts of continuous power. Societal attitudes toward a HAAP and its propulsion systems were also considered.

Solar-powered HAAP concepts are extremely large, and conventionally shaped configurations cannot provide adequate surface for the required solar cells because of the combined requirements of maintaining station against high winter windspeeds and storing energy for use during the long winter nights. The development of all technologies to advanced levels projected herein could lead to a viable blimp design of manageable size. Near-term technology levels should result in a reasonable sized blimp designed for lesser airspeeds. For HAAP applications, solar power appears to be more readily acceptable by society than the other propulsion methods considered in this study.

Microwave-powered HAAP concepts do not require nighttime energy storage, and should result in relatively small vehicles that can perform the year-around mission; however, these concepts are restricted to

operation near a ground station. Current societal attitudes could result in controversy over the use of microwave-powered systems even though the required ground station would only transmit power at levels comparable to current satellite communications stations.

Nuclear-powered HAAP concepts may be technically feasible; however, current societal attitudes toward the use of nuclear power would appear to prohibit the development of this concept.

## CHAPTER 2

### INTRODUCTION

Evolutionary advances in science and technology transform dreams into realities. The landing of a man on the Moon is one vivid example. Another, and one which has become an integral part of our society, is television.

This report addresses the use of current and near-term science and technology to transform perhaps another dream into reality, that of a vehicle flying continuously without refueling. Of specific interest is a remotely powered, remotely piloted vehicle which flies continuously, and at high altitudes, in performing a variety of missions. This class of aircraft has been frequently referred to as a High-Altitude Aircraft Platform (HAAP), and includes both blimp-type and airplane-type concepts.

Three propulsion systems are of interest for a HAAP. One of primary interest is a solar-voltaic power system which uses direct energy from the Sun. This propulsion concept has been highly publicized over the past year by the flights of a solar-powered airplane, "Solar Challenger," developed by Dr. Paul MacCready (ref. 1). However, the requirement of high altitude and continuous (24 hours each day) flight for a HAAP is a much greater technological demand than that for MacCready's "Challenger." Another propulsion system of primary interest is a microwave system. This system entails the collection and conversion of microwave energy transmitted through the air, to usable electric energy. Both of these systems provide exciting challenges for the

application of new technologies. Nuclear power, because of its relatively long time periods between refueling, may also be a viable propulsion system for a HAAP.

## 2.1 BACKGROUND

The idea of developing an aircraft platform for a variety of purposes has been proposed for years. Platforms such as instrumented balloons have long been used for obtaining atmospheric data. More recently, however, increasing interest has focused on the need for a powered aerial platform capable of maintaining station for long periods and at a relatively high altitude.

The National Aeronautics and Space Administration (NASA) has been involved in assessing the feasibility of a High-Altitude Aircraft Platform (HAAP). In 1977, NASA funded two HAAP related studies. One study (ref. 2) was performed by the Stanford Research Institute (SRI) to determine the technological feasibility of a HAAP concept and to estimate costs associated with the various HAAP configurations. The second study (ref. 3) was performed concurrently by Battelle Columbus Laboratories (BLC). This study was to determine potential applications for the HAAP, the payloads for each application, and to compare the cost of the HAAP system for each application with the cost of competing systems. In addition to these studies, other HAAP related activities have also been undertaken.

### 2.1.1 SRI HAAP Feasibility Study

In reference 2, Sinko concluded that the most practical and economical propulsion method for a HAAP was a microwave propulsion system.

Consequently, essentially all of this study was devoted to microwave-powered vehicle concepts. Sinko also concluded that the only other practical alternative system would be chemical, i.e., hydrazine or jet fuel, with aircraft rotation or refueling. Aircraft rotation or refueling was determined to be uneconomic. A nuclear-powered HAAP was deemed technically feasible but unlikely because of safety concerns. A solar-powered HAAP was considered technically prohibitive for a "reasonable" size "airship." Specific concept comparisons were absent from this study report. Figure 2.1 illustrates concepts favored by Sinko.

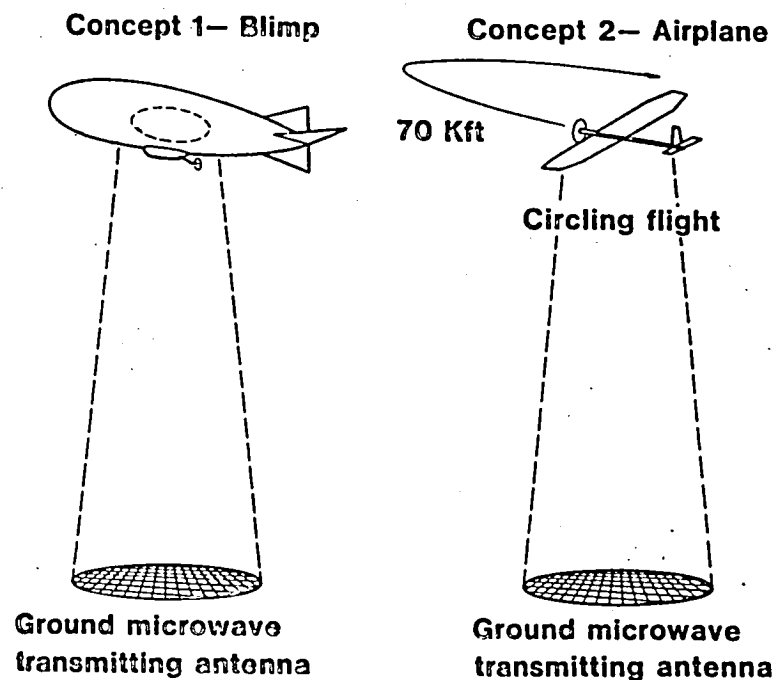


Figure 2.1 - Two proposed High-Altitude Aircraft Platform concepts.

Sinko estimated that the construction cost for either blimp or airplane concept would range between \$0.2 to \$0.4 million (ref. 2, page 49).

### 2.1.2 BCL HAAP Applications Study

This study (ref. 3) examined potential remote sensing and communications applications for a HAAP that would fly in a circle above a ground-based microwave power installation at an altitude of 70,000 feet.

Kuhner, et al. (ref. 3) concluded that for most remote sensing applications, a HAAP was more expensive and less flexible than aircraft that currently perform those missions, but two classes of remote sensing tasks were identified for which HAAP's are particularly suited. HAAP's were determined to be competitive with aircraft where very frequent coverage is required (more than once per day) and where wide-angle sensors are applicable for large areas to be viewed. Remote sensing missions specifically identified for HAAP were:

- (1) Forest fire detection
- (2) Marine traffic surveillance
- (3) Great Lakes ice mapping

The study also identified communications applications that were well suited for HAAP's as being:

- (1) Direct broadcast to home televisions
- (2) Communications experiments
- (3) Mobile communications

### 2.1.3 BCL HAAP User Definition Study

Kuhner and McDowell at Battelle surveyed a group of scientists (ref. 4), representative of selected scientific areas, on future scientific requirements. The three broad discipline areas considered were atmospheric science (chemistry, physics, and pollution monitoring),

remote sensing of the Earth's surface, and astrophysics (radiation monitoring). This study concluded that the high-altitude platform has a " . . . definite potential as an astronomical platform for infrared and cosmic ray investigations and, to a lesser degree, as a tool for upper atmospheric research and remote sensing . . ."

### 2.1.3 Other HAAP-Related Studies

In reference 5, Youngblood, et al., discuss HAAP mission scenarios that could be performed by a solar- or microwave-powered airplane. These scenarios included marine monitoring, such as the ocean disposal of waste materials.

References 6 and 7 discuss solar-powered HAAP concepts. Parry (ref. 6) discusses the feasibility of a solar-powered blimp or airplane performing missions at an altitude of 100,000 ft. Parry concludes that the airplane, because it depends on dynamic lift to remain aloft, did not appear feasible. According to Parry, existing wing structural weight technology (1974) was the limiting factor. A blimp concept was deemed feasible since it depended only on static lift to remain aloft, requiring no power to maintain altitude at night. In reference 7, Phillips discusses some of the practical aspects of a solar-powered HAAP airplane design. Phillips concludes that existing solar cell technology is adequate for operating a HAAP, but that existing rechargeable batteries are too heavy. A flight plan consisting of climbing during the day to store energy and gliding at night is not feasible because the altitude lost during the night is excessive.

A microwave-powered HAAP airplane concept is discussed by Heyson in reference 8. Heyson discusses an airplane that cyclically climbs to an altitude of about 75,000 ft while in the microwave power beam, and then glides over 100 miles in a linear flight profile. Heyson concludes that this concept, which takes advantage of the inherent forward speed of the airplane, is feasible, but that substantial research and development would be needed to insure success within a reasonable period of time. Morris (ref. 9) and Turriziani (ref. 10) each discuss the effects of varying flight parameters on the feasibility of the Heyson (ref. 8) concept.

In a microwave-powered system, the transmission efficiency decreases rapidly as the microwave beam is pointed away from boresight; thus, there is concern for minimizing the ground track of the aircraft. Sinko discusses minimum ground tracks for circling flight in reference 11. Sinko concludes that for wind velocities below 0.35 of the airspeed, the minimum ground track is "D"-shaped (except in zero wind where the shape is a circle). When wind speed is greater than 35 percent of the airspeed, the minimum ground track is a figure-8 pattern. When the wind and airspeeds are equal, the aircraft can simply hover so that the ground track degenerates to a point.

#### 2.1.4.1 The Hufnagel Report

In March 1978, the Department of Defense requested that the Inter-agency Committee on Search and Rescue examine emergency communications requirements, assess the ability of existing communications systems to meet the requirements, and if appropriate, develop a plan for an



Emergency Response Communications System. The Committee was composed of 11 federal agencies and, for this task, was chaired by Air Force Major Ray Hufnagel. The Committee concluded that "... under emergency conditions, existing communication systems exhibit significant deficiencies in coverage . . ." The study (ref. 12) proposed a single geosynchronous communications satellite to provide coverage for the U.S. and its territories. It was anticipated that such a system would serve about 20,000 users. However, the Communications System ground rules were that the federal government would pay for the research and development, and the user would pay operational costs. This system cost was considered "... extremely difficult . . ." to assess, but thought to be, perhaps, too costly for a state government to meet its individual needs.

Nonreferencible documentations internal to NASA have suggested that a system of HAAP's would be a lower cost alternative to the Emergency Response Communications System discussed in the Hufnagel report (ref. 12). These documents indicate that perhaps as few as 13 HAAP's could provide coverage for the contiguous U.S.

#### 2.1.5 Summary of Proposed HAAP Applications

Table 2.1 summarizes the applications that have been proposed for a HAAP.

TABLE 2.1 - SUMMARY OF PROPOSED HAAP APPLICATIONS

Military

- Communications Relay
- Ballistic Missile Early Warning
- Aircraft Tracking
- Weather Monitoring
- Ocean Surveillance
- Battlefield Tactical Intelligence
- Nuclear Explosion Cloud Sampling

Scientific

- Astronomical Observations
- Atmospheric Research
- Oceanographic Research

Civil

- 200 Mile Fishery Enforcement
- Border Patrol Surveillance
- Water Pollution Monitoring
- Atmospheric Pollution Monitoring
- Resource Management
- UHF TV Broadcasts
- National TV Distribution
- Ice Surveying/Mapping of Waterways
- Emergency Response Communications
  
- Forest Fire
- Flash Flood Alert
- Severe Weather
- National Disasters
- Man-Made Disasters
- Search and Rescue

2.2 PROJECT PURPOSE AND OBJECTIVES

The foregoing discussion has identified and summarized some of the studies which indicate a need for, or at least an interest in, a high-altitude aircraft platform. Feasibility studies of various HAAP configuration concepts and propulsion systems have also been summarized.

To date, no systematic evaluation of the various HAAP proposals have been made. The purpose of this research project is to perform that evaluation. Specific objectives of this research project were:

- (1) To determine the technology readiness in areas which impact the current and near-term feasibility of a HAAP.
- (2) To perform a systematic technical evaluation of blimp and air-plane concepts using current and near-term capabilities, with emphasis on solar-voltaic and microwave propulsion systems.
- (3) To identify the technologies that have the greatest impact on the overall concept feasibility of a HAAP, and the possible levels of future improvement.
- (4) To identify societal influences which may constrain or enhance HAAP performance or development.

### 2.3 PROJECT APPROACH

The approach used to accomplish the project research objectives is as follows:

- (1) Identify pertinent HAAP-related technologies and determine their technology readiness.
  - (a) Conduct literature searches.
  - (b) Acquire, review, and assess pertinent documents..
  - (c) Consult with recognized experts in specific areas.

- (2) Develop tools for the analysis of HAAP concept.
  - (a) Develop a computer code to analyze solar-voltaic and microwave-powered blimps.
  - (b) Develop a computer code to analyze solar-voltaic and microwave-powered airplanes.
- (3) Evaluate concepts via parametric analyses.
  - (a) Determine the sensitivity of concept feasibility to parametric variations.
- (4) Identify environmental concerns toward HAAP technologies.
  - (a) Conduct literature searches.
  - (b) Acquire, review, and assess pertinent documents.

## CHAPTER 3

### THE OPERATIONAL ENVIRONMENT

A major concern in providing for the systematic evaluation of a High-Altitude Aircraft Platform (HAAP) is a definition of its operational environment. The civil argument for the justification of a HAAP has been based on its utilization within the confines of the United States (U.S.). Thus, in this study, the region considered for HAAP operation is the 48 contiguous states of the U.S. In global coordinates, the 48 contiguous states and its territorial waters approximately encompass the region between 24 and 49 degrees north latitude and between 60 and 130 degrees west longitude (see Figure 3.1). (The importance of global coordinates will become clear in Chapter 4.)

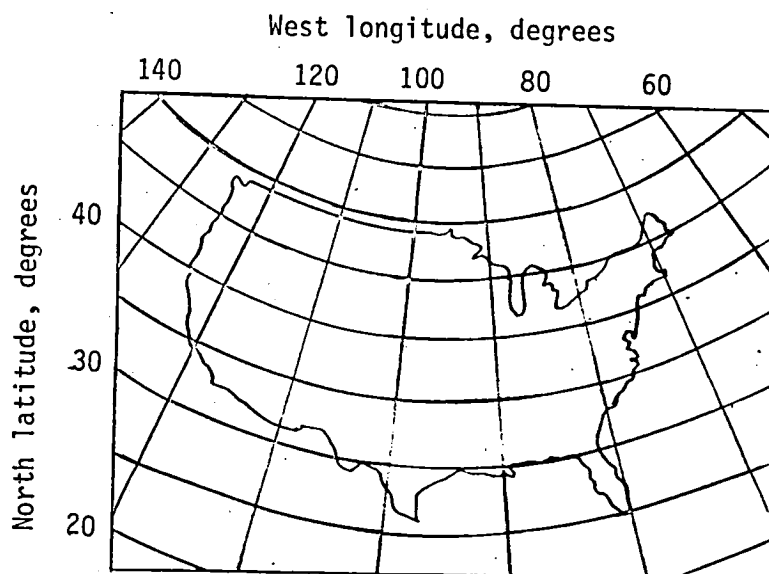


Figure 3.1 - Location of U.S. in global coordinates.

### 3.1 WINDS

Because the missions for HAAP require that the platform be able to maintain station, the wind speeds that the platform will encounter become a significant design constraint. The general shape of wind profiles across the United States resembles that shown in Figure 3.2 which is given in reference 13 (page 8.91) as a design criterion for the launch of aerospace vehicles. In this figure, the 99 percentile line, for example, means that 99 percent of the time the wind speed is equal to, or less, than that shown for the indicated altitude.

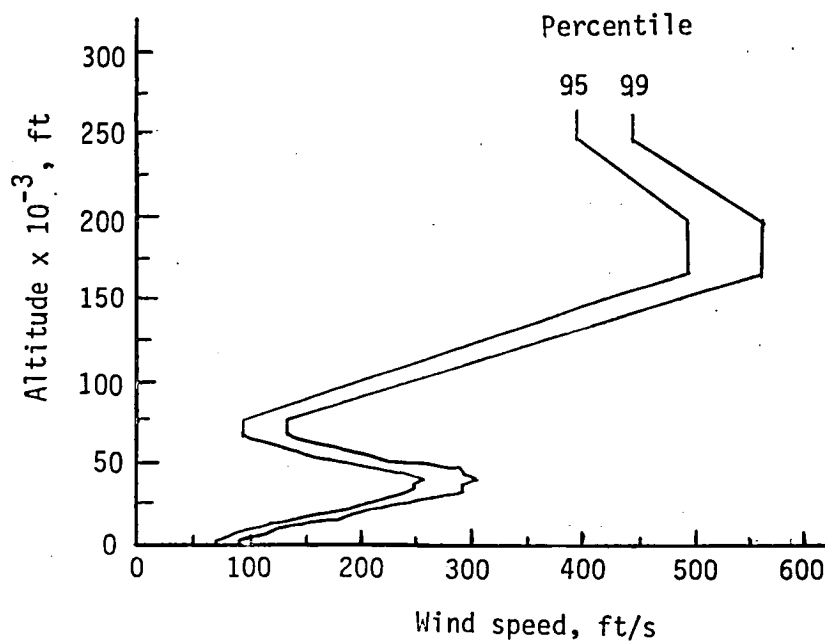


Figure 3.2 - Wind profiles for aerospace vehicle design.

The peak in wind speed near 50,000-ft altitude as shown in the figure is the maximum speed of the "jet stream" region that is familiar to commercial aircraft pilots. It is apparent from Figure 3.2 that the

magnitude of the wind speeds to which a HAAP will be subjected is sensitive to operational altitudes.

The published literature on HAAP proposes an operational altitude of about "70,000 feet" (21 km). This altitude falls in a region of minimum winds. Except for supersonic transports and military aircraft, it is also well above any air traffic anticipated for the reasonably near future.

Reference 14 is a survey of available wind-aloft data performed especially for the design of a high-altitude platform. The statistical data shown in Table 3.1 (ref. 14, page 11) represent years of climatic measurements at altitudes from 53,000 to 82,000 ft, and are the most thoroughly gathered data of this type readily available.

TABLE 3.1 - HAAP WIND DESIGN CRITERIA  
(53,000 to 82,000 ft altitude)

Design speed	Season	Station keeping probability (percent of time)
52 ft/s 30 knots	Winter Spring Summer Fall	60 90 98 90
68 ft/s 40 knots	Winter Spring Summer Fall	75 95 99.6 95
84 ft/s 50 knots	Winter Spring Summer Fall	85 98 99.6 98
127 ft/s 75 knots	Winter Spring Summer Fall	95 99.5 99.7 99.5

If HAAP operation is performed on a yearly basis (as contrasted to a seasonal basis) as its missions indicate, and if it is to perform with at least a 95-percent probability of maintaining station, a HAAP must have at least the capability of operating in maximum winds of about 127 ft/s. The average winds in which the HAAP must operate are modest. The highest average seasonal wind speed in this altitude region, about 50 ft/s, occurs in the winter (ref. 14, page 14).

Although gust phenomena at extreme altitudes are not well understood, some data based on flight measurements are available. NASA has used both the U-2 and XB-70 aircraft to record high-altitude gust data. The Air Force, in its High-Altitude Clear Air Turbulence Program (HICAT), also used a U-2 airplane to measure turbulence. Some results of these measurements are reported in references 15 to 17. Figure 3.3 (from ref. 17, page 983) illustrates the variation in recorded turbulence measurements.



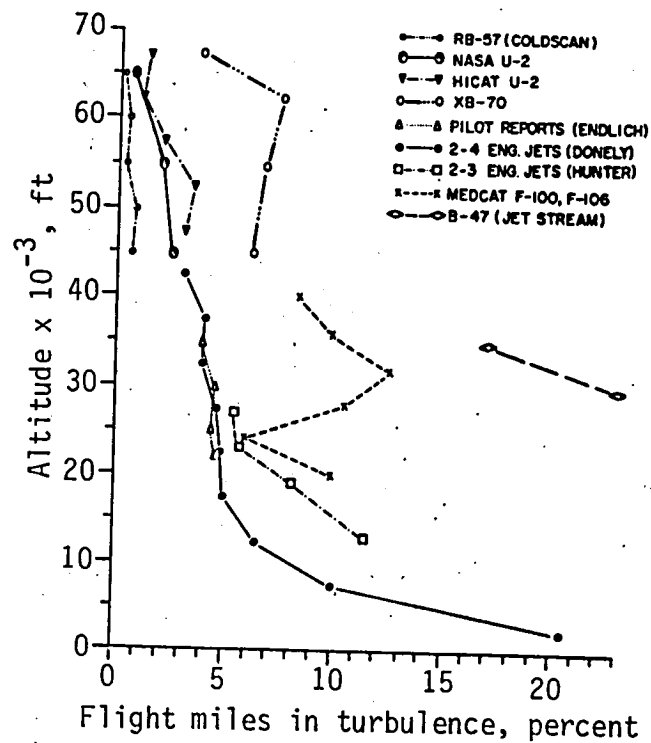


Figure 3.3 - Comparison of turbulence measurements.

Figure 3.3 indicates a general lessening of turbulence at the altitudes considered herein (60,000 to 70,000 ft); however, the data, which are sparse, indicate an uncertainty of an order of magnitude in the percentage of flight miles in turbulence.

It has often been assumed that the gust and turbulence environment at HAAP altitudes is benign and that the structural design requirements may be relaxed in favor of lighter weight. This philosophy tends to overlook a significant difference between conventional aircraft and HAAP vehicles. A conventional aircraft flies for a very few hours upon which it lands and can be inspected for damage. On the other hand, a HAAP vehicle flies continuously for about a year (8760 hours). During this period, there is no opportunity for inspection, repair, or overhaul. A

fatigue crack, once started, continues to propagate with a significant possibility of catastrophic failure during the long flight. The structural design criteria for a HAAP must account for these possibilities. In view of the imperfect knowledge of the environment and the lack of experience with such long flight times, the initial choice of HAAP structural criteria may have to be more severe than those which are applied to conventional aircraft.

### 3.2 TEMPERATURES

The seasonal variation in atmospheric temperature with altitude, as well as the extreme temperatures recorded over Edwards Air Force Base, California (ref. 13, page 10.28), are shown in Figure 3.4. These curves resemble the average global temperature profile (ref. 18), and are thought to be representative of temperatures over the United States. Note in Figure 3.4 that minimum temperatures occur near the 70,000-ft altitude region proposed for HAAP operation.

Using the Edwards' data as indicative of the ambient temperatures for HAAP, that range is about from  $-58^{\circ}\text{F}$  to  $-112^{\circ}\text{F}$ , including extreme weather conditions.

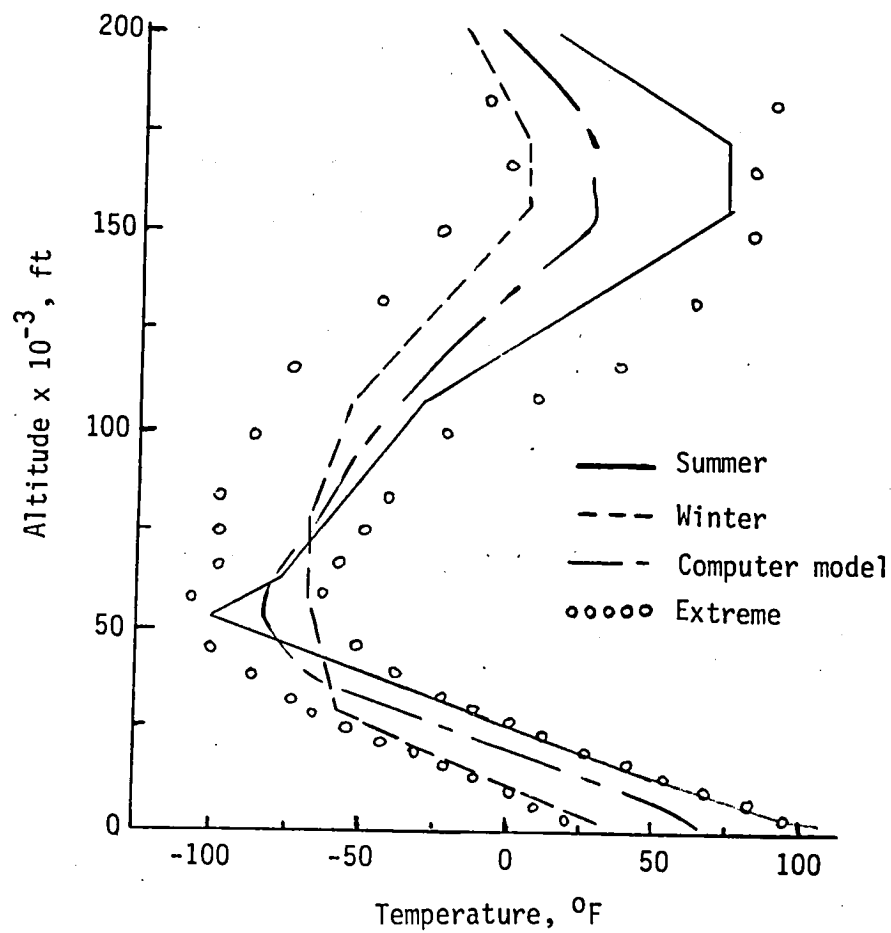


Figure 3.4 - Temperature profile over Edwards Air Force Base, California.

### 3.3 ENVIRONMENTAL PARAMETER SUMMARY

Reference 18 provides characteristic air properties such as density and kinematic viscosity for the HAAP altitude range. Table 3.2 is a summary of the HAAP operational environment.

TABLE 3.2 - SUMMARY OF HAAP ENVIRONMENTAL PARAMETERS

Altitudes, ft	53,000 to 82,000
Wind speeds, ft/s	42 to 130
Temperatures, °F	-112 to -58
Densities $\times 10^3$ , slugs/ft <sup>3</sup>	0.321 to 0.008
Pressures, lb/ft <sup>2</sup>	216 to 53
Kinematic viscosities $\times 10^6$ , ft <sup>2</sup> /s	8 to 34

## CHAPTER 4

### SOLAR-VOLTAIC POWER TECHNOLOGY

Solar-voltaic power technology is concerned with the direct conversion of energy from the Sun to electrical energy.

#### 4.1 GLOBAL INTEREST

The published literature covering the various technological aspects of solar power is massive. Ongoing efforts in solar-voltaic power research and development are being conducted in France, West Germany, Japan, Italy, Great Britain, and Canada (ref. 19). Currently, the U.S. has a large financial commitment to furthering solar power technology. The National Photovoltaics Act authorized expenditure of \$1.5 billion over a 10-year period for photovoltaic research, development, and demonstration. This Photovoltaic Systems Program, which had a \$100 million budget in 1979 and \$130 million in 1980, is administrated by the U.S. Department of Energy. The European effort is coordinated through the Commission of the European Economic Community and plans to spend about \$50 million over a 4-year period on similar efforts. This global effort is primarily aimed at terrestrial application; that is, as an alternate energy source to petroleum based fuels. The primary focus for this application is on reasonable efficiency and low system cost for overall acceptability as an alternative to petroleum fuels. System weight is not a significant consideration.

Solar-voltaic power technology focused on space application is being conducted primarily in the U.S. and Japan. Space application

focuses on high efficiency, reliability, and long life. Solar power system weight is of concern because it has major impact on launch weight for the spacecraft. However, once the spacecraft is in orbit, the solar power system weight imposes no penalty on the craft's operation, although it can affect dynamics when large panels are unfolded.

A HAAP solar power system is faced with stringent constraints. It must not only have relatively high efficiency, but also low weight. The energy obtained through the solar power system must be used, in part, to keep the airplane, including the weight of the solar power system aloft. For HAAP, the requirements are similar to those of space technology rather than terrestrial application.

#### 4.2 THE SUN AND ITS ENERGY

The Earth daily rotates about its own axis and annually orbits about the Sun as shown in Figure 4.1 (ref. 20, page 41). The energy

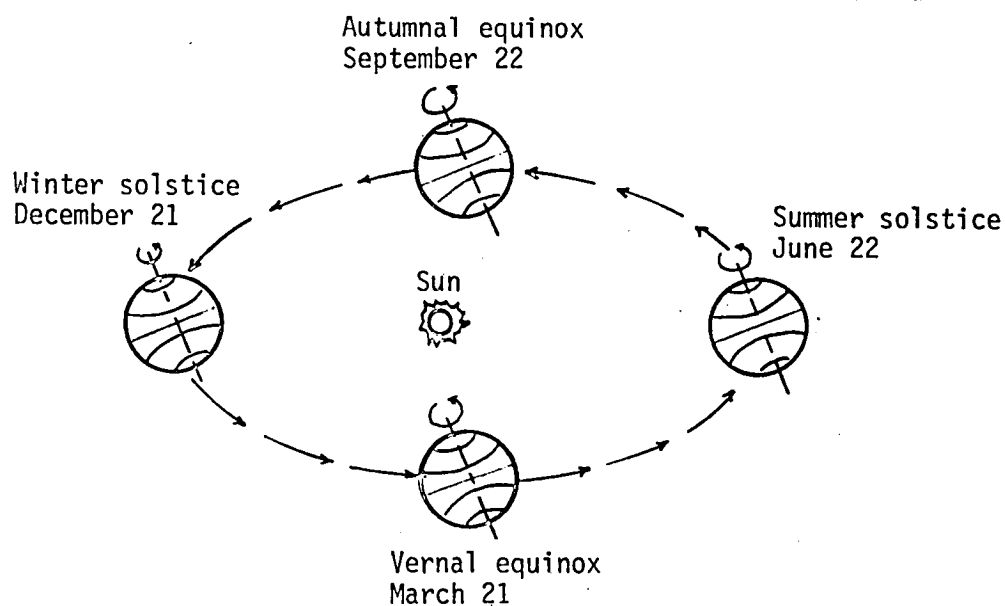


Figure 4.1 - The Earth's orbit.

that the Earth receives from the Sun varies slightly over the course of its yearly orbit. However, an average value for the Sun's energy flux on the Earth has been determined by satellite experiments to be about  $127 \text{ W/ft}^2$  ( $1368 \text{ W/m}^2$ ). This value (within 1 percent) is well established (ref. 21).

The "top of the Earth's atmosphere" is often considered to be at 30-km (98,425-ft) altitude because, for theoretical purposes, absorption and scattering of the Sun's energy in the Earth's atmosphere does not occur at altitudes greater than 30 km. Figure 4.2 (from ref. 22, page 44) shows the annual theoretical daily distribution of energy about the Northern Hemisphere at 30-km altitude. For the latitude region of the U.S. ( $24^\circ$  to  $49^\circ$ ), the daily solar insolation (energy) is greatest in the months of June and July. Figure 4.2 shows that,

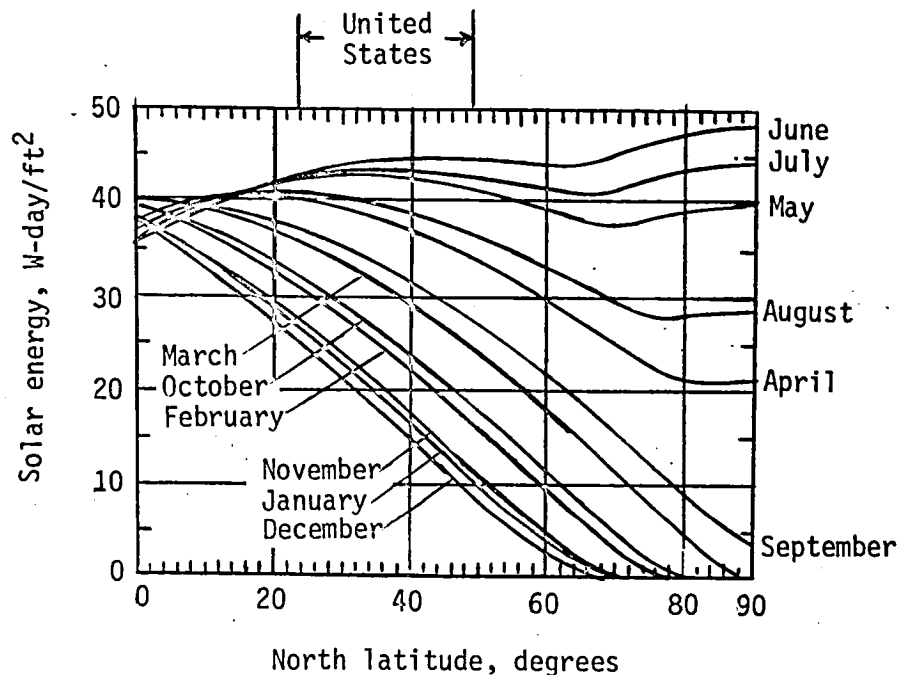


Figure 4.2 - Theoretical daily distribution of solar energy on the Northern Hemisphere.

during the year, incident daily solar energy at the "top of the atmosphere" over the U.S. varies from about 9 to 45 Watt-Day/ft<sup>2</sup>. This solar energy, only part of which is visible, is distributed over the wavelength spectrum shown in Figure 4.3 (ref. 22, page 5).

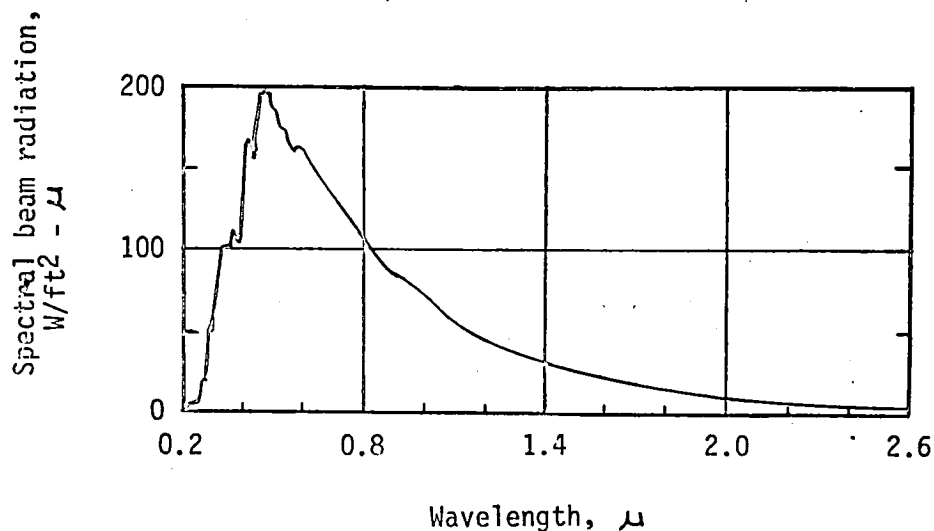


Figure 4.3 - Wavelength distribution of solar energy.

If the area under the curve of Figure 4.3 is integrated over all wavelengths, the calculated value will approximate that of the "solar constant" (127 W/ft<sup>2</sup>). The distribution of solar energy in wavelength regions is shown in Table 4.1.

TABLE 4.1 - DISTRIBUTION OF SOLAR ENERGY IN WAVELENGTH REGIONS

Region, μ	Distribution, percent
Ultraviolet (below 0.38)	7.0
Visible (0.38 to 0.75)	44.7
Infrared (above 0.75)	48.3



#### 4.3 THE SOLAR CELL

The solar cell is a photovoltaic device which responds to electromagnetic radiation, generally in the visible wavelength region, and directly converts a portion of this energy to usable d-c (direct-current) electricity. References 23 to 33 provide a thorough background for understanding solar cell technology. Ongoing research efforts include the study of many materials, metallic and nonmetallic, as well as organic and inorganic, to determine their photovoltaic properties and suitability for use in solar cells.

Reference 29 is the single most comprehensive document on solar cell characteristics behavior and subsequent design, and much of the subsequent discussion is from that source. Currently, the two most advanced types of solar cells are Si (silicon) and GaAs (gallium arsenide). The principal advantages of Si cells are that silicon is a more abundant material (which contributes to the cell being more economical to manufacture) and it has less mass. GaAs cells are less susceptible to radiation damage which gives them longer lifetime in a space environment, and in that environment they are more efficient in converting solar-to-electrical energy. The maximum theoretical efficiencies are about 0.22 for the Si cell and about 0.27 for the GaAs (ref. 33, page 11). Table 4.2 illustrates some differences in typical Si and GaAs solar cells with identical volumetric size and surface area.

TABLE 4.2 - COMPARISON OF TYPICAL SOLAR CELLS

Characteristics	Solar cell	
	Silicon	Gallium arsenide
Size, in. $\times$ in. $\times$ in.	0.79 $\times$ 0.79 $\times$ 0.010	0.79 $\times$ 0.79 $\times$ 0.010
Mass, slugs $\times 10^5$	1.93	3.49
Efficiency (at 77°F; 298°K)	0.148	0.157

Note the temperature associated with the rated conversion efficiency in Table 4.2. Temperature has a significant effect on cell efficiency. The efficiency of Si cells typically changes by  $-0.005/^{\circ}\text{K}$  and GaAs by  $-0.024/^{\circ}\text{K}$  from the values at the reference temperature shown in the table (from ref. 33, page 23).

Figures 4.4 (ref. 30, page 11.3-4) and 4.5 (ref. 1, page 4) are indicative of the relative response characteristics for solar cells when exposed to simulated space sunlight at 77°F (298°K).

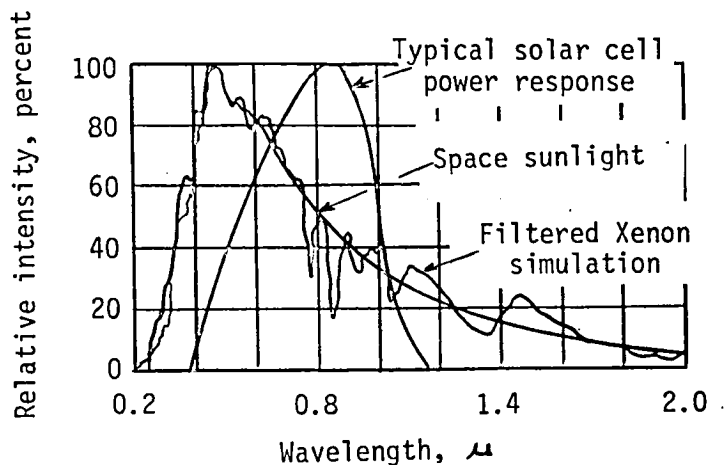


Figure 4.4 - Typical solar cell response characteristics.

The curves in Figure 4.4 show the distribution of solar energy at the "top of the atmosphere" (space sunlight), the simulation of that solar energy in the laboratory (filtered xenon simulation), and the bell-shaped curve which is the response of the solar cell to the simulated solar spectrum. The solar cell response curve indicates maximum cell power conversion efficiency occurs for incident power having a specific wavelength, in this example, about  $0.85 \mu$  ( $2.8 \times 10^{-6}$  ft). A relative decrease in cell conversion efficiency occurs for incident power at wavelengths either longer or shorter than this optimum wavelength.

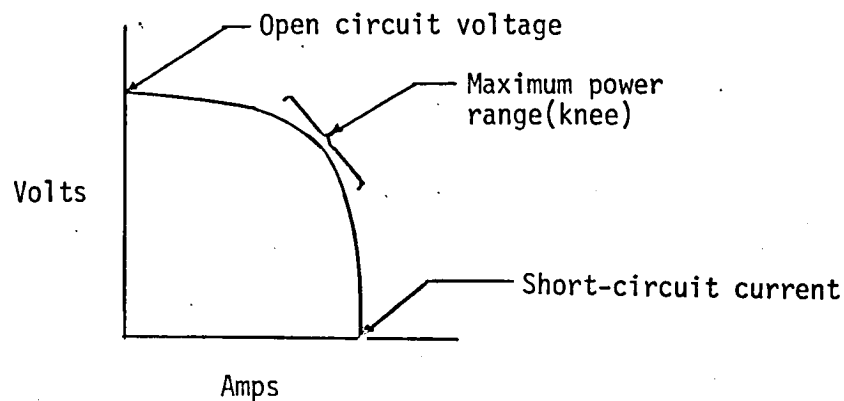


Figure 4.5 - Typical solar cell power output characteristics.

Although solar cells can be produced in a number of sizes and shapes, they are typically  $0.79 \times 0.79$  in. ( $2 \times 2$  cm) or  $0.79 \times 1.58$  in. ( $2 \times 4$  cm) with thicknesses from about 0.004 to 0.012 in. Figure 4.5 illustrates the electrical characteristics typical of  $0.79 \times 0.79$  in. ( $2 \times 2$  cm) solar cells when exposed to the reference solar radiation ( $126 \text{ W/ft}^2$ ) at  $77^\circ\text{F}$  ( $298^\circ\text{K}$ ). Electrical characteristics vary with

thickness and material type, but are typically operated at about 0.5 volt and about 0.15 amps for a 0.79 x 0.79 in. cell. Maximum power occurs at the knee of the curve.

#### 4.3.1 Arrays

In space application, solar cells are encapsulated by a cover for environmental protection, especially from charged particles which degrade cell performance. Space radiation is of less concern in the HAAP operational environment, but a thin cover would be used to protect the cells from environmental effects such as moisture. Figure 4.6 (ref. 29, page 6.2-15) illustrates 9 cells electrically interconnected to form a sub-array. Typically, the cells are connected in both series and parallel electrical networks to obtain a desired system voltage and current. In turn, the sub-arrays are also electrically interconnected. The network can be wired so that in the case of a cell failure, only a few cells in the corresponding series network become inoperative.

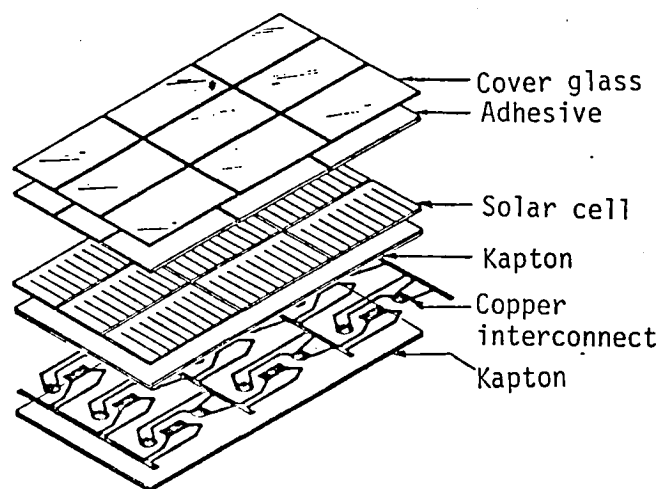


Figure 4.6 - Illustration of a solar cell array.

The wiring technique which was used on the 16,000 cell Solar Challenger airplane allowed a cell to fail without significantly affecting the other cells in the electrical network (ref. 1, page 8).

Historically, solar cell arrays have been used in space application since 1958 when an array provided power (about 1 watt) on board the U.S. satellite Vanguard I (ref. 29, pages 1.1-1 to 1.1-4). The individual solar cells were about 0.79 x 0.20 in. with a rated (at 82°F) conversion efficiency of 10 percent. Since that time, most spacecraft have used solar cell arrays as the primary power source. Power systems on spacecraft have, at times, used well over 100,000 individual solar cells in their design.

#### 4.4 TECHNOLOGY STATUS

Solar-voltaic energy is a proven technology which has been demonstrated for about 25 years while undergoing continuous evolution. Figure 4.7 illustrates trends in solar cell efficiencies obtained from a variety of sources. The figure indicates the time lag associated with transferring laboratory results to production line status and includes both Si and GaAs cells. The trend curves of Figure 4.7 have been adjusted to the current standard of 1353 W/m<sup>2</sup>, and include the effect of a number of changes in the standards under which solar cell efficiency has been measured over the years. In 1971, a redefinition of the solar constant from 130 W/ft<sup>2</sup> (1396 W/m<sup>2</sup>) to 126 W/ft<sup>2</sup> (1353 W/m<sup>2</sup>) resulted in an apparent increase in cell efficiency of about 3 percent. (The current reference value for the solar constant used in solar cell technology is 1353 W/m<sup>2</sup> although the actual value is now believed to

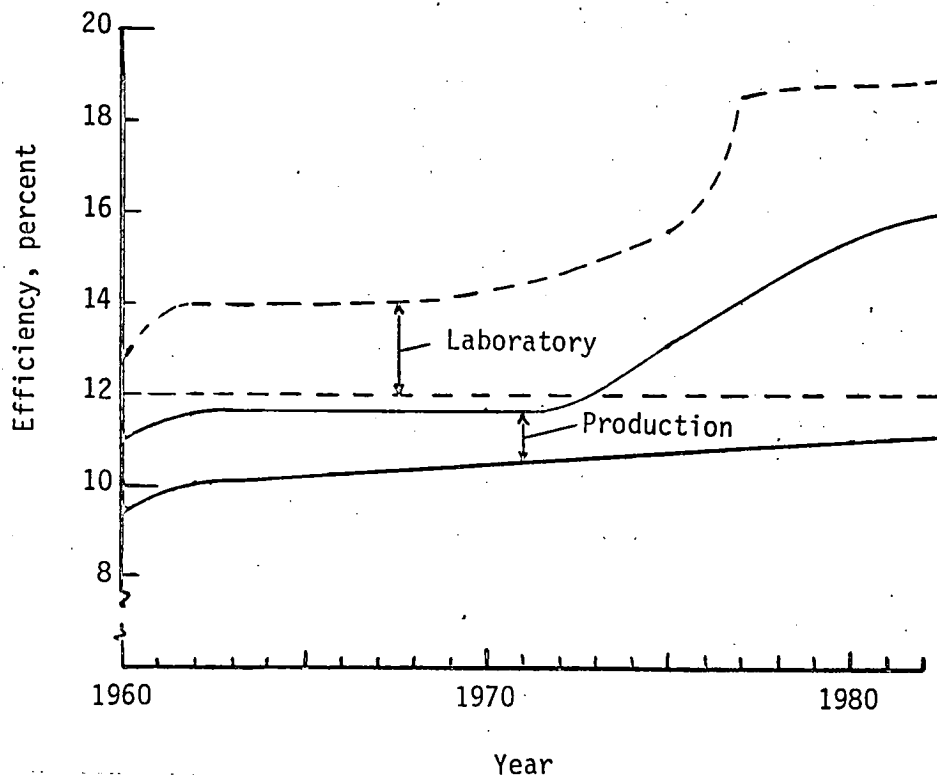


Figure 4.7 - Historical evolution of solar cell efficiency.

be  $1368 \text{ W/m}^2$ .) A general decrease in reference test temperature from  $82^\circ\text{F}$  to  $77^\circ\text{F}$  resulted in an apparent 2-percent increase in cell efficiency (ref. 29, page 3.12-1). Cells have become thinner in an effort to reduce spacecraft propulsion system mass, and this change also reduces efficiency.

Current solar cell production line technology is represented in Table 4.3, and reflects recent discussion with representatives of the solar cell manufacturers (see Appendix B.1).

TABLE 4.3 - CURRENT STATUS OF SOLAR CELL TECHNOLOGY

Cell type	Si	Si	Si	GaAs
Cell size, in. × in.	0.79 × 0.79	0.79 × 0.79	0.79 × 0.79	0.79 × 0.79
Cell thickness, in.	0.004	0.008	0.010	0.010
Efficiency (77°F)	0.140	0.146	0.148	0.157
Mass × 10 <sup>5</sup> , slugs	0.97	1.60	1.93	3.49
Weight × 10 <sup>3</sup> , lb	0.31	0.51	0.62	1.12
Specific power, W/lb	244.4	154.9	129.2	75.9

The higher specific power system, silicon, is advantageous to HAAP application.

Table 4.4 characterizes a silicon solar cell array system specifically designed for HAAP application using current and near-term technologies. The values shown for efficiency have been temperature adjusted to a HAAP representative operating temperature.

TABLE 4.4 - TECHNOLOGY STATUS OF SOLAR-VOLTAIC POWER FOR HAAP DESIGN

	Current	Near-term (2-4 years)
Cell type	Silicon	Silicon
Cell size, in. × in. × in.	0.79 × 0.79 × 0.004	1.57 × 2.36 × 0.004
Rated efficiency, (at 77°F; 298°K)	0.140	0.145
Operating efficiency (at -76°F; 213°K)	0.155	0.160
Array weight, lb/ft <sup>2</sup>	0.09	0.08
Specific power, W/lb	197.5	227.2
W/ft <sup>2</sup>	17.5	18.9

The values shown for near-term technology will be used in determining the feasibility of solar-powered HAAP concepts. In addition, to account for atmospheric effects such as absorption, scattering, etc., and more significantly, the misalignment of the solar cells with the Sun's rays (including flight orientation and latitude) which prevents capturing the maximum available energy, a value of  $111 \text{ W/ft}^2$  ( $1200 \text{ W/m}^2$ ) will be assumed herein to represent the average incident solar energy.

The performance of a solar cell array specifically designed for HAAP will be considerably different from that of the Solar Challenger airplane. The "Challenger" used rejected space quality solar cells obtained from the U.S. Air Force through NASA. Values provided by Aerovironment, Inc. (see Appendix B.1), builder of the Solar Challenger, specify an array weight of about  $0.20 \text{ lb/ft}^2$  and an average array operating efficiency, on a clear day, of about 0.125. It is important to note that the efficiency for the Solar Challenger is based on a different energy spectrum (one that includes atmospheric effects) than that for HAAP (see Fig. 4.3). The reference solar energy appropriate for the Solar Challenger is approximately  $93 \text{ W/ft}^2$  ( $1000 \text{ W/m}^2$ ).



## CHAPTER 5

### MICROWAVE POWER TECHNOLOGY

The microwave portion of the electromagnetic spectrum (see Table 5.1) has been used for long-distance communications, navigation, and radar for decades. The lower microwave frequencies (longer wavelengths, i.e., about  $10^6 \mu$ ) are being used daily and worldwide for radio and television transmission. In all of these applications, usable a-c or d-c power is converted to "radio" (microwave) frequencies and transmitted over "free-space." The technology of converting usable power to microwaves and the transmission of these microwaves over free-space has become a mature technology which has been readily accepted by society at the power levels typically used in communications.

#### 5.1 TECHNOLOGY BACKGROUND

Although the daily transmission of low power microwave radiation is customary in our society, a technology which is in its infancy and which is vital to the concept of a microwave-powered high-altitude platform (HAAP), is collecting transmitted microwave energy and converting it back into usable energy. Reference 34 by Brown is an excellent summary of work on the collection and rectification of transmitted microwave energy for military applications.

In recent years, emphasis on space applications of microwave power transmission and conversion in the U.S. has stemmed from a societal need. In 1973, the United States was confronted with an embargo by the oil exporting nations. Subsequently, in an effort to become "energy

TABLE 5.1 - SPECTRUM OF ELECTROMAGNETIC RADIATION

Frequency, Hz	Type of radiation	Wavelength, $\mu$
$10^{22}$	Cosmic rays	$10^{-8}$
$10^{20}$	Gamma rays	$10^{-6}$
$10^{18}$	X-rays	$10^{-4}$
$10^{16}$	Ultraviolet	$10^{-2}$
$10^{14}$	Visible light	$10^0$
$10^{12}$	Infrared	$10^2$
$10^{10}$	Submillimeter waves	$10^4$
$10^8$	Microwaves (radar)	$10^6$
$10^6$	Television and FM Radio	$10^8$
$10^4$	Short Wave	$10^{10}$
	AM radio	
	Maritime communications	

independent," the U.S. government embarked on an effort to determine the feasibility of using large satellites to collect solar energy, convert that energy to microwave energy, transmit the microwave energy over free-space, and, finally, to collect and convert that to electrical power suitable for nationwide distribution. The system proposed for obtaining this objective is called the Solar Power Satellite (SPS). References 35 and 36 discuss many efforts, both ongoing and complete, which relate to the Solar Power Satellite concept, and which, in part, address microwave power systems. A conceptual sketch of an SPS system is presented in Figure 5.1.

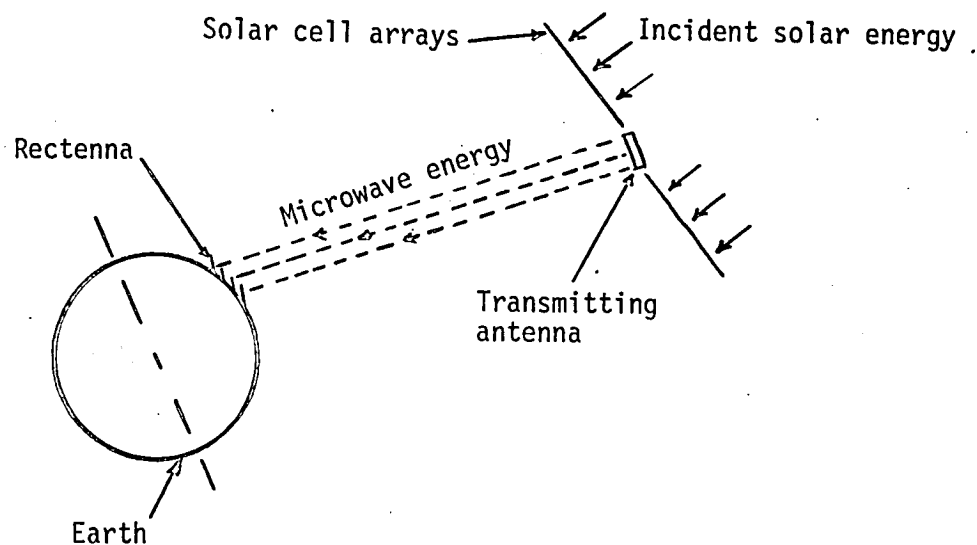


Figure 5.1 - Concept of a solar-powered satellite.

Although SPS does promote advances in microwave power transmission and reception technology, there is one fundamental difference between SPS efforts and those needed for a High-Altitude Aircraft Platform (HAAP). Efforts in SPS are focused on lightweight transmitting antenna which must be transported into Earth orbit. The receiving antenna for the system will be located on the Earth (land). Weight for this antenna to collect and rectify the microwave energy poses little concern. SPS emphasis is on conversion efficiency and low cost. An operational HAAP must be concerned about the weights of the various systems which must be carried on board. Emphasis for a HAAP becomes that of a low-weight rectifying antenna (rectenna) system. Figure 5.2 illustrates the concept of a microwave-powered HAAP. In the example, a HAAP airplane performs as a communications relay station while in circling flight.

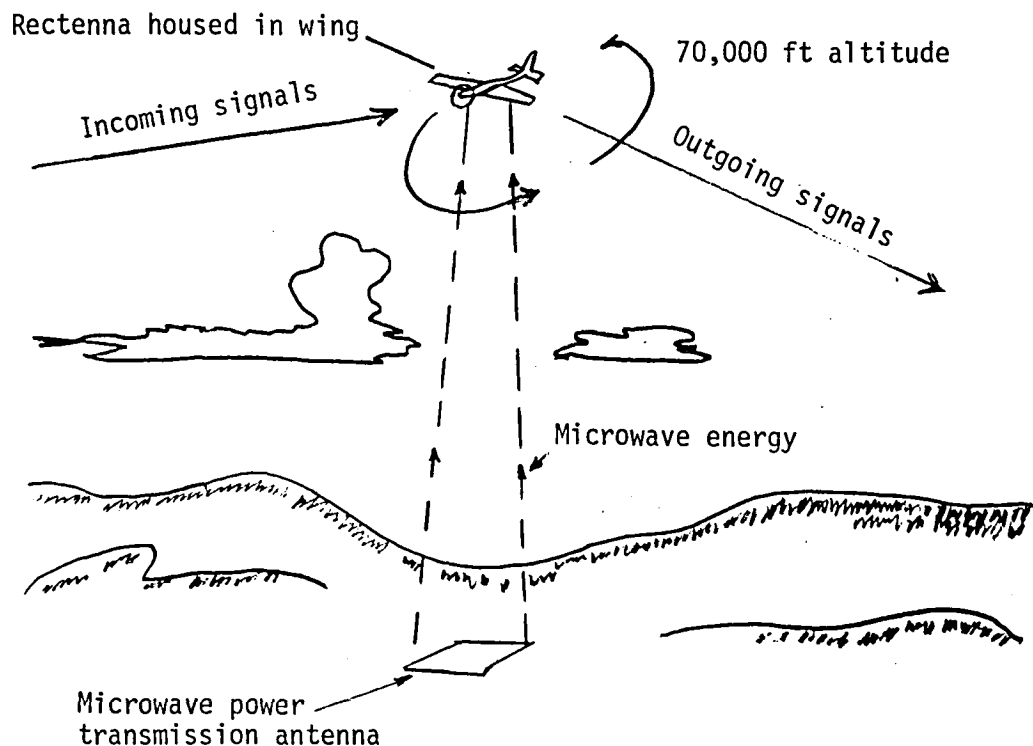


Figure 5.2 - Concept of a microwave-powered HAAP airplane system.

## 5.2 MICROWAVE POWER TRANSMISSION, RECEPTION, AND CONVERSION

The process of microwave power transmission, reception, and conversion is illustrated in Figure 5.3 (from ref. 38) with the laboratory measured efficiencies associated with each process. The complete laboratory experiment is reported by Dickinson and Brown in reference 39. This experiment is particularly important in that the capability of collecting and rectifying microwave power to usable d-c power was quantified.

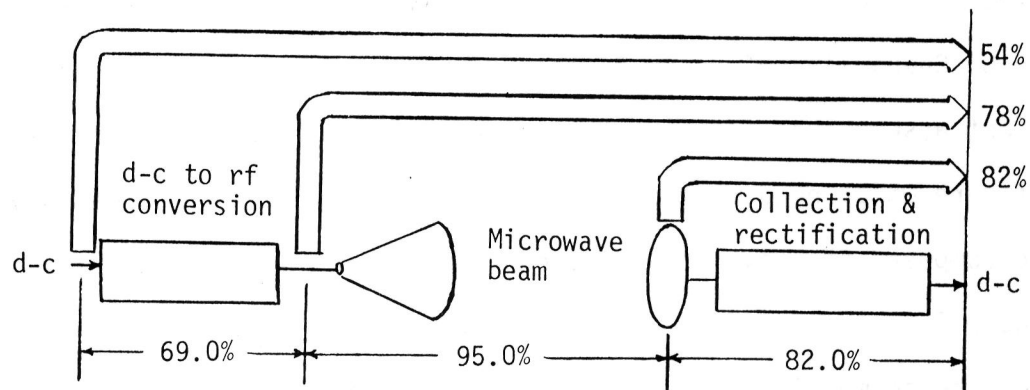


Figure 5.3 - Overall and subsystem efficiencies of a microwave power transmission system.

The process in Figure 5.3 which converts d-c power to microwave power is part of a mature technology. Radio and television stations perform this type of conversion daily. This type of power conversion is also performed in home microwave ovens. A device which performs this power conversion in the microwave oven (ref. 40, page 2.19) - a magnetron - is illustrated in Figure 5.4.

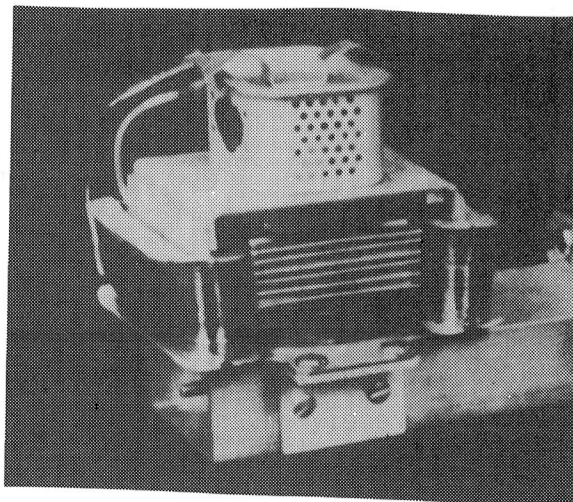
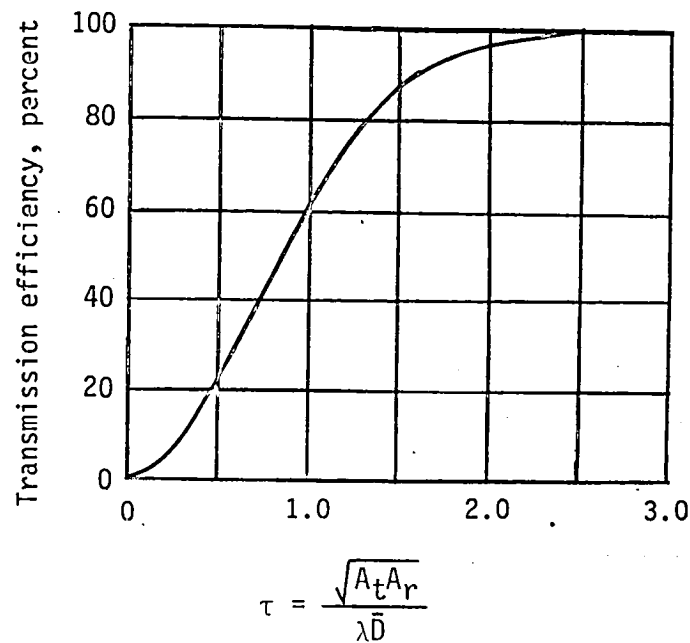


Figure 5.4 - Microwave oven magnetron.

The efficiency associated with microwave power transmission as discussed by Gaubau in reference 37 is shown in Figure 5.5. There are two important assumptions associated with the efficiency relationship in this figure which need mentioning. First, the transmitting device, which may be composed of many individual converters such as the magnetron shown in Figure 5.4 is assumed to be performing as a single transmitter. Second, the geometric shape (i.e., circle) of the transmitting surface is the same as that of the receiving surface. It should be noted that, theoretically, the wavelength of the microwaves could be made sufficiently short that the transmission losses are negligible.  $A_t$  in



where  $A_t$  = area of transmitting antenna  
 $A_r$  = area of receiving antenna  
 $\lambda$  = the wavelength of the radiation  
 $\bar{D}$  = the distance between the two antennas

Figure 5.5 - Relationship for microwave transmission efficiency.

Figure 5.5 would correspond to the surface area of the microwave power transmitting antenna shown in Figure 5.3.  $A_r$  would correspond to the surface area of the incident rectenna housed in the airplane.  $\bar{D}$  is the actual linear distance between the two rectenna (between  $A_t$  and  $A_r$ ). When the airplane is directly over the transmission station as shown in Figure 5.2,  $\bar{D}$  equals 70,000 ft. (The economics associated with the efficiency of a microwave power transmission system is discussed in Chapter 14 (pages 194-195).)

### 5.3 THE RECTENNA

The process of receiving and converting microwaves to d-c power as depicted in Figure 5.3 is performed with a collecting and rectifying device called a rectenna. The energy is collected by simple dipole antennas. Conversion to d-c power is achieved by adding a solid-state electrical circuit using rectifying diodes at each dipole. A comprehensive literature search indicates only W. C. Brown and his development team (Raytheon Company) to be actively engaged in the technical development of a rectenna to be used specifically by a HAAP.

In 1963, microwave power (about 100 watts) was successfully collected and rectified to operate a d-c motor (ref. 41, page 5). This experiment led to a demonstration for using microwave power in 1964 when a small tethered helicopter was powered by microwaves. In this demonstration (ref. 42), the 5-lb helicopter hovered 50 ft above the transmitting antenna. Usable d-c motor power was about 200 watts. In 1976, a microwave power transmission field demonstration was performed at the Goldstone Facility in the Mojave Desert (ref. 43). In this

experiment, microwave power was transmitted over a distance of about 1 mile with an average power density at the rectenna of about  $121 \text{ W/ft}^2$ . The average efficiency of the rectenna system was about 0.815, which validated the laboratory measurement of 0.82 (see Fig. 5.3). Figure 5.6 (ref. 43, page 18) illustrates the 5-in.-thick rectenna array system used at Goldstone. Figure 5.7 (ref. 41, page 18) shows an individual dipole and the associated rectifying circuit as used in the array. The rectenna dipole (Fig. 5.7) was made of aluminum. The circuit shown included a solid-state diode rectifier which was made of gallium arsenide and attached to the aluminum transmission line (gold coated at the joints) to enhance thermal conductivity. The rectenna element, as shown, weighed about 0.009 lb.

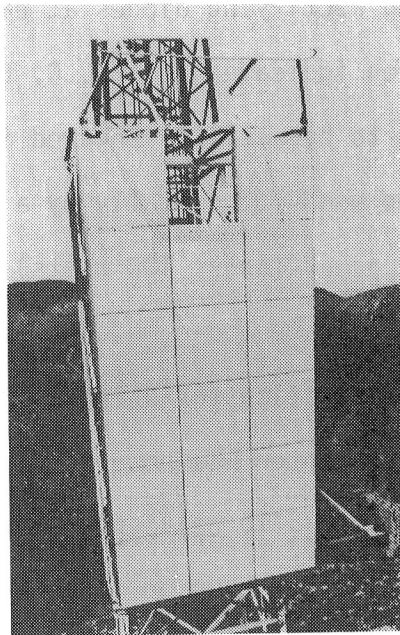


Figure 5.6 - Rectenna array used in microwave power transmission field demonstration.



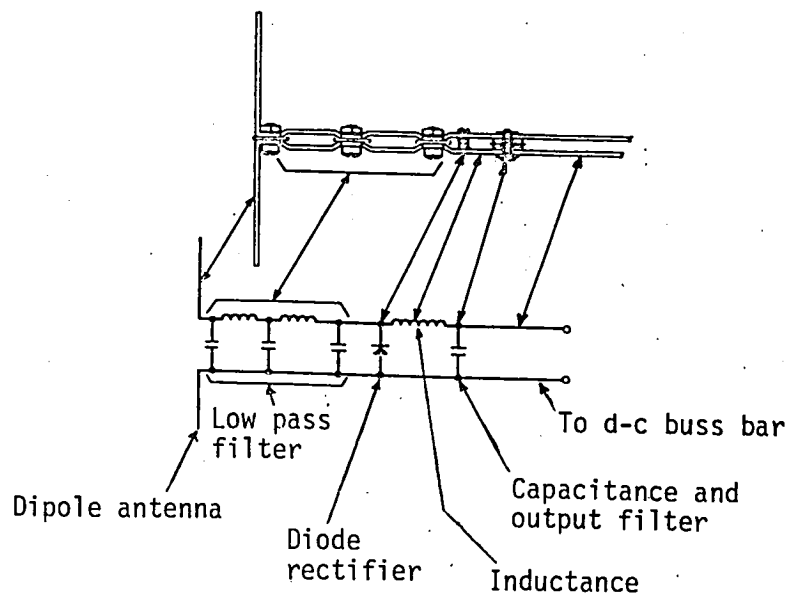


Figure 5.7 - Rectenna used in Goldstone experiment.

A thin-film rectenna specifically designed for a High-Altitude Aircraft Platform (HAAP) blimp is illustrated in Figure 5.8, and is described by Brown in reference 44. This rectenna is photoetched copper

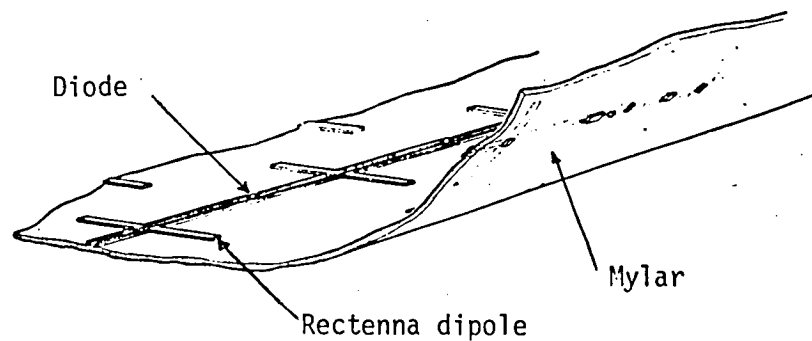


Figure 5.8 - Thin film rectenna proposed for HAAP.

on 1-mil thick Mylar. The diode heat sink uses a layer of platinum and one of gold at the copper junction point to prevent thermal damage, and performs electrically like the Goldstone diode circuit. The thin-film rectenna was designed to perform at ambient atmospheric pressure and temperature characteristic of the HAAP operational altitude (70,000 ft). Laboratory design tests were performed at an incident power density of  $16 \text{ W/ft}^2$ . The  $0.03 \text{ lb/ft}^2$  thin-film rectenna had an average conversion efficiency of 0.75.

An important note for rectenna array design is that the diodes are self-fused. If a diode should fail, only that single rectenna element becomes inoperative. This rectenna characteristic was demonstrated at Goldstone. It should also be noted that the maximum rectenna conversion efficiency is 0.50 unless it has a reflecting plane behind it (ref. 44, page 3.27). The reflecting planes used in the previously referenced rectenna experiments have been thin aluminum deposits. A metallic film about 0.08 mil thick is sufficient (ref. 44, page 3-27). In addition, experiments have indicated that a rectenna packing density of about  $19 \text{ rectenna/ft}^2$  is about optimum. All of the rectenna development work has been conducted at microwave transmission frequencies of approximately 2.45 gigahertz (0.40-ft wavelength).

#### 5.4 TECHNOLOGY STATUS

The overall technology status of microwave power transmission and reception is reflected in reference 35. However, this assessment specifically addresses a Solar Power Satellite (SPS), which has requirements different from a High-Altitude Aircraft Platform (HAAP).

A rectenna designed for HAAP application (low atmospheric density) is currently in the laboratory development stage. Mr. W. C. Brown (Raytheon Company) is conducting this development effort. The current version of the thin-film rectenna is copper imbedded in a Kapton film, instead of the Mylar film described in reference 44. Kapton's material properties are not as degradable in the HAAP environment, and it can withstand higher temperatures than Mylar. Currently, limitations on incident power density are based on acceptable diode temperatures.

Table 5.2 summarizes the current laboratory status for the thin-film HAAP rectenna.

TABLE 5.2 - TECHNOLOGY STATUS IN MICROWAVE POWER  
CONVERSION FOR HAAP DESIGN

Thin film	1-mil thick Kapton
Rectenna weight, lb/ft <sup>2</sup>	0.03
Maximum incident power:	
No convection, W/ft <sup>2</sup>	16
With convection, W/ft <sup>2</sup>	37
Conversion efficiency	0.80

Although some of the values shown in Table 5.2 appear in the literature, some that do not were personally provided by Mr. Brown and represent his latest laboratory results. The values shown for the rectenna weight do not include the reflecting plane. For HAAP blimp design, a lightweight honeycomb structure has been considered for

housing the reflector. Figure 5.9 illustrates how this structure might look. The weight associated with the additional structure is estimated to be about  $0.05 \text{ lb/ft}^2$  which would give a total HAAP blimp rectenna system weight of about  $0.08 \text{ lb/ft}^2$ .

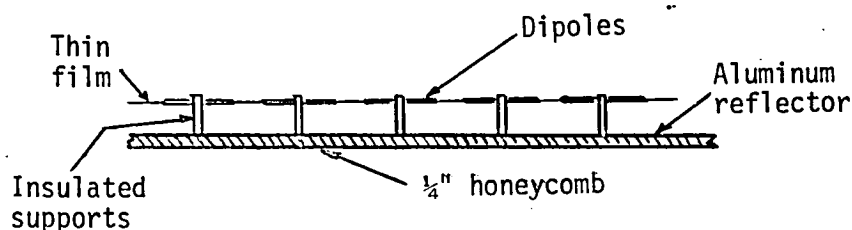


Figure 5.9 - A possible rectenna and reflecting plane structure.

For HAAP airplane application, the rectenna-reflector structure might appear the same as for a blimp; however, the "insulated support" shown in the figure could be a part of the airframe structure. An engineering estimate for a HAAP airplane reflecting plane composed of aluminum film bonded to 1/2-mil thick Kapton is  $0.01 \text{ lb/ft}^2$ , which gives a total HAAP airplane rectenna system weight of about  $0.04 \text{ lb/ft}^2$ .

In this study, the rectenna is assumed to be in contact with a surface covering on the bottom of the HAAP blimp or airplane that does not reflect microwaves, thus permitting the rectenna to receive total incident power. It is also assumed that convection of heat at the rectenna is achieved through the rectenna surface covering. Table 5.3 shows the values used for microwave power technology in this study.

TABLE 5.3 - DESIGN PARAMETERS FOR A  
MICROWAVE-POWERED HAAP

Concept	Blimp	Airplane
Maximum incident power, W/ft <sup>2</sup>	37	37
Rectenna system weight, lb/ft <sup>2</sup>	0.08	0.04
Conversion efficiency	0.80	0.80

## CHAPTER 6

### ALTERNATE POWER TECHNOLOGIES

Because solar-voltaic and microwave propulsion systems have been most frequently mentioned in the literature as applicable for a HAAP, emphasis has been placed on solar-voltaic and microwave power technologies in this study. Alternate propulsion system technologies have also been studied to determine the status of their suitability for powering a HAAP.

#### 6.1 LASER POWER TECHNOLOGY

The laser (Light Amplification by Stimulated Emission of Radiation) is an oscillator-type device that can produce a single electromagnetic frequency at high intensities. These frequencies are in the optical region and, when viewed by man, resemble a concentrated beam of light. Since its invention in 1960, the laser has found a number of applications in society. These applications include performing as a tool in medical surgery, and reading the prices of products purchased at the supermarket.

Lasers used in medical surgery are solid state lasers that emit about 50 watts of power (ref. 45). These solid state systems are low power devices, and do not appear capable of providing sufficient power for HAAP applications; therefore the remainder of this discussion will be confined to gaseous laser systems.

A survey of CO<sub>2</sub> (gas) lasers used for industrial applications was performed by Locke (ref. 46). Survey results showed that these laser

systems varied in output power from about 2 to 15 kilowatts. A gas laser system designed and built by the NASA Lewis Research Center of even higher power output (70,000 watts) is discussed in reference 47. The lasers discussed in references 46 and 47 use carbon dioxide ( $\text{CO}_2$ ) as the medium for achieving the laser power, and correspondingly, are referred to as  $\text{CO}_2$  lasers. Figure 6.1 (from ref. 47) is presented to illustrate schematically the  $\text{CO}_2$  laser system of reference 47.

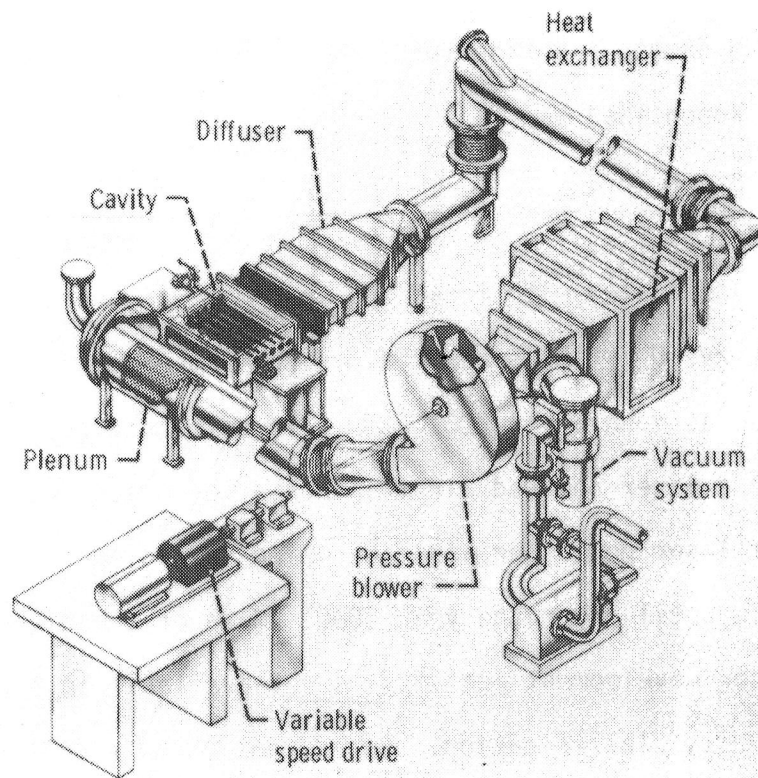


Figure 6.1 - Schematic illustration of an NASA developed high power laser.

Although  $\text{CO}_2$  laser systems are more highly developed, systems which use other gases such as carbon monoxide ( $\text{CO}$ ) also exist. Bain (ref. 48) discusses these types of lasers and their current technology status. Rudko (ref. 49) discusses recent developments to extend the wavelength

region in which lasers operate. Table 6.1 shows some types of gaseous lasers and their characteristic operating wavelengths.

TABLE 6.1 - SOME LASER WAVELENGTH CHARACTERISTICS

Laser type	Wavelength, $\mu$
Carbon dioxide (CO <sub>2</sub> )	10.6
Carbon monoxide (CO)	5.3
Hydrogen bromide (HBr)	4.2
Hydrogen fluoride (HF)	2.8
Xenon (Xe)	2.0
Argon (Ar)	1.3

The power associated with laser applications vary considerably. In medical surgery 50 watts is about a typical power level. Industrial applications use as much as 15,000 watts. In reference 50, Hertzberg, et al., discuss a laser-powered air transportation system requiring 40 megawatts of laser power per airplane using technology which would not be available until after the year 2000. Much of the high power (megawatts) laser development activity is not available in the literature because of security classification. An indication of recent developments has been made known through newspaper and television accounts of the U.S. military having demonstrated the capability of destroying flying aircraft by laser beams.

Although Bain (ref. 48, page 30) states that high power lasers (greater than 100,000 watts) operate reliably for only a few minutes,



laser reliability is not the only concern in a propulsion system. Equally important is the capability of converting laser energy to a usable energy, whether it is to propel a transport aircraft (ref. 50) or to propel a HAAP. The current technology for converting laser energy to electrical energy is discussed by Bain (ref. 48) and by Lee in reference 51.

Lee (ref. 51) discusses the historical evolution of research efforts in laser energy conversion as well as predictions for the future. He discusses energy conversion schemes such as the photovoltaic conversion of laser energy with solar cells. These cells would be optimized for wavelength compatibility with the laser beam. He also discusses heat engines which, in principle, absorb laser energy through a working medium such as helium. A thermodynamic process is used to convert the thermal energy to mechanical or electrical energy. Material properties limit the engine temperatures to less than 3100°F, and thus the efficiencies at which these engines could operate.

Both references 48 and 51 are excellent papers on laser power technology, especially the energy conversion aspect. These papers indicate no practical near-term conversion system for laser energy. Matching the wavelengths of the emitted laser energy and the wavelength to which the conversion device or fluid medium responds is crucial to the development of practical laser propulsion systems. Developed photovoltaic cells, for example, respond to wavelengths less than 1.3  $\mu$ , a value lower than the wavelengths of developed lasers, as can be seen in Table 6.1.

Because the present study is focused on near-term technologies (2 to 7 years), and laser power technology appears insufficiently developed for practical use within that period, it will not be considered further in this study.

## 6.2 NUCLEAR POWER TECHNOLOGY

In recent years, nuclear power has become an increasingly controversial societal issue; however, nuclear devices have been and continue to be contemplated for space application. In reference 32, Szego discusses space power systems and their state of the art in the early 1960's. The SNAP program (Systems for Nuclear Auxiliary Power) is thoroughly discussed. In this program, both nuclear reactor and radioisotope power systems were launched into orbit. The successfully launched SNAP 10A was the only nuclear reactor orbited; however, there have been many radioisotope thermoelectric generators (RTG's) orbited. Although these nuclear devices have been used for powering satellite payloads, the same power source could be used to power a propeller-driven high-altitude aircraft platform.

The nuclear reactor system uses a nuclear fission process to generate heat which is transferred to a working fluid in a thermodynamic process such as a Rankine or Brayton cycle. The thermal energy can be converted to electrical energy by means of a generator or a thermoelectric converter. In a radioisotope thermoelectric generator system, the heat source is the radioisotope. The heat energy is thermoelectrically converted to electrical energy by means of a differential temperature process which is, in essence, a thermocouple. The specific

characteristics of the nuclear reactor development in the SNAP program are provided by Cockeram in reference 52. Figure 6.2 provides a physical illustration of the SNAP 10A thermal nuclear reactor assembly. Table 6.2 describes the system.

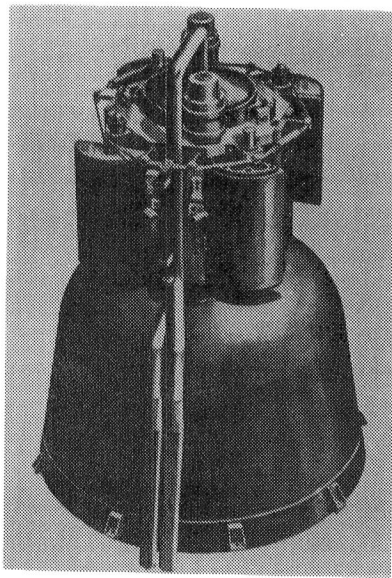


Figure 6.2 - SNAP 10A reactor shield assembly concept.

In reference 53, Schulman discusses radioisotope thermoelectric generators (RTG's) developed in the SNAP program. The SNAP 19 RTG, which was flown on the Nimbus B satellite in 1967, is shown in Figure 6.3 (from ref. 53, page 89). SNAP 19 characteristics, some of which were obtained from reference 54, are presented in Table 6.3.

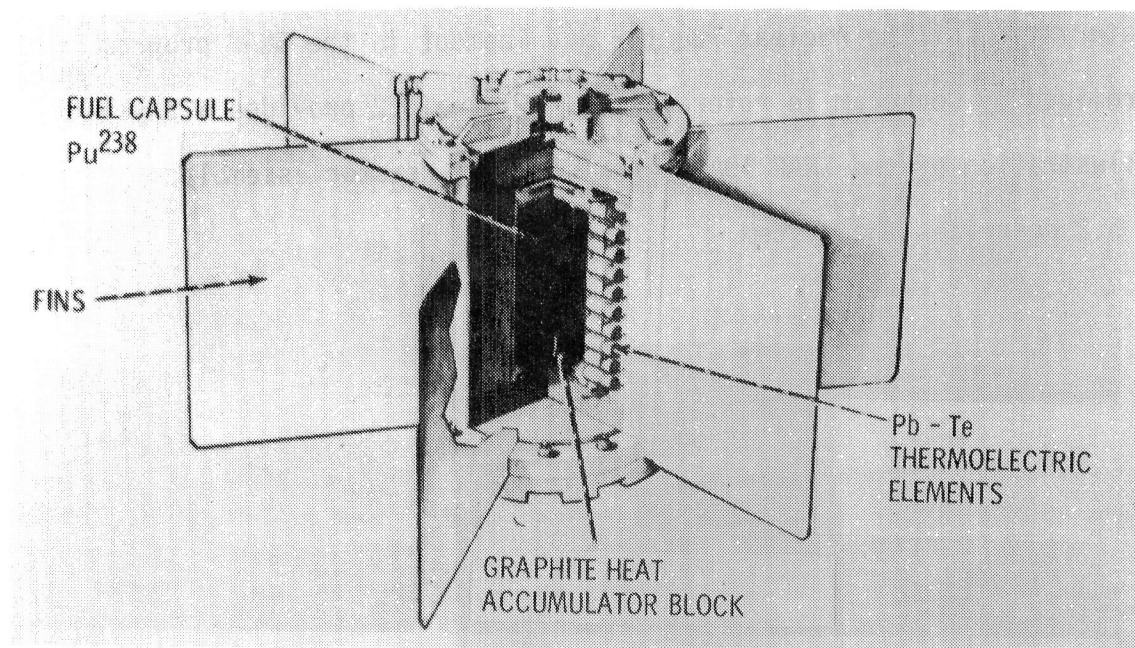


Figure 6.3 - SNAP 19 radioisotope thermoelectric generator concept.

TABLE 6.2 - SNAP 10A THERMAL NUCLEAR REACTOR CHARACTERISTICS

Thermal power, W . . . . .	35,000
Electrical power, W . . . . .	500
Power conversion efficiency . . . . .	0.014
Reactor outlet temperature, °F . . . . .	1000
Reactor diameter, ft . . . . .	1.41
Reactor weight, lb . . . . .	270
System unshielded weight, lb . . . . .	650
Total system weight, lb . . . . .	960

TABLE 6.3 - SNAP 19 RADIOISOTOPE THERMOELECTRIC  
GENERATOR (RTG) CHARACTERISTICS

Thermal power, W . . . . .	645
Electrical power, W . . . . .	30
Power conversion efficiency . . . . .	0.047
Peak temperature, °F . . . . .	980
RTG diameter, ft . . . . .	1.31
RTG height, ft . . . . .	0.92
RTG weight, lb . . . . .	30

The SNAP program was terminated about 1973, and with it the development of space nuclear reactor systems ceased (ref. 55). The revival of U.S. nuclear reactor technology for space application is being conducted by Los Alamos National Laboratory in the SPAR (Space Power Advanced Reactor) program. Discussions with Mr. David Buden, the SPAR program manager and an expert in nuclear technology, indicate that it would take about as much time, but not as much money, to recoup the technology status that existed in the SNAP program as to complete the SPAR program efforts. References 55 and 56 discuss the SPAR program and system design. The system is being designed to produce up to 100,000 watts of thermoelectrical power with an operational life of 7 years. A technology demonstration is scheduled for the 1984-85 time period. Table 6.4 provides some SPAR system design parameters.

TABLE 6.4 - SPAR NUCLEAR REACTOR SYSTEM DESIGN PARAMETERS

Thermal power, kW	110	550	1110
Electrical power, kW	10	50	100
Conversion efficiency	0.09	0.09	0.09
Reactor temperature, °F	2060	2060	2060
Reactor diameter, ft	1.71	1.71	1.71
Reactor height, ft	1.64	1.64	1.64
Reactor weight, lb	881	881	881
Shield weight, lb	562	760	837
System weight, lb	1785	2765	3911

The current status and development efforts on radioisotope thermoelectric generators (RTG's) are discussed in reference 57. According to Mullin, et al. (ref. 57), who are responsible for NASA's space power program, current RTG systems, including shielding, have a specific power of about 2.2 W/lb with a thermal power-to-electrical power conversion efficiency of about 0.06. NASA's 10-year program effort is to double RTG performance. Personal conversations with Mullin revealed that all RTG's to date have operated at less than 600 watts of electrical output. Table 6.5 summarizes RTG technology status and development plans.

TABLE 6.5 - RADIOISOTOPE THERMOELECTRIC GENERATOR

## TECHNOLOGY SUMMARY

	Current	Near-term (5 years)	Far-term (10 years)
Electrical power, W	<1000	<1500	<2000
Conversion efficiency	0.06	0.09	0.12
Specific power, W/lb	2.22	3.34	4.45

Shielding requirements for space nuclear systems are discussed by Szego (ref. 32, page 644). Shield weight is a stronger function of mission than unit power. Of course, a detailed shielding analysis is performed for each mission over a range of operating powers. In lieu of this, Szego indicates manned applications generally require 15 to 20 times the shielding required for unmanned missions. Shielding is based on a space utilization safety requirement of ". . . no undue risk to the public or the environment . . ." (ref. 56, page 15). Shielding weights associated with RTG's and shown for the SPAR system (Table 6.4) are for the unmanned environment. Crashworthiness, which would be a prime concern for HAAP operations, has not been a safety design factor. A suitable data base for the design of a crashworthy nuclear reactor system has not been developed. The launching of the SNAP 10 reactor system was conducted with the system inert; the system was activated only after orbit was achieved. RTG safety requirements are essentially the same as for the reactor; and, in reference 58 (page 18-23), Streb specifically discusses RTG safety philosophy.

The shielding weight required to provide a crashworthy nuclear-powered HAAP can significantly affect the system specific power.

Because of this weight uncertainty, nuclear propulsion for HAAP concepts will be studied parametrically by varying the system weight.

### 6.3 SOLAR-THERMAL POWER TECHNOLOGY

Solar-thermal energy systems are concerned with focusing reflected or collected solar energy onto a pipe containing a working fluid such as cesium, for example. The energy imparted to the fluid is used in a thermodynamic process such as a Rankine or Brayton cycle. The thermodynamic cycle operates a converter system which converts the thermal energy to electrical energy. Figure 6.4 schematically illustrates the solar-thermal energy system designed for a propeller-driven High-Altitude Platform (HAAP).

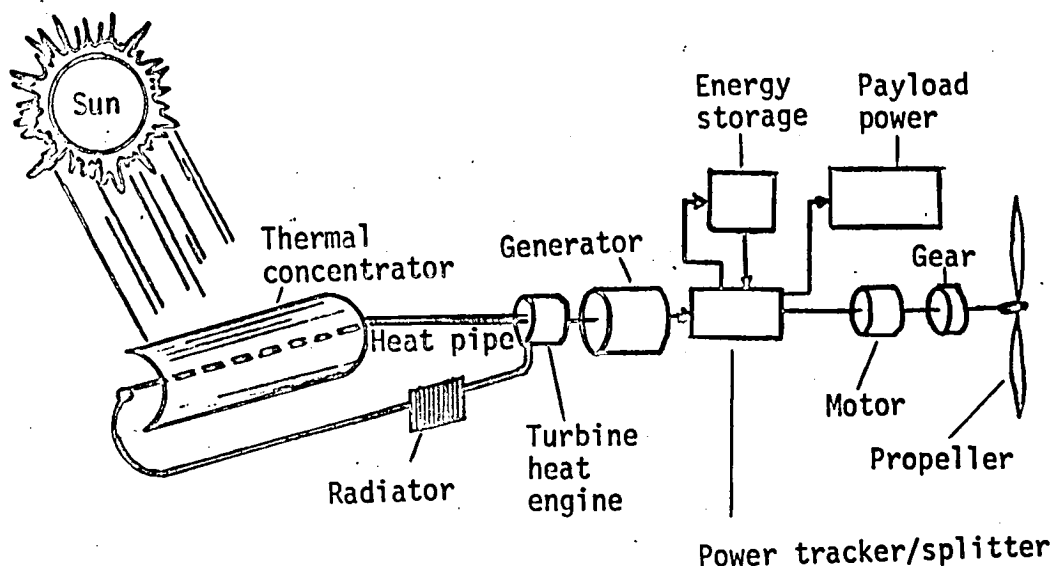


Figure 6.4 - Schematic propulsion diagram for a solar-powered HAAP.



It should be noted that the solar cell array in a solar-voltaic system is replaced by a solar-thermal system composed of a reflector (concentrator), a thermodynamic subsystem (heat pipe, heat engine, and radiator), and generator.

Two types of solar collectors or concentrators are shown in Figure 6.5 (ref. 30). These concentrators focus the Sun's energy onto a pipe which contains the working fluid.

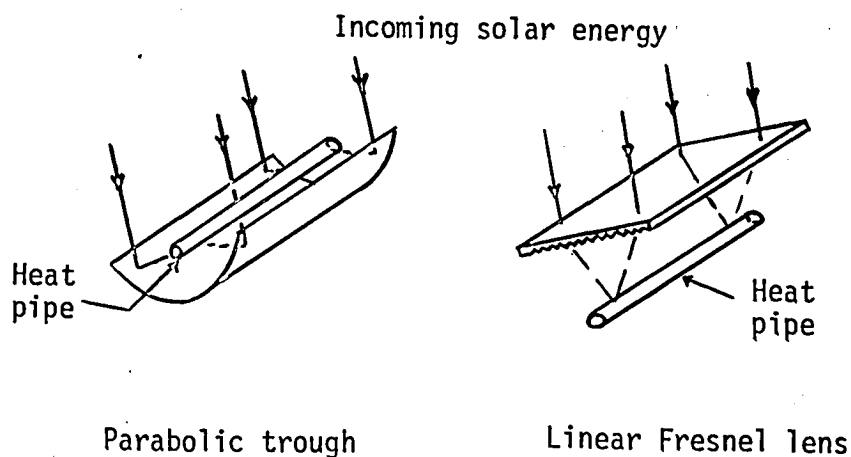


Figure 6.5 - Two types of solar concentrators (ref. 30).

In reference 19 (page 119), Javetski discusses innovative efforts to increase the efficiency of these concentrators to collect the incident solar energy and to transfer the heat energy. One effort involves using a special dye to form a sheet on the surface of the concentrator which traps the energy within the surface coating. The energy eventually "bounces" down the sheet to heat a pipe at its edge. The efficiency of concentrators to transmit energy vary with such design features as surface material and shape or type of concentrator. The optimal efficiency

in transferring solar energy incident at the concentrator surface to the fluid in the heat pipe is about 0.6 (refs. 59, page 6, and 60, page 16). The efficiency value of 0.6 includes losses associated with concentrator reflectivity, heat pipe shadowing, focusing, and heat pipe absorptivity. Although this value is based on terrestrial solar energy, it is thought to be representative of a space solar energy system. Reference 22 discusses, in detail, the entire solar-thermal energy process.

A heat pipe can be used to transport the thermal energy received from the concentrator to the electrical conversion equipment. A heat pipe is a tube with a working fluid that is vaporized in the heated end and is condensed back to a liquid at the heat extraction end. A wick in the tube wall returns the liquid by capillary action to the concentrator. Figure 6.6 illustrates a heat pipe cross section.

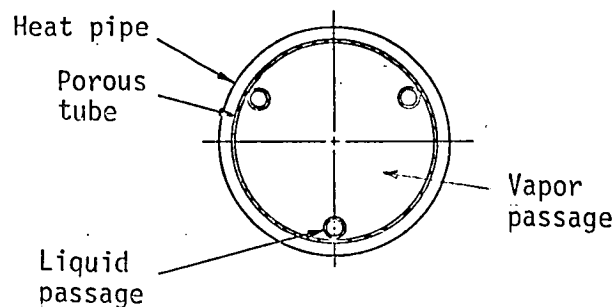


Figure 6.6 - Illustration of a heat pipe cross section.

Reference 61, the proceedings of a workshop on energy conversion, discusses the performance of thermodynamic systems in converting thermal energy to electrical energy. Reference 61 concludes that current and

near-term materials technology limits this energy conversion process to an efficiency of about 0.21.

Table 6.6 summarizes some system characteristics pertinent for HAAP design.

TABLE 6.6 - SOME SOLAR-THERMAL PROPULSION SYSTEM  
CHARACTERISTICS FOR HAAP DESIGN

Concentrator/fluid system efficiency	0.60
Thermodynamic system energy conversion efficiency	0.21
Overall system energy conversion efficiency	0.13

Although values for system weight were not readily available, inspection (see Fig. 6.4) indicates the solar-thermal system should be considerably heavier and more complex than the solar-voltaic system. From the viewpoint of total energy collected, the concentrator is four times more efficient than solar cells; however, the overall efficiency is less than that of the solar-voltaic system after the heat has been converted to a usable energy form. The overall impact on design is that the solar-thermal system requires more collector area than the solar-voltaic system for a given power requirement. Consequently, solar-voltaic systems are the currently preferred propulsion methods when using solar energy, and solar-thermal propulsion systems will not be given further consideration in this study.

## CHAPTER 7

### SELECTED FLIGHT SYSTEMS TECHNOLOGIES

#### 7.1 ENERGY STORAGE SYSTEMS

The energy storage system in a High-Altitude Aircraft Platform (HAAP) is required to provide the energy required to power the aircraft and operate the payload whenever the primary source energy is not available. In the case of a solar-powered HAAP, the stored energy would be needed at night when direct energy from the Sun is not available. In the case of microwave- and nuclear-powered systems, the stored energy could provide operational power during emergency conditions when it might become necessary to shut off the primary source power. Three energy storage systems which are discussed in the literature, batteries, fuel cells, and flywheels, will now be assessed.

##### 7.1.1 Batteries

The conventional battery is a device which contains all of its chemical reactants, and therefore all of its energy, in an electrolytic cell; that is, the chemical system is built into the cell at the time of manufacture. References 62 and 63, both proceedings of battery workshops, discuss current research and development efforts in battery technology. Ongoing developmental efforts are concerned with many chemical combinations such as Ag-H<sub>2</sub> (silver-hydrogen) and with several Li (lithium) compounds. These technology efforts focus on both primary (non-rechargeable) and secondary (rechargeable) batteries.

In addition to battery specific energy (maximum stored energy per unit weight), and overall battery efficiency (ratio of energy that the battery can deliver-to-the energy delivered to the battery), the depth of discharge is of major importance in the performance of a rechargeable battery. The depth-of-discharge is a direct measure of the amount of stored energy that can be withdrawn from the rechargeable battery without decreasing the overall efficiency. A depth-of-discharge of 0.4 and an overall efficiency of 0.8, for example, imply that 40 percent of the stored energy can undergo repetitive charge-discharge cycles while maintaining an overall efficiency of 80 percent. Should more than 40 percent of the stored energy undergo the cycles, the overall efficiency will decrease. It should be noted that for a specific battery type (i.e., nickel-cadmium battery), battery life in terms of the number of charge-discharge cycles tends to be inversely proportional to the depth-of-discharge.

Because of the long duration mission requirement for a HAAP, the energy storage system must be rechargeable. Both Ni-Cd (nickel-cadmium) and Ni-H<sub>2</sub> (nickel-hydrogen) are advanced rechargeable or secondary battery systems. Nickel-cadmium (Ni-Cd) has demonstrated its performance capability as a secondary battery during two decades of utilization on spacecraft. The Ni-Cd battery is the standard for comparison in rechargeable energy systems. Detailed Ni-Cd battery performance characteristics are discussed by Thierfelder in reference 64 and reflects current technology. Wolter, et al. (ref. 65, page 69) indicate that

Ni-Cd batteries provide about 1 kW-h/ft<sup>3</sup>. Figure 7.1 illustrates a Ni-Cd battery assembly.

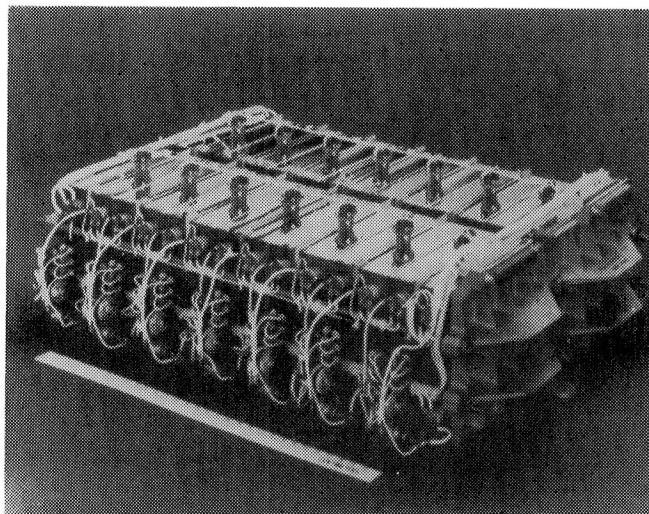


Figure 7.1 - A nickel-cadmium battery assembly.

Nickel-hydrogen (Ni-H<sub>2</sub>) batteries have been under development by the U.S. Air Force as a rechargeable battery system for about 10 years. In 1977, the U.S. Navy launched the Navigation Technology Satellite-2 (NTS-2) which used a rechargeable Ni-H<sub>2</sub> battery system. The performance of the batteries as well as a description of the system are reported in reference 66 by Stockel, Dunlop, and Betz. The unit was a 14-cell, 630-watt-hour battery system with specific energy of 15.4 W-h/lb. The system performed at an overall efficiency of about 0.69 with a depth-of-discharge of about 0.57. According to Fordyce (ref. 67, page 162), Ni-H<sub>2</sub> currently requires about 1.5 to 2.0 times the volume of an equivalent Ni-Cd battery. Figure 7.2 illustrates a Ni-H<sub>2</sub> battery system arrangement. The cells are typically about 4.5 in. in diameter.

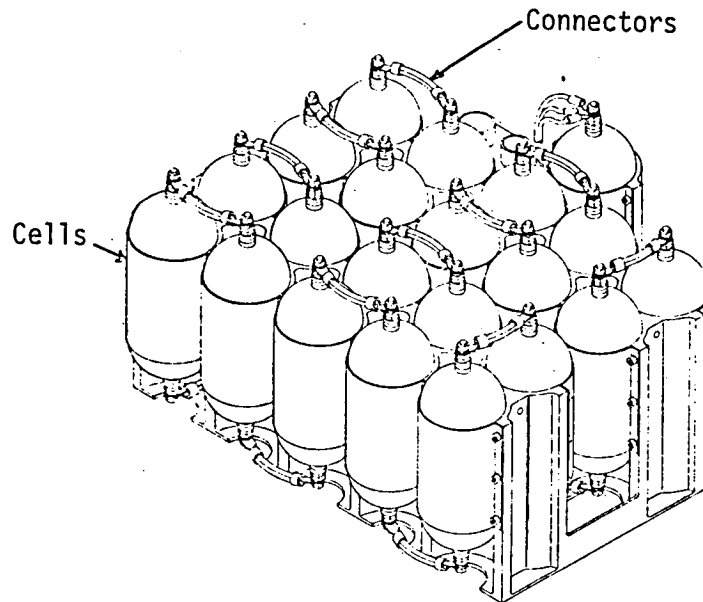


Figure 7.2 - Illustration of a nickel-hydrogen battery assembly.

Considerable effort has been made to not only characterize current and near-term battery technology for HAAP applications, but also to directly compare Ni-Cd and Ni-H<sub>2</sub> battery systems. Trout (ref. 68) provides a comprehensive assessment and performance comparison of Ni-Cd and Ni-H<sub>2</sub> battery systems as well as regenerative (rechargeable) fuel cells for 1985 applications. NASA internal correspondence on the subject, which is not generally available, has also been studied. In addition, researchers, supervisors, and managers within NASA who work in the area of battery technology have been personally consulted. Table 7.1 is a composite summary of rechargeable battery technology for HAAP application.

TABLE 7.1 - RECHARGEABLE BATTERY TECHNOLOGY STATUS  
FOR HAAP DESIGN

Type	Ni-Cd		Ni-H <sub>2</sub>	
	Current	1985	Current	1985
Stored specific energy, W-h/lb	11.0	15.0	13.0	18.0
Depth-of-discharge (6000 cycles)	.60	.65	.80	.85
Usable specific energy, W-h/lb	6.6	9.8	10.4	15.3
Overall efficiency	.80	.80	.80	.85

The values shown do not, in general, deviate significantly from those appearing in the literature. The values are representative of a 20-amp-hour battery system capable of 6000 charge-discharge cycles. It should be noted that this battery development is being driven by space application requirements. The 6000 cycles is representative of about 1 year of operation on a low-earth-orbit satellite.

#### 7.1.2 Fuel Cells

The fuel cell differs from a conventional battery in that its electrolytic cell is supplied continuously with chemicals that are stored outside the cell. The chemicals react in the cell simultaneously, but one chemical reacts at the positive electrode and another chemical at the negative electrode. Figure 7.3 illustrates simplistically, the difference in operational principles between the conventional battery cell and the fuel cell.

A fuel cell which uses hydrogen (H<sub>2</sub>) as the fuel and oxygen (O<sub>2</sub>) as the oxidizer was used as the primary source of electrical power on



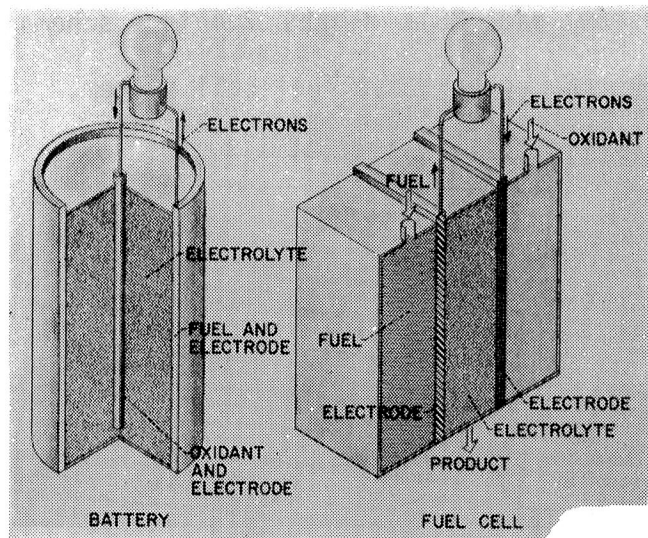


Figure 7.3 - Operational comparison of battery and fuel cell.

the Gemini and Apollo manned space programs. An  $H_2-O_2$  fuel cell system is currently being used on the Space Shuttle. Existing fuel cell systems lack the capability for being regenerated (recharged); however, there are ongoing efforts to develop a regenerative (rechargeable) fuel cell system. This regenerative system would be designed for future space missions and should also be suitable for a HAAP.

Currently, regenerative fuel cell system feasibility studies and development efforts are being conducted by NASA through its Johnson Space Center and Lewis Research Center. In reference 69, McBryar discusses the regenerative fuel cell program and results of an industry (McDonnell-Douglas Aircraft Corporation) study comparing anticipated fuel cell performance with both Ni-Cd and Ni- $H_2$  battery systems. For the mission studies, the regenerative fuel cell system weight was 25 to 50 percent lighter than the batteries. It was also determined that deep

discharge (up to 100 percent) has no adverse effect on regenerative fuel cell performance (ref. 69, page 86). Figure 7.4 is a schematic diagram of a solar-voltaic powered regenerative fuel cell system.

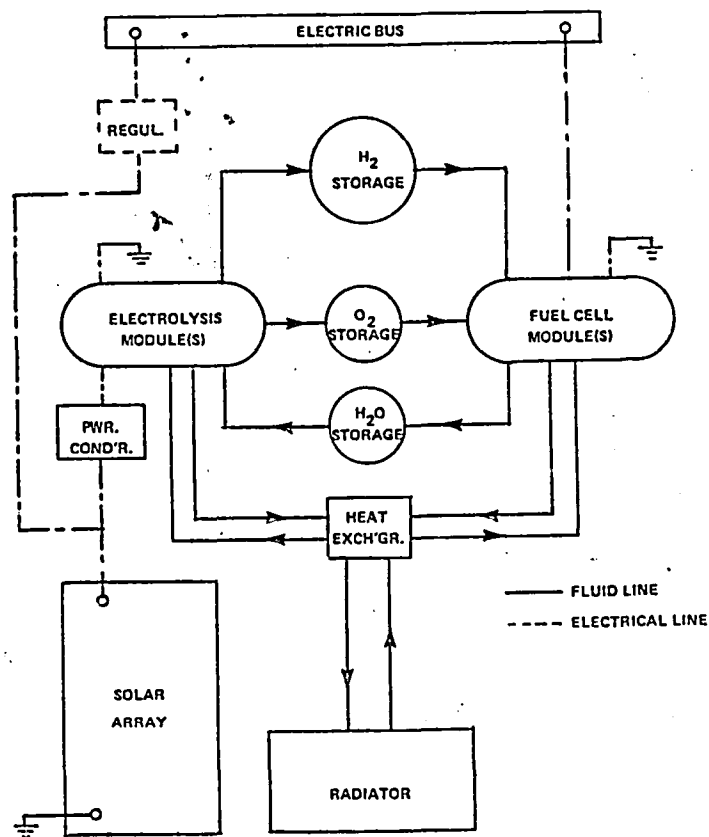


Figure 7.4 - Schematic diagram of a regenerative fuel cell system.

Other studies on regenerative fuel cells have also been performed. Trout (ref. 67) discusses fuel cell technology readiness anticipated for the year 1985. Reference 70 provides a detailed report on a study of regenerative fuel cell design conducted by the General Electric Company. These studies (refs. 67 and 70) are for systems providing power in the 35-kW to 250-kW range which may be somewhat higher than

anticipated for a HAAP airplane. In reference 71, both a 40-kW and a 10-kW regenerative fuel cell system design study prepared by B-K Dynamics, Inc., are discussed. Table 7.2 summarizes some of the regenerative fuel cell system characteristics published in the references cited.

TABLE 7.2 - SUMMARY OF SOME REGENERATIVE FUEL CELL SYSTEM STUDIES

Study	General Electric Co. (ref. 70)	B-K Dynamics, Inc. (ref. 71)		Trout (ref. 67)		
Power output, kW	100	10	40	35	100	250
Specific power, W/lb	21.5	15.1	20.0	13.8	18.7	19.1
Specific reactant rate, lb/hr/kW	.78	.78	.78	.78	.78	.78
System overall efficiency	.45	.60	.60	.50	.50	.50
Baseline technology year	1979	1982	1982	1979	1979	1979
System readiness year	1985	--	--	1985	1985	1985

When determining system specific energy, account must be made for the number of fuel cell discharging hours and the associated reactant weight. The specific reactant rate shown in the table is about 11 percent  $H_2$  and 89 percent  $O_2$ . It should be noted that the system specific energy increases with the number of discharging hours, since only the size of the various tanks in the system (which can vary in pressure from 30 to 200 psi depending on system design) must increase to accommodate a longer discharge cycle. The current status of regenerative fuel cell

technology development was obtained through personal conversations with Mr. Hoyt McBryar, project manager for regenerative cell development at the NASA Johnson Space Center. According to Mr. McBryar, both the fuel cell mode and the regenerative mode of a laboratory cell system have operated successfully in an independent mode. Efforts currently underway to integrate these two components into a system are being conducted by the General Electric Company. A system technology demonstration test is scheduled for 1986. After consultation with Mr. McBryar, the characteristics summarized in Table 7.3 are thought to be representative of 1986-87 fuel cell technology for HAAP application. The values shown are engineering estimates based on the information sources mentioned, and are of the power levels required for all of the HAAP concepts considered in this study.

TABLE 7.3 - REGENERATIVE FUEL CELL TECHNOLOGY  
STATUS FOR HAAP DESIGN

Specific power, W/lb	14.0
Specific reactant rate, lb/hr/kW	0.78
System overall efficiency	0.50
Depth-of-discharge	0.90

### 7.1.3 Flywheels

The flywheel is a mechanical device which stores kinetic or inertial energy. Its primary development thrusts have been focused on terrestrial applications such as in electric automobiles and for solar-energy homes.

In reference 72, Rabenhorst discusses, in part, a 70-passenger bus developed in Switzerland by the Oerlikon Company which operates solely by flywheel energy storage. The range of the bus is limited to one or two bus stops before recharging. According to reference 73 (page 2), the Oerlikon bus, which uses a pure flywheel system, delivers about 3 W-h/lb and recharges about every 0.25 mile.

In the United States the emphasis on using flywheels as an energy storage device for ground transportation has been in conjunction with batteries on all electric propulsion systems. In this capacity, the flywheel provides power needed for rapid acceleration at low speeds, thus decreasing the required battery size. At higher vehicle speeds, the flywheel is recharged by the battery, which is the primary energy source. Reference 74 (page 61) indicates about 15 to 20 times greater range for the hybrid (flywheel/battery) system than for the pure flywheel system.

Millner (ref. 75) discusses a flywheel energy storage system suitable for solar power system in the house. The overall efficiency (ratio of energy out-to-energy in) using 1985 technology is expected to be about 0.73. Figure 7.5 is presented to illustrate the basic components of a flywheel system. Flywheel rotors are housed in a vacuum to reduce the drag associated with the rotation speed. Rotation speeds vary from about 2,000 to over 35,000 rpm depending on the system design. The motor drives the transmission to store the mechanical energy in the rotor system. The rotors, in turn, mechanically turn a generator which

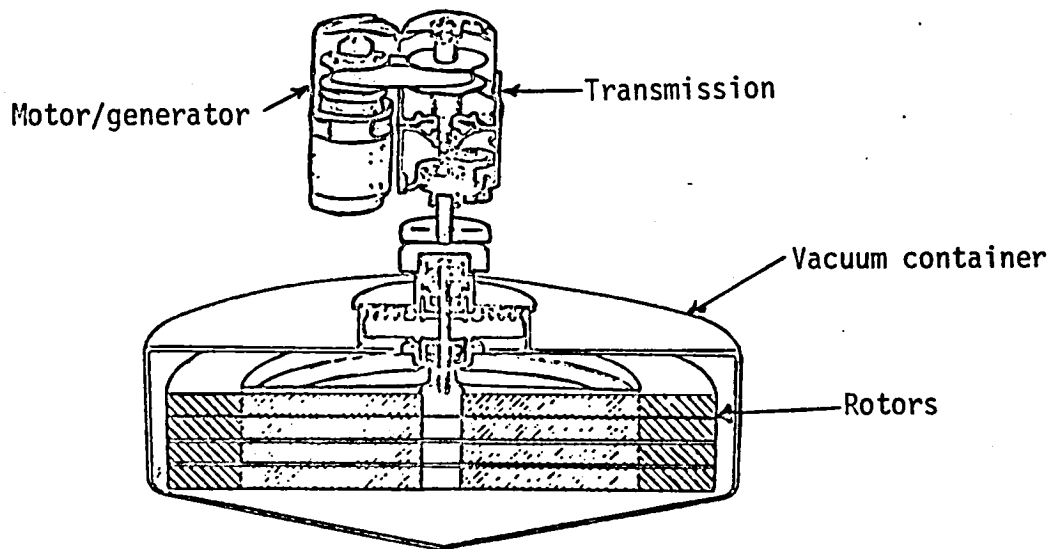


Figure 7.5 - Basic components of a flywheel energy storage system.

produces the electrical energy when needed. Electronic switching permits a single unit to operate in both motor and generator modes.

Flywheel technology applicable for space and for possible HAAP application is discussed in reference 76, which highlights some of the flywheel technology efforts at the NASA Goddard Space Center. These technology efforts attempt to use composite materials such as Kevlar to obtain much higher rotor strength-to-weight ratios than possible with metals. In addition, the use of powerful rare earth magnets in magnetic suspension systems (ref. 77) significantly reduces frictional losses in the system. These two technological advances make the flywheel potentially competitive in performance with conventional batteries. It should be noted that the use of composite rotors in flywheels for energy storage is an infant technology.

Discussions with Mr. Philip Studer of the NASA Goddard Space Center indicate a concern for system integrity when using composites or magnetic suspension. Composites such as Kevlar have "broken up" at high (greater than 10,000) rotor rpm. Since the rotor tip operates at supersonic velocities and momentum is quite high, suspension system failure could be catastrophic. These concerns are verified, in part, by flywheel experiments discussed in reference 78. These experiments are part of a current technology program to advance composite flywheel technology. Nimmer, et al. (ref. 78), conclude that composite flywheel energy density that can be expected is only about 80 percent of the predicted values. The failure criterion is based on fiber breakage at the center of the rotor disc.

Discussions with Mr. Claude Keckler of the NASA Langley Research Center have been most informative on flywheel energy storage devices. A 1.5-kW-h flywheel with a solid titanium rotor (ref. 79) that was designed and constructed by Rockwell International is located at NASA Langley. Unpublished experiments have confirmed the system design. This system uses roller bearing suspension and the rotor shape is designed for constant stress.

Table 7.4 compares the titanium flywheel system characteristics (ref. 79) with those anticipated for a space quality composite flywheel system. The value shown for efficiency excludes the losses associated with power conditioning (i.e., losses external to the flywheel assembly).

An engineering estimate has been made for a composite flywheel system, since the source reference (ref. 78) based its performance value on rotor-alone weight.

TABLE 7.4 - FLYWHEEL ENERGY STORAGE TECHNOLOGY FOR HAAP DESIGN

Rotor type	Titanium	Composite (Kevlar)		
		Rotor	Advanced rotor	Advanced system (estimate)
Rated power, kW	2.5	-	-	2.5
Stored energy, kW-h	1.5	-	1.0	1.0
Depth-of-discharge	0.75	-	-	0.75
Usable energy, kW-h	1.1	-	-	0.75
Efficiency	0.87	-	-	0.90
Rotor speed, rpm	35,000	31,000	37,000	37,000
Rotor diameter, ft	0.75	1.5	1.5	1.5
System weight, lb	170	-	-	70
Usable specific energy, W-h/lb	6.5	18	30	10.7
Technology readiness year	Now	Now	1982	1985

#### 7.1.4 Summary

Table 7.1 shows that, on a basis of usable specific energy, the Ni-H<sub>2</sub> battery is more suitable than a Ni-Cd battery for HAAP vehicles using 1985 technology. Table 7.4 lists flywheel characteristics which show that the battery is a more desirable energy storage candidate than the titanium flywheel. The Ni-H<sub>2</sub> battery is preferable to the 1985-technology



version of a composite flywheel. However, it appears that as composite flywheel technology matures, it could surpass the battery as an energy storage device.

Determining whether the battery is more or less desirable than the regenerative fuel cell (Table 7.3) is not straightforward, since the specific energy of the fuel cell increases with the number of hours the cell must operate. The weight associated with the increase in operating hours is small; only that for the additional reactants and slightly larger storage tanks.

Table 7.5 summarizes usable specific energy, which is used as a performance parameter for the various storage devices using 1985-86 technology.

TABLE 7.5 - SUMMARY OF ENERGY STORAGE CAPABILITY  
FOR HAAP DESIGN

	Regenerative fuel cell	Ni-H <sub>2</sub> battery	Composite flywheel
Usable specific energy, W-h/lb	Discharge time		
	1-hr 12.5	15.3	10.7
	1.2-hr 14.9		
	2-hr 24.7		
	4-hr 48.3		
	8-hr 92.7		
	12-hr 133.7		
	16-hr 171.6		
Efficiency	0.50	0.85	0.90

As can be seen in Table 7.5, the battery is preferred over the flywheel at all times, and over the fuel cell if energy storage is required for 1.2 hours or less. The fuel cell becomes increasingly preferable to the battery for hours of operation greater than 1.2.

## 7.2 ELECTRIC MOTORS

An electric motor(s) would be used to turn the propeller(s) of the HAAP. The use of "rare earth" magnets in motors designed for aerospace application is discussed in reference 80. These motors employ electronic, instead of mechanical, commutation which eliminates the associated electromagnetic interference. According to Klass (ref. 80), when compared to conventional motors the rare earth magnet motors have better response time, are more efficient, and have greater reliability. The rare earth magnets, especially samarium cobalt, are being used on-board aircraft in alternators, accelerometers, and electric motors.

The design of a samarium cobalt d-c motor is discussed by Sawyer and Edge in reference 81. This specific motor was designed for the electromechanical actuator on the Space Shuttle Orbiter elevon. The motor develops about 12,900 W (17.1 hp) at 9,000 rpm, weighs 17.16 lb, is 0.94 ft long, and has an operating efficiency of about 0.95. Figure 7.6 illustrates this complete motor assembly.

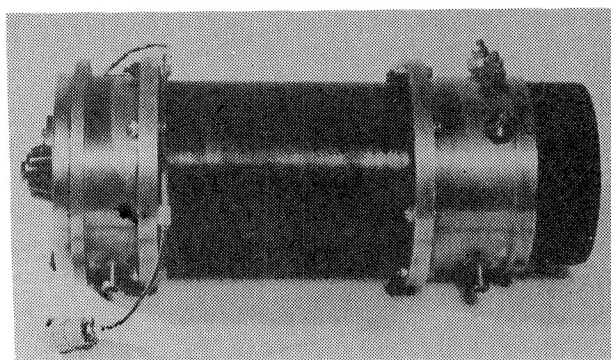


Figure 7.6 - Complete samarium-cobalt magnet motor assembly.

Additional experiments on rare earth magnet motor performance are discussed by Maslowski (ref. 82). Tests were performed on samarium cobalt and strontium ferrite motors at rotor speeds up to 26,000 rpm. Both types of motors consistently performed at efficiencies greater than 0.93, while delivering up to 26 kW (35 hp) of power. In some instances, where the rpm was greater than 22,000 for maximum power, a cooling fan weighing about 6 lb was used.

A gear or gearing system of some design would be used to connect the motor with a propeller. According to Anderson and Loewenthal (ref. 83, page 5) a well-designed gear will have an operating efficiency of at least 0.98. Information on gear weight design for small (less than 375 kW (500 hp)) gears was not readily available. References 84 and 85 provide a methodology for the detailed design of gear boxes, including weight. Reference 85 indicates that operational reduction gear efficiencies in excess of 0.99 are not uncommon. In lieu of a detailed analysis for gear weight, a crude gear weight approximation method was used.

Mr. Robert Boucher (Astroflight, Inc.) designed the motor and gear box for the Solar Challenger, which is thought to be in the general class of a propulsion requirement as a HAAP. Boucher's 27:1 reduction gear weighed 1.5 lb for a maximum motor power of 4.1 kW (5.5 hp). The linear approximation relationship shown (eq. (7.1)) is thought to be valid in this power regime; that is

$$\text{Gear weight (lb)} = 0.3 \times \text{maximum motor horsepower} \quad (7.1)$$

This crude method is within 0.3 lb of Boucher's gear design and within 15 percent of the detailed gear design for a 4500-hp motor discussed in reference 85.

Table 7.6 summarizes the motor and reduction gear characteristics for HAAP design.

TABLE 7.6 - MOTOR AND GEAR-BOX TECHNOLOGY  
FOR HAAP DESIGN

<u>Motor</u>	
Type	Samarium cobalt d-c brushless
Specific power, W/lb	746
Efficiency	0.95
<u>Gear</u>	
Type	Reduction
Specific power, W/lb	2461
Efficiency	0.99
<u>System</u>	
Specific power, W/lb	573
Efficiency	0.94

The values presented in Table 7.6 represent currently available technology. Significant near-term improvements in motor and gear-box technology appear unlikely.

### 7.3 POWER PROCESSING

Power conditioning, controlling, and processing are all synonymous terms which are used to categorize the overall electronics needed to

support and integrate the various systems (i.e., solar array, batteries) required for the flight vehicle. Power processing includes devices such as fuses, switches, circuit breakers, inverters, and transformers which are used in managing the vehicle power system. Although a detailed system design is required for precise weight values for the power conditioning system, it is customary to estimate this weight based on the total amount of power to be managed. In reference 86 Slifer and Billenbeck provide a detailed discussion on space quality power processing technology. They assess current (1978) power conditioning technology at about 23 W/lb. However, a group of energy conversion experts conclude in reference 61 (page 80) that current (1980) power processing technology is ". . . on the order of . . ." 45 W/lb. In 1977, Goldsmith and Reppucci (ref. 87) projected 1980 power control technology to be about 49 W/lb. In 1976, a demonstration by Schwarz (ref. 88) indicated that advanced power processing techniques using available technology could give values of about 55 W/lb. The efficiency of the power processing system is nominally about 0.90.

In this study, the weight for power processing equipment is not only applied to the payload, but to other power needs. The weight for such items as wiring and regulators for propulsion power has been determined by using non-referenceable information characteristic of power distribution equipment for advanced military aircraft. Table 7.7 summarizes power processing technology thought to be applicable for this study.

TABLE 7.7 - SUMMARY OF POWER PROCESSING TECHNOLOGY  
FOR HAAP DESIGN

	Current	1985-86
Payload specific power, W/lb	45	54
Propulsion specific power, W/lb	225	250
Efficiency	0.90	0.92

## CHAPTER 8

### AERODYNAMIC CONSIDERATIONS

#### 8.1 BLIMP

Conventional blimps develop their lift in accordance with equation (8.1)

$$L = V \left( \rho_a - m \frac{P_a}{RT_a c} \right) g + L_d \quad (8.1)$$

where

L	total lift (lb)
V	blimp volume displacement (ft <sup>3</sup> )
$\rho_a$	ambient density (slugs/ft <sup>3</sup> )
m	molecular weight of lifting gas (gm/mole)
$P_a$	ambient pressure (lb/ft <sup>2</sup> )
R	universal gas constant (ft-lb/°K-mole)
$T_a$	ambient temperature (°K)
g	gravitational acceleration (ft/s <sup>2</sup> )
c	conversion constant (gm/slug)
$L_d$	dynamic lift (lb)

In this study, the blimp is assumed to be a sealed, constant volume, "superpressured" vehicle. The blimp becomes fully inflated during ascent and reaches its equilibrium altitude having a superpressured envelope. The superpressure varies with the internal gas temperature of the blimp. There is no gas bleed-off or replenishment during the day-night temperature cycle. The minimum superpressure,  $\Delta P_{\min}$ , normally occurs at night when the blimp temperature is approximately equal to the ambient. The

magnitude of  $\Delta P_{\min}$  must be sufficient to prevent structural buckling of the blimp envelope (ref. 89, page 65). The maximum superpressure,  $\Delta P_{\max}$ , depends on the ratio of maximum temperature to minimum temperature. This superpressure relationship is expressed in equation (8.2).

$$\frac{P_a + \Delta P_{\min}}{T_{\min}} = \frac{P_a + \Delta P_{\max}}{T_{\max}} \quad (8.2)$$

where

$\Delta P_{\min}$       minimum superpressure  
 $\Delta P_{\max}$       maximum superpressure  
 $T_{\min}$         minimum blimp temperature  
 $T_{\max}$         maximum blimp temperature

But  $T_{\min} \approx T_a$ , and equation (8.1) becomes equation (8.3) for a superpressured blimp.

$$L = V \left( \rho_a - m \frac{P_a + \Delta P_{\min}}{RT_a c} \right) g + L_d \quad (8.3)$$

The mass of the displaced air is  $V\rho_a$ , and the mass of the lifting gas is  $V m \frac{P_a + \Delta P_{\min}}{RT_a c}$ . Since the volume is constant, only pressure changes with  $T$ ; thus,  $L = \text{Constant}$ . In reference 90, Lagerquist and Kean discuss the structural design of a superpressured HAAP. According to reference 90 (page 5) the value of  $\Delta P_{\min}$  is about  $5.2 \text{ lb/ft}^2$  and the value of  $\Delta P_{\max}$  is about  $31.3 \text{ lb/ft}^2$ .

If heat were added to the lifting gas by channelling heat from the operation of equipment such as a fuel cell, a superheat term,  $\Delta T$ , would be incorporated in equation (8.3) to yield equation (8.4).



$$L = V \left[ \rho_a - m \frac{P_a + \Delta P_{min}}{R(T_a + \Delta T)c} \right] g + L_d \quad (8.4)$$

where  $\Delta T$  = superheat.

Dynamic lift,  $L_d$ , is developed by the blimp moving at angles of attack and is used to counteract temperature-induced lift changes associated with conventional (non-superpressured) blimps. A detailed mathematical formulation is provided by Azuma for both superheat (ref. 91, page 467) and dynamic lift (ref. 91, page 469) effects. Layton (ref. 92) provides some dynamic lift and drag coefficient relationships empirically determined from conventional blimp concepts. Theoretically, the superpressured blimp operates at a constant altitude using only its static lift. In practice, it tends to seek a region of constant ambient density which has some altitude variation with time. Because the superpressured blimp considered herein would use little, if any, dynamic lift during normal operations, dynamic lift will be neglected in the present study.

The drag coefficient associated with blimps is expressed as

$$C_D = C_{D,S} + \frac{S C_{L_d}^2}{\pi A V^{2/3}} \quad (8.5)$$

where

- $C_D$         total drag coefficient
- $C_{D,S}$      static lift drag coefficient
- $S$          blimp planform area (ft<sup>2</sup>)

$C_{L_d}$	dynamic lift coefficient (based on planform area)
A	aspect ratio
V	volume (ft <sup>3</sup> )

Since the superpressured blimp in this study does not use dynamic lift,  $C_{L_d} = 0$  and equation (8.5) reduces to  $C_D = C_{D,S}$ . For a blimp, the drag coefficient is generally expressed in terms of  $v^{2/3}$ ; thus, the drag is

$$D = \frac{1}{2} C_D \rho_a v^2 v^{2/3} \quad (8.6)$$

where  $v$  = airspeed (ft/s). The value of the blimp drag coefficient is of particular concern since estimated values for HAAP blimp concepts vary considerably. Table 8.1 summarizes some of the blimp characteristics from other HAAP studies.

The HAAP blimp vehicles characterized in Table 8.1 are of different propulsion classes. The Sinko (ref. 2) and Kuhn (ref. 93) studies were based on a criteria for long-duration (continuous) flight. Sinko assumed microwave power to meet all propulsion needs and a battery to power the payload. Kuhn assumed a solar-voltaic/regenerative fuel cell system to meet all power requirements. Beemer, et al. (ref. 89), provided for a high-altitude mission, but for short durations. They considered a fuel cell for all power requirements which limited the flight duration to only 7 days. Petrone and Wessel (ref. 94) considered a solar-voltaic and fuel-cell system to provide up to 30 days of flight operation.

TABLE 3.1 - SUMMARY OF CHARACTERISTICS FROM VARIOUS  
HAAP BLIMP CONCEPT STUDIES

Study	Sinko (ref. 2)	Sinko (ref. 2)	Kuhn (ref. 93)	Kuhn (ref. 93)	Beemer, et al. (ref. 89)	Petrone, et al. (ref. 94)
Primary propulsion	Microwave	Microwave	Solar-fuel cell	Solar-fuel cell	Solar-fuel cell	Solar-fuel cell
$C_D$ (operating)	0.050	0.050	0.050	0.050	0.050	0.036
Airspeed, ft/s	-	-	65.6	98.4	26.9	33.8
Altitude, ft	70,000	70,000	69,000	69,000	69,000	70,000
Payload, lb	1587	287	220	220	220	-
Structural weight fraction	0.33	0.36	0.41	0.28	-	0.33
Total weight, lb	4801	1857	2311	19,472	4081	
Volume $\times 10^{-3}$ , ft <sup>3</sup>	1300	500	491	4142	1034	800
Length, ft	-	-	289	589	371	333
Fineness ratio			5	5	5	5
Kinematic viscosity $\times 10^4$ , ft <sup>2</sup> /sec	21.56	21.56	20.39	20.39	20.39	21.56

Table 8.1 shows that the values for  $C_D$  are at least 0.050 with the exception of the Petrone and Wessel study (ref. 94). Although reference 94 uses a  $C_D$  of 0.036, concern was expressed that  $C_D$  might be as much as 50 percent higher (ref. 94, page 2). Goldschmied (ref. 95) discusses an optimal high-altitude blimp hull design with extensive regions of laminar flow. Reference 95 concludes that a  $C_D$  of 0.018 for a fineness ratio 3 concept is obtainable. Warner and Haigh (ref. 96) also discuss applying laminar flow control by body shaping the blimp. Reference 96 (page 21) indicates that at altitudes of 55,000 ft and an airspeed of 135 ft/s,  $C_D$  can be as low as 0.008 to as high as 0.022, depending on the relative lengths of laminar and turbulent flows.

After reviewing many publications on blimp and body drag, for this study, a drag coefficient of 0.035 was chosen as representative of 1985 technology in blimp aerodynamics. A body fineness ratio of 5 is also assumed. Helium will be considered as the lifting gas. Although hydrogen can provide more lift, it is not considered because of its extreme flammability. The gas composition is 95 percent pure helium and 5 percent air. No superheat,  $\Delta T$  in equation (8.4), is considered for the baseline concept.

## 8.2 AIRPLANE

The airplane develops its lift dynamically, by air flowing over the wing. The relationship for the lift is expressed in equation (8.7).

$$L = \frac{1}{2} C_L \rho_a v^2 S_{ref} \quad (8.7)$$

where

$L$	lift (lb)
$C_L$	wing lift coefficient
$v$	airspeed (ft/s)
$\rho_a$	ambient density (slugs/ft <sup>3</sup> )
$S_{ref}$	wing reference (planform) area (ft <sup>2</sup> )

Equations (8.8) and (8.9) define the relationships for drag and drag coefficient.

$$D = \frac{1}{2} C_D \rho_a v^2 S_{ref} \quad (8.8)$$

$$C_D = C_{D,0} + \frac{C_L^2}{\pi e A} \quad (8.9)$$

where

$D$	drag (lb)
$C_D$	total drag coefficient
$C_{D,0}$	profile drag coefficient
$A$	wing aspect ratio
$e$	Oswald airplane efficiency factor

Table 8.2 summarizes some of the characteristics of HAAP airplane concepts from various other studies. The solar-powered concept study by Phillips (ref. 7) considered airplanes with aspect ratios of 35 and 20 which operated at  $L/D$ 's of 37.5 and 19.7, respectively. The higher aspect ratio aircraft takes advantage of the correspondingly lower induced drag coefficient indicated by equation (8.9). The Parry study (ref. 6) of a solar-powered HAAP was performed for flight at an altitude

TABLE 8.2 - SUMMARY OF CHARACTERISTICS FROM VARIOUS  
HAAP AIRPLANE CONCEPT STUDIES

	Solar-powered			Microwave-powered		
	Phillips (ref. 7)	Phillips (ref. 7)	Parry (ref. 6)	Sinko (ref. 2)	Sinko (ref. 2)	Heyson (ref. 8)
$C_L$ (operating)	1.50	1.50	1.50	0.93	1.00	0.90
$C_D$ (operating)	0.040	0.076	0.058	0.058	0.065	0.020
L/D (operating)	37.5	19.7	26.1	16.0	15.4	45
Airspeed, ft/s	59-112	59-112	100	131	197	216
Altitude, ft	65,600	65,600	100,000	70,000	70,000	Varies
Kinematic viscosity $\times 10^4$ , ft <sup>2</sup> /s	17.212	17.212	95.490	21.561	21.561	Varies
Payload, lb	-	-	100	287	1587	1100
Wing loading, lb/ft <sup>2</sup>	0.42	0.42	0.25	0.90	2.78	2.92
Aspect ratio	35	20	20	6	6	30
Wing span, ft	159.4	91.9	280	98	98	190
Wing chord, ft	4.56	4.54	14	16.3	16.3	6.3
Wing chord Reynolds number $\times 10^{-6}$	0.16-0.30	0.16-0.30	0.15	1.00	1.50	0.78

somewhat higher than currently considered. However, the aspect ratio 20 concept with an operating lift coefficient of 1.5 used by Parry was the same as that used by Phillips.

The microwave-powered concept study performed by Sinko (ref. 2) considered airplanes with different payloads. His operational lift coefficients are comparable with that used by Heyson (ref. 8) in his study, but the aspect ratios of the aircraft in the two studies vary considerably. It should be noted that the Heyson study was based on a linear flight profile which used powered and glide phases between a series of microwave power transmitting stations. However, the characteristics presented in Table 8.2 for that study are thought to be representative of those for the aircraft in powered level or circling flight.

Table 8.2 indicates that the lift coefficient of 1.5 needed by the solar-powered aircraft must be achieved at a Reynolds number between 0.1 and 0.3 million. The Reynolds number is of concern because it has a major influence on airfoil lift and drag characteristics. The influence of Reynolds number becomes increasingly critical as it decreases to or less than about 0.5 million. At these low values, the airflow often separates and reattaches to the airfoil; a phenomenon sometimes called a "separation bubble." In reference 97, Mueller and Batill discuss this aerodynamic behavior and present some photographs which vividly show the "bubble" as it occurred during wind-tunnel tests. Figure 8.1 (from ref. 97) illustrates the "laminar separation bubble."

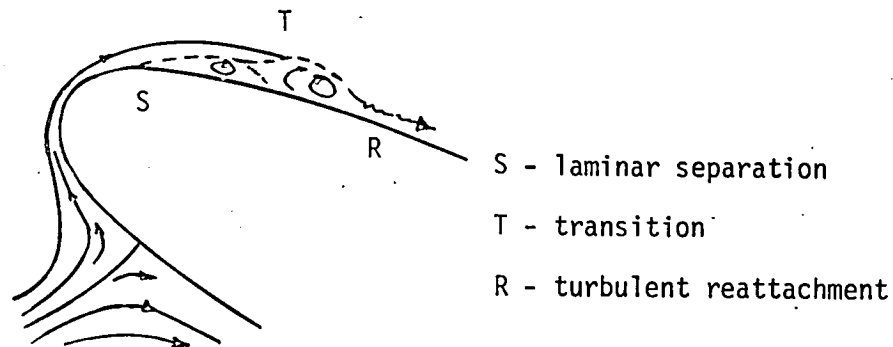


Figure 8.1 - Illustration of airflow separation and reattachment on an airfoil.

An extreme, but not uncommon, example of airfoil separation and reattachment on the airfoil lift and drag coefficient characteristics is shown in Figure 8.2.

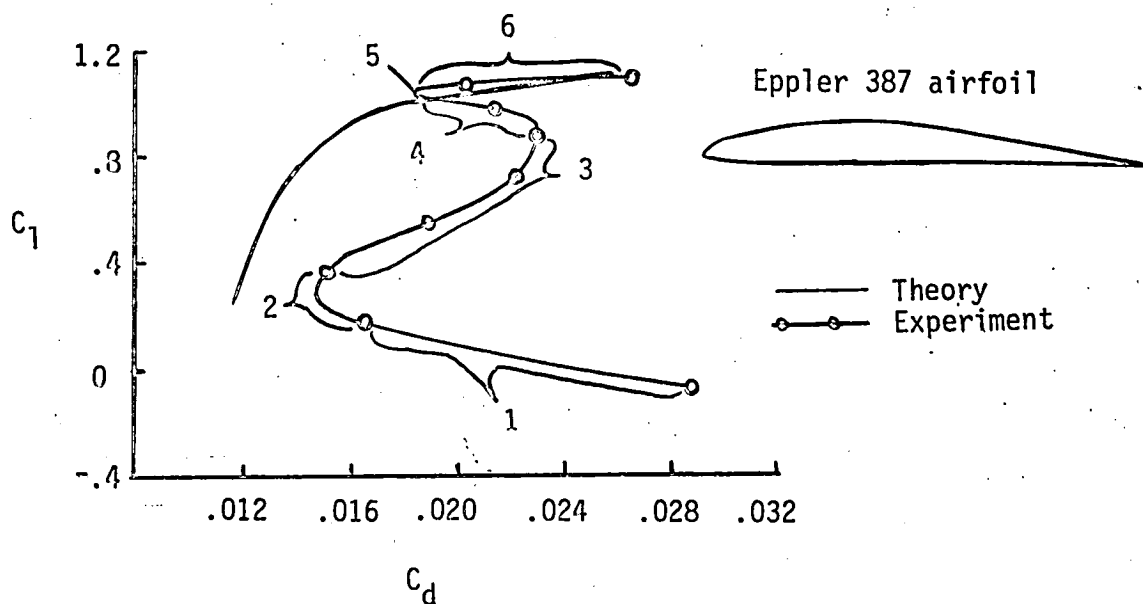


Figure 8.2 - Comparison of theoretical and experimental results on an airfoil at 0.1 million Reynolds number.



Figure 8.2 compares theoretical and experimental data on the Eppler 387 airfoil at a Reynolds number of 0.1 million. The theoretical predictions were obtained using the computer code of Eppler and Somers (ref. 98). As shown in the figure, there are significant differences between the experimental and theoretical behavior for the airfoil. A possible explanation for the experimental behavior is given by the following sequence of airflow characteristics identifiable with Figure 8.2:

1. Separation on lower surface
2. "Bubble" on lower surface
3. "Bubble" on upper and lower surfaces
4. Lower surface reattachment
5. Attached flow on upper and lower surfaces
6. Upper surface separation

The Eppler design and prediction code, which is thought to be representative of the state of the art for low-speed airfoils, contains only an attached boundary-layer code. It can estimate the start of separation, but it cannot predict reattachment to form a bubble. Regardless of whether or not the flow reattaches to form a bubble, the code is inadequate to compute the performance accurately once separation has occurred. Although the specific comparison presented in Figure 8.2 is not in a referenceable report, Patrick (ref. 99) reports similar behavior of the same airfoil with experimental data obtained from both Delft (Netherlands) and Cranfield (United Kingdom) Universities.

It is because of the degradation in airfoil performance generally associated with the low Reynolds numbers at which the solar-powered

HAAP airplane, in particular, would operate (see Table 8.2) that airfoil selection is of concern. A review of airfoil characteristics in reference 100 (Abbott and von Doenhoff), reference 101 (Riegels), and reference 102 (Althaus and Wortmann) indicates only a few airfoils with the potential for obtaining a  $C_l$  of 1.5 in the 0.1 to 0.3 million Reynolds number regime apparently needed for a solar-powered HAAP. One older airfoil that exhibits unusually high  $C_l$ 's at low Reynolds numbers is the Göttingen 227 (ref. 101, page 239).

Efforts to develop high lift, low drag airfoils at low Reynolds numbers of interest to HAAP have been pursued by Dr. Robert Liebeck at the McDonnell-Douglas Corporation. The Liebeck airfoil design method attempts to avoid flow separation on the airfoil along the entire pressure recovery region. The airfoil is designed for extensive regions of laminar flow on the upper surface. Immediately prior to laminar separation, airfoil contouring is used to deliberately trip the laminar boundary layer to turbulent. An attempt is made to maintain attached flow to the trailing edge by designing the turbulent boundary layer to flow against the maximum pressure gradient it can tolerate without separation (a Stratford recovery (ref. 103)). Liebeck discusses his design philosophy in detail in reference 104, and also presents some experimental results.

Figure 8.3 compares the characteristics of the Göttingen 227 and two Liebeck airfoils, the LA 2566 and the L 1003M. These airfoils were tested at Reynolds numbers ( $R_n$ ) of 0.1, 0.25 (design condition), and 1.0 (design condition) million, respectively.

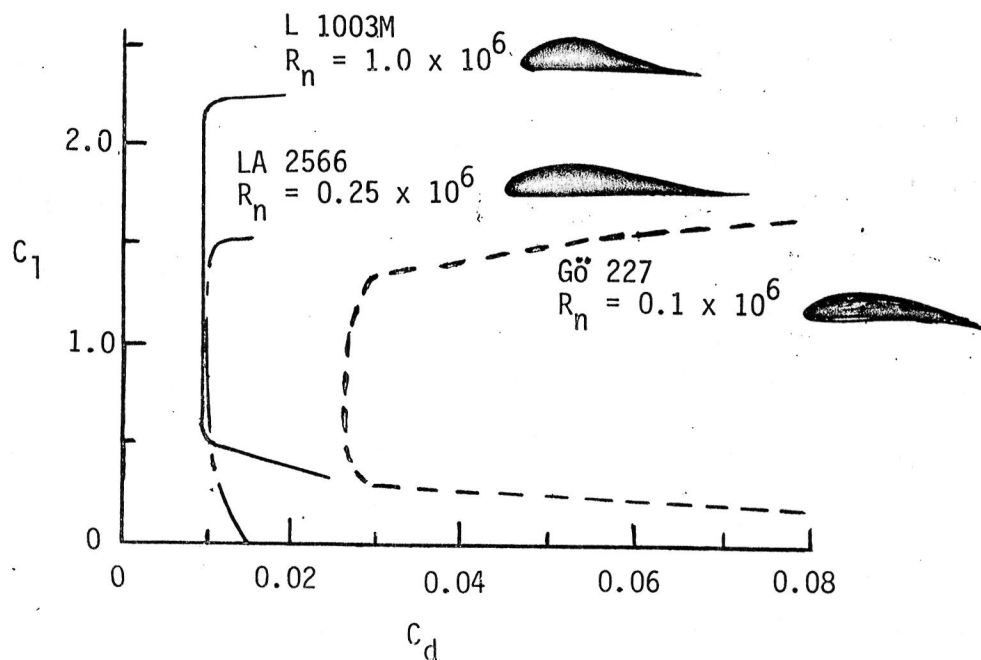


Figure 8.3 - Comparison of three airfoils having high lift at low Reynolds number.

The three airfoils have significantly different camber lines and thickness forms. The general character of the data is similar for all three airfoils; however, the actual  $C_d$  and  $C_l$  levels differ considerably. (Tests performed on the L 1003M airfoil with a negative flap deflection extended the low-drag range to  $C_l = 0$ .) A portion of these differences may be due to the  $R_n$  of the tests, but insufficient data exist to separate the effects due to  $R_n$  and those due to shape. Figure 8.3 shows clearly that it is possible in the  $R_n$  range of interest herein, to obtain high values of  $C_l$  simultaneously with low values of  $C_d$  that are almost independent of angle of attack. Most likely the indication of improved performance for the Liebeck airfoil sections over the Göttingen section results from the use of modern computational

techniques. This gives some confidence that additional efforts, both experimental and computational, will provide airfoil sections suitable for HAAP vehicles.

Personal conversations with Dr. Liebeck indicate that his LA 5055 airfoil is the most promising to date in obtaining high lift and low drag at low Reynolds numbers. Experimental data on this airfoil at conditions of interest to HAAP are not readily available. However, since an earlier Liebeck airfoil, the LA 2566 demonstrated a  $C_l > 1.4$  and  $C_{d,0} \approx 0.01$  at  $R_n = 0.25$  million (ref. 96, page 551), it is assumed that future airfoils of this class will have even better performance (see Table 8.3).

Because the Liebeck airfoils characteristically develop lift coefficients over a wide range without a significant change in drag coefficient (see Fig. 8.3), it is assumed that this type of airfoil could contribute to an aircraft having a reasonably high Oswald airplane efficiency factor. An efficiency factor of 0.85 is assumed for this study.

Table 8.3 summarizes the status of current and near-term airfoil technology suitable for HAAP design application.

TABLE 8.3 - STATUS IN AIRFOIL TECHNOLOGY FOR HAAP DESIGN

	Current	1985-86
Type	Liebeck LA 2566	Future
$C_l$ , max	1.4	1.8
$C_{d,0}$	0.010	0.008
$R_n$ , million	0.25-0.50	0.1-1.5

In concluding this section, a few additional thoughts merit discussion. In general, low-speed experimental measurements on airfoils at  $R_n$  less than 0.3 million are unsatisfactory. Different wind tunnels give different answers for the same airfoil. This is due, in part, to airflow separation along the wind-tunnel walls. At the NASA Langley Research Center, a wind tunnel is currently undergoing extensive modification to facilitate this type of testing. In addition, NASA Langley is initiating a low-level effort to develop high lift, low drag airfoils at low  $R_n$  (i.e.,  $C_l = 1.5$  at  $R_n = 0.3$  million).

### 8.3 PROPELLERS

The design and successful demonstration of lightly loaded propellers which use new lightweight materials such as the graphite fabric used on the Solar Challenger airplane is discussed by MacCready, et al. (ref. 2, page 9). Personal conversations with Mr. Ray Morgan, the Solar Challenger project manager, indicated that the propeller weight-to-thrust ratio was the primary design criterion for the Challenger's propeller. A weight-to-thrust ratio of about 0.06 lb/lb was used in that design, and is assumed for this study. The Challenger's propeller efficiency was estimated at about 0.86.

In the HAAP aircraft studies, Heyson (ref. 8, page 4) provides airplane propeller design information, and Petrone and Wessel (ref. 94, page 3) provide details of a propeller designed to power a HAAP blimp. Table 8.4 summarizes some propeller design data determined from references 8 and 94.

TABLE 8.4 - SUMMARY OF CHARACTERISTICS FOR PROPELLERS  
DESIGNED FOR HAAP AIRCRAFT

Study	Petrone and Wessel (ref. 94)	Heyson (ref. 8)
HAAP aircraft	Blimp	Airplane
Number of blades	3	3
Diameter, ft	25	24
RPM	90-144	450
Altitude, ft	70,000	65,500
Kinematic viscosity $\times 10^4$ , $\text{ft}^2/\text{s}$	21.56	17.21
Airspeed, $\text{ft/s}$	34.3 and 57.2	216
Characteristic $R_n$ , million	0.1	0.1
Efficiency	0.79	0.87-0.92

Table 8.4 indicates that the propellers will operate at a nominal Reynolds number of about 0.1 million. The propeller lift coefficient would be considerably less than that for an airfoil, reducing slightly the performance demands on the propeller relative to the airfoil for solar-powered flight. In this study, a propeller efficiency of 0.85 is assumed.

## CHAPTER 9

### MATERIALS, STRUCTURES, AND PAYLOADS

#### 9.1 MATERIALS AND STRUCTURES

Lightweight materials such as Kevlar, graphite, and plastic derivatives are being incorporated into the construction of blimps (ref. 105, page 4) and of airplanes (ref. 2, pages 8-9). The advantage of using these materials is lighter structural weight. For this study, a constant structural weight fraction is assumed. Based on the summary data presented in Table 8.3, a structural weight fraction of 0.33 is assumed for the HAAP blimp. In using this value, note that the weight of the lifting gas is not included in the total vehicle loads.

A minimum structural weight fraction assumed for the HAAP airplane is that for the Minisniffer II, a high-altitude remotely piloted vehicle discussed by Reed in reference 106. The minimum structural weight fraction assumed for the HAAP airplane is 0.17 (determined from ref. 106, page 36). An additional structural constraint must also be considered, the ratio of structural weight to wing planform area. The Solar Challenger airplane is thought to be representative of current ultra-light aircraft technology. Its value for the structural weight to wing planform area ratio was about  $0.5 \text{ lb/ft}^2$ . The minimum value for that ratio selected for this study is  $0.40 \text{ lb/ft}^2$ .

The degradation of these lightweight materials when exposed to the expected low radiation levels in the case of a nuclear-powered HAAP is

not known. However, the same structural weight ratio will be used for the nuclear aircraft as for the solar- and microwave-powered aircraft.

## 9.2 PAYLOADS

Payload type, weight, volume, and power requirements will vary with the many possible uses discussed in Chapter 2. A study of these many types of payload instrumentation is beyond the scope of this project. As an alternative, a simple weight allowance is used herein. However, the payload selected is thought to be representative of the small payloads and power levels that might be used on the advanced communications satellites anticipated for the mid-1980's (ref. 107, page 76). A payload weight of 100 lb with a continuous power requirement of 1000 watts is assumed for this study.



## CHAPTER 10

### ANALYSIS CONSIDERATIONS

#### 10.1 HAAP DESIGN PHILOSOPHY

##### 10.1.1 Solar-Powered Concepts

Of major concern in the practical operation of a solar-powered HAAP is its orientation to the Sun. Figure 10.1 illustrates positions for relatively high and low exposure of the solar cells to the Sun's rays for a HAAP blimp.

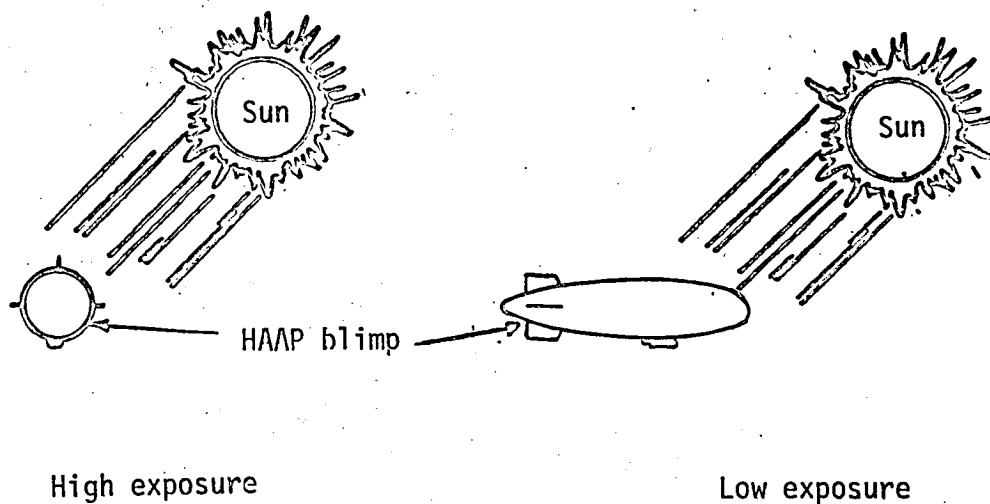


Figure 10.1 - Illustration of Sun angle effect on energy to a solar-powered HAAP blimp.

The solar-powered blimp must operate throughout the entire day; thus, many additional solar cells may be required so that an adequate number are illuminated at all hours of the day. The direction of flight will be determined by the direction of the winds aloft. Under certain combinations of wind direction and solar aspect, the majority of the

cells may receive light only at grazing angles with a consequent reduction in power output. These considerations will not be addressed further herein since the objective of the current study is primarily a gross assessment of the technical feasibility of the HAAP.

Figure 10.2 illustrates the importance of Sun orientation for a solar-powered HAAP airplane.

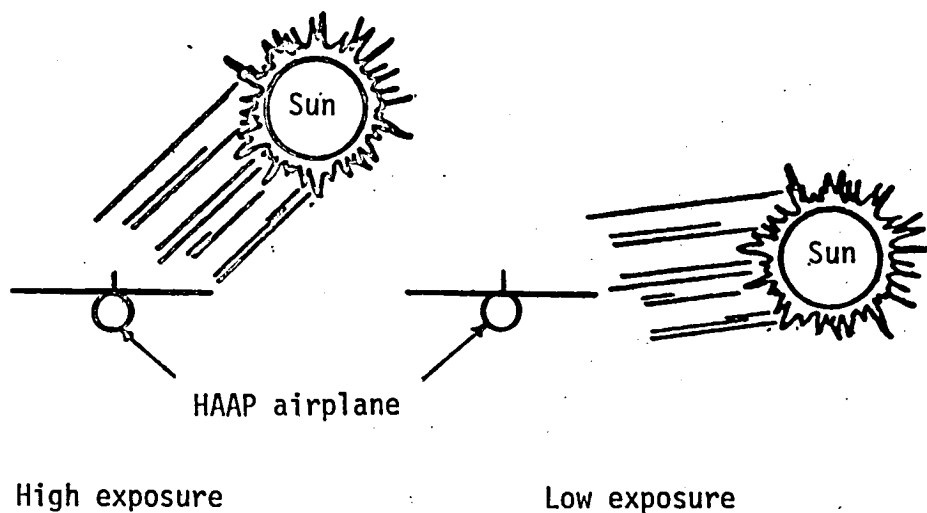


Figure 10.2 - Illustration of Sun angle effect on energy to a solar-powered HAAP airplane.

The present study assumes that the solar cells are mounted on the essentially horizontal upper surface of the wing. As indicated by figure 10.2, when the Sun is low on the horizon, either because of the hour of day or because of very high latitude, the cells receive only grazing energy from the Sun. Operation under such conditions indicates a requirement for cells on vertical as well as horizontal surfaces. Some possible configurations have been suggested to accommodate this need in non-referenceable documents. The present study is intended only

as a first order feasibility study and will not address this aspect of the problem.

#### 10.1.2 Microwave-Powered Concepts

Of importance in the design of a microwave HAAP system is the alignment of the energy transmitting and energy receiving (rectenna) antenna. (It should be noted that the direction of a HAAP blimp is chosen by the direction of the wind, and that a HAAP airplane must circle to maintain station.) If both transmitter and rectenna use linear polarization, the energy transferred diminishes significantly with misalignment; approximately with the phase angle between the two units. If the antenna transmits with circular polarization, the linear polarization of the rectenna produces a sinusoidal variation in apparent amplitude of each wave form at the rectenna. As a result, the average energy level at the rectenna is only half that for linear polarized alignment. In this study, the details associated with linear or circular polarization of the transmitted microwaves are neglected; thus, circular polarization of both antennae is implicitly assumed. Linear polarization would impact the results to some extent; however, the present treatment should suffice for a first-order feasibility study.

#### 10.1.3 Blimps

The HAAP blimp design philosophy is relatively straightforward since there is no concern for dynamic lift. After defining the flight system characteristics (Chapters 4 through 7), aerodynamic characteristics (Chapter 8), and structural weight relationships (Chapter 9), the winds which will be encountered (Chapter 3) determine the power, and

eventually the blimp size. The design maximum airspeed assumed for this study is 140 ft/s, which permits some degree of maneuverability in the severe winter wind environment.

For the solar-powered HAAP blimp, energy must be stored to provide power for nighttime operation. During this nighttime operation, it is assumed that the average airspeed will not exceed 50 ft/s; this highest seasonally averaged airspeed at HAAP altitudes occurs during the winter.

#### 10.1.4 Airplanes

For maintaining station, the airplane would, ideally, fly into the headwind at equal airspeed, as in the blimp case. Since the wind speed is variable, and sometimes zero, for simplicity, the HAAP airplane is designed for circling flight at a constant 140 ft/s, the maximum required airspeed. In addition, the HAAP airplane is designed to operate at minimum power. The relationship for operating at minimum power is derived by Loftin in reference 108 (page 343). Equation (10.1) expresses that relationship.

$$C_{L,opt} = \sqrt{3C_{D,0}\pi Ae} \quad (10.1)$$

where

- |             |                                   |
|-------------|-----------------------------------|
| $C_{L,opt}$ | lift coefficient at minimum power |
| $C_{D,0}$   | profile drag coefficient          |
| $A$         | aspect ratio                      |
| $e$         | Oswald airplane efficiency factor |

Then the relationship defining lift coefficient in cruise:

$$C_L = \frac{W}{\frac{1}{2} \rho v^2 S} \quad (10.2)$$

can be used to define the required wing area as

$$S = \frac{W}{\frac{1}{2} \rho v^2 C_{L,opt}} \quad (10.3)$$

when operating at minimum power, where

S	wing planform area (ft <sup>2</sup> )
W	airplane total weight (lb)
$\rho$	ambient density (slugs/ft <sup>3</sup> )
v	airspeed (ft/s)

The relationship for wing area is based on aerodynamic loads, and does not account for the solar-cell or rectenna area required to meet the airplane power demands.

An aspect ratio 20 wing is selected for the baseline configuration in this study. The operating cruise  $C_L$  is defined by equation (10.1) with a maximum operating cruise lift coefficient ( $C_{L,max op}$ ) of 1.50.

## 10.2 COMPUTER CODES

To facilitate the technical evaluation of the various HAAP concepts, two interactive FORTRAN computer codes were developed to aid in the analysis. One computer program is designed to analyze blimp concepts; another program to analyze airplanes. Each program can represent solar-, microwave-, or nuclear-propulsion systems as desired.

The computer codes contain appropriate modeling of the atmosphere, developed from the data contained in reference 18 (the U.S. Standard Atmosphere). Temperature, density, and pressure profiles of the atmosphere are modeled to an altitude of 260,000 ft. A 15-term Chebychev approximation method is used to determine density and pressure for a specified altitude. The airplane analysis code uses only the atmospheric density model.

The computer codes are interactive, which permits the user to conveniently select values for many parameters such as altitude, airspeed, or drag coefficient. Should the user choose not to provide a value for a specific parameter, a default value is provided in the program. The default values are generally representative of the near-term technologies applicable for a microwave-powered HAAP concept. The default values and the input dimensional units for all major system components (i.e., battery efficiency) are displayed on the screen of the interactive terminal. Should the user input "0" for the amount of energy (power) that is incident to the aircraft, the analysis is conducted on the assumption that the aircraft is nuclear-powered.

The effect of varying any one parameter on the size of the HAAP concept can be evaluated readily. The user may select any parameter, such as propeller efficiency, and then select different values for efficiency. The effect of propeller efficiency is shown on the plotted data output. Blimp size is measured by volume and airplane size by wing span.

The methodology used to find a solution for the aircraft size is based on excess-lift-fraction, which is expressed as

$$\text{Excess-lift-fraction} = \frac{\text{Lift}}{\text{Weight}} - 1. \quad (10.4)$$

The logic of the computer code is to increment blimp volume or to wing area, both of which produce lift. When blimp volume or wing area is too small, a negative value is calculated for excess-lift-fraction. Conversely, if blimp volume or wing area is too large, a positive value is calculated for excess-lift-fraction. The blimp volume or wing area (expressed in terms of wing span), for which the excess-lift-fraction equals zero, is the design size. Figure 10.3 illustrates this method of logic for determining blimp size.

The computer analysis codes do not contain any graphics capability. The codes use an output data format compatible with complex graphics codes at the NASA Langley Research Center that plot the generated data on the computer terminal screen. Figure 10.4 is a flow chart which illustrates the logic used in the analysis programs. Appendix A provides a listing of the two codes.

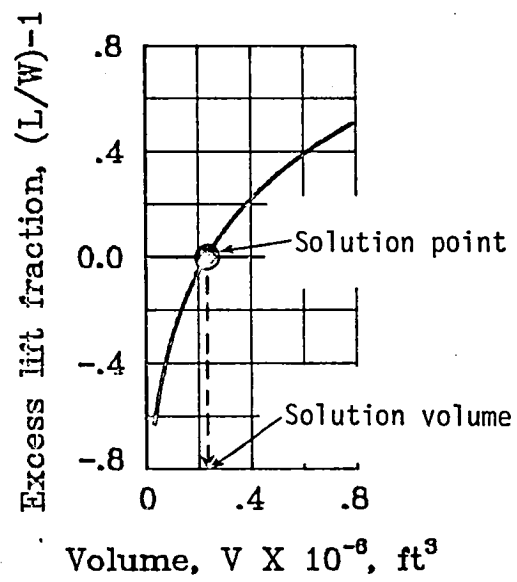


Figure 10.3 - Illustration of sizing methodology for a HAAP concept solution.



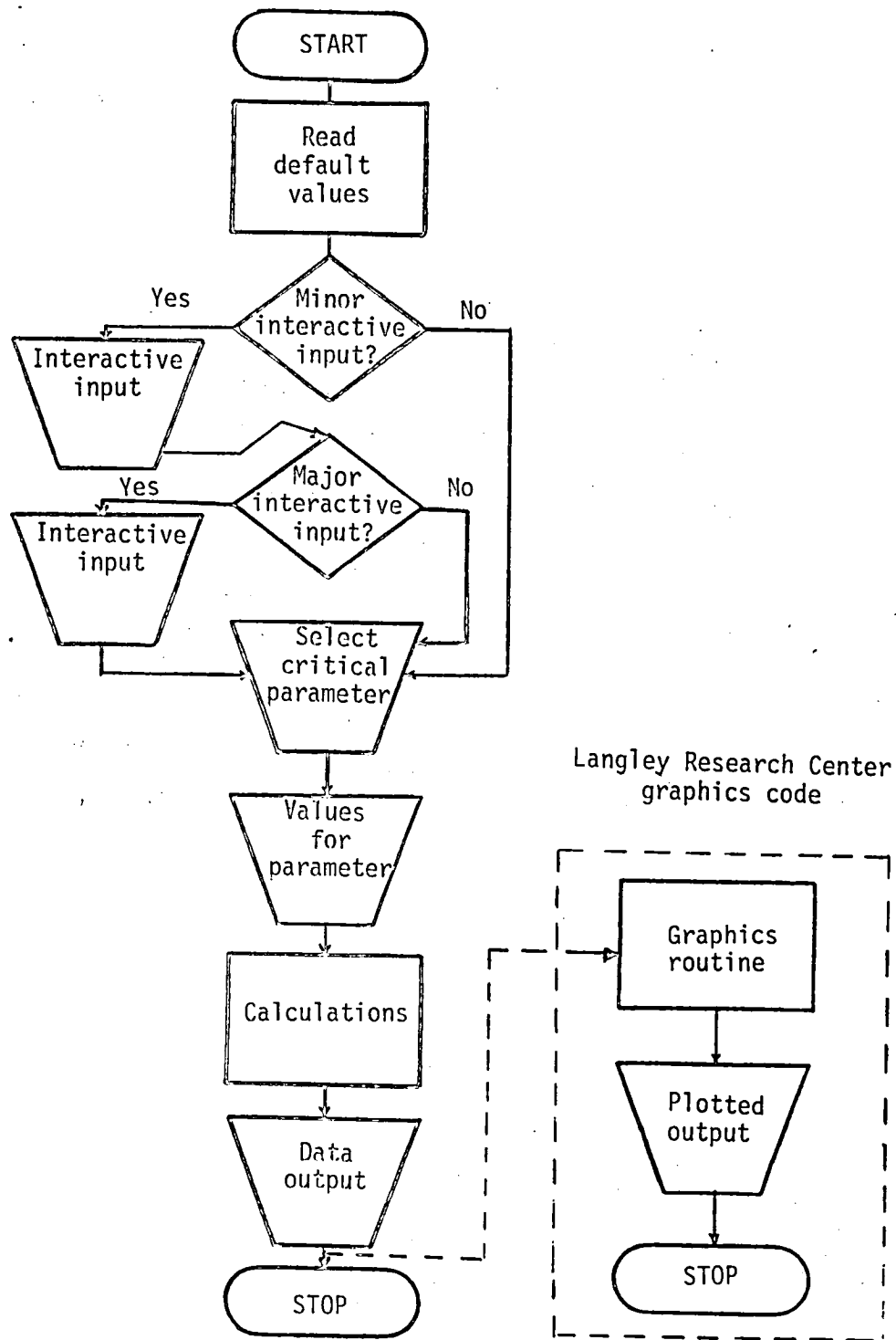


Figure 10.4 - HAAP computer analysis codes flow chart.

### 10.3 HAAP POWER SYSTEM SCHEMATIC

Figure 10.5 illustrates the generalized propulsion and power system arrangement for a HAAP.

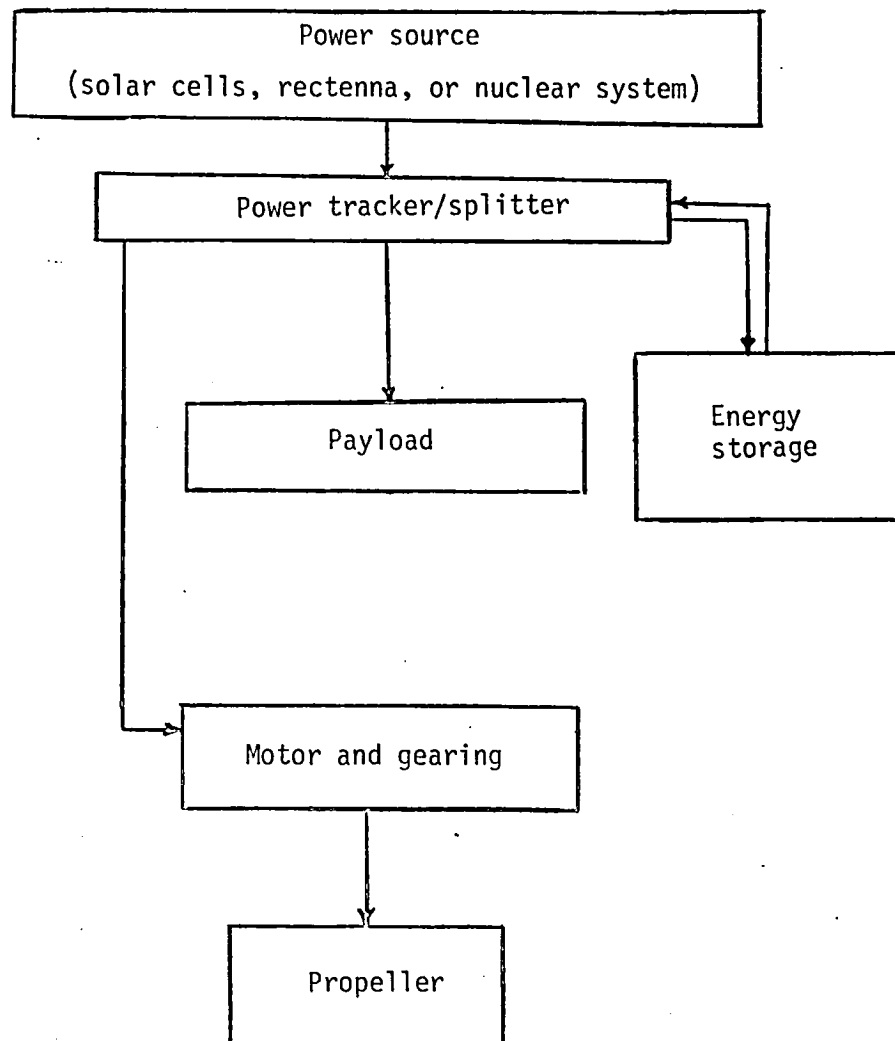


Figure 10.5 - HAAP power system schematic diagram.

#### 10.4 HAAP CONCEPT ENERGY REQUIREMENTS

Conventional relationships are used to determine power and energy requirements. The following fundamental relationships are used for thrust, motor power, and system energy in the calculations. Aerodynamic relationships were discussed in Chapter 8.

$$T = \frac{1}{2} C_D \rho_a v^2 S_{ref} \quad (10.5)$$

$$P_m = \frac{Tv}{\eta_p} \quad (10.6)$$

$$E = \frac{\left( \frac{P_m}{\eta_m} + P_p \right) \left( 24 - P_{off} + \frac{P_{off}}{\eta_{es}} \right)}{\eta_{pp}} \quad (10.7)$$

where

$C_D$	drag coefficient
$E$	daily (24-hour) energy delivered by power source (W-h) (see Fig. 10.2)
$P_m$	power delivered by motor (W)
$P_p$	payload power (W)
$P_{off}$	number of hours energy storage device is operated (h)
$S_{ref}$	wing reference area for airplane (ft <sup>2</sup> ) (volume) <sup>2/3</sup> for blimp (ft <sup>2</sup> )
$T$	required thrust (lb)
$v$	characteristic airspeed (ft/s)
$\rho_a$	ambient density (slugs/ft <sup>3</sup> )
$\eta_{es}$	energy storage efficiency

$\eta_m$	motor efficiency
$\eta_p$	propeller efficiency
$\eta_{pp}$	power processing efficiency

## 10.5 SUMMARY OF SYSTEM PARAMETERS

Chapters 3 through 9 discussed the technology status of various systems for application to a High-Altitude Aircraft Platform (HAAP). Tables 10.1 to 10.3 summarize the technology statuses of the components used in this study, most of which are near-term (1985-86). Details associated with any system can be found in the prior chapters. Table 10.1 summarizes various baseline values of the system parameters used herein to evaluate the HAAP concepts.

TABLE 10.1 - SUMMARY OF GENERAL SYSTEM PARAMETERS  
FOR HAAP DESIGN

SYSTEM

Energy Storage

Batteries

Usable energy-weight ratio, W-h/lb . . . . .	15.3
Efficiency . . . . .	0.85

Fuel Cell

Usable energy-weight ratio, W-h/lb:	
4-hour storage . . . . .	48.3
8-hour storage . . . . .	92.7
12-hour storage . . . . .	133.7
16-hour storage . . . . .	171.6
Efficiency . . . . .	0.50

Motor and Gearing

Power-weight ratio, W/lb . . . . .	573
Efficiency . . . . .	0.94

Power Processing

Power-weight ratio (payload), W/lb . . . . .	54
Power-weight ratio (propulsion), W/lb . . . . .	250
Efficiency . . . . .	0.92

Structure

Blimp weight-total load ratio . . . . .	0.33
Minimum airplane airframe weight-total weight ratio . . . . .	0.17
Minimum airplane airframe weight-wing area ratio, lb/ft <sup>2</sup> . . . . .	0.40

Aerodynamic Characteristics

Propeller

Weight-thrust ratio, lb/lb . . . . .	0.06
Efficiency . . . . .	0.85

Airplane maximum operating lift coefficient, $C_{L,max op}$ . . . . .	1.50
---	------

Airplane profile drag coefficient, $C_{D,0}$ . . . . .	0.010
--	-------

Airplane (Oswald) efficiency factor . . . . .	0.85
---	------

Airplane aspect ratio . . . . .	20 or 30
---------------------------------	----------

Blimp drag coefficient, $C_D$ . . . . .	0.035
---	-------

Due to the technological uncertainty of energy-weight ratios for regenerative fuel cells, particularly for a small number of storage capability hours, the battery system is used for energy storage requirements less than 4 hours.

Table 10.2 summarizes the system parameters uniquely associated with each propulsion system under consideration in this study.

TABLE 10.2 - SUMMARY OF SPECIFIC PROPULSION SYSTEM  
PARAMETERS FOR HAAP DESIGN

Solar Power System

Solar cell array

Weight-area ratio, $\text{lb/ft}^2$ . . . . .	0.07
Efficiency . . . . .	0.16
Sun energy flux, $\text{W/ft}^2$ . . . . .	111

Microwave Power System

Rectenna

Weight-area ratio (blimp), $\text{W/lb}$ . . . . .	0.08
Weight-area ratio (airplane), $\text{W/lb}$ . . . . .	0.04
Efficiency . . . . .	0.80
Microwave energy flux, $\text{W/ft}^2$ . . . . .	37

Nuclear Propulsion System

Power-weight ratio, $\text{W/lb}$ . . . . .	10 to 30
---	----------

Table 10.3 summarizes payload and operating parameters for the HAAP aircraft.

TABLE 10.3 - SUMMARY OF PAYLOAD AND OPERATING  
PARAMETERS FOR HAAP DESIGN

Payload

Weight, lb . . . . .	100
Power, W . . . . .	1000

Operating conditions

Altitude, ft . . . . .	70,000
------------------------	--------

Blimp:

Maximum airspeed, ft/s . . . . .	140
Average airspeed, ft/s . . . . .	50
Minimum superpressure, lb/ft <sup>2</sup> . . . . .	5.2
Superheat, °F . . . . .	0
Helium-gas fraction . . . . .	0.95

Airplane:

Airspeed, ft/s . . . . .	140
--------------------------	-----

## CHAPTER 11

### HAAP BLIMP FEASIBILITY AND ANALYSIS

The current analysis compares the relative feasibilities of solar-voltaic- and microwave-powered HAAP blimps using near-term technologies appropriately common to each propulsion concept. A solar-powered concept designed to operate over the United States is significantly influenced by the long nights in the winter and the long days in the summer. In addition, the energy flux incident on the solar cells is physically limited by the maximum energy available from the Sun, about  $127 \text{ W/ft}^2$ .

A microwave-powered concept is more heavily influenced by technological progress. Energy available with this concept is influenced by the magnitude of the incident microwave flux that can be rectified reliably. Near-term technology estimates for this flux are about  $37 \text{ W/ft}^2$ . Solar-voltaic and microwave power technologies are discussed in detail in Chapters 4 and 5, respectively. Other near-term technologies essential to this study were discussed in previous chapters, and summarized in Tables 10.1, 10.2, and 10.3.

There is a high degree of uncertainty about the propulsion system weight for a nuclear-powered system; therefore HAAP blimps using nuclear power are only analyzed parametrically.

Figure 11.1 illustrates the required sizes of a solar-voltaic and a microwave-powered HAAP blimp as determined from a weight balance analysis.



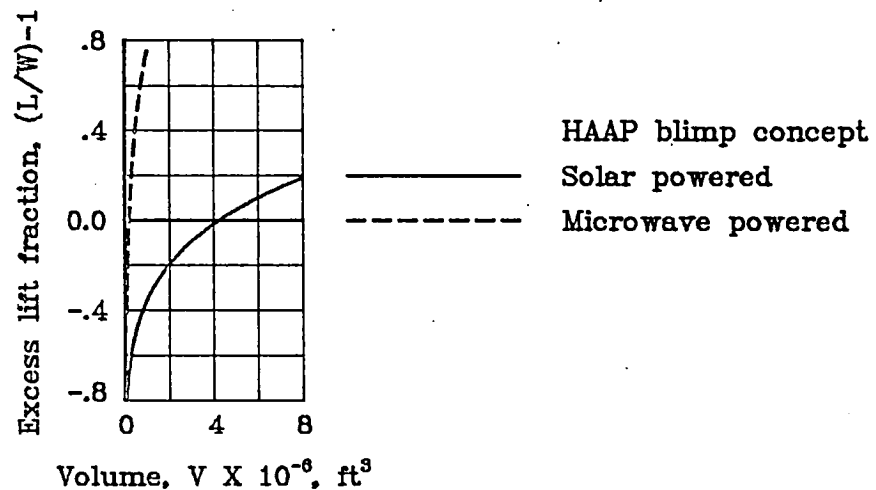


Figure 11.1 - HAAP blimp sizes.

#### 11.1 SOLAR-POWERED CONCEPT

Figure 11.1 indicates, from a weight analysis viewpoint, that a solar-powered HAAP blimp would be about 4 million cubic feet in size. The concept is sized to operate on days with 8 hours of sunlight, which is, on the average, about the smallest number of daylight hours encountered in the United States each year. During the daylight hours, the blimp is powered by solar cells mounted on its surface. During the hours of darkness, the blimp is powered by a regenerative fuel cell system. Table 11.1 summarizes some of the specific characteristics of this solar-powered HAAP blimp concept.

Table 11.1 shows that the solar-powered HAAP blimp would be about 678 feet in length. Particular note should be given to the required solar cell area and reference area. The required solar cell area provides all power needs and includes a 10-percent redundancy. The reference area is simply the blimp projected planform area, and is the maximum

TABLE 11.1 - SOLAR-VOLTAIC POWERED HAAP BLIMP SUMMARY CHARACTERISTICS

Design conditions:

Altitude, ft	70,000
Cruise airspeed, ft/s	50
Maximum airspeed, ft/s	140
Incident energy flux, W/ft <sup>2</sup>	111
Solar cell efficiency	0.16
Stored energy, h	16
Payload power, W	1,000
Payload weight, lb	100
Structural weight fraction	0.33
Cruise drag coefficient, $C_D$	0.035

Motor size, hp	373
----------------	-----

Weights, lb

Propeller	74
Motor-gear	485
Payload	100
Solar cell array	6988
Fuel cell system	1349
Power processing system	1130
<u>Structure</u>	4987
Total weight	15,114

Gas mass, lb	3567
--------------	------

Blimp dimensions:

Volume x 10 <sup>-6</sup> , ft <sup>3</sup>	4.2
Maximum diameter, ft	136
Length, ft	678
Reference planform area, ft <sup>2</sup>	59,800
Solar cell area, ft <sup>2</sup>	99,800

Cruise Reynolds number	15,800,000
------------------------	------------

Daily incident energy required, kW-h	630
--------------------------------------	-----

effective area subjected to the rays of the Sun for obtaining power. The required solar cell area is about 1.7 times the planform area. This means that there is insufficient area on a conventionally shaped blimp to locate the necessary solar cells. Figure 11.2 illustrates a twin-bodied blimp which conceptually can provide the necessary area by carrying the solar cell arrays between the bodies. If aerodynamic forces on the solar panel were neglected, each hull of the twin body configuration would be about 4 million ft<sup>3</sup> in volume and about 670 ft in length.

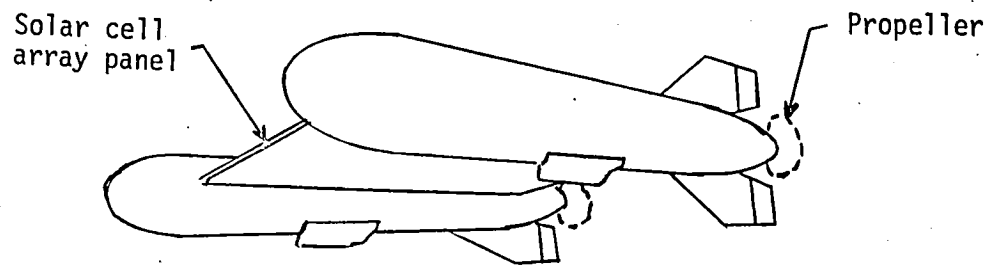


Figure 11.2 - A possible solar-powered HAAP blimp concept.

If drag due to the solar panel is considered, the drag coefficient for the blimp concept is modified as shown in equation (11.1).

$$C_D = C_{D,h} + C_{D,0} \frac{S_{ref}}{v^{2/3}} \quad (11.1)$$

where

- $C_D$             concept total drag coefficient
- $C_{D,h}$         blimp hull drag coefficient (based on  $v^{2/3}$ )  
                  (formerly  $C_D$  in eq. (8.5))

$C_{D,0}$       solar panel profile drag coefficient  
 $S_{ref}$       solar panel area (ft<sup>2</sup>)  
 $V$           blimp hull volume (ft<sup>3</sup>)

A value of 0.005 was selected as representative of  $C_{D,0}$ , and is based on flat plate drag estimates. Temporary modifications were made to the computer program of Appendix A.1, to examine the hull sizes required for the twin hull configuration. The results of this brief study are shown in Figure 11.3 for several assumed values of wing weight.

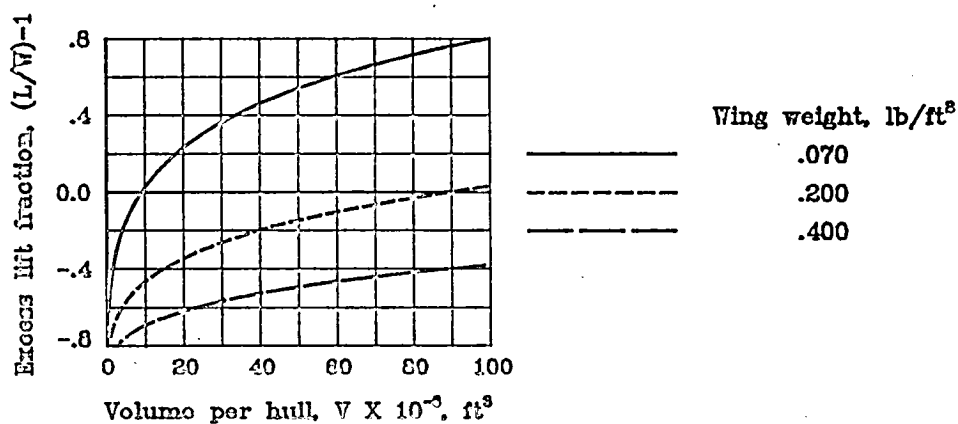


Figure 11.3 - Effect of wing weight on twin-body solar-powered HAAP blimp size.

The drag penalty due to the wing (wing weight = 0.07) changes the hull volume from 4.2 million ft<sup>3</sup> (see Fig. 11.1) to about 10 million ft<sup>3</sup>, and results in a 1900-ft vehicle length. Small increments in wing weight to provide structural integrity have a remarkable effect on hull volume. A wing weight of 0.2 lb/ft<sup>2</sup>, for example, results in a 90 million ft<sup>3</sup> volume for each hull. In practice, however, the wing could be used to house some of the lifting gas, which in turn reduces hull size. In any

event, with practical values for wing weight, solar blimps of this configuration appear to be so immense as to be impractical. This configuration will not be considered further in this report.

#### 11.1.1 Parametric Variations

Considerable effort was involved in determining the near-term technology capabilities which were assumed in this study. Because the feasibility of a solar-powered HAAP blimp is subject to change with level of technology, a sensitivity analysis was conducted. The results of this analysis will be presented in the next several sections of this paper. The following analysis illustrates the size of a single hull carrying the design payload, and neglects aerodynamic forces that may be on a connecting solar panel.

##### 11.1.1.1 Maximum Airspeed

The 140 ft/s design maximum airspeed selected for this study is based on available high-altitude windspeed data (Table 3.1, page 15), and permits a small degree of maneuverability in the most severe windspeeds anticipated. Figure 11.4 illustrates the dramatic effect maximum airspeed has on the size of a solar-powered HAAP blimp.

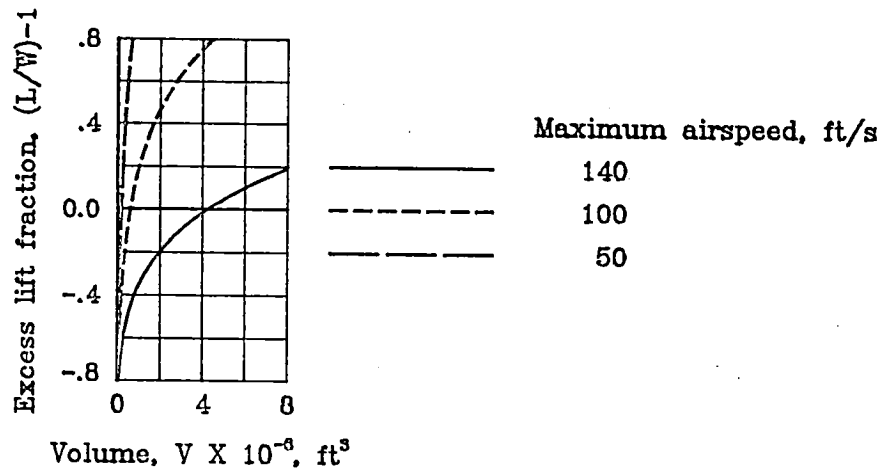


Figure 11.4 - Effect of maximum airspeed on solar-powered HAAP blimp size.

Figure 11.4 vividly exemplifies that power required, and the corresponding system weights, varies with airspeed cubed ( $v^3$ ). A design maximum airspeed of 100 ft/s results in a blimp size of about 0.6 million  $\text{ft}^3$ , based on a weight balance analysis. When additional solar cells are provided for a practical concept which would permit the capture of energy from either a left- or right-side facing Sun, the size increases to about 3.2 million  $\text{ft}^3$ . This concept would be extensively covered with solar cells and about 620 ft in length. This 100 ft/s maximum airspeed design represents about the maximum design airspeed for which a conventional single-body concept is feasible, using near-term technology. It should be noted that concept feasibility is achieved at significant sacrifice to station keeping capability during the winter season.

#### 11.1.1.2 Drag Coefficient, $C_D$

One of the major inconsistencies in the literature on HAAP blimps is the operational drag coefficient. Some studies have assumed a drag coefficient of 0.050 while others have assumed values of about 0.020. The drag coefficient (0.035) assumed in this study is thought to be representative of a flight configuration constructed within 5 to 6 years. In determining the 0.035 drag value, many experimental and theoretical documents on blimp drag were reviewed and the sensitivity of size to drag coefficient was investigated.

The results of the parametric study of drag coefficient are shown in Figure 11.5. A solar-powered HAAP blimp with a relatively high drag

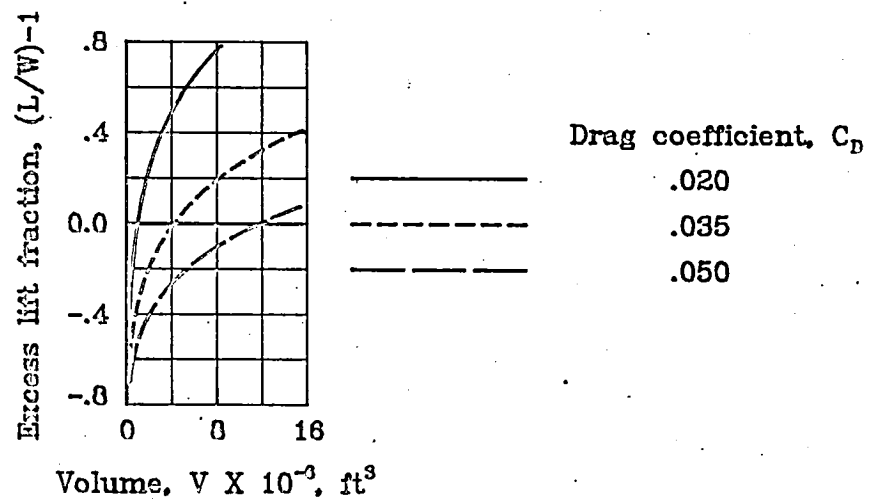


Figure 11.5 - Effect of drag coefficient on solar-powered HAAP blimp size.

coefficient of 0.050 would have a volume of about 12 million  $\text{ft}^3$  and a length of 960 feet. A more aerodynamically refined configuration having

a  $C_D$  of 0.020 would have a volume of about 1 million  $\text{ft}^3$  and a length of 420 feet. The most important impact of the variation in  $C_D$  is not the change in size, but the relative areas required for solar cells. The concept with  $C_D = 0.050$  needs more than twice the available planform area for installing the solar cells, while the  $C_D = 0.020$  vehicle needs about 97 percent of the planform area for cells.

If a conventionally shaped HAAP blimp could be designed with a  $C_D$  of 0.020, each body of a twin-body configuration (similar to the baseline concept shown in Fig. 11.2) would have a volume of about 1 million  $\text{ft}^3$ . Although the lower  $C_D$  (0.020) makes a single-body concept more feasible, it would need to be almost entirely covered with solar cells. Slightly less than half of the cells would be on the dark side of the blimp and provide no contribution to propulsion power. The excessive amount of solar cell weight would result in a concept considerably larger than 1 million  $\text{ft}^3$  - about 12 million  $\text{ft}^3$ .



### 11.1.1.3 Propeller Efficiency

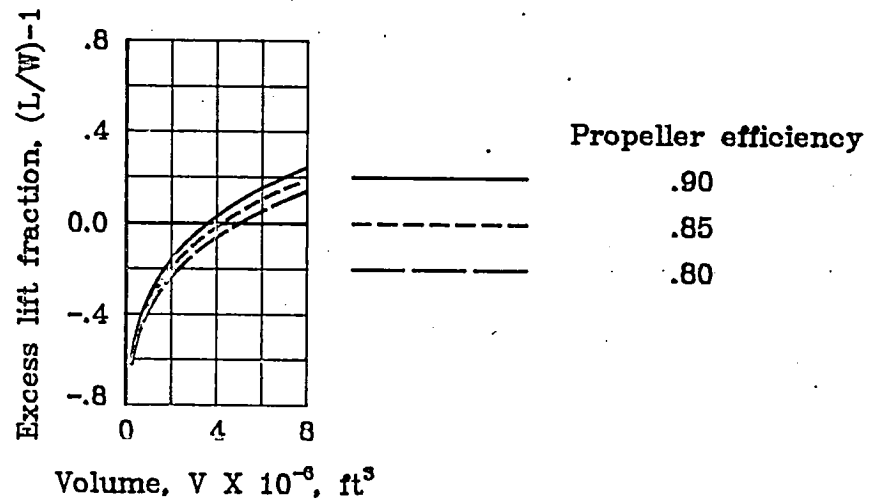


Figure 11.6 - Effect of propeller efficiency on solar-powered HAAP blimp size.

A propeller efficiency of 0.85 was assumed for this study. A change in propeller efficiency of 5 percent (Fig. 11.6) changes the volumetric size of the blimp by about 15 percent. The effect of propeller efficiency is relatively minor.

#### 11.1.1.4 Solar Cell Efficiency

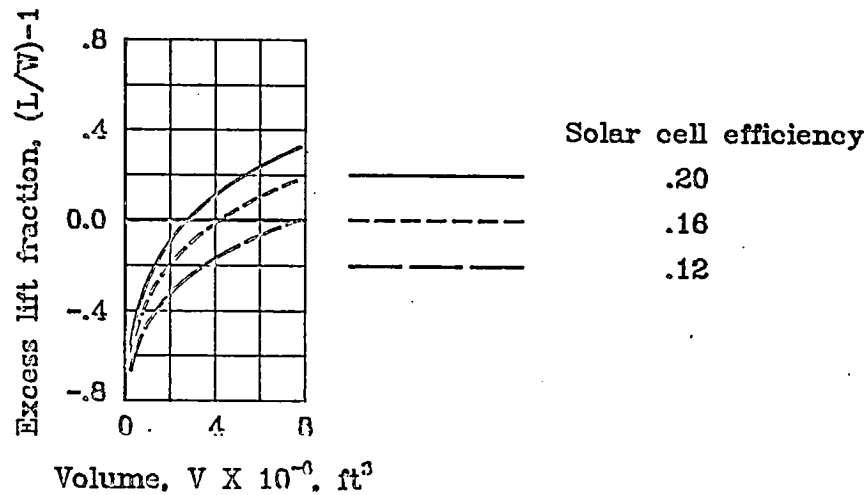


Figure 11.7 - Effect of solar cell efficiency on solar-powered HAAP blimp size.

Solar cell array efficiency can significantly affect the solar-powered HAAP blimp size (Fig. 11.7). If the arrays operated at 12 percent efficiency, the blimp would require almost double the volume of a blimp with the 16-percent efficient array. A 20-percent efficient solar cell array system could decrease blimp size by about 1 million  $\text{ft}^3$ , but would still require 30 percent more cell area than available on the conventional blimp platform.

#### 1.1.1.5 Incident Solar Power

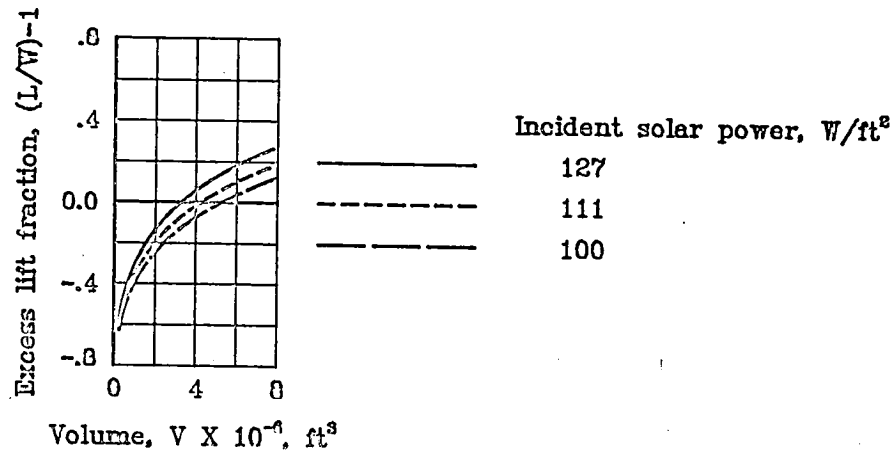


Figure 11.8 - Effect of incident solar power on solar-powered HAAP blimp size.

An incident solar energy flux of  $111 \text{ W/ft}^2$  was assumed in this study. It is an average value for each hour of the day that sunlight is incident on the vehicle. Values less than  $111 \text{ W/ft}^2$  result in larger blimps (Fig. 11.8). If  $127 \text{ W/ft}^2$  is assumed, which represents about the maximum possible energy flux, the blimp size is reduced, but 25 percent more solar cell area is still required than available on the platform.

#### 11.1.1.6 Fuel Cell Weight

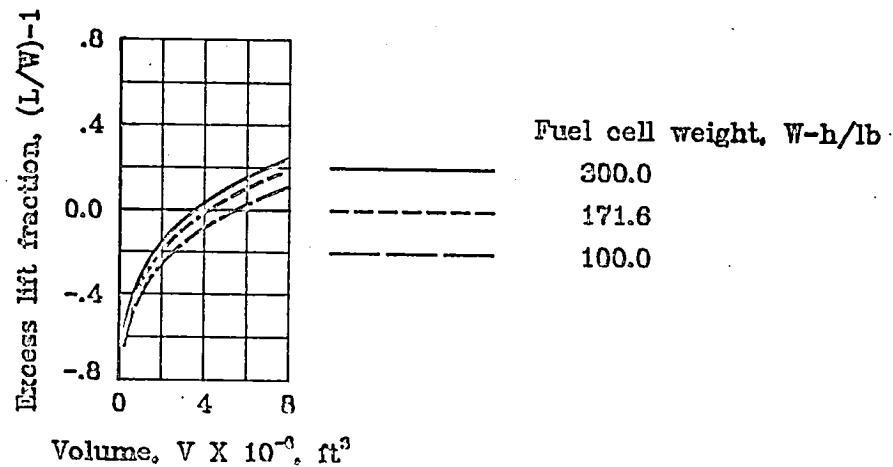


Figure 11.9 - Effect of fuel cell weight on solar-powered HAAP blimp size.

In this study, the weight of a regenerative fuel cell system designed for an 8-hour charge--16-hour discharge cycle is characterized by a value of 171.6 W-h/lb. This value is thought to be representative of regenerative fuel cell energy storage technology when the system is introduced and becomes available for use. Higher characteristic values for an introductory system have been estimated. Figure 11.9 indicates the effect of fuel cell system weight on the resultant HAAP blimp size. The fuel cell weight has negligible effect on the relative area required for solar cell arrays.

#### 11.1.1.7 Structural Weight Fraction

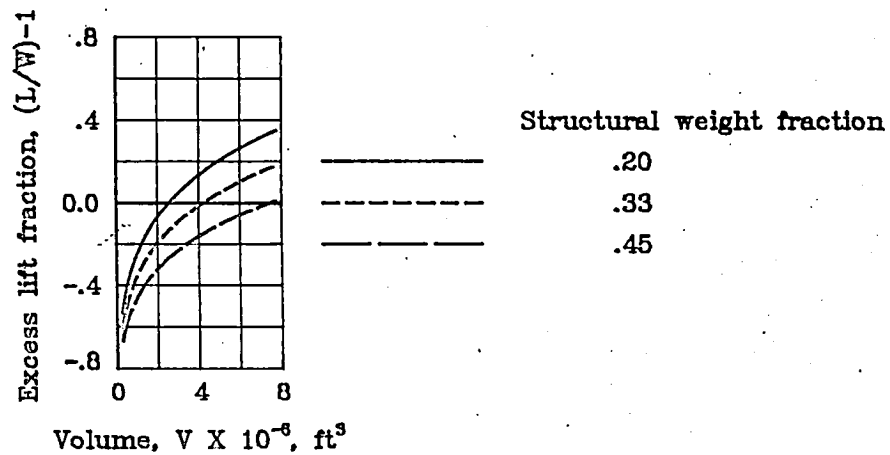


Figure 11.10 - Effect of structural weight fraction on solar-powered HAAP blimp size.

The superpressure blimp represents a considerably different construction technology than the conventional blimps associated with the "Goodyear" television commercials. The structural weight fraction assumed for this study of 0.33 is based primarily on results from in-depth studies on the structural design of superpressure HAAP type blimps. The structural weight fraction value does not include the weight of the lifting gas. Figure 11.10 demonstrates the major impact of structural weight fraction on the blimp size. The effect on relative solar cell area is negligible.

#### 11.1.1.8 Payload Weight

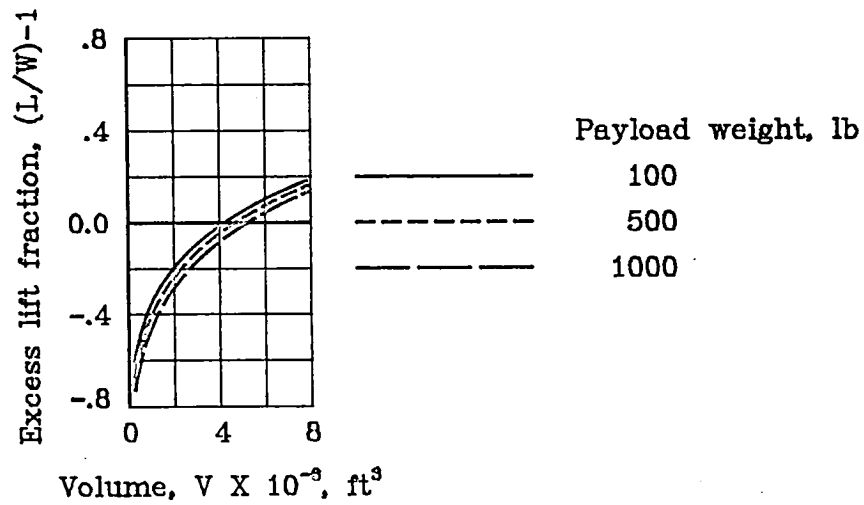


Figure 11.11 - Effect of payload weight on solar-powered HAAP blimp size.

Larger payload weights can be accommodated readily without compromising the HAAP blimp concept feasibility. Increasing the payload by a factor of 10 (Fig. 11.11) results in only a relatively small increase in volume. This result should be anticipated since the payload represents only a small fraction of the total weight.

#### 11.1.1.9 Helium Gas Fraction

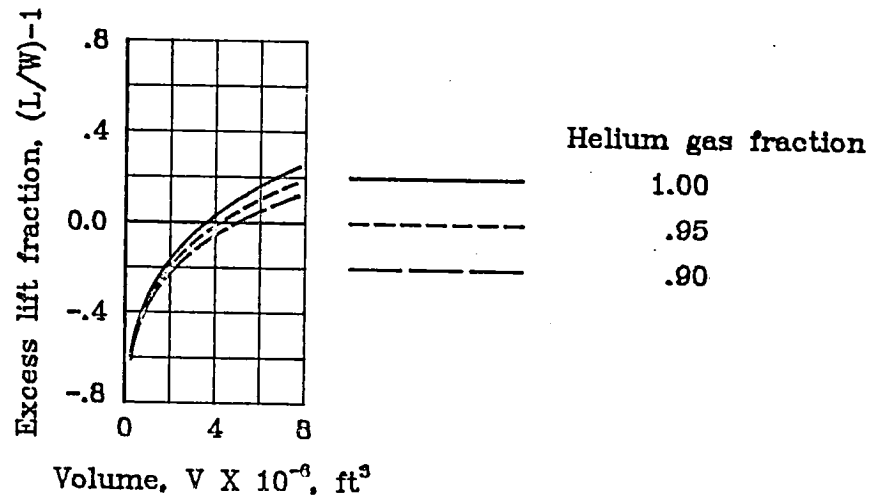


Figure 11.12 - Effect of helium gas fraction on solar-powered HAAP blimp size.

A helium gas fraction of 0.95 was used in this study. This means that the lifting gas is 95 percent pure helium with the remaining 5 percent being air. The literature on blimp operational gases generally reflect a 94-percent pure helium gas content. Figure 11.12 indicates that about a 15-percent change in blimp volumetric size results from a 5-percent change in the purity of helium.

#### 11.1.1.10 Superpressure

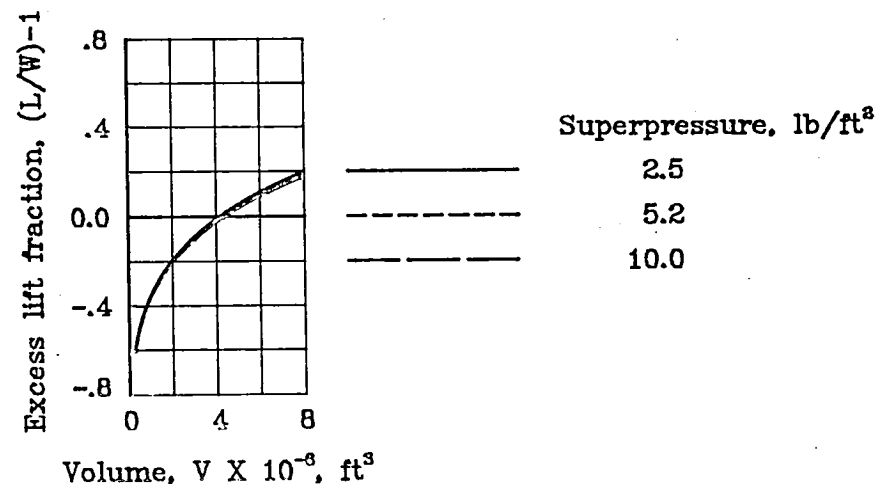


Figure 11.13 - Effect of superpressure on solar-powered HAAP blimp size.

Figure 11.13 shows that small changes in blimp design superpressure would have an almost insignificant effect on the blimp concept size and feasibility for the HAAP missions considered in this study.



#### 11.1.1.11 Advanced Technology Solar-Powered HAAP Blimp

Figure 11.14 illustrates the size of a single-body solar-powered HAAP blimp concept representative of far-term technology.

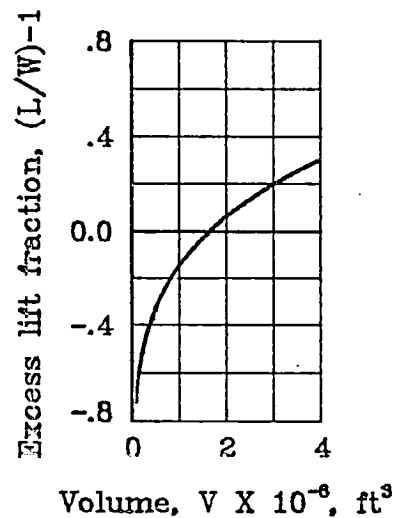


Figure 11.14 - Solar-powered HAAP blimp size using far-term technology.

Table 11.2 indicates the technology advances (far-term) required for the advanced vehicle design (Fig. 11.14) in comparison to those used in this study (near-term). The advanced vehicle concept would be a single-body about 500 ft in length, and extensively covered with solar cells. Observe that success of this venture requires the development of all the technologies in Table 11.2 to the "far-term" levels indicated.

TABLE 11.2 - SOME TECHNOLOGY ADVANCES FOR A SINGLE-BODY  
SOLAR-POWERED HAAP BLIMP CONCEPT

	Near-Term	Far-Term
Solar cell array operating efficiency	0.16	0.20
Structural weight fraction	0.33	0.20
Cruise drag coefficient, $C_D$	0.035	0.020
Propeller efficiency	0.85	0.90
Fuel cell energy-weight ratio, W-h/lb	171.6	300.0
Helium purity fraction	0.95	1.00
Superpressure, lb/ft <sup>2</sup>	5.2	2.5

#### 11.1.2 General Remarks

A primary concern in the design of a solar-powered HAAP blimp is the excessive area needed for the solar arrays. A twin-bodied design illustrated in Figure 11.2 is one configuration which could resolve that concern, but it would be an impractically large vehicle when designed for maximum station keeping capability (140 ft/s). Detailed analysis indicated that a single-body solar-powered blimp to perform the HAAP mission becomes more feasible as the design changed to operation with increasing number of daylight hours. For example, HAAP blimp designed to operate with up to 16 hours of daylight would be a single body, about 7 million ft<sup>3</sup> in volume and about 800 ft in length. This concept would be sufficiently covered with solar cells to provide power without regard to whether its left or right side were facing the Sun. The minimum number of daylight hours for which a single-body solar-powered HAAP appears

feasible with near-term technology is about 13 hours. Such a concept would be on the order of 15 million  $\text{ft}^3$  in volume and 1000 ft in length. The full development of all pertinent technologies reduces the size of the solar-powered HAAP blimp to manageable proportions. A substantial degree of success in these developments would be required before starting the blimp development in order to reduce the risk to a reasonable level.

A conventional single-body solar-powered HAAP blimp with reduced station keeping capability (100 ft/s maximum airspeed) appears to be feasible in the near-term. The concept would be about 3.2 million  $\text{ft}^3$  in volume and about 620 ft in length.

The solar-powered, superpressured, HAAP blimp concepts derived from this study can be compared with that derived by Kuhn (ref. 93) for a similar solar-cell/regenerative fuel cell system. Kuhn's study considered hydrogen as the lifting gas and a drag coefficient of 0.050 for several payload sizes and design airspeeds. For a 220-lb payload design capable of an airspeed of about 115 ft/s at 70,000 ft altitude, Kuhn determined that a single-bodied blimp slightly over 16 million  $\text{ft}^3$  in volume and about 930 ft in length is required. Kuhn does not discuss the incompatibility between the blimp surface area and the required solar cell area that occurs with increase in design airspeed.

## 11.2 MICROWAVE-POWERED CONCEPT

Figure 11.1 indicates that a microwave-powered HAAP blimp would be about 0.2 million  $\text{ft}^3$  in volume, which is almost identical to the volume of the "Goodyear blimp." The HAAP blimp concept is sized to operate continuously, converting incident microwave power which is

beamed from a nearby ground-transmission station. There is no energy storage requirement for this concept. Table 11.3 summarizes the blimp characteristics.

Table 11.3 describes a microwave-powered HAAP blimp as having a length of 242 ft and requiring a 48-hp motor. The area required for the rectenna is about 20 percent of the available planform. The rectenna area includes 10 percent redundancy. Because the microwaves readily transmit through blimp surface materials, the rectenna arrays can be housed within the blimp envelope without significantly compromising the design or size.

The concept described in Table 11.3 is less than half the volume of the microwave-powered HAAP blimp proposed by Sinko in reference 2. This current study considered a superpressure blimp whereas Sinko's study was based on the conventional blimp that houses the lifting gas in ballonets (gas bags) carried inside the hull. Sinko's 0.50 million  $\text{ft}^3$  concept had 50 lb of batteries to power the 287-lb payload; however, his assumption of a drag coefficient of 0.060 is the probable reason for the greater volume of his proposed blimp.

TABLE 11.3 - MICROWAVE-POWERED HAAP' BLIMP SUMMARY CHARACTERISTICS

Design conditions:

Altitude, ft	70,000
Cruise airspeed, ft/s	50
Maximum airspeed, ft/s	140
Incident energy flux, W/ft <sup>2</sup>	37
Rectenna efficiency	0.80
Stored energy, h	0
Payload power, W	1,000
Payload weight, lb	100
Structural weight fraction	0.33
Cruise drag coefficient, C <sub>D</sub>	0.035
Motor size, hp	48
<u>Weights, lb</u>	
Propeller	9
Motor-gear	61
Payload	100
Rectenna	124
Battery system	0
Power processing system	160
<u>Structure</u>	<u>224</u>
Total weight	679
Gas mass, lb	161
Blimp dimensions:	
Volume x 10 <sup>-6</sup> , ft <sup>3</sup>	0.19
Maximum diameter, ft	48
Length, ft	242
Reference (planform) area, ft <sup>2</sup>	7600
Rectenna area, ft <sup>2</sup>	1555
Cruise Reynolds number	5,800,000
Daily incident energy required, kW-h	71

A microwave-powered HAAP would resemble the conventionally configured blimp illustrated (not to scale) in Figure 11.15.

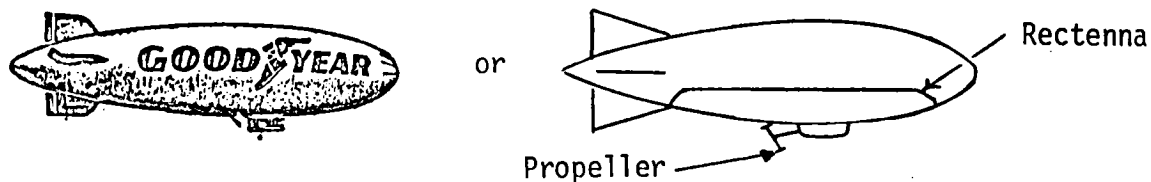


Figure 11.15 - A feasible microwave-powered HAAP blimp concept.

### 11.2.1 Parametric Variations

The sensitivity of a microwave-powered HAAP blimp concept to changes in the level of technology is presented in the same manner as for the solar-powered HAAP blimp.

#### 11.2.1.1 Drag Coefficient, $C_D$

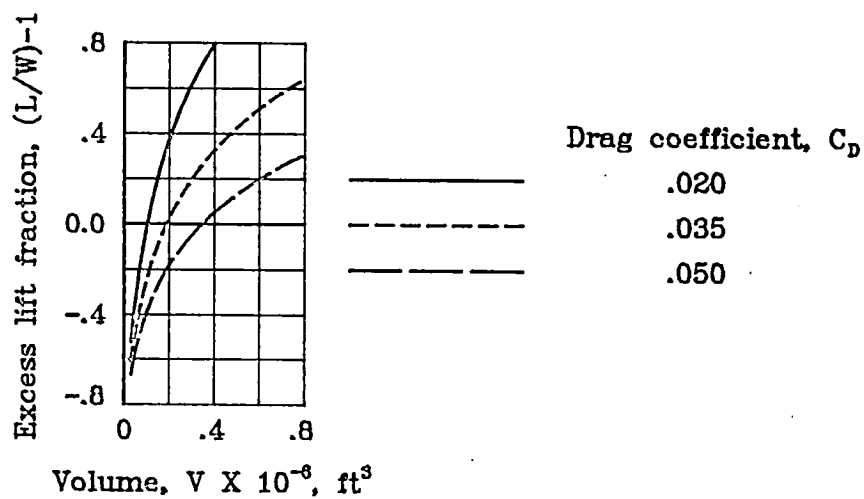


Figure 11.16 - Effect of drag coefficient on microwave-powered HAAP blimp size.

Figure 11.16 shows that the drag coefficient assumed for the microwave-powered HAAP blimp can significantly affect its size. The representative high ( $C_D = 0.50$ ) and low ( $C_D = 0.20$ ) values for blimp drag coefficient which appear in the literature can double or halve the volume of the baseline concept for which a  $C_D$  of 0.035 was assumed. The  $C_D$  values shown in Figure 11.13 have no significant effect on overall concept feasibility.

#### 11.2.1.2 Propeller Efficiency

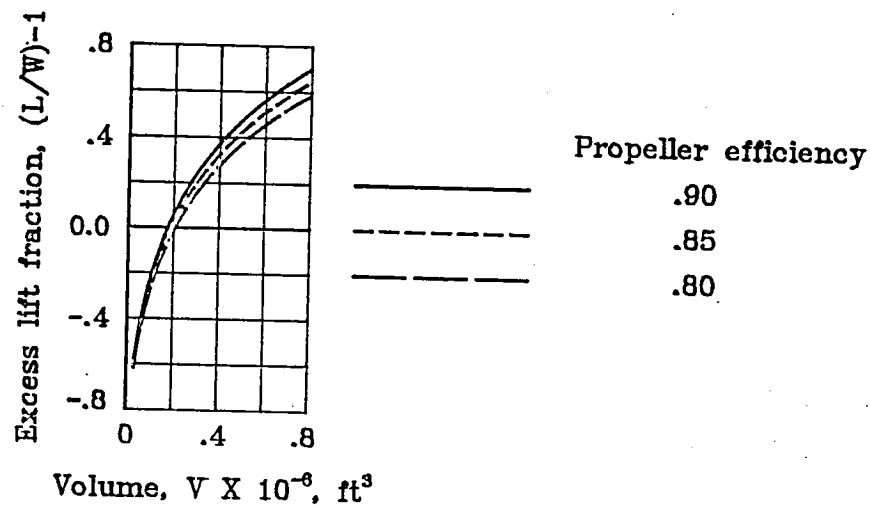


Figure 11.17 - Effect of propeller efficiency on microwave-powered HAAP blimp size.

Figure 11.17 shows that reasonable variations in propeller efficiency have little effect on the microwave-powered HAAP blimp size or feasibility.

### 11.2.1.3 Rectenna Efficiency

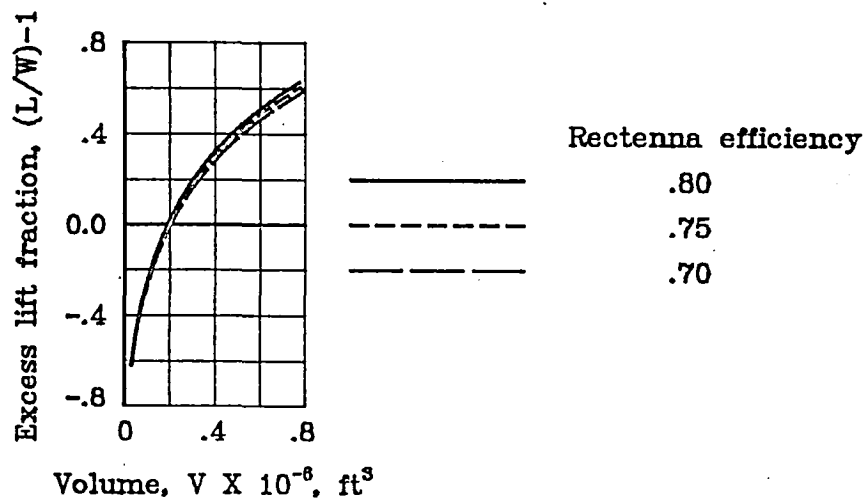


Figure 11.18 - Effect of rectenna efficiency on microwave-powered HAAP blimp size.

Figure 11.18 shows that reasonable variations in the efficiency of the rectenna system have little effect on the blimp size or feasibility. The 80-percent efficient system assumed in this study needs 0.20 of the available planform area for rectenna; a system with a rectenna efficiency of 70 percent needs about 0.23 of the available area.



#### 11.2.1.4 Incident Microwave Power

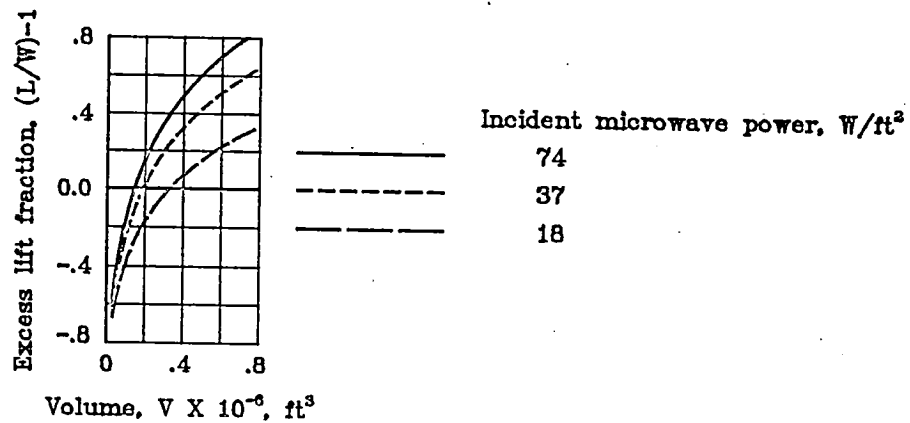


Figure 11.19 - Effect of incident microwave power on microwave-powered HAAP blimp size.

Microwave power incident to the blimp surface was assumed to be 37 W/ft<sup>2</sup>. As shown in Figure 11.19, doubling the amount of incident power reduces the volume by about 20 percent. If the incident power was reduced by about 50 percent, the volume would need to be increased by about 80 percent. For the beam power levels shown in the figure, the conventional blimp planform provides more than twice the area needed for rectenna.

#### 11.2.1.5 Structural Weight Fraction

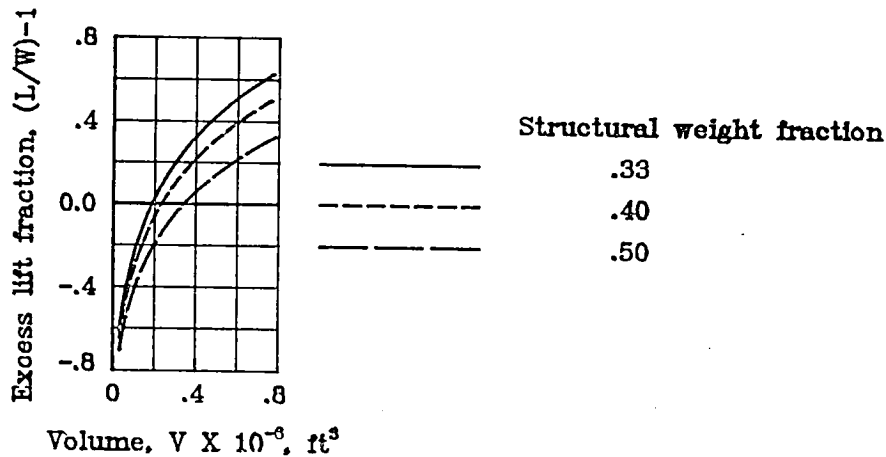


Figure 11.20 - Effect of structural weight fraction on microwave-powered HAAP blimp size.

The structural weight fraction of 0.33 determined to be representative of near-term superpressure blimp construction, and used in this study, was applied to all blimp concepts regardless of their propulsion system. Because the microwave-powered HAAP blimp is relatively small, a more conservative weight fraction might be appropriate. Figure 11.20 indicates that if 50 percent of the total weight (excluding the weight of the lifting gas) were structural, the HAAP would increase in volume by about 80 percent. However, it would still be a relatively small vehicle less than 300 ft in length.

#### 11.2.1.6 Payload Weight

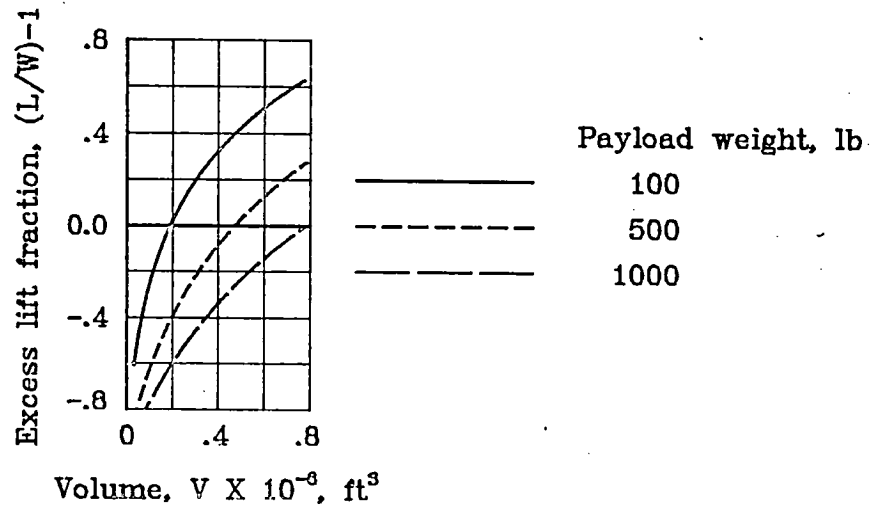


Figure 11.21 - Effect of payload weight on microwave-powered HAAP blimp size.

Unlike the solar cell powered blimp, the payload is a significant fraction of the total weight of the microwave-powered blimp; therefore, the volume of the microwave-powered HAAP blimp is very sensitive to payload weight. Figure 11.21 shows that increasing payload weight from 100 lb to 1000 lb requires a blimp with about four times the volume of the baseline blimp.

#### 11.2.1.7 Helium Gas Fraction

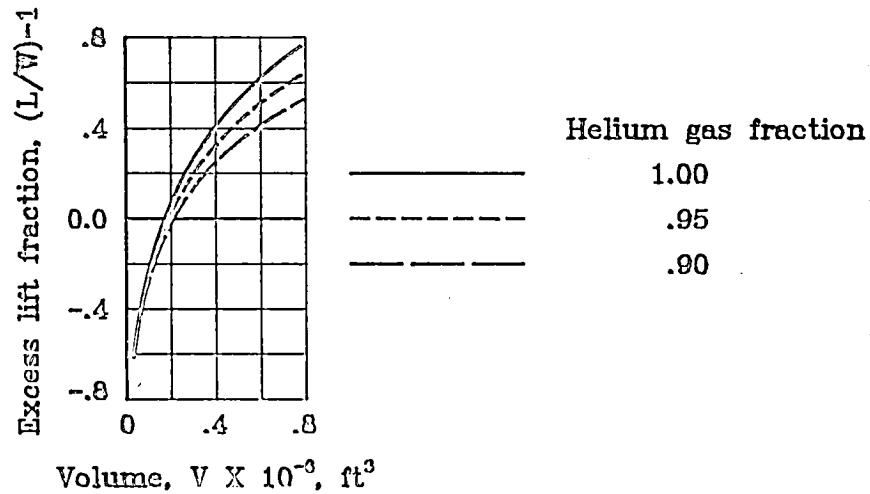


Figure 11.22 - Effect of helium gas fraction on microwave-powered HAAP blimp size.

Figure 11.22 shows that reasonable variations in the purity of the helium used as a lifting gas result only in small changes in blimp size.

#### 11.2.1.8 Superpressure

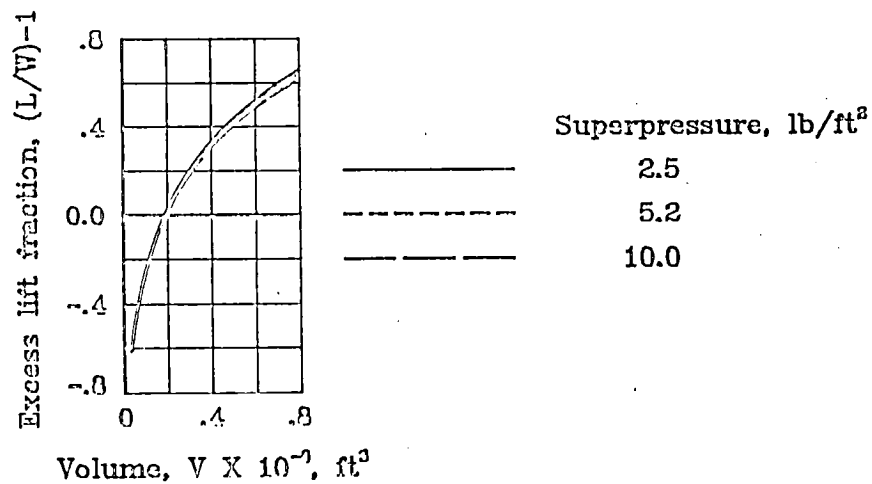


Figure 11.23 - Effect of design superpressure on microwave-powered HAAP blimp size.

Figure 11.23 shows that reasonable changes in HAAP blimp super-pressure have an insignificant effect on size and feasibility.

#### 11.2.2 General Remarks

A microwave-powered HAAP blimp can be relatively small in size, about the same size as a Goodyear blimp. There appears to be ample area in or on a conventionally configured blimp to house the required rectenna. With the exceptions of drag coefficient and payload weight, reasonable parametric variations had little effect on concept size or feasibility. Larger values for both drag coefficient and payload weight would result in a larger blimp, but the increase in size would not significantly compromise the feasibility of the concept.

#### 11.3 NUCLEAR-POWERED CONCEPT

The technology status of radioisotope thermonuclear generators and of nuclear reactor propulsion systems was discussed in detail in Chapter 6. Because of the uncertainty of the weights and power of these systems, especially with crashworthy shielding designed to provide environmental protection, the nuclear-powered HAAP blimp was analyzed parametrically.

Figure 11.24 illustrates the effect of propulsion system weight on the size of a nuclear-powered HAAP blimp. This figure indicates that theoretically, for a given nuclear propulsion system weight (characterized in terms of specific power, i.e., 10 W/lb) there is a blimp size that will accommodate that system. There is, of course, a practical limit to the construction size of such a vehicle. If a 20-W/lb nuclear system could be achieved, including radiator and shielding weights,

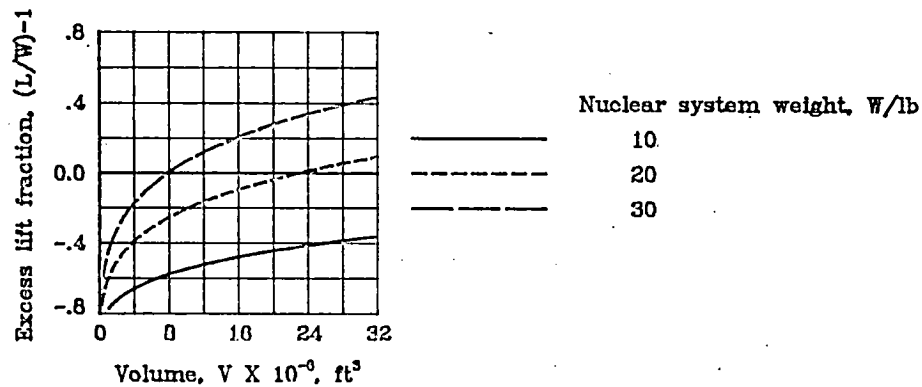


Figure 11.24 - Effect of propulsion system weight on nuclear-powered HAAP blimp size.

Figure 11.24 shows the HAAP blimp would have a volume of about 23 million  $\text{ft}^3$ . Table 11.4 summarizes the characteristics of a nuclear-powered HAAP blimp with a 20-W/lb propulsion system.

If the weights shown in Table 11.4 could be achieved safely, and without regulatory restraints, the nuclear-powered blimp would be the most flexible of the blimp concepts considered for performing the HAAP missions. Like the microwave powered blimp, the nuclear-powered vehicle could have a conventional single-body design; however, it could operate anywhere without the necessity of being close to a ground transmitter.

TABLE 11.4 -- SUMMARY CHARACTERISTICS OF A 20-WATT PER POUND  
NUCLEAR-POWERED HAAP BLIMP

Design conditions:

Altitude, ft	70,000
Cruise airspeed, ft/s	50
Maximum airspeed, ft/s	140
Stored energy, h	0
Payload power, W	1,000
Payload weight, lb	100
Structural weight fraction	0.33
Cruise drag coefficient, $C_D$	0.035

Motor size, hp	1,158
<u>Weights, lb</u>	

Propeller	232
Motor-gear	1,507
Payload	100
Nuclear system	49,989
Battery system	0
Power processing system	3,473
<u>Structure</u>	<u>27,238</u>
<u>Total weight</u>	<u>82,539</u>

Gas mass, lb	19,536
--------------	--------

Blimp dimensions:

Volume $\times 10^{-6}$ , ft <sup>3</sup>	23
Maximum diameter, ft	239
Length, ft	1,195
Reference (planform) area, ft <sup>2</sup>	185,500

Cruise Reynolds number	27,900,000
------------------------	------------

Daily energy required, kW-h	1,118
-----------------------------	-------

## CHAPTER 12

### HAAP AIRPLANE FEASIBILITY AND ANALYSIS

The idea of using a remotely piloted airplane to perform a variety of long-duration missions at very high altitudes has been discussed in the technical literature. Propulsion systems proposed for this High-Altitude Aircraft Platform (HAAP) have been based on the use of solar or microwave power. Some feasibility studies have been conducted on the use of each of these propulsion systems in a HAAP airplane, but a detailed comparison has not previously been published. The present analysis compares the relative feasibilities of solar-voltaic and microwave-powered HAAP airplane concepts using technologies appropriate to each concept that should be available within the next 5 to 7 years. In addition, a nuclear-powered HAAP vehicle has also been analyzed, but in less detail.

The HAAP airplane is to operate continuously over the United States at an altitude of 70,000 ft, and it must withstand environmental variations in the weather due to seasonal changes. The operational environment, as well as the technologies essential to a HAAP airplane, have been discussed in previous chapters. Chapter 10 includes a summary of the technology assumptions and a brief discussion of the airplane design philosophy of flying as close as possible to minimum power conditions.

The sizes of HAAP airplanes powered by solar-voltaic and by microwave power that might be technically feasible with a 100-lb payload are illustrated in Figure 12.1.



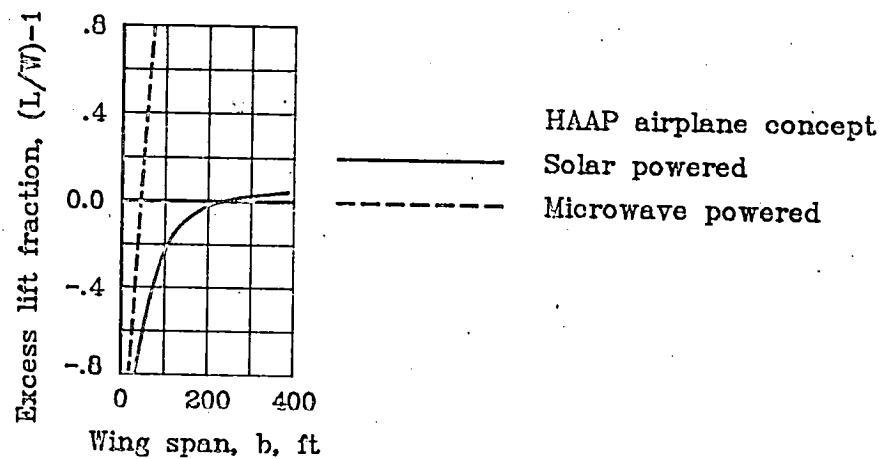


Figure 12.1 - HAAP airplane sizes.

## 12.1 SOLAR-POWERED CONCEPT

Figure 12.1 indicates that, from a weight analysis viewpoint, a solar-powered HAAP airplane would have a span of about 240 ft. The concept is sized to operate on days with only 8 hours of sunlight, which is about the smallest average number of daylight hours that would be encountered over the United States each year, and which constitutes the most severe operational case. During the daylight hours, the airplane is powered by solar cells mounted on its surfaces. During the 16 hours of darkness, the airplane is powered by a regenerative fuel cell system which is "charged" during the day. Table 12.1 summarizes some of the specific characteristics of this solar-powered HAAP airplane concept.

Note in Table 12.1 that it was necessary to increase the wing aspect ratio to 30 in order to obtain a feasible weight solution. A feasible design which performed the HAAP mission and used near-term technologies could not be obtained using an aspect ratio 20 wing. The structural

TABLE 12.1 - SOLAR-VOLTAIC POWERED HAAP AIRPLANE  
SUMMARY CHARACTERISTICS

Design conditions:

Altitude, ft	70,000
Cruise airspeed, ft/s	140
Design airspeed, ft/s	140
Incident energy flux, W/ft <sup>2</sup>	111
Solar cell efficiency	0.16
Stored energy, h	16
Payload power, W	1000
Payload weight, lb	100
Structural weight fraction	0.20

Airplane performance parameters:

Cruise lift coefficient, $C_L$	1.50
Cruise drag coefficient, $C_D$	0.038
Motor size, hp	30

Weights, lb

Propeller	6
Motor-gear	39
Payload	100
Solar cell	580
Fuel cell system	2294
Power processing system	107
<u>Structure</u>	<u>781</u>
Total weight	3907

Airplane geometry:

Aspect ratio	30
Span, ft	240
Wing planform area, ft <sup>2</sup>	1920
Solar cell area, ft <sup>2</sup>	8281
Wing loading, lb/ft <sup>2</sup>	2.0
Cruise Reynolds number	500,000
Daily incident energy required, kW-h	1070

weight fraction was increased to 0.20 from the 0.17 baseline value in Table 10.1 to meet the structural weight-wing area ratio requirement of  $0.4 \text{ lb/ft}^2$ . The concept operates at a constant airspeed of 140 ft/s. A significant result is that this specific HAAP concept needs an area of solar cells which is more than four times the wing planform area. (This area includes a 10-percent redundancy factor for the cells.) Although this is not an optimized concept, it is sufficiently close to one to recognize that this important solar cell area characteristic cannot be readily overcome. Figure 12.2 illustrates what a solar-voltaic HAAP might resemble conceptually. The solar-panel shown in the figure is analogous to a flat plate, and is not intended to provide lift, although there would be obvious weight and drag penalties.

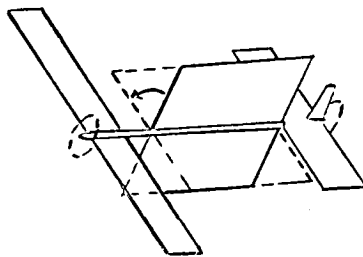


Figure 12.2 - An unconventionally configured solar-powered HAAP airplane concept.

This analysis can be compared with that performed by Phillips (ref. 7) for solar-powered aircraft which must operate in up to 16 hours of darkness. Phillips' study considered flight at 70,000 ft for airplanes of aspect ratio 20 and 30, but confined the location of the solar cells to the wing planform. In limiting the solar cells to the wing

planform area, the resultant wing loading was about  $0.83 \text{ lb/ft}^2$ .

Phillips assumes that the solar cells are kept normal to the rays of the Sun, which can be accomplished by the concept in Figure 12.3 by tilting the solar panel. A solar-powered airplane concept proposed by Phillips is presented in Figure 12.3.

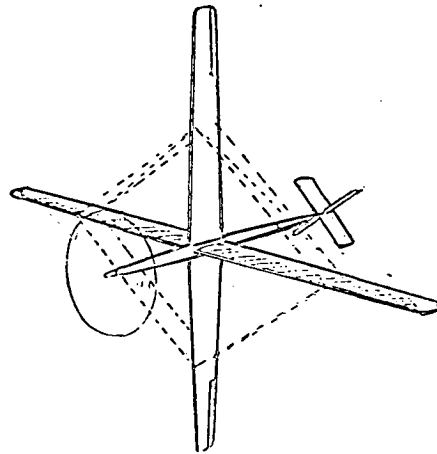


Figure 12.3 - A cruciform wing solar-powered airplane concept.

Phillips' cruciform wing concept permits banking the aircraft to maintain the solar cells perpendicular to the Sun line (the dashed lines in Fig. 12.3 indicate wire bracing). The true airspeed of this concept at 70,000-ft altitude is, at best, about 80 ft/s which is about 60 percent of the airspeed required to maintain station in performing the year-around HAAP mission.

#### 12.1.1 Parametric Variations

The feasibility of a solar-powered HAAP airplane concept is subject to change with changing technology assumptions. The following discussion

is presented to indicate the sensitivity of that feasibility with a few of the more important assumptions.

#### 12.1.1.1 Design Airspeed

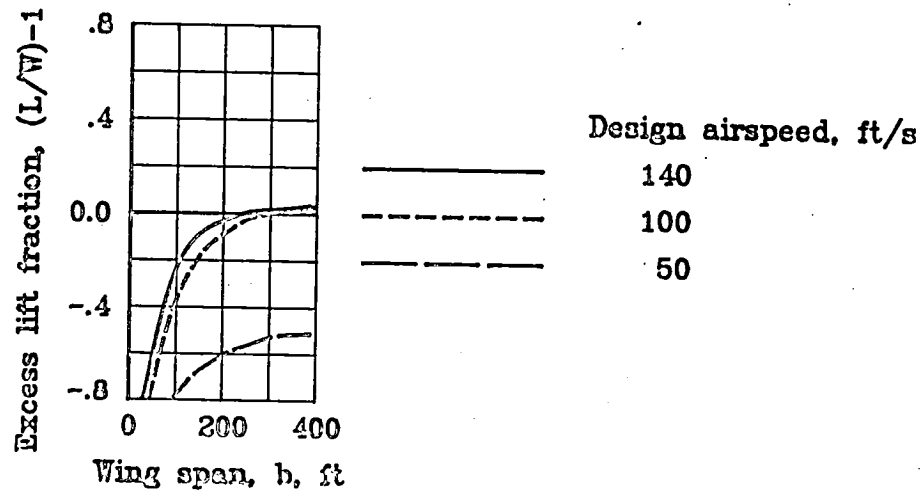


Figure 12.4 - Effect of design airspeed on solar-powered HAAP airplane size.

The effect of design airspeed on the size of a solar-powered HAAP airplane is shown in Figure 12.4. Lower design airspeeds result in larger aircraft with little beneficial change in the ratio of solar cell area required to wing area available.

### 12.1.1.2 Maximum Operating Lift Coefficient

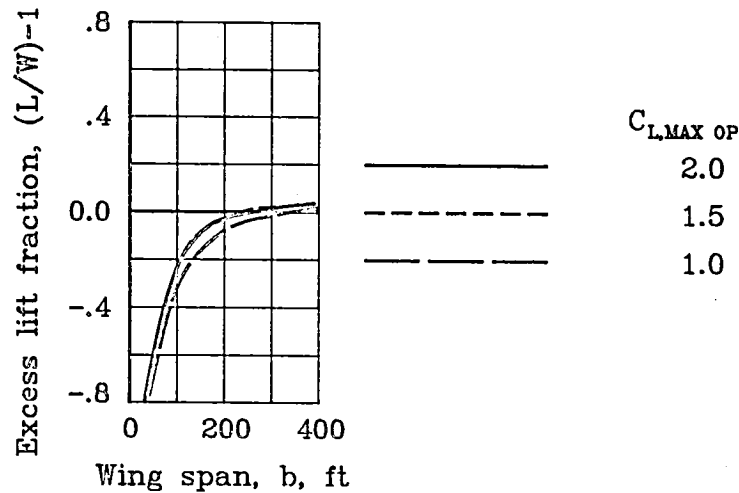


Figure 12.5 - Effect of maximum operating lift coefficient on solar-powered HAAP airplane size.

Figure 12.5 indicates that, if airfoil development was to provide an airfoil capable of operating up to a  $C_L$  of 2.0, there would be negligible change in the span from the airfoil with  $C_{L,max op} = 1.50$ . This is because the baseline aspect ratio 30 airplane wants to fly at  $C_L = 1.55$  for minimum power flight. Limiting the 1.55 value of  $C_L$  to 1.50 has little impact; however, limiting  $C_{L,max op}$  to 1.00 changes the span to about 340 ft, a 40-percent increase in span. A HAAP designed to operate at  $C_L = 1.00$  as compared to 1.50 reduces the solar cell area required to about 2.5 times from about 4.3 times the wing area; however, the airplane weight increases from 3900 to about 5200 lb.

### 12.1.1.3 Profile Drag Coefficient, $C_{D,0}$

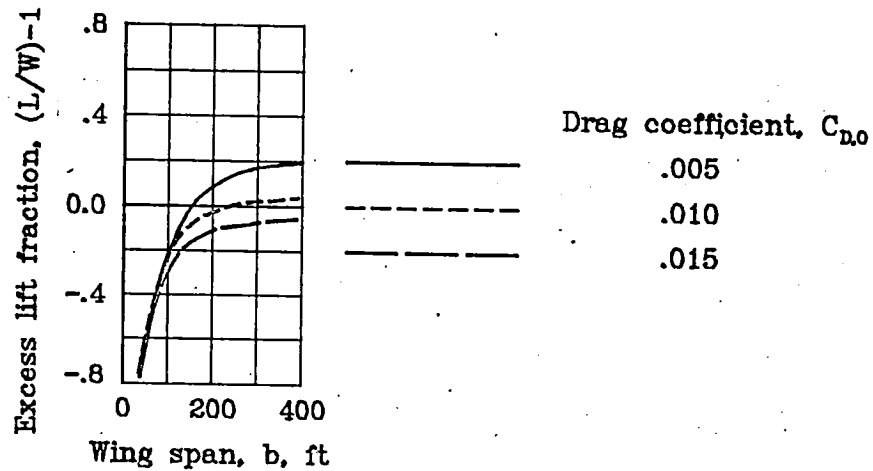


Figure 12.6 - Effect of drag coefficient on solar-powered HAAP airplane size.

If the baseline profile drag coefficient assumed for this study ( $C_{D,0} = 0.010$ ) could be reduced to 0.005, the resultant HAAP airplane span (Fig. 12.6) would be reduced about 33 percent and the airplane would weigh about 65 percent less. The smaller airplane would still need more than twice the wing planform area for solar cells. A  $C_{D,0}$  of 0.015 results in an exceptionally large vehicle.

#### 12.1.1.4 Propeller Efficiency

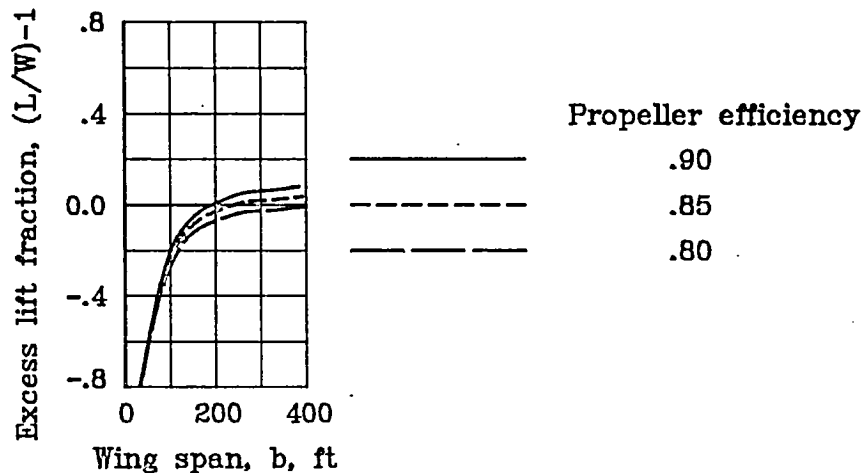


Figure 12.7 - Effect of propeller efficiency on solar-powered HAAP airplane size.

Figure 12.7 shows that relatively small changes in the propeller efficiency can significantly affect the design of a solar-powered HAAP airplane. A propeller efficiency of 0.90 (where the baseline efficiency was 0.85) can reduce the span from 240 ft to 185 ft and vehicle weight from 3900 to 2300 lb. A propeller efficiency of 0.80 results in a 400-ft span, 11,000-lb vehicle. The propeller efficiency has little effect on the ratio of solar cell area to wing planform area.



#### 12.1.1.5 Solar Cell Efficiency

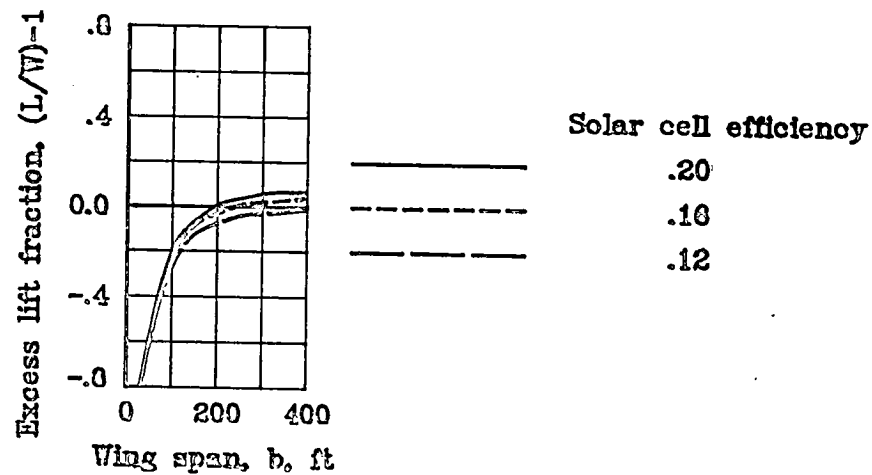


Figure 12.8 - Effect of solar cell efficiency on solar-powered HAAP airplane size.

The operating efficiency of the solar cell array can significantly affect the HAAP airplane size. Sixteen-percent efficient cells were assumed in this study. Figure 12.8 shows that 20-percent efficient solar cells would result in a 2600-lb vehicle with a 195-ft wing span. The relative solar cell area needed is still quite large, 3.5 times the wing planform.

#### 12.1.1.6 Incident Solar Power

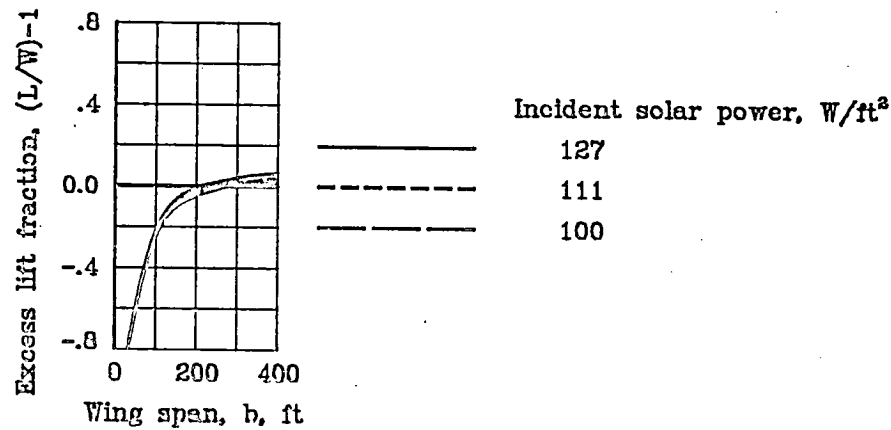


Figure 12.9 - Effect of incident solar power on solar-powered HAAP airplane size.

One assumption in this study is that the energy from the Sun incident to the solar cells would average about 111  $W/ft^2$ . This value includes the Sun declination angle, which varies considerably over the year as well as misalignment due to maneuvering while in flight. As shown in Figure 12.9 if a value of 100  $W/ft^2$  were assumed, the span would increase to about 280 ft and the weight to about 5300 lb which may be compared to the baseline value of 111  $W/ft^2$  and the resultant 240-ft span, 3900-lb aircraft. The value of 127  $W/ft^2$  represents about the maximum possible incident energy and results in a 2900-lb aircraft with a 205-ft span. With 127  $W/ft^2$  incident on the airplane, 3.8 times the available wing area is required for solar cells.

#### 12.1.1.7 Fuel Cell Weight

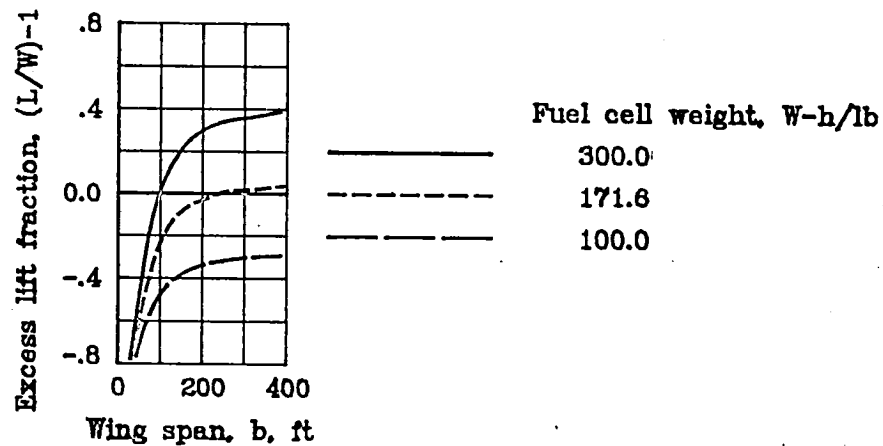


Figure 12.10 - Effect of fuel cell weight on solar-powered HAAP airplane size.

Current estimates of regenerative fuel cell system weights vary widely since these systems are in an early stage of development. The 171.6 W-h/lb system used in this study is thought to be representative of this device when introduced into operation for an 8-hour charge, 16-hour discharge cycle. Figure 12.10 shows that a 300 W-h/lb system would reduce the HAAP airplane substantially, to a 100-ft span, 700-lb aircraft. The weight of the fuel cell system is reduced from about 2300 lb in the baseline configuration to about 300 lb. The solar cell area needed on the smaller aircraft is about 5 times that available on the wing planform.

#### 12.1.1.8 Structural Weight-Wing Area Ratio

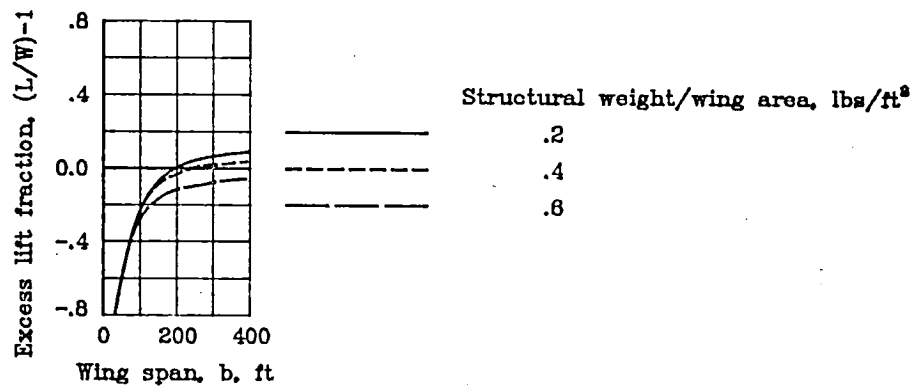


Figure 12.11 - Effect of structural weight-wing area ratio solar-powered HAAP airplane size.

The ratio of the structural weight to wing area is an important constraint on the design of the HAAP vehicle. In sizing the vehicle, weight is added to the structure until the ratio requirement is met or slightly exceeded. The  $0.4 \text{ lb/ft}^2$  value used in this study is thought to be reasonable with the use of advanced construction techniques and high-strength ultra-lightweight materials. If unforeseen technological advances permit a  $0.2 \text{ lb/ft}^2$  flight vehicle (Fig. 12.11), it could be as small as 195 ft span and weigh about 2600 lb. If a more detailed structural analysis led to greater structural weight (i.e.,  $0.60 \text{ lb/ft}^2$ ), the size would increase considerably.

### 12.1.1.9 Payload Weight

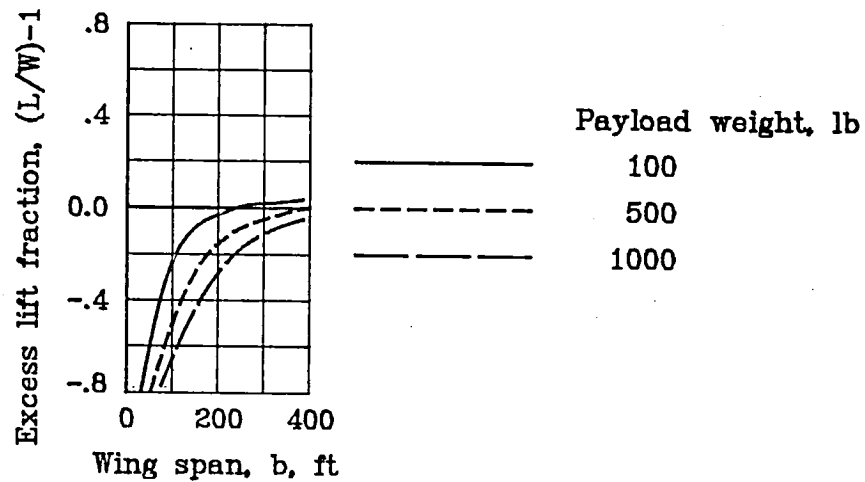


Figure 12.12 - Effect of payload weight on solar-powered HAAP airplane size.

If a heavier payload was required, the HAAP would increase in size.

Figure 12.12 shows that a 500-lb payload requirement would result in a 400-ft span vehicle weighing about 11,000 lb.

### 12.1.1.10 Aspect Ratio

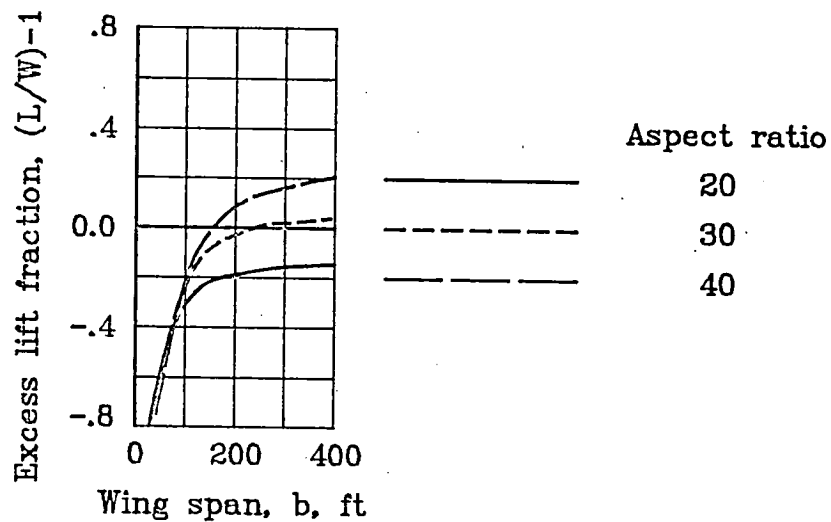


Figure 12.13 - Effect of aspect ratio on solar-powered HAAP airplane size.

Figure 12.13 shows the effect of wing aspect ratio on the HAAP airplane size with the Oswald's airplane efficiency factor held at a constant value of 0.85. In practice, increasing aspect ratio, on an otherwise fixed configuration, decreases the Oswald efficiency. A solar-powered HAAP of reasonable wing span would need a wing aspect ratio near 30. If it were possible to build an aspect ratio 40 aircraft using the technology assumptions of this study, Figure 12.13 shows that the wing span could be reduced to about 153 ft and vehicle weight to about 1200 lb. However, the concern about excessive solar cells would not be reduced; 4 times the wing planform area would be required.

#### 12.1.1.11 Oswald's Airplane Efficiency Factor

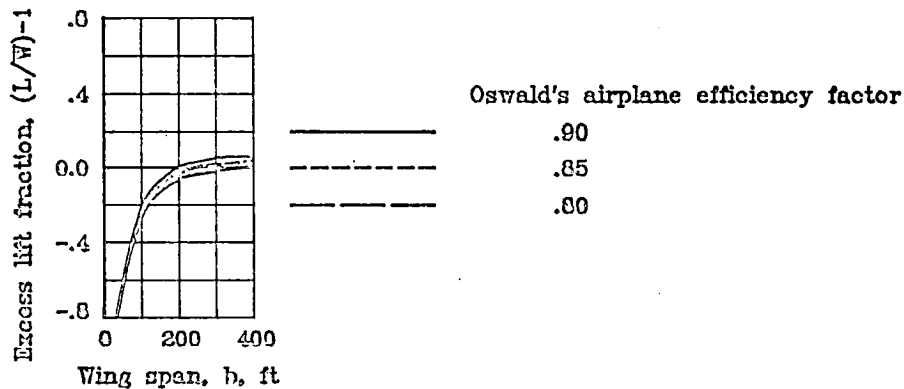


Figure 12.14 - Effect of Oswald's airplane efficiency factor on solar-powered HAAP airplane size.

An Oswald's airplane efficiency factor (e) of 0.85 was assumed for an aerodynamically refined flight concept with a wing aspect ratio (A)

of 30. The product of aspect ratio and  $e$  may be considered as an effective aspect ratio in the following equation:

$$C_D = C_{D,0} + \frac{C_L^2}{\pi e A} \quad (8.9)$$

where

- $C_D$             total drag coefficient
- $C_{D,0}$         profile drag coefficient
- $A$              wing aspect ratio
- $e$              Oswald's airplane efficiency factor

It is readily seen in the equation that as the  $eA$  term increases, the total drag coefficient decreases. With  $A$  held constant at 30 (Fig. 12.14), the airplane size varies from about a 195-ft span to a 370-ft span vehicle as the Oswald's efficiency factor changes from 0.90 to 0.80, respectively. The relative solar cell area required is essentially unchanged.

#### 12.1.2 General Remarks

A primary concern in the design of a solar-powered HAAP airplane is the excessive area needed for the solar cell arrays. The general design philosophy used in this study is to design the aircraft to fly at minimum power. This design philosophy provides a smaller vehicle, but does not provide for minimizing the amount of excess solar cells. The minimal amount of excess solar cells, that is, minimizing the required cell area to wing area ratio, is obtained when this HAAP is designed to operate at a lift coefficient of approximately 1; however, the resulting airplane

concept is quite large, with a span of about 340 ft and weight of about 5200 lb. The associated cell area-wing area ratio is about 2.5.

The solar-powered aircraft could meet the requirements of housing all the needed solar cells on the wing (with 10 percent redundancy) if it would fly with 24 hours of sunlight. Its airspeed would be about a constant 120 ft/s, which is slightly less than that required for the HAAP mission scenarios. The corresponding span would be about 65 ft, and without any need for energy storage, it would weigh about 200 lb.

An important footnote to the analysis of solar-powered HAAP airplanes is that when attempting to confine the required solar cell area to that of the combined wing and tail planform, decreasing the number of daylight hours must be generally compensated by reducing the airspeed.

## 12.2 MICROWAVE-POWERED CONCEPT

Figure 12.1 indicates that a microwave-powered HAAP airplane would have a wing span of about 50 ft. The concept is sized to operate entirely on rectified microwave power that is continuously beamed to the aircraft; and requires no stored energy in its operation. Table 12.2 summarizes some of the HAAP microwave-powered airplane characteristics.

The microwave-powered HAAP operates at a constant 140 ft/s and needs about 90 percent of the wing planform for rectenna installation (including 10 percent redundancy). Note in Table 12.2 that a structural weight fraction of 0.24 was needed to meet the structure weight-wing area requirement of  $0.4 \text{ lb/ft}^2$ . A microwave-powered HAAP might resemble a conventional sailplane as illustrated in Figure 12.15.



TABLE 12.2 - MICROWAVE-POWERED HAAP AIRPLANE  
SUMMARY CHARACTERISTICS

Design conditions:

Altitude, ft	70,000
Cruise airspeed, ft/s	140
Design airspeed, ft/s	140
Incident energy flux, W/ft <sup>2</sup>	37
Rectenna efficiency	0.80
Stored energy, h	0
Payload power, W	1000
Payload weight, lb	100
Structural weight fraction	24

Airplane operating parameters:

Cruise lift coefficient, $C_L$	1.27
Cruise drag coefficient, $C_D$	0.040
Motor size, hp	2

Weights, lb

Propeller	2
Motor-gear	4
Payload	100
Rectenna	4
Battery system	0
Power processing system	24
Structure	41
Total weight	173

Airplane geometry:

Aspect ratio	20
Span, ft	45
Wing planform area, ft <sup>2</sup>	101
Rectenna area, ft <sup>2</sup>	93
Wing loading, lb/ft <sup>2</sup>	1.7
Cruise Reynolds number	150,000
Daily incident energy required, kW-h	60

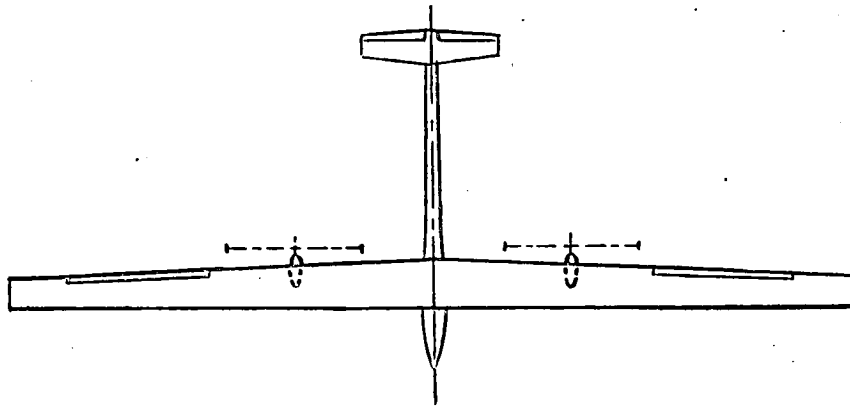


Figure 12.15 - A microwave-powered HAAP airplane concept.

This concept resembles that proposed by Heyson (ref. 8) for a microwave sailplane which operated in a powered-unpowered flight mode in performing selected HAAP missions. Heyson employed an aspect ratio 30 wing and had a heavier payload (1100 lb), resulting in a 190-ft span, 3500-lb vehicle.

#### 12.2.1 Parametric Variations

The feasibility of a microwave-powered HAAP airplane concept is subject to change with changing technology assumptions. The following discussion is presented to indicate the sensitivity of that feasibility to a few of the more significant assumptions.

### 12.2.1.1 Maximum Operating Lift Coefficient

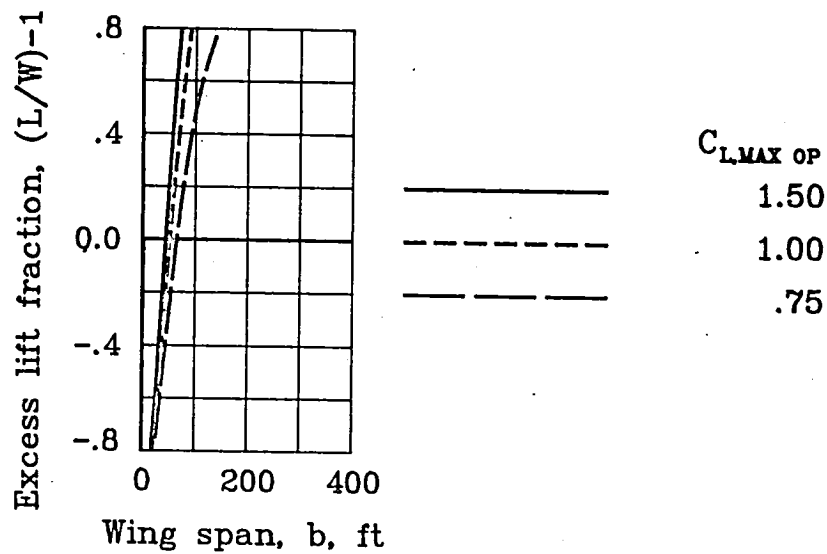


Figure 12.16 - Effect of maximum operating lift coefficient on microwave-powered HAAP airplane size.

An aspect ratio 20 airplane with a  $C_{D,0}$  of 0.010 if designed for minimum power flight, wants to fly at a  $C_L$  of 1.27. The maximum operating lift coefficient of 1.50 assumed for this study permits a minimum power design concept. As shown in Figure 12.16, if maximum operating lift coefficient is limited to a value less than 1.27, the HAAP airplane span and weight increases. A  $C_{L,max\ op}$  of 1.00 results in a 55-ft span, 200-lb vehicle. A  $C_{L,max\ op}$  of 0.75 results in a 70-ft span, 240-lb HAAP airplane.

### 12.2.1.2 Profile Drag Coefficient, $C_{D,0}$

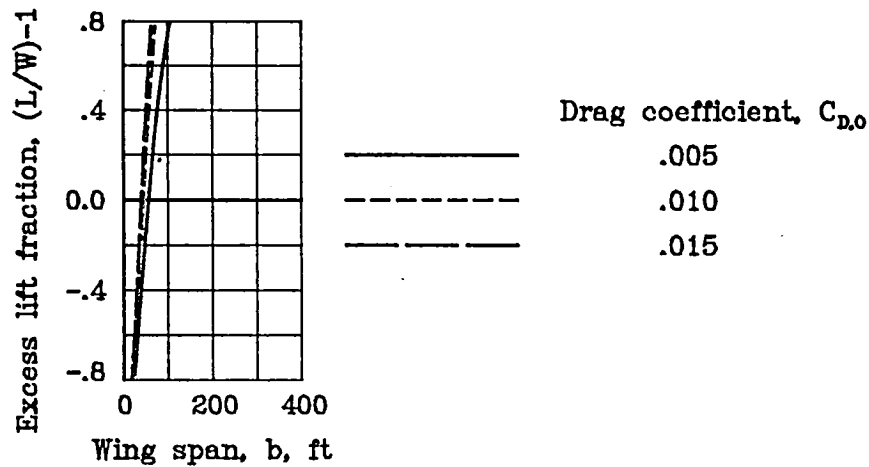


Figure 12.17 - Effect of profile drag coefficient on microwave-powered HAAP airplane size.

Changes in profile drag coefficient indicate that as this drag value increases, the wing span decreases. Equation (10.1) (page 100), which governs minimum-power flight, explains the behavior.

$$C_L = \sqrt{3 A e C_{D,0}} \quad (10.1)$$

where

- A wing aspect ratio
- e Oswald's airplane efficiency factor
- $C_{D,0}$  profile drag coefficient

Profile drag coefficients of 0.005, 0.010, and 0.020 lead to  $C_L$  values of 0.90, 1.27, and 1.50 ( $C_{L,max}$ ), respectively, for the aspect ratio 20 concept. For the same lifting capability, the lower  $C_L$

value requires more wing area, and correspondingly, more span. The span increases shown in Figure 12.17 (with decreases in  $C_{D,0}$ ) are associated with increases in vehicle weight from about 170 lb to about 195 lb. The effect of  $C_{D,0}$  on the required rectenna area is far more important. The ratio of rectenna area-wing planform area is about 0.5 for  $C_{D,0} = 0.005$ , 0.9 for  $C_{D,0} = 0.010$ , and 1.3 for  $C_{D,0} = 0.020$ . The 10-percent rectenna redundancy factor is included in this analysis. Thus, for  $C_{D,0}$  values much greater than 0.010, area in addition to the wing planform must be used to locate the rectenna.

#### 12.2.1.3 Propeller Efficiency

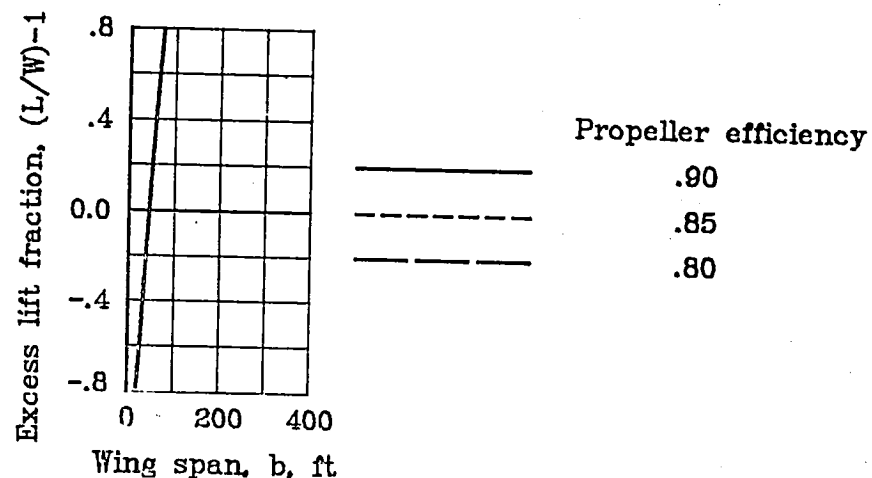


Figure 12.18 - Effect of propeller efficiency on microwave-powered HAAP airplane size.

As shown in Figure 12.18, reasonable changes in propeller efficiency have negligible impact on the concept span or weight. The decrease in efficiency requires a larger percentage of the wing for very lightweight

rectenna. A propeller efficiency of 0.90 requires about 89 percent of the wing planform for rectenna, whereas an efficiency of 0.80 requires about 95 percent.

#### 12.2.1.4 Rectenna Efficiency

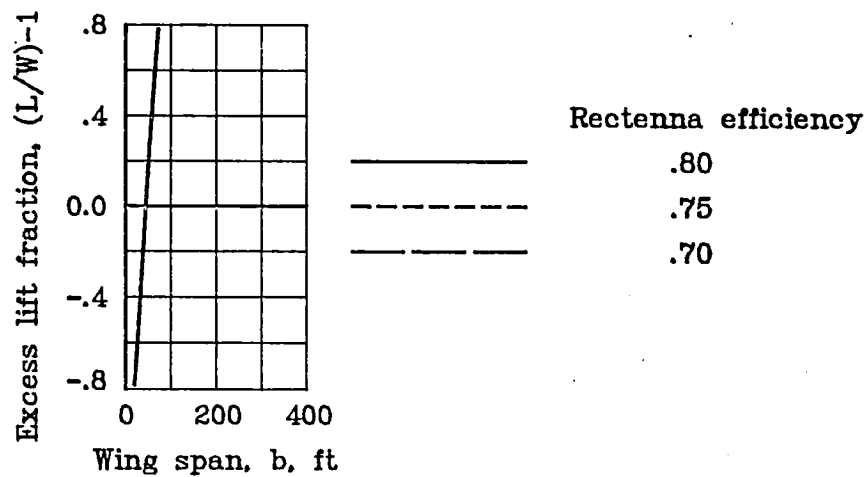


Figure 12.19 - Effect of rectenna efficiency on microwave-powered HAAP airplane size.

Figure 12.19 shows that reasonable changes in rectenna efficiency have negligible effect on the HAAP airplane span or weight. Reductions in rectenna efficiency increase the rectenna area required. A rectenna conversion efficiency of 0.80, for example, leads to using about 92 percent of the wing planform for rectenna. An efficiency of 0.70 requires about 5 percent more area for rectenna than is available on the wing.

### 12.2.1.5 Incident Microwave Power

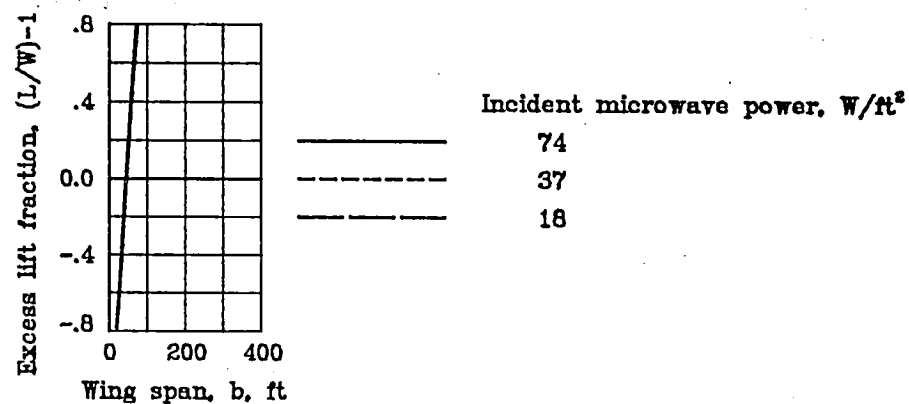


Figure 12.20 - Effect of incident microwave power on microwave-powered HAAP airplane size.

Figure 12.20 shows that if the microwave energy incident to the HAAP airplane were doubled (74.0 W/ft<sup>2</sup>) or about halved (18.0 W/ft<sup>2</sup>) from the 37.0 W/ft<sup>2</sup> baseline value used in this study, the impact on vehicle span and weight would be small. For example, an 18.0 W/ft<sup>2</sup> beam increases vehicle weight by about 10 lb to a 180-lb vehicle. The effect incident power has on required rectenna area is more dramatic. A 74 W/ft<sup>2</sup> beam needs less than half of the wing planform for rectenna, whereas an 18 W/ft<sup>2</sup> beam requires about 85 percent more area for rectenna than is available on the wing.

#### 12.2.1.6 Structural Weight-Wing Area Ratio

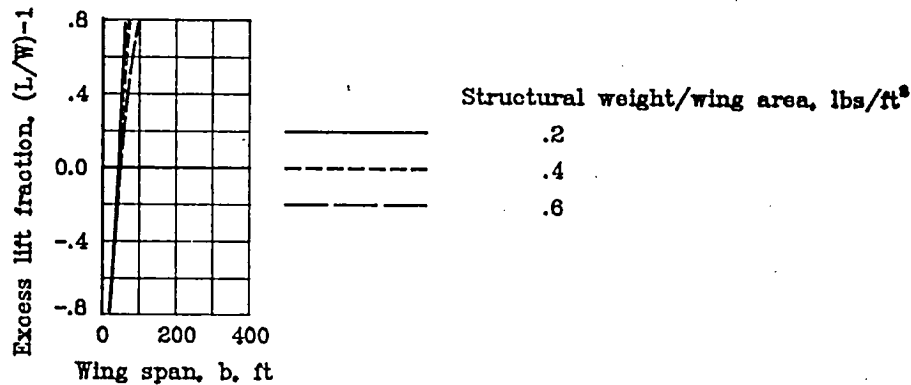


Figure 12.21 - Effect of structural weight-wing area ratio on microwave-powered HAAP airplane size.

Figure 12.21 shows that the structural weight-wing area requirement has relatively little impact on the HAAP airplane feasibility. If current construction technology, which requires about  $0.6 \text{ lb/ft}^2$  was used, the HAAP airplane would be about 50 ft in span and weigh about 210 lb.

#### 12.2.1.7 Payload Weight

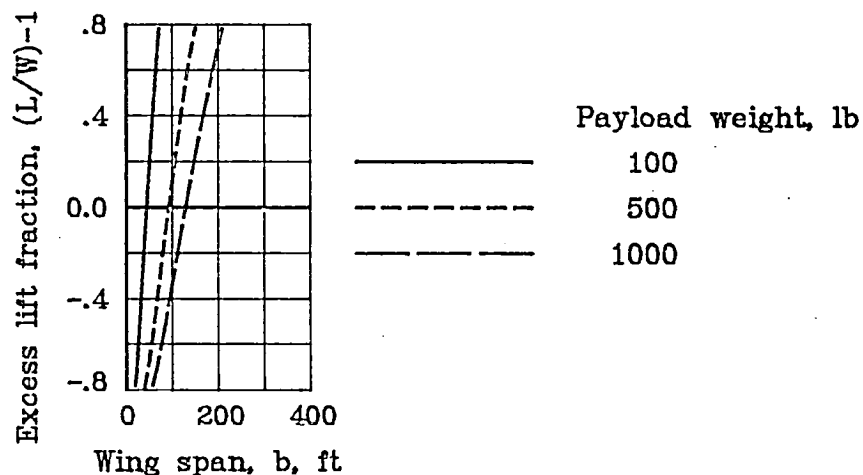


Figure 12.22 - Effect of payload weight on microwave-powered HAAP airplane size.



A microwave-powered HAAP airplane designed for a heavier payload would, of course, be larger. Figure 12.22 shows that designing for a 500-lb payload would result in a 95-ft span, 750-lb vehicle. A 1000-lb payload design would result in a 130-ft span HAAP weighing about 1450 lb. Because of the relatively small size of the vehicle, payload weight has a major impact on gross weight.

#### 12.2.1.8 Aspect Ratio

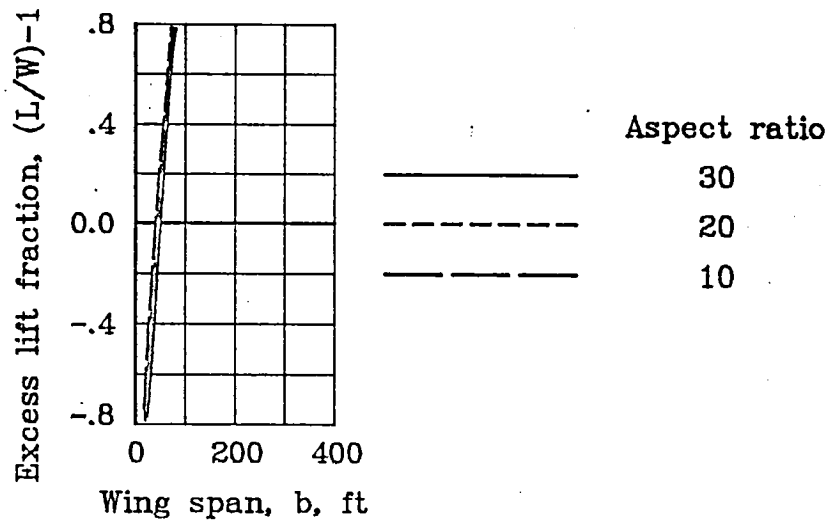


Figure 12.23 - Effect of aspect ratio on microwave-powered HAAP airplane size.

Figure 12.23 shows the effect of wing aspect ratio on the microwave-powered HAAP airplane span while holding the Oswald efficiency constant at 0.85. Increasing aspect ratio from 20 to 30 results in slightly greater wing span (4 ft), and somewhat less weight (9 lb) and planform area (21 ft<sup>2</sup>). The reduction in wing area due to improved aerodynamic performance also reduces the area available for rectenna. Thus, the

aspect ratio 30 configuration requires 100 percent of the planform for rectenna. In contrast, the aspect ratio 10 concept is about 30 lb heavier than the baseline (aspect ratio = 20) concept with about 67 ft<sup>2</sup> more planform. This results in more than ample area for rectenna; only 76 percent of the planform is required for the rectenna.

#### 12.2.1.9 Oswald's Airplane Efficiency Factor

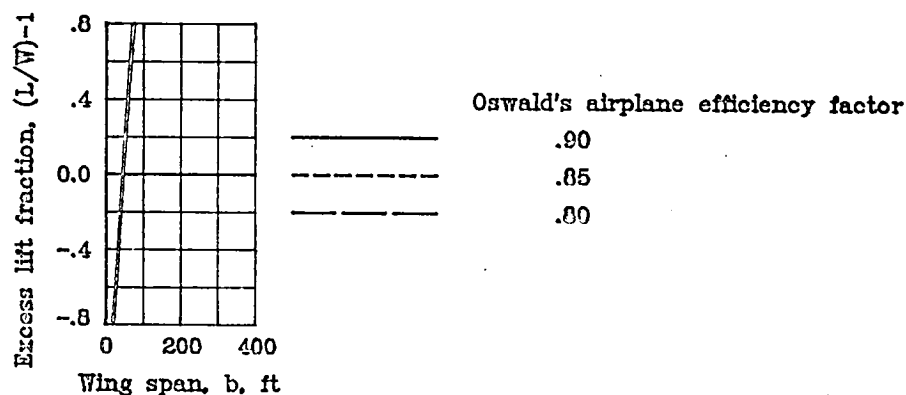


Figure 12.24 - Effect of Oswald's airplane efficiency factor on microwave-powered HAAP airplane size.

As shown in Figure 12.24, reasonable variation in Oswald's airplane efficiency has little effect on the microwave-powered HAAP airplane. Span remains the same, within a few feet. Weight remains the same within a few pounds. The rectenna and wing planform area vary somewhat, but the wing planform always provides at least 5 percent more area than required to house the rectenna.

#### 12.2.2 General Remarks

The feasibility of a microwave-powered HAAP is relatively insensitive to reasonable variations in parameters, with the obvious exception

of payload weight. The primary design concern with varying some parameters is that the area required for housing the rectenna may exceed the wing area. For the few conditions when excessive rectenna area would be required, the excess appears sufficiently reasonable that the additional rectenna could be located on the fuselage and tail surfaces without unduly compromising the design.

Design of a microwave-powered HAAP airplane for heavier, but still reasonable, payloads also appears feasible with no special concerns associated with the heavier payloads.

### 12.3 NUCLEAR-POWERED CONCEPT

The technology status in nuclear power systems possibly suitable for HAAP propulsion was discussed in detail in Chapter 5. Some literature surveyed on this subject indicated, but did not specify, that perhaps the technology in radioisotope thermoelectric generator (RTG) systems might be more advanced than the published (unclassified) literature indicates. Because of this uncertainty and because the unclassified literature indicated near-term technologies incapable of providing a feasible aircraft, the nuclear-powered HAAP concept was analyzed parametrically.

Figure 12.25 indicates that an aspect ratio 20 airplane capable of performing the HAAP mission must have a nuclear system specific power approaching 15 W/lb. The value for system specific power contains all components of the nuclear system, including radiator and shielding.

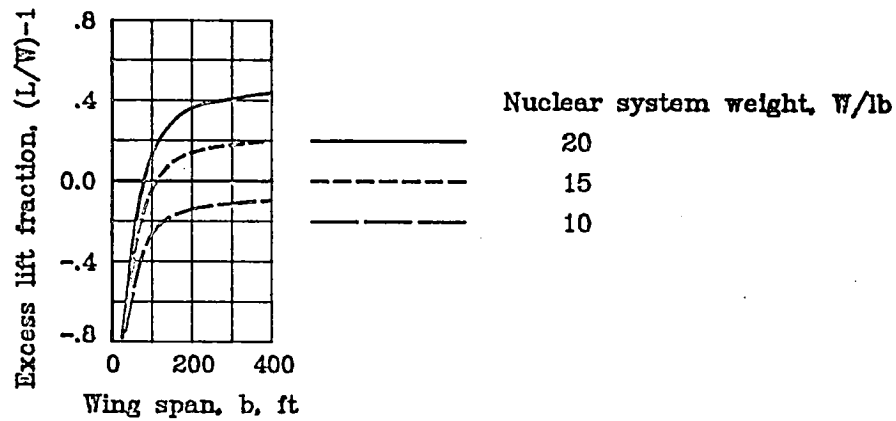


Figure 12.25 - Effect of propulsion system weight on the feasibility of a nuclear-powered HAAP airplane.

Table 12.3 summarizes the characteristics of a nuclear-powered HAAP airplane contingent on a 15 W/lb nuclear propulsion system.

Theoretically, an aspect ratio 30 airplane could perform the HAAP mission with a nuclear system specific power of 10 W/lb. This airplane would have a wing span of about 180 ft and would weigh about 2200 lb.

In performing HAAP missions, the nuclear-powered concept would be the most flexible of the propulsion systems discussed. It would share the advantage of the microwave system in that it would not require batteries. In addition, its operation would not require proximity to a ground station. If the systems weights could be achieved, and if it could be done safely and without regulatory restraints, this would be the optimum system.

TABLE 12.3 - SUMMARY CHARACTERISTICS FOR A 15-WATT PER POUND  
NUCLEAR-POWERED HAAP AIRPLANE CONCEPT

Design conditions:

Altitude, ft	70,000
Cruise airspeed, ft/s	140
Design airspeed, ft/s	140
Stored energy, h	0
Payload power, W	1000
Payload weight, lb	100
Structural weight fraction	0.24

Airplane operating parameters:

Cruise lift coefficient, $C_L$	1.27
Cruise drag coefficient, $C_D$	0.038
Motor size, hp	12

Weights, lb

Propeller	2
Motor-gear	15
Payload	100
Nuclear propulsion system	746
Power processing system	54
Structure	290
Total weight	1207

Airplane geometry:

Aspect ratio	20
Span, ft	120
Wing planform area	720
Wing loading, lb/ft <sup>2</sup>	1.7
Cruise Reynolds number	390,000
Daily energy required, kW-h	269

## CHAPTER 13

### LAUNCH CONSIDERATIONS

The current study has placed considerable emphasis on the feasibility of operating a remotely piloted, high-altitude aircraft platform (HAAP) in a year-around, 70,000-ft altitude environment. Primary emphasis has been on operation at the design altitude; however, there are constraints in low-altitude operation which affect the launch and climb to design altitude. A brief discussion of methods for launching the HAAP to operating altitude is now provided.

#### 13.1 BLIMPS

At launch, the blimp envelope is almost empty; yet, at operational altitude it is fully inflated and pressurized. Methods proposed in the literature to accomplish this transition are similar in technique. The fundamental procedures common to the launch of a superpressure blimp are discussed by Eney in reference 109 (which also includes some photographs of blimp model deployment tests). Figure 13.1 simplistically illustrates in five steps this deployment technique.

In step 1 (Fig. 13.1) the amount of helium needed for full, superpressured inflation at 70,000 ft is encapsulated in a bubble in the stern end, and contained by a reefing collar. The whole HAAP blimp system slowly lifts until at an appropriate point (step 2) the reefing collar is jettisoned, and the entire unit is allowed to rise freely. As it rises in altitude, the helium expands (step 3) to fill the entire shape (step 4) and reach equilibrium at 70,000 ft (step 5). At

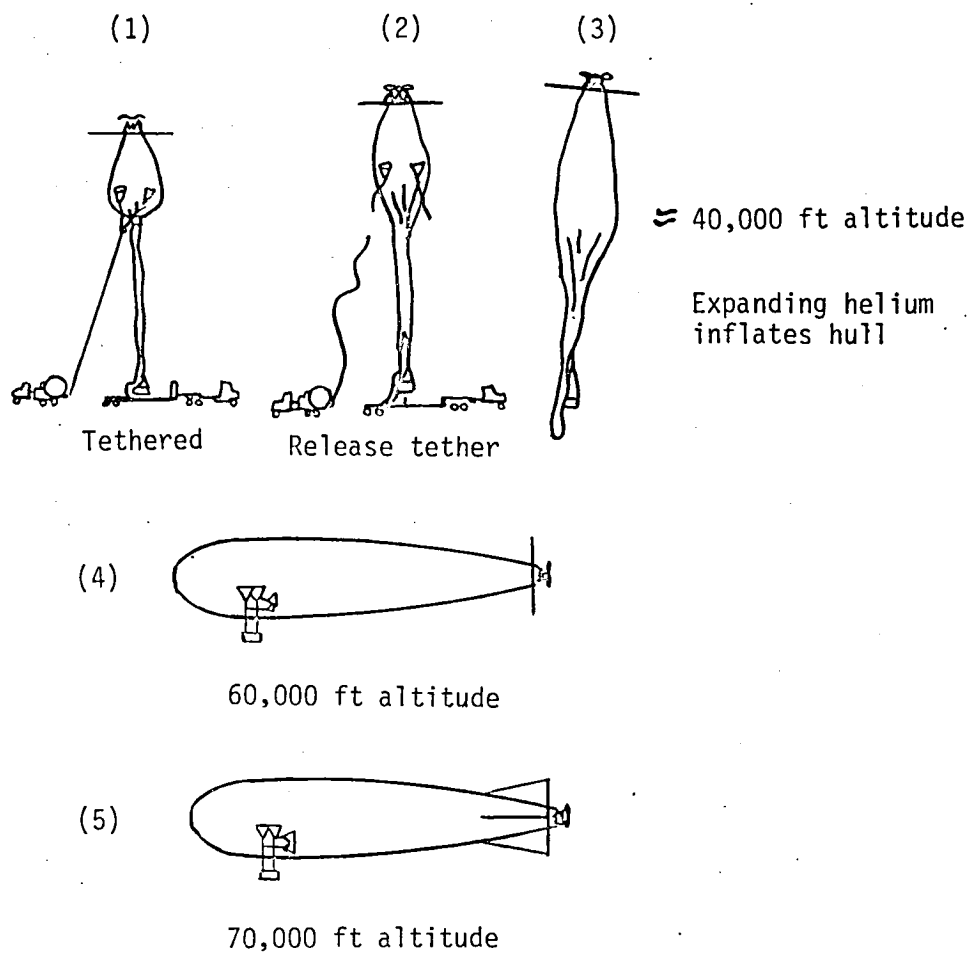


Figure 13.1 - A superpressure blimp launch sequence.

70,000 ft the fins would unfurl and mission operations would begin.

It should be noted that Figure 13.1 illustrates a fundamental launch process for superpressure blimps, and that some modifications (with considerable thought in its detailed design) may be required to facilitate a specific propulsion system. A microwave-powered concept, for example, might employ a collapsible rectenna system that is vertically mounted and extends the entire length within the blimp envelope. It might begin its launch sequence with a modified version of step (2) in Figure 13.1. The rectenna would unfold as the envelope expanded with increasing altitude. Another suggestion for the launch of a microwave-powered blimp is to attach the rectenna to pressurized splines extended inside the envelope, so that collapsing the rectenna becomes unnecessary. In launching a solar-powered HAAP blimp, the specific techniques used would be chosen to minimize possible damage to the solar cells. A nuclear-powered concept might be launched in accordance with Figure 13.1, since the propulsion unit would be housed in a rigid container either internal or external to the envelope.

Variations of the fundamental launch scheme illustrated in Figure 11.1 have also been proposed. Excess initial-helium inflation has been suggested to decrease ascent time (with no excess gas, ascent would take about 1 hour). Helium gas bleed-off would occur with altitude gain. To decrease ascent time, the no-excess-gas blimp concept could also be towed to higher altitudes by an airplane.



Rapid launch addresses the concern for the blimp drifting into the flight paths of other aircraft. Tethering could be used during the ascent phase at lower altitudes to prevent drift; however, because of its weight, the tethering line would have to be severed at some reasonable distance from the ground. The concern for excessive drift could be alleviated by using an airborne control station to guide the blimp into range of the ground control station. Excessive drift by a microwave-powered HAAP poses an additional concern since the power source, which is also ground-based, would also be out-of-range. The microwave-powered concept might necessitate an energy storage system, entailing additional weight for the batteries, to provide sufficient power to get within transmission range. This battery system could be expendable; that is, used only during critical launch phases and then ejected, but the associated ground hazard would appear to limit launch regions. It has also been suggested that weather balloons might be released prior to HAAP blimp launch to either indicate its launch path or to determine a desirable launch site.

It appears that the successful launch of a HAAP superpressure blimp concept will require considerable design detail, and special packaging techniques depending on the propulsion system. Even if modifications to facilitate launch enlarges the baseline concept, its technical feasibility should not be jeopardized.

## 13.2 Airplanes

The launch of a HAAP airplane poses different concerns than those for a HAAP blimp. The HAAP is designed to operate efficiently and perform its missions at 70,000-ft altitude, but may be launched and required to climb near sea level, where the atmospheric density is 10 times that at the design condition. The following text discusses some concerns associated with the launch of HAAP airplanes with various propulsion systems.

### 13.2.1 Solar-Powered

The launch of a solar-powered HAAP airplane was not discussed in detail in the available literature. Parry (ref. 6, page 6) implies a conventional take-off, and for his design concept, sea level airspeed is limited to less than 12 ft/s.

The current study indicates that airspeeds of about 80 ft/s can be achieved at sea level at a  $C_L$  of about 0.3, if the design propeller efficiency of 0.85 is assumed. This assumption is questionable, however, since propeller efficiency is known to be a function of airspeed; that is, the propeller designed to operate at the HAAP operational airspeed of 140 ft/s could suffer substantial reduction in propeller efficiency when operating at lower airspeeds, such as 80 ft/s. The loss in propeller efficiency during launch could be a major factor in establishing launch methods since climb rates would also be reduced. Propeller efficiency relationships are discussed by Perkins and Hage (ref. 110, pages 147 to 150). Propeller efficiency,  $\eta_p$ , is a function of advance ratio,  $J$ , and the relationship is illustrated in Figure 13.2.

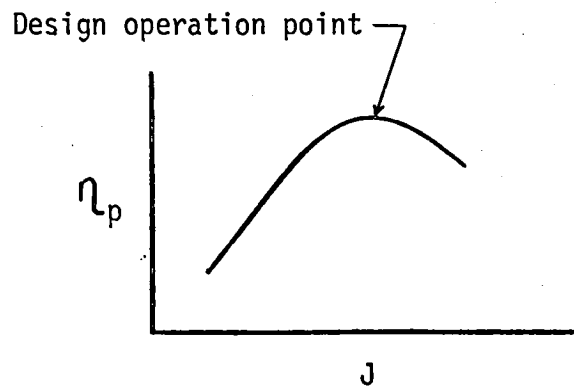


Figure 13.2 - Illustration propeller efficiency variation.

Figure 13.2 illustrates an approximate propeller efficiency relationship where

$\eta_p$	propeller efficiency
$J$	advance ratio, $J = \frac{v}{nd}$
$v$	airspeed (ft/s)
$n$	propeller rotational speed (revolutions/s)
$d$	propeller diameter (ft)

Figure 13.2 indicates that maximum propeller efficiency occurs at the peak of the curve, the design condition. A reduction in airspeed,  $v$ , reduces advance ratio,  $J$ , and results in a corresponding decrease in propeller efficiency,  $\eta_p$ . Propeller rotational speed,  $n$ , could theoretically be adjusted to produce a  $J$  value to maintain high efficiency by using a variable speed gearbox; however, variable speed gearboxes are complex and have found limited application.

Since the airplane may be susceptible to windspeeds of 50 ft/s or higher at low altitudes (see Fig. 3.2, page 13), which would probably

exceed the HAAP station keeping capability during climb, an appropriate launch day may need to be chosen to reduce this problem. If the airplane drifts off-station during launch, an airborne control station could be used to guide the HAAP airplane to within ground-based signals after it has reached operational altitude. A method of towing the HAAP airplane to higher altitudes with, for example, an agricultural aircraft as suggested by Heyson (ref. 8, page 6) might be utilized even though Heyson specifically suggests this method for a microwave-powered HAAP airplane. It has also been suggested that an expendable, lightweight, non-rechargeable, battery system might be used for added power only during the launch phase and then jettisoned, but this method poses a ground hazard which would restrict launch near populated areas.

Another concern during launch would be the aerodynamic loads on the panels which carry much of the required solar cell area (see Fig. 12.2, page 134). In addressing this concern, perhaps collapsible panels might be used that are folded during launch. A fully charged regenerative fuel cell system could provide the power for a nighttime launch. Upon reaching operational altitude, the solar panels would unfold, collecting the solar energy during the day to provide energy for flight and to recharge the fuel cell system.

#### 13.2.2 Microwave-Powered

Because the operational design of the microwave-powered HAAP airplane receives its energy from a power beam and includes no stored energy, conventional take-off methods are not readily suitable. Heyson (ref. 8, page 6) suggests a microwave-powered HAAP might be towed by an

agricultural-type aircraft to altitudes near 10,000 ft where it would be released. The airplane would climb, using transmitted microwave power, until operational altitude is reached. The launch method proposed by Heyson is suitable for the current concept. The current concept would, however, be limited to a maximum airspeed of about 90 ft/s at 10,000-ft altitude at a  $C_L$  of 0.23 and a propeller efficiency of 0.85.

Station-keeping during launch can be of primary importance for the current microwave HAAP concept design since power for flight is entirely dependent on the transmitted beam of microwave power. Additional power can be made available for the launch environment by modifying the current concept somewhat. The current design uses about 0.92 of the wing planform area for rectenna, and includes 10-percent redundancy. The remaining wing planform area, fuselage bottom surface, and horizontal tail surfaces could be used to house additional rectenna area. The minor increase in rectenna weight and a slightly heavier and more powerful motor add small increments to aircraft weight and span while providing a substantial increase in power (perhaps as much as 40 percent).

The use of an expendable, lightweight, non-rechargeable battery system for use only during launch and subsequently jettisoned also appears feasible, but the associated ground hazard would restrict launch near populated areas.

### 13.2.3 Nuclear-Powered

Although a nuclear-powered HAAP airplane could take off conventionally, this current design is confronted with marginal power to simultaneously climb and combat low-altitude winds. This marginal power becomes a particularly critical concern when the prospect of reduced propeller efficiency, previously discussed for HAAP airplanes, is confronted. An oversized nuclear power system could be employed in the basic design which would be adequate to facilitate the launch environment, but would result in a larger aircraft. Perhaps an expendable lightweight, battery system, previously discussed, could be used only during the launch phase to provide the additional power required. In either case, the technical feasibility of a nuclear-powered HAAP airplane (which is contingent on a 15-W/lb propulsion system) does not appear to be jeopardized by launch considerations.

### 13.2.4 General Remarks

Common to the launch of any HAAP airplane concept is the apparent marginal climb performance in the low-altitude wind environment. The performance is attributed, in part, to an anticipated reduction in propeller efficiency associated with lowering the flight airspeed. The marginal climb performance is also attributed to the large change in atmospheric density between the high (70,000 ft) altitude used for concept design, and the low (0 to 10,000 ft) altitudes associated with launch. Some methods discussed to facilitate launch include providing

additional power, which in turn, would mean a larger motor and greater airplane size. Those increases appear to be relatively small with little, if any, impact on the overall technical feasibility of the concept.

## CHAPTER 14

### SOCIETAL CONSTRAINTS

The current study was initiated on the premise that a High-Altitude Aircraft Platform (HAAP) would perform a variety of missions (see Chapter 2, page 10), and, correspondingly, provide a service to society. At the same time, society constrains all activities, including those proposed in this study, to conform to norms which provide an acceptable level of safety. It is society's perception of danger, not necessarily the real (as defined by technological experts) danger that governs. Because permissiveness in society is an ever-changing whim, the following discussion briefly addresses some current societal issues that might constrain or prevent HAAP development.

#### 14.1 HAAP AIRSPACE

Although the proposed operational altitude of 70,000 ft is well above any civil air traffic anticipated for the reasonably near future (except, perhaps, supersonic transports), the HAAP would still be subject to societal regulation. The Federal Aviation Administration (FAA) regulates the use of this nation's (United States) airways. Any anticipated ruling by the FAA on the operation of an unmanned HAAP vehicle would, at this time, be speculative; however, it does not seem unreasonable that a HAAP might be allotted restricted or controlled airspace in which to operate. This type of airspace is currently allotted to military airports and to other selected sites, such as flight test ranges.



## 14.2 HAAP PROPULSION METHODS

### 14.2.1 Solar Power

The current public perception of solar power is that it is a cost-free source of energy without environmental problems, and that it should be exploited. The discussion in Chapter 4 indicates the global prospect of finding more practical uses for solar power. Solar-thermal systems are being used to heat and cool many homes and offices, but they were found unsuitable for a HAAP. Solar-voltaic devices are being used in toys, watches, and to provide power for an increasing number of devices in society. Solar-voltaic systems have also been used to provide power for several manned experimental aircraft. Perhaps the most notable was the 294-lb (with pilot) "Solar Challenger" airplane which performed day-time flights in both the United States and Europe during 1980 and 1981.

At this time, there appears to be a favorable reaction toward the use of solar power for any purpose, including flight.

### 14.2.2 Microwave Power

Radio frequencies are routinely used in our society to transmit radio and television signals to the home and office. The higher radio frequencies, called microwaves, include UHF-television, radar, and satellite communication transmission frequencies. Although the aforementioned uses of microwave energy, as well as the use of microwave ovens, are generally acceptable in today's society, the effects of these transmissions on mankind and the surrounding environment is becoming an increasingly controversial issue.

#### 14.2.2.1 Controversial Issues

The singular most significant source of controversy over the use of microwave energy stems from the large discrepancies in the acceptable levels of human exposure as adopted by the United States and by Russia. Additional concern about microwave utilization emanates from books, published research studies, and news media releases which highlight reported biological effects of microwave radiation.

##### 14.2.2.1.1 Safety standards

Using references 111, 112, and 113 as data sources, Table 14.1 is presented to illustrate the large discrepancies in the United States and Russian views on microwave safety.

The United States bases its environmentally safe level for microwave exposure on the thermal effects of microwave radiation on the human body; primarily, rises in body temperature due to microwave absorption. Russia bases its safe levels on the non-thermal effects of microwave radiation, typified by headache, dizziness, and loss of memory attributed to microwave absorption. Canada, which had previously accepted the U.S. guidelines as its standards, has recently adopted more stringent safety standards.

For persons periodically exposed to microwave radiation, the North Atlantic Treaty Organization (NATO) standard uses the formula

$$t = \frac{6000}{p^2}$$

where

- |   |   |
|---|---|
| t | permitted exposure time, in minutes, during any 1-hr period |
| P | power density in mW/cm <sup>2</sup>                         |

TABLE 14.1 - SUMMARY OF STANDARDS FOR HUMAN EXPOSURE TO MICROWAVE RADIATION

Environment	Country	Frequencies, GH	Average exposure, W/ft <sup>2</sup> (mW/cm <sup>2</sup> )	Duration, per day
General public	U.S. (& Western Europe)	0.01-300	9.3 (10)	24 hr
	Canada	0.01-300	0.9 (1)	24 hr
	Russia	0.3-300	0.0009 (0.001)	24 hr
Occupational	U.S. (& Western Europe)	0.01-300	9.3 (10)	8 hr
	Canada	0.01 < 1	0.9 (1)	8 hr
		1-300	4.6 (5)	8 hr
	Russia	0.05-0.3	0.009 (0.01)	Work day-stationary antennas
		0.3-300	0.09 (0.10)	Work day-rotating antennas

According to Lindsay (ref. 111), the formula has a practical limitation of  $50 \text{ mW/cm}^2$  ( $46 \text{ W/ft}^2$ ).

It should be noted that according to references 111 (page 8) and 113 (page 2-5), that the U.S. "standard" for human exposure to microwave radiation is actually a guideline since no specific enforcement or punitive actions are provided for violations. This guideline, as it applies to the popular microwave oven requires no more than  $0.93 \text{ W/ft}^2$  ( $1 \text{ mW/cm}^2$ ) leakage at the time of manufacture, and no more than  $4.65 \text{ W/ft}^2$  ( $5 \text{ mW/cm}^2$ ) leakage thereafter (ref. 111, page 5). This requirement is based on measurements about 2 in. (5 cm) from the oven surface; therefore, the whole-body human exposure due to leakage would be significantly less.

The standards and guidelines shown in Table 14.1 generally reflect the scientific literature, which indicates that the environmental effects of microwaves are strong functions of both frequency and exposure time. The frequency generally considered for a HAAP power transmission system is 2.45 gigahertz (GH).

#### 14.2.2.1.2 Environmental effects

There are many ongoing research activities to determine the biological effects of microwave radiation. Reference 114 is a publication which summarizes these research activities, as well as highlights appropriate news items and meetings on the subject. Reference 115 presents the results of a comprehensive review of papers on the biological effects of microwave radiation to determine the potential impact of a Solar Power Satellite (SPS) on biological and ecological systems. This

reference discusses specific biological studies ranging from cataracts to nervous system response to microwaves. Greenstone performed a similar study on environmental uncertainties relating to a HAAP which is reported in reference 116. The results of these studies are perhaps best characterized by a quotation from reference 117, another microwave biological effects study. ". . . The results of all experiments purporting to demonstrate a significant non-thermal biological effect have been disputed; in fact, very few experiments in the entire field have ever been replicated, a situation which should be rectified . . ."

The study of Brodeur (ref. 118) is in marked contrast to the opinions reported in references 115 to 117 which argue that there is little technical evidence to substantiate any claims of the detrimental effects of low level microwave radiation on the human body. Brodeur's book (ref. 118) created a media and public sensation in this country in 1977, partly because it discussed and documented events surrounding the low level microwave bombardment of the American Embassy in Moscow, Russia. The Russians had been directing radiation at the Embassy to jam sophisticated American listening devices. The effects of the daily exposure of American Embassy personnel to these microwaves has resulted in a statistically high number of reported cases of dizziness, headaches, eye damage, and cancer (ref. 111, page 8).

The Embassy radiation had been monitored by the Defense Advanced Research Projects Agency (DARPA) which reported that the highest level was ". . . 18 microwatts . . ." per square centimeter ( $0.016 \text{ W/ft}^2$ ). This DARPA reported value was contradicted by one member of the

investigative team who recalled that the maximum radiation in the Embassy was much higher, about 3.7 W/ft ( $4 \text{ mW/cm}^2$ ). Regardless of which value is more accurate, they are both substantially lower than the current U.S. guideline of 9.3 W/ft ( $10 \text{ mW/cm}^2$ ) for continuous public exposure. (See ref. 118, pages 116-118.)

The exposure time of occupants of an airplane that might fly through a microwave beam would be limited to a few seconds (ref. 116, page 1-7). In addition, the metal surface of the airplane would shield the occupants from most of the radiation. The microwave transmission system could also be turned off before an aircraft traversed the beam.

Greenstone's report, which summarizes a number of studies on the environmental concerns about microwave power transmission, indicates that HAAP microwave transmitters might interfere with communication transmissions (ref. 116, pages 1-6, 2-8, and 3-14). The microwave generators would produce some noise power outside the proposed 2.45 ( $\pm 0.05$ ) GHz transmission band; however, this should be a minor problem if the antenna systems are designed with particular attention to suppression of beam sidelobes.

#### 14.2.2.2 Public Perception

The public perception of microwave radiation appears mixed. A negative connotation is often associated with the word "radiation." This is perhaps an association with memories of the World War II atomic bomb blast over Hiroshima, Japan, and the subsequent human devastation due to Gamma- and X-radiation. Gamma- and X-frequencies are highly

energized and are termed "ionizing radiation." Ionizing radiation behaves, in effect, like highly energized particles and excessive exposure is known to cause many adverse biological effects to humans, such as skin burns, genetic mutation, and cancer. Microwaves and the other radio frequencies contain far less energy, are termed "non-ionizing radiation," and characteristically behave like waves. Excessive exposure to radio frequencies (microwaves) can result in human body overheating, resulting in cell damage, and cataracts if the eye is exposed. The non-thermal effects of microwave radiation on the human body are controversial in Western society. Microwave radiation exposure standards have been previously discussed in the section on "Safety Standards."

In contrast to the negative connotation of "microwave radiation," the current sales of microwave ovens indicate public acceptance of this device, even though they are sources of microwaves in the home. The microwave oven has become a relatively common household device even though "Consumer Reports" (refs. 119 and 120), a popular consumer magazine had "not recommended" any microwave oven due to ". . . the lack of knowledge about the possibly hazardous effect of long-term low-level microwave radiation . . ."

The microwave oven saga illustrates that society weighs risks against benefits, and conditions itself to accept risk, or to negate the belief of risk, depending on the benefit which it perceives in return. The perceived benefit from the microwave oven, for example, is energy conservation and less cooking time (less time in the kitchen) relative to conventional cooking.

#### 14.2.2.3 Microwave Transmission Station

The microwave power transmission station would need a restricted zone around the transmitting antenna. Since some of the missions proposed for a HAAP would be performed near populated areas, the size of the required station might influence its societal acceptance.

Table 14.2 illustrates some relative ground-based transmitting antenna characteristics compatible with the baseline microwave-powered HAAP concepts resulting from this study.

TABLE 14.2 - SOME COMPARATIVE MICROWAVE TRANSMITTING  
ANTENNA CHARACTERISTICS

HAAP concept	Transmission efficiency	Antenna size, ft <sup>2</sup>	Average power density, W/ft <sup>2</sup>	Total transmitted power, W
Blimp (airplane)	0.80	887,000 (14,804,000)	0.081 (0.0003)	71,900 ( 4,300)
	0.60	489,200 (8,160,000)	0.196 (0.0007)	95,900 ( 5,800)
	0.40	278,900 (4,653,000)	0.515 (0.002)	143,800 ( 8,600)
	0.20	107,800 (1,793,000)	2.668 (0.010)	287,600 (17,200)
	0.10	45,800 (764,700)	12.55 (0.045)	575,200 (34,500)
	0.05	18,400 (306,700)	62.56 (0.225)	1,150,000 (68,000)
	0.016	4,100 (68,800)	871 (3.13)	3,595,000 (215,500)

Table 14.2 is presented to provide a trade-off comparison between antenna size and total transmitted microwave power for this study's



baseline HAAP blimp and airplane concepts. The antenna sizes greatly determine the construction costs, whereas the total transmitted power influences the yearly operational costs. An additional parameter, average power density at the transmitter, can influence the perception of environmental safety. The baseline HAAP blimp and airplane have rectenna areas of 1554 ft<sup>2</sup> and 93 ft<sup>2</sup>, respectively. Thirty-seven (37) W/ft<sup>2</sup> of power is incident at the rectenna surface. As can be seen in Table 14.2, high transmission efficiencies mean low transmitted power, but large antenna areas. Low transmission efficiencies yield smaller antenna, but the transmitted and average power increase. The relationship between transmission efficiency, antenna size, and rectenna size is discussed in Chapter 5 (see Fig. 5.5, page 35).

Table 14.3 (ref. 111, page 40) is presented to provide a comparison of a HAAP transmission station power characteristic to transmitters which already exist in society.

TABLE 14.3 - CHARACTERISTICS OF MICROWAVE SOURCES BY CATEGORIES

Source	Maximum power density, W/ft <sup>2</sup>	Near-field distance, ft	Distance to 9.3 W/ft <sup>2</sup> guideline, ft
Satellite communication			
Earth terminals	2 to 90	300 to 20,000	-
Radars			
Search and tracking	11 to 744	21 to 72	32 to 364
Air traffic control	2 to 14	61 to 102	Out to 158
Aircraft weather	27 to 76	2 to 6	7 to 16
UHF-TV	0.03 to 0.23	-	-

The "near-field distance" in Table 14.3 is the distance from the transmitter to where "maximum power density" was measured. The "distance to guideline" is the distance from the transmitter to where  $9.3 \text{ W/ft}^2$  was measured. By comparing the power density levels shown in Table 14.3 with those in Table 14.2, it appears that a well designed HAAP microwave transmission station would pose no more a radiation safety concern than some facilities that already exist in society.

This study will not attempt to determine the specific economics of the microwave-powered HAAP concepts developed or of the associated transmission stations, but some other studies have. Sinko (ref. 2) has considered these costs, which are summarized in Table 14.4.

TABLE 14.4 - SINKO'S MICROWAVE HAAP COST ESTIMATES

Costs	Blimp (\$M)	Airplane (\$M)
Vehicle	0.21	0.20
Antenna/transmitter	1.60	2.40
Annual	0.47	0.42
(electricity)	(0.06)	(0.09)

Sinko's HAAP blimp is  $0.5 \text{ million ft}^3$  in size. His HAAP airplane has a 98-ft span, wing area of  $1614 \text{ ft}^2$ , and weighs 1788 lb. Sinko states that due to the uncertainty associated with his cost estimates, they should be used with caution. He does not specifically discuss antenna size, operating power, or operating efficiency for his microwave-powered HAAP system.

In contrast to Sinko's somewhat cursory approach to microwave HAAP system costs, Brown (ref. 44, pages 2-1 to 2-11) provides a rather detailed analysis of HAAP microwave power transmission system costs. Brown derives cost relationship equations, and illustrates some selected antenna-rectenna systems sizes for minimum power transmission system costs. Estimates for some cost parameters, such as unit antenna construction costs, must be made. Brown indicates that minimum overall transmission costs occur when the transmission antenna costs and power costs are approximately equal. Brown also indicates that these minimum costs occur at very low transmission efficiencies.

#### 14.2.3 Nuclear Power

The current public perception of nuclear power is generally very negative, that is, that it poses a threat to our society and to the safety of mankind. This is a widespread belief, in spite of a lack of statistical evidence to substantiate the belief. The current belief perhaps stems, in part, from war-time uses of nuclear power, and the devastating effect of the atomic bomb blast over Hiroshima, Japan, during World War II. The resultant "ionizing radiation" caused severe skin burns, genetic defects, and a high incident of cancer among the people exposed.

Although nuclear power serves the military (nuclear-powered aircraft carriers and submarines), it also has non-military roles. Nuclear reactors have been used to provide electric power for public utilization since about 1955. Nuclear power in the form of radioisotopes has been used to provide operational power for satellites. In medicine,

minute quantities of selected radioisotopes are injected into the human body, and serve as "tracers" to aid in the diagnosis of diseases.

Essentially all forms of nuclear power or radioactive materials in this country, whether its in the production, handling, or utilization phase, are subjected to some, and often many, forms of governmental regulations. The regulations are intended to reduce the probability of human exposure to ionizing radiation. Just as there are standards for human exposure to microwave (non-ionizing) radiation, there are also standards for human exposure to ionizing radiation. A basic unit of measurement for any kind of ionizing radiation absorption is the "rad." One rad is defined as 100 ergs/gr ( $1.26 \times 10^{-6}$  W-h/lb). The "rem" is a unit used to express the estimated equivalent of any type of radiation that would produce the same biological effect as 1 rad delivered by X or gamma radiation. The Ionizing Radiation section of the Langley Safety Manual (ref. 121, pages 22-23) reflects current guides for exposure to this radiation. These are summarized in Table 14.5. The current general philosophy for ionizing radiation safety is to maintain levels ". . . as low as reasonably achievable . . ."

The standards and safety precautions associated with ionizing radiation do not appear to be well understood by the general public. The general public is influenced by sensational events, such as the incident at the "Three Mile Island," Pennsylvania nuclear power reactor on March 28, 1979. The resultant threat of radioactive gas being released into the atmosphere created near-panic locally, and was headline material for newspapers and television for weeks. Since the

TABLE 14.5 - SUMMARY OF IONIZING RADIATION STANDARDS

Environment	Maximum exposure
Controlled areas (radiation workers)	
Whole body, head and trunk; active blood forming organs; lens of eyes; or gonads	1.25 rem/calendar quarter
Hands and forearms; feet and ankles	18.75 rem/calendar quarter
Skin of whole body	7.50 rem/calendar quarter
Uncontrolled areas (general public)	
Whole body	0.5 rem/calendar year
Dose for minors	10 percent of that for controlled areas

"Three Mile Island" accident, all aspects of radiation safety have undergone scrutiny in the news media. The use of radioactive materials, including nuclear wastes, remains a subject of attention and controversy.

As part of this study, the views of Dr. Donald P. Hearth, Director and chief executive officer of the Langley Research Center, on the use of nuclear power in a flight vehicle were solicited. Dr. Hearth had a key administrative role in NASA's Voyager, Viking, and Pioneer space programs which all used RTG's (radioisotope thermonuclear generators) as power sources. Dr. Hearth points out that to get regulatory approval to launch these systems was a "... very, very, format process ..." that involved "... lots of paperwork ...", and included the participation of subgroups of the National Security Council. He also points out that

this very time-consuming process (conducted in the early 1970's) was in an environment when nuclear power was more acceptable than it is today. In the current societal environment, the use of nuclear power in a HAAP aircraft is, perhaps, best summarized by another quote from Dr. Hearth, "The need isn't high enough to justify the . . . risk."

#### 14.3 GENERAL REMARKS

The attitude of society towards a High-Altitude Aircraft Platform (HAAP), and the benefits derived from it, will undoubtedly influence its development and operation. The current method of regulating this nation's airspace by the Federal Aviation Administration (FAA) does not appear to prohibit HAAP operation, especially since precedence for controlled or restricted airspace has been set. In terms of HAAP propulsion methods, solar energy appears to be readily acceptable, whereas nuclear energy appears to be unacceptable. The societal acceptance of microwave energy for a HAAP system is not easily evaluated. Although microwave transmitters which emit power densities comparable to those anticipated for a HAAP system already exist in our society, they provide a valued service. Ground transmitters for satellite communications systems have relatively high power density levels, but provide a service to society which currently outweighs the environmental risks. In the "selling" of a microwave-powered HAAP, whether the perceived benefits outweigh the perceived risks, remains to be seen.

## CHAPTER 15

### CONCLUSIONS

The current study has identified and integrated near-term technologies anticipated to be available within the next 5 to 7 years in determining the feasibility of remotely powered aircraft to perform year-around missions at 70,000-ft altitudes over the United States. Solar-, microwave-, and nuclear-powered blimp and airplane concepts have been analyzed. In addition, societal issues which might influence the development or operation of this High-Altitude Aircraft Platform (HAAP) have been evaluated. A 100-lb payload requiring 1000 watts of continuous power was used for analysis purposes throughout this study.

#### 15.1 SOLAR-POWERED HAAP CONCEPTS

Solar-powered HAAP systems are extremely large, and conventionally shaped vehicles do not provide adequate surface area to accommodate the required solar cells. The long nights of the winter season place a severe demand on this propulsion mode, since all energy must be collected during the daylight for both day- and nighttime operation. The short days of the winter are accompanied by the greatest windspeeds (up to 140 ft/s) and, thus, the greatest power requirement. As a result, the critical nature of winter operation leads to very large vehicles. An unconventional, twin-bodied concept that carries a solar panel between the hulls could provide sufficient area for the cells, but appears prohibitive because of its immense size - about 90 million ft<sup>3</sup> per hull. Increased levels of technological advancement in the areas

of solar-cell efficiency, fuel-cell weight, aerodynamics, and structures, when used collectively could provide a conventional single-body HAAP blimp less than 2 million  $\text{ft}^3$  in volume.

A solar-powered HAAP blimp designed for reduced station keeping capability (maximum airspeed of 100 ft/s) appears feasible with near-term technology. This concept could be a single-body, conventionally shaped aircraft about 3.2 million  $\text{ft}^3$  in volume, and about 620 ft in length.

A solar-powered HAAP airplane would have much too little area on the wing, fuselage and tail surfaces to house the required solar cells. No viable configuration to overcome this problem was found.

In terms of societal acceptance, solar propulsion appears to be the most readily acceptable of the concepts studied.

## 15.2 MICROWAVE-POWERED HAAP CONCEPTS

Microwave-powered HAAP systems do not require nighttime energy storage and should result in relatively small, conventionally shaped vehicles that can satisfy all of the mission requirements. A super-pressure blimp concept would be about the size of a "Goodyear blimp" (0.2 million  $\text{ft}^3$  in volume and 240 ft in length). The airplane concept, with an aspect ratio 20 wing, would have about a 45-ft span and weigh about 175 lb. These concepts, however, would be restricted to operation near a ground power transmission station.

Microwave-powered HAAP systems appear to be a potentially controversial issue; however, ground stations compatible with the microwave



concepts that can perform the mission of this study would not require transmitted power levels greater than that for existing satellite communications ground stations.

### 15.3 NUCLEAR-POWERED HAAP CONCEPTS

Nuclear-powered HAAP systems appear to be feasible depending on the specific power of the nuclear propulsion system; however, with society's current attitude towards nuclear power, it seems unlikely that such a vehicle would be acceptable.

## BIBLIOGRAPHY AND REFERENCE LIST

1. MacCready, P. B.; Lissaman, P. B. S.; Morgan, W. R.; and Burke, J. D. Sun Powered Aircraft Design. Presented at the AIAA Annual Meeting and Technical Display on Frontiers of Achievement. Long Beach, California. AIAA 81-0916. May 12-14, 1981.
2. Sinko, J. W. High Altitude Platform Cost and Feasibility Study. Stanford Research Institute. SRI Project 5655-502, Contract NASW-2962. October 1977.
3. Kuhner, M. B.; Earhart, R. W.; Madigan, J. A.; and Ruck, G. T. Applications of a High-Altitude Powered Platform (HAPP). Battelle Columbus Laboratories. Report No. BCL-OA-TFR-77-5. September 1977.
4. Kuhner, M. B.; and McDowell, J. R. User Definition and Mission Requirements for Unmanned Airborne Platforms. Battelle Columbus Laboratories. NASA CR-156861. 1979.
5. Youngblood, James W.; Darnell, Wayne L.; Johnson, Robert W.; and Harriss, Robert C. Airborne Spacecraft - A Remotely Powered, High-Altitude RPV for Environmental Applications. NASA paper presented at Electronics and Aerospace Systems Conference. Arlington, Virginia. October 9-11, 1979.
6. Parry, J. F. W. A Solar Powered Observation Platform. R&D Associates. RDA-TR-4300-008, ARPA Order No. 2558, July 1974.
7. Phillips, William H. Some Design Considerations for Solar-Powered Aircraft. NASA TP-1675. June 1980.
8. Heyson, Harry H. Initial Feasibility Study of a Microwave Powered Sailplane as a High-Altitude Observation Platform. NASA TM-78809. December 1978.
9. Morris, Charles E. K., Jr. Parametric Study of Microwave-Powered High-Altitude Airplane Platforms Designed for Linear Flight. NASA TP 1981. November 1981.
10. Turriziani, R. Victor. Sensitivity Study for a Remotely Piloted Microwave-Powered Sailplane Used as a High-Altitude Observation Platform. Kentron International, Inc. NASA CR-159089. June 1979.
11. Sinko, J. W. Circling Flight in Wind for HAAP Aircraft. SRI International. Technical Note SED-716. Contract NASW-3166. August 1978.

12. Anon. Emergency Response Communications Program. Report of Interagency Committee for Search and Rescue Ad Hoc Working Group, Hufnagel Committee. Prepared by ORI, Inc., Silver Spring, Md. Contract NAS 13-126. June 1979.
13. Kaufman, John W. Terrestrial Environment (Climatic) Criteria Guidelines for Use in Aerospace Vehicle Development, 1977 Revision. NASA TM 78118. 1977.
14. Strganac, Thomas W. Wind Study for High Altitude Platform Design. NASA RP-1044. December 1979.
15. Coleman, Thomas L.; and Steiner, Roy. Atmospheric Turbulence Measurements Obtained From Airplane Operation at Altitudes Between 20,000 and 75,000 Feet for Several Areas in the Northern Hemisphere. NASA TN D-548. 1960.
16. Waco, David E.; and Ashburn, Edward V. "Turbulence Variations During the High Altitude Clear Air Turbulence (HICAT) Program." Journal of Aircraft. P. 56-58. Vol. 10. No. 1. January 1973.
17. Waco, David E. "Variation of Turbulence With Altitude to 70,000 Ft." Journal of Aircraft. P. 981-986. Vol. 13. No. 12. December 1976.
18. Anon. U.S. Standard Atmosphere, 1976. NOAA-S/T 76-1562. 1976.
19. Jayetski, John. "A Burst of Energy in Photovoltaics." Electronics. P. 105-122. July 19, 1979.
20. Battan, Louis J. Fundamentals of Meteorology. Prentice-Hall, Inc. Englewood Cliffs, N.J. 1979.
21. Anon. Solar Electromagnetic Radiation. NASA SP-8005. May 1971.
22. Duffie, John A.; and Beckman, William A. Solar Energy Thermal Processes. John Wiley & Sons, Inc. New York, N.Y. 1974.
23. Anon. Conference Record of the Fourteenth IEEE Photovoltaic Specialists Conference. IEEE No. 80CH17508-1. 1980.
24. Anon. Sun II. Proceedings of the International Solar Energy Society. Atlanta, GA. Vol. 2. Pergamon Press, New York. May 1979.
25. Anon. Space Photovoltaic Research and Technology 1980-High Efficiency, Radiation Damage, and Blanket Technology. Proceedings of a conference held at NASA Lewis Research Center, Cleveland OH. October 15-17, 1980.

26. Billman, Kenneth W. (edited by). Radiation Energy Conversion in Space. Technical Papers Prepared for the Third NASA Conference on Radiation Conversion. NASA Ames Research Center. Published by AIAA. January 16-18, 1978.
27. DeWinter, Francis; and Cox, Michael (edited by). Sun - Mankind's Future Source of Energy. Proceedings of the International Solar Energy Society Conference. Vol. 2. New Delhi, India. Pergamon Press, New York. January 1978.
28. Anon. The Final Proceedings of the Solar Power Satellite Program Review. Lincoln, Nebraska. DOE Conf-800491. April 22-25, 1980.
29. Rauschenbach, H. S. Solar Cell Array Design Handbook. Vols. I & II. NASA Jet Propulsion Lab. JPL SP43-48. October 1976.
30. Treble, F. C. "Solar Cells." IEE Review. IEE Proc. Vol. 127, Pt. A. No. 8. P. 505-525. November 1980.
31. Salama, A. M.; Rowe, W. M.; and Yasui, R. K. "Stress Analysis and Design of Silicon Solar Cell Arrays and Related Material Properties." P. 146-157. Conference Record of the Ninth IEEE Photovoltaic Specialists Conference. IEEE No. 72 CHO 613-0-ED. May 1972.
32. Szego, G. C. "Space Power Systems State of the Art." Journal of Spacecraft and Rockets. Vol. 2. No. 5. P. 641-659. September-October 1965.
33. Anon. "Energy Conversion Systems Studies." Space Based Solar Power Conversion and Delivery Systems Study. Vol. 4. Final Report (Little, Arthur D., Inc.). NASA CR 150297. 29 Mar 1977.
34. Brown, William C. "The History of the Development of the Rectenna." Solar Power Satellite Microwave Power Transmission and Reception. P. 271-280. Proceedings of a Workshop held at Johnson Space Center, Houston, Texas. NASA Conference Publication 2141. January 15-18, 1980.
35. Anon. Solar Power Satellite Microwave Power Transmission and Reception. Proceedings of a Workshop held at Johnson Space Center. Houston, Texas. NASA Conference Publication 2141. January 15-18, 1980.
36. Anon. The Final Proceedings of the Solar Power Satellite Program Review. DOE Conf-800491. July 1980.
37. Gaubau, G. "Microwave Power Transmission From an Orbiting Solar Power Station." Journal of Microwave Power. P. 223-231. Vol. 5. No. 4. 1970.

38. Brown, William C. "The Technology and Application of Free-Space Power Transmission by Microwave Beam." Proceedings of the IEEE. Vol. 62. No. 1. January 1974.
39. Dickinson, R. M.; and Brown, W. C. Radiated Microwave Power Transmission System Efficiency Measurements. JPL TM 33-727. May 1975.
40. Brown, William C. Satellite Power System (SPS) Magnetron Tube Assessment Study. Prepared for Marshall Space Flight Center. Contract NAS 8-33157. PT-5653. 10 July 1980.
41. Brown, William C. Electronic and Mechanical Improvement of the Receiving Terminal of a Free-Space Microwave Power Transmission System. NASA CR-135194. August 1, 1977.
42. Brown, W. C. "Experiments Involving a Microwave Beam to Power and Position a Helicopter." IEEE Transactions on Aerospace and Electronic Systems. Vol. AES-5. No. 5. P. 692-702. September 1969.
43. Dickinson, R. M. Evaluation of a Microwave High-Power Reception-Conversion Array for Wireless Power Transmission. JPL TM 33-741. September 1, 1975.
44. Brown, William C. Design Definition of a Microwave Power Reception and Conversion System for Use on a High Altitude Powered Platform. NASA CR-156866. 1981.
45. Raloff, Janet. "Seeking Coherent Answers." Science News. Vol. 120. No. 12. P. 184-187. September 19, 1981.
46. Locke, Edward V. "Multi-Kilowatt Industrial CO<sub>2</sub> Lasers - A Survey." Industrial Applications of High Power Laser Technology. Proceedings of the Society of Photo-Optical Instrumentation Engineers. Vol. 86. P. 2-7. August 1976.
47. Lancashire, R. B.; Alger, D. L.; Manista, E. J.; Slaby, J. G.; Dunning, J. W.; and Stubbs, R. M. "NASA High Power Carbon Dioxide Laser-Versatile Tool for Laser Applications." Industrial Applications of High Power Laser Technology. Proceedings of the Society of Photo-Optical Instrumentation Engineers. Vol. 86. P. 11-19. August 1976.
48. Bain, Claud N. "Power From Space by Laser." Astronautics & Aeronautics. P. 28-39. March 1979.

49. Rudko, R. I. "Mini Transversely Excited Atmospheric (TEA) CO<sub>2</sub> Lasers." Advances in Laser Engineering and Applications. Proceedings of the Society of Photo-Optical Instrumentation Engineers. Vol. 247. P. 69-73. August 1980.
50. Hertzberg, Abraham; Sun, Kenneth; and Jones, Wayne S. "Laser Aircraft." Astronautics & Aeronautics. P. 41-49. March 1979.
51. Lee, George. "Status and Summary of Laser Energy Conversion." Radiation Energy Conversion in Space. 3rd Conference. Moffett Field, CA. P. 549-565. January 26-28, 1978.
52. Cockeram, D. J. "SNAP 2, 8, and 10 Reactor Programs Progress Report." Space Power Systems Engineering Progress in Astronautics and Aeronautics. Vol. 16. P. 393-415. (Edited by Szego, G. C.; and Taylor, J. E.). Academic Press. New York. 1966.
53. Schulman, Fred. "Isotopes and Isotope Thermoelectric Generators." Space Power Systems Advanced Technology Conference. NASA SP-131. P. 73-93. August 1966.
54. Layton, J. Preston. Space Power Systems: Retrospect and Prospect. Presented at the International Astronautical Federation (IAF) XXVth Congress. Amsterdam. 30 Sept. - 5 Oct. 1974. 74-082.
55. Buden, D.; and Angelo, J. A., Jr. Reactors for Nuclear Electric Propulsion. Presented at AIAA, Japan Society for Aeronautical and Space Sciences and DGLR, 15th International Electric Propulsion Conference. Las Vegas, Nev. AIAA 81-0697. April 21-23, 1981.
56. Buden, D.; Ranken, W. A.; and Koenig, D. R. Space Nuclear Reactor Power Plants. Los Alamos Scientific Laboratory. Report No. LA-8223-MS. January 1980.
57. Mullin, J. P.; Randolph, L. P.; and Hudson, W. R. "Progress in Space Power Technology." Proceedings of the 15th Intersociety Energy Conversion Engineering Conference. Vol. 1. P. 83-88. Seattle, Washington. August 18-22, 1980.
58. Streb, Alan J. "Radioisotope Power Systems for Manned Space Stations." Space Power Systems Engineering Progress in Astronautics and Aeronautics. Vol. 16. (Edited by Szego, G. C.; and Taylor, J. E.). P. 3-29. Academic Press. New York. 1966.
59. Allen, J.; Reed, K.; Levitz, N.; Schertz, W.; Rabi, A.; and Winston, R. "Development of Compound Parabolic Concentrators for Solar Thermal Application?" Presented at the American Society of Mechanical Engineers, Winter Annual Meeting. New York, N.Y. Paper 76-WA/Sol-11. December 1976.

60. Schuster, J. R.; Neill, J. M.; and Bass, J. "Fixed Mirror Solar Concentrator for Application to a 100 MW(e) Electric Generating Plant." Intersociety Energy Conversion Engineering Conference. Proceedings of the 14th Intersociety Energy Conversion Engineering Conference. Vol. 1. P. 15-19. American Chemical Society. Washington, DC. August 1979.
61. Anon. The Final Report of the SPS Energy Conversion and Power Management Workshop. Marshall Space Flight Center. Huntsville, Ala. DOE/CS/34218. February 1980.
62. Anon. The 1978 Goddard Space Flight Center Battery Workshop. NASA CP-2088. November 1978.
63. Anon. The 1980 Goddard Space Flight Center Battery Workshop. NASA CP-2177. November 1980.
64. Thierfelder, H. "DSCS III Battery Tests." The 1980 Goddard Space Flight Center Battery Workshop. P. 317-327. NASA CP 2177. November 1980.
65. Wolter, John G.; Gilbert, John A.; and Leonard, James V. "Current State-of-the-Art of Electrochemical Batteries From a Users Point of View." Proceedings of the 4th Annual Conference on Energy. P. 64-70. University of Missouri (Rolla). 1978.
66. Stockel, J. F.; Dunlop, J. D.; and Betz, F. "NTS-2 Nickel-Hydrogen Battery Performance." Journal of Spacecraft and Rockets. Vol. 17. No. 1. P. 31-34. January-February 1980.
67. Fordyce, Stuart J. "Technology Status-Batteries and Fuel Cells." Future Orbital Power Systems Technology Requirements. NASA CP 2058. P. 157-166. 1978.
68. Trout, J. Barry. Energy Storage for Low Earth Orbit. Presented at the AIAA/NASA Conference on Advanced Technology for Future Space Systems. Hampton, Virginia. AIAA 79-0885. May 1979.
69. McBryar, Hoyt. "Electrochemical Orbital Energy Storage (ECOES) Technology Program." Synchronous Energy Technology. NASA CP 2154. P. 81-96. 1980.
70. Erickson, A. C.; Austin, J. F.; and Moulthrop, L. C. Electrochemical Cell Technology for Orbital Energy Storage. General Electric Company. NASA CR-160878. June 1980.

71. Kuhn, Ira F., Jr.; Reiss, Keith W.; Schubert, Franz H.; and Stedman, Jay K. Regenerative Fuel Cell System Final Design Report. B-K Dynamics, Inc. Rockville, Maryland. Contract F33657-80-C-0343. January 1981.
72. Rabenhorst, David W. "Energy Conservation With Flywheels." Johns Hopkins APL Technical Digest. Vol. 1. No. 2. P. 114-119. April-June 1980.
73. Benoit, Jean. "La Propulsion De Vehicules Per Rove D'Inertic." Proceedings of Urbanization and Pollution Symposium. P. 1-11. Quebec, Canada. May 1977.
74. Lawson, L. J.; Smith, A. K.; and Davis, G. D. Study of Flywheel Energy Storage Final Report Volume 1, Executive Summary. UMTA-CA-06-0106-77-1. September 1977.
75. Millner, Alan R. "Flywheels for Energy Storage." Technology Review. P. 32-39. November 1979.
76. Renner-Smith, Susan. "Flywheels in Space." Popular Science. P. 86-87. August 1980.
77. Poubeau, P. C. "Satellite Flywheels With Magnetic Bearings and Passive Radial Centering." Journal of Spacecraft and Rockets. P. 93-98. Vol. 17. No. 2. March-April 1980.
78. Nimmer, R. P.; Torossian, K.; and Hickey, J. Laminated Composite Disc Flywheel Development. (Third Interim Report.) Prepared by the General Electric Company for Lawrence Livermore Laboratory. Subcontract No. 2479309. SRD-80-091. February 1980.
79. Anon. Design Report for the Rotating Assembly for an Integrated Power/Attitude Control System. Prepared by Rockwell International for the Langley Research Center. Contract NAS1-13008. SD 74-SA-0100. September 1974.
80. Klass, Phillip J. "Powerful Magnets Find Aerospace Role." Aviation Week & Space Technology. P. 66-70. August 8, 1977.
81. Sawyer, Bert; and Edge, J. T. "Design of a Samarium Cobalt Brushless DC Motor for Electromechanical Actuator Applications." Proceedings of the IEEE 1977 National Aerospace and Electronics Conference. P. 1108-1112. 77CH1203-9 NAECON. May 1977.
82. Maslowski, Edward A. Electronically Commutated dc Motors for Electric Vehicles. DOE/NASA/51044-14. NASA TM 81654. January 1981.



83. Anderson, Neil E.; and Loewenthal, Stuart H. Design of Spur Gears for Improved Efficiency. NASA TM 81625. December 1980.
84. Imwalle, D. E. High Performance Epicyclic Gears for Gas Turbines. ASME Paper No. 76-GT-88. March 1976.
85. Anon. Quiet Clean Short-Haul Experimental Engine (QCSEE) Main Reduction Gears Detailed Design Final Report. Prepared by Curtiss-Wright Corporation for NASA Lewis Research Center. March 1975.
86. Slifer, Luther W., Jr.; and Billerbeck, Wilfred J. Synchronous Orbit Power Technology Needs. Presented at the AIAA/NASA Conference on Advanced Technology for Future Space Systems. Hampton, Virginia. AIAA 79-0916. May 1979.
87. Goldsmith, P.; and Reppucci, G. M. Advanced Photovoltaic Power Systems. AIAA Paper No. 77-506. March 1977.
88. Schwarz, Francis C. Advanced Power Processing Techniques for DC to DC Converters. Prepared for U.S. Army Electronics Command. ECOM-74-0968-1. April 1976.
89. Beemer, Jack D.; Parsons, Roger N.; Rueter, Loren L.; Seuferrer, Paul A.; and Swiden, LaDell R. POBAL-S, the Analysis and Design of a High Altitude Airship. Prepared for the Air Force Cambridge Research Laboratory by Raven Industries, Inc. Sioux Falls, S.D. AD-A012292. February 1975.
90. Lagerquist, D. R.; and Kean, L. B. Structural Design of a High-Altitude Superpressure Powered Aerostat. Presented at the AIAA Lighter Than Air Technology Conference. Snowmass, Colorado. AIAA Paper No. 75-933. July 1975.
91. Azuma, Akira. "Fundamental Formulation of Airship Performance and Flight Dynamics." Institute of Space and Aeronautical Science, University of Tokyo, Report No. 536. Vol. 40. P. 457-489. December 1975.
92. Layton, D. M. "Quasi-Hybrid Airships." AIAA Lighter-Than-Air Systems Technology Conference. P. 86-89. AIAA Paper No. 81-1333. July 1981.
93. Kuhn, Ira F. "High-Altitude, Long Endurance Sensor Platform for Wide Area Defense of the Fleet." Proceedings of the High Altitude Platform Workshop. P. 23-49. Coordinated by the Lighter-Than-Air Project Office. Naval Air Development Center. Warminster, PA. July 1978.

94. Petrone, Francis J.; and Wessel, Paul R. HASPA Design and Flight Test Objectives. Presented at the AIAA Lighter-Than-Air Technology Conference. Snowmass, Colorado. AIAA 75-924. July 1975.
95. Goldschmied, Fabio R. "Aerodynamic Hull Design for HASP LTA Optimization." Journal of Aircraft. P. 634-638. Vol. 15. September 1978.
96. Warner, D. J.; and Haigh, W. W. "Feasibility of Applying Laminar Flow Control to an LTA Vehicle." AIAA Lighter-Than-Air Technology Conference. P. 17-23. AIAA CP 815. July 1981.
97. Mueller, T. J.; and Batill, S. M. Experimental Studies of the Laminar Separation Bubble on a Two-Dimensional Airfoil at Low Reynolds Number. AIAA 13th Fluid and Plasma Dynamics Conference. AIAA-80-1440. July 1980.
98. Eppler, Richard; and Somers, Dan J. A Computer Program for the Design and Analysis of Low-Speed Airfoils. NASA TM 80210. 1980.
99. Patrick, J. T. "Aerofoils Down to Critical Reynolds Numbers and the Performance of Remotely Controlled Gliders." P. 12.1-12.6. International Conference on Remotely Piloted Vehicles. Bristol, UK. September 1979.
100. Abbott, Ira H.; and von Doenhoff, Albert E. Theory of Wing Sections. Dover Publications, Inc. New York. 1958.
101. Riegels, Dr. Friedrich Wilhelm (Translated from German by Randall, D. G.). AEROFOIL SECTIONS - Results From Wind-Tunnel Investigations - Theoretical Foundations. Butterworth & Co., Ltd. London. 1961.
102. Althaus, Dieter; and Wortmann, Franz Xaver. Stuttgarter Profil-katalog I. Friedr. Vieweg & Sohn. Braunschweig, Germany. 1979.
103. Stratford, B. S. "The Prediction of Separation of the Turbulent Boundary Layer." Journal of Fluid Mechanics. P. 1-16. Vol. 5. January 1959.
104. Liebeck, R. H. "Design of Subsonic Airfoils for High Lift." Journal of Aircraft. Vol. 15. No. 9. P. 547-561. September 1978.
105. Alley, V. L., Jr.; and McHatton, A. D. Structural Materials Research for Lighter-Than-Air Systems. Presented at AIAA Lighter-Than-Air Technology Conference. Snowmass, Colorado. AIAA Paper 75-935. July 1975.

106. Reed, R. Dale. "High-Flying Mini-Sniffer RPV: Mars Bound?" Astronautics & Aeronautics. P. 26-39. Vol. 16. No. 6. June 1978.
107. Koelle, D. E.; Kellermeier, H.; and Fetzer, K. "Spacecraft Design Aspects for Advanced Communications Satellites." Satellite Broadcasting. Proceedings of a Technical Symposium held in Stockholm. P. 75-85. (European Space Agency. Paris). ESA-SP-122. November 1976.
108. Loftin, Laurence K., Jr. Subsonic Aircraft: Evolution and the Matching of Size to Performance. NASA RP 1060. August 1980.
109. Eney, John A. "HASPA-I Program Status." Proceedings of the High Altitude Platform Workshop. P. 85-99. Coordinated by the Lighter-Than-Air Project Office. Naval Air Development Center. Warminster, PA. July 1978.
110. Perkins, Courtland D.; and Hage, Robert E. Airplane Performance Stability and Control. John Wiley & Sons, Inc. New York. June 1960.
111. Sosnicky, Andrew Peter. Sources and Biological Effects of Nonionizing Electromagnetic Radiation. (A Master's Degree Thesis.) Naval Postgraduate School. Monterey, California. September 1976.
112. Lindsay, I. R. Microwave Radiation: Biological Effects and Exposure Standards. A Paper Presented at the International Symposium on Solar Power Satellites. Toulouse, France. June 25-27, 1980.
113. Anon. Environmental Assessment for the Satellite Power System - Concept Development and Evaluation Program - Microwave Health and Ecological Effects. DOE/ER/10035-2. November 1980.
114. Anon. Biological Effects of Nonionizing Electromagnetic Radiation. Prepared by the Franklin Institute Research Laboratories for the U.S. Navy. Volume 11. No. 4. June 1978.
115. Justesen, D. R.; Ragan, H. A.; Rogers, L. E.; Gay, A. W.; Hjeresen, D. C.; Hinds, W. T.; and Phillips, R. D. Compilation and Assessment of Microwave Bioeffects: A Selective Review of the Literature on Biological Effects in Relation to the Satellite Power System. DOE Contract No. EY-76-C-06-1830. May 1978.
116. Greenstone, Reynold. Environmental and Technical Uncertainties Related to the High Altitude Powered Platform (HAPP) Concept. Prepared by ORI. Silver Spring, Md. for NASA Headquarters. Contract No. NASW-2961. December 1977.

117. Ruderman, Marvin A.; and MacDonald, Gordon J. On the Interaction of Non-Ionizing Radiation With People. Prepared by SRI International for the Defense Advanced Research Projects Agency. JASON Technical Report JSR-79-14. February 1980.
118. Brodeur, Paul. The Zapping of America. W. W. Norton & Co., Inc. New York. 1977.
119. Anon. "Microwave Ovens." Consumer Reports. Vol. 38. No. 4. P. 221-230. April 1973.
120. Anon. "Microwave Ovens: Still Not Recommended." Consumer Reports. Vol. 38. No. 8. P. 489. August 1973.
121. Anon. Ionizing Radiation. NASA Langley Research Center. LHB 1710.5. January 1978.

# APPENDIX A

## COMPUTER PROGRAM LISTINGS

### A.1 BLIMP

C	PROGRAM GRAVES (INPUT,OUTPUT,TAPE1=INPUT,TAPE5,TAPE6=OUTPUT)	0001	1
C	*****	0001	2
C	*****	0001	3
C	*****	0001	4
C	PROGRAM GRAVES AIDS IN THE FEASIBILITY ANALYSIS OF	0001	5
C	SOLAR-, MICROWAVE-, AND NUCLEAR-POWERED BLIMPS	0001	6
C	*****	0001	7
C	TAPE1 IS INPUT FROM INTERACTIVE TERMINAL	0001	8
C	TAPE5 IS A PLOTTING PROGRAM INPUT TAPE	0001	9
C	TAPE6 IS OUTPUT TO INTERACTIVE TERMINAL	0001	10
C	*****	0001	11
C	*****	0001	12
C	DIMENSION A(15),B(15),C(15),YPLT(6),E(4)	0001	13
C	REWIND 5	0001	14
C	WRITE(5,550)	0001	15
C	WRITE(6,54)	0001	16
C	WRITE(6,53)	0001	17
C	*****	0001	18
C	CONSTANTS	0001	19
C	*****	0001	20
C	PI IS PI(THE MATHEMATICAL TERM)	0001	21
C	PI=3.14159	0001	22
C	*****	0001	23
C	RHO0 IS AMBIENT DENSITY AT SEA LEVEL(SLUGS/FT/FT/FT)	0001	24
C	RHO0=.0023769	0001	25
C	*****	0001	26
C	P0 IS AMBIENT PRESSURE AT SEA LEVEL(LBS/FT/FT/)	0001	27
C	P0=2116.21695	0001	28
C	*****	0001	29
C	G0 IS GRAVITATIONAL ACCELERATION AT SEA LEVEL(FT/S/S)	0001	30
C	G0=32.174	0001	31
C	*****	0001	32
C	CPP IS PROPULSION POWER PROCESSING SPECIFIC POWER(W/LB)	0001	33
C	CPP=250.	0001	34
C	*****	0001	35
C	CC1 CONVERTS(FT-LB/S) TO W	0001	36
C	CC1=1.355818	0001	37
C	*****	0001	38
C	CR1 CONVERTS SLUGS TO GRAMS	0001	39
C	CR1=14.5939E+03	0001	40
C	*****	0001	41
C	R IS UNIVERSAL GAS CONSTANT(FT-LB/K-MOLE)	0001	42
C	R=6.134	0001	43
C	*****	0001	44
C	PC IS PRISMATIC COEFFICIENT(SHAPE FACTOR)	0001	45
C	PC=.45	0001	46
C	*****	0001	47
C	GMOLAIR IS MOLECULAR WEIGHT OF AIR AT SEA LEVEL(GM/MOLE)	0001	48
C	*****	0001	49
C	*****	0001	50
C	GMOLAIR=28.9644	0001	51
C	*****	0001	52
C	GMOLENE IS MOLECULAR WEIGHT OF HELIUM(GM/MOLE)	0001	53
C	GMOLENE=4.003	0001	54
C	*****	0001	55
C	AC=242.467	0001	56
C	AC2=328.084	0001	57
C	KA=1	0001	58
C	LINEN=0	0001	59
C	E(4)=160000.123456789	0001	60

C	*****	DOC1	60
C		DOC1	61
C	***** DEFAULT VALUES *****	DOC1	62
C	DEFAULT VALUES ARE THOSE FOR A MICROWAVE-POWERED BLIMP	DOC1	63
C		DOC1	64
C	*****	DOC1	65
C		DOC1	66
C	PWTPD IS POWER PROCESSING POWER-TO-WEIGHT RATIO(W/LB)	DOC1	67
C	PWTPD=53.4	DOC1	68
C		DOC1	69
C		DOC1	70
C	PPYLD IS PAYLOAD POWER(W)	DOC1	71
C	PPYLD=1000.	DOC1	72
C		DOC1	73
C	WTPYLD IS PAYLOAD WEIGHT(LBS)	DOC1	74
C	WTPYLD=100.	DOC1	75
C		DOC1	76
C	VLD IS LENGTH-TO-MAXIMUM DIAMETER RATIO	DOC1	77
C	VLD=5.0	DOC1	78
C		DOC1	79
C	ALT IS ALTITUDE(THOUSANDS OF FT)	DOC1	80
C	ALT=70.000	DOC1	81
C		DOC1	82
C	ASPFED IS AVERAGE AIRSPEED(FT/S)	DOC1	83
C	ASPFED=50.	DOC1	84
C		DOC1	85
C	VMAX IS MAXIMUM CAPABLE AIRSPEED(FT/S)	DOC1	86
C	VMAX=140.	DOC1	87
C		DOC1	88
C	PWNJKE IS NUCLEAR SYSTEM POWER-TO-WEIGHT RATIO(W/LB)	DOC1	89
C	PWNJKE=20.	DOC1	90
C		DOC1	91
C	PWMOTDR IS MOTOR POWER-TO-WEIGHT RATIO(W/LB)	DOC1	92
C	PWMOTDR=573.	DOC1	93
C		DOC1	94
C	EWBAT IS BATTERY ENERGY-TO-WEIGHT RATIO(W-H/LB)	DOC1	95
C	EWBAT=15.3	DOC1	96
C		DOC1	97
C	EFBAT IS BATTERY EFFICIENCY	DOC1	98
	EFBAT=.85	DOC1	99
C		DOC1	100
C	EFCOLL IS RECTENNA(OR SOLAR CELL) EFFICIENCY	DOC1	101
C	EFCOLL=.80	DOC1	102
C		DOC1	103
C	WTFRACS IS STRUCTURAL WEIGHT FRACTION	DOC1	104
C	WTFRACS=.33	DOC1	105
C		DOC1	106
C	EFMOTDR IS MOTOR-GEAR BOX EFFICIENCY	DOC1	107
C	EFMOTDR=.94	DOC1	108
C		DOC1	109
C	FFPD IS POWER PROCESSING EFFICIENCY	DOC1	110
C	FFPD=.92	DOC1	111
C		DOC1	112
C	WPROPT IS PROPELLER WEIGHT-TO-THRUST RATIO(LB/LB-THRUST)	DOC1	113
C	WPROPT=.06	DOC1	114
C		DOC1	115
C	WACOLL IS RECTENNA(OR SOLAR CELL) WEIGHT-TO-AREA RATIO(LB/FT/FT)	DOC1	116
C	WACOLL=.08	DOC1	117
C		DOC1	118
C	EFLUX IS INCIDENT BEAM POWER(W/FT/FT)	DOC1	119
C	EFLUX=37.	DOC1	120
C		DOC1	121
C	FHE IS HELIUM GAS FRACTION	DOC1	122
C	FHE=.95	DOC1	123
C		DOC1	124
C	SC1 IS RECTENNA(OR SOLAR CELL) REDUNDANCY FRACTION	DOC1	125
C	SC1=0.10	DOC1	126
C		DOC1	127
C	SR1 IS BATTERY REDUNDANCY FRACTION	DOC1	128
C	SR1=2.0	DOC1	129
C		DOC1	130
C	POFF IS NUMBER OF HOURS BATTERY PROVIDES ALL POWER NEEDS	DOC1	131
C	POFF=0.	DOC1	132
C		DOC1	133
C	FFPRJP IS PROPELLER EFFICIENCY	DOC1	134
C	FFPRJP=.85	DOC1	135

C			
C	DELPMIN IS MINIMUM SUPERPRESSURE(LB/FT/FT)	DQC1	136
	DELPMIN=5.2	DQC1	137
C		DQC1	138
C	TSMIET IS SUPERHEAT(K)	DQC1	139
	TSMIET=0.	DQC1	140
C		DQC1	141
C		DQC1	142
C	CD IS DRAG COEFFICIENT	DQC1	143
C	CD=.335	DQC1	144
C		DQC1	145
C	*****	DQC1	146
		DQC1	147
C			
C	CHERYCHEV--A() VALUES--USED IN CALCULATING AMBIENT DENSITY	DQC1	148
C		DQC1	149
	A(1)=-.10960632E+02	DQC1	150
	A(2)=-.55717132E+01	DQC1	151
	A(3)=-.90116555E-01	DQC1	152
	A(4)=-.61044847E-01	DQC1	153
	A(5)=-.14304157	DQC1	154
	A(6)=-.29492088E-02	DQC1	155
	A(7)=-.58789604E-02	DQC1	156
	A(8)=-.20421324E-02	DQC1	157
	A(9)=-.71033206E-02	DQC1	158
	A(10)=-.10314086E-01	DQC1	159
	A(11)=-.34100737E-02	DQC1	160
	A(12)=-.41764325E-02	DQC1	161
	A(13)=-.39151559E-02	DQC1	162
	A(14)=-.11227820E-02	DQC1	163
	A(15)=-.15751053E-02	DQC1	164
C		DQC1	165
C		DQC1	166
C	CHERYCHEV--B() VALUES--USED IN CALCULATING AMBIENT PRESSURE	DQC1	167
C		DQC1	168
	B(1)=-.11385925E+02	DQC1	169
	B(2)=-.56937011E+01	DQC1	170
	B(3)=-.52666476E-01	DQC1	171
	B(4)=-.77884294E-01	DQC1	172
	B(5)=-.11064083	DQC1	173
	B(6)=-.17572339E-01	DQC1	174
	B(7)=-.48546337E-02	DQC1	175
	B(8)=-.17694405E-02	DQC1	176
	B(9)=-0.18165298E-02	DQC1	177
	B(10)=-0.26635086E-02	DQC1	178
	B(11)=-0.35645433E-02	DQC1	179
	B(12)=-0.02257517E-03	DQC1	180
	B(13)=-0.10363683E-02	DQC1	181
	B(14)=-0.57053477E-03	DQC1	182
	B(15)=-0.19023078E-03	DQC1	183
C		DQC1	184
C	*****	DQC1	185
C		DQC1	186
C	INTERACTIVE PROGRAM INPUT	DQC1	187
C		DQC1	188
C	*****	DQC1	189
C		DQC1	190
	WRITE(6,112)	DQC1	191
	READ(1,100)CD	DQC1	192
C		DQC1	193
C	IF CD INPUT GREATER THAN 81.,ALL DEFAULT VALUES ARE USED	DQC1	194
C		DQC1	195
		DQC1	196
	IF(FDF(1)) 2,2	DQC1	197
	2 IF(CD.GE.81.) GOTO 23	DQC1	198
	WRITE(6,111)	DQC1	199
	READ(1,100)ASPEED	DQC1	200
	IF(FDF(1)) 3,3	DQC1	201
	3 WRITE(6,777)	DQC1	202
	READ(1,100)POFF	DQC1	203
	IF(FDF(1)) 4,4	DQC1	204
	4 WRITE(6,113)	DQC1	205
	READ(1,100)FFPROP	DQC1	206
	IF(FDF(1)) 5,5	DQC1	207
	5 CONTINUE	DQC1	208
	WRITE(6,740)	DQC1	209

	READ(1,750)OPTION	DOC1	210
	WRITE(6,52)	DOC1	211
	IF(E7F(1)) 7,6	DOC1	212
	6 IF(OPTION.EQ.1HY)66,7	DOC1	213
	6A WRITE(6,110)	DOC1	214
	READ(1,100)ALT	DOC1	215
	IF(E7F(1))67,67	DOC1	216
	67 WRITE(6,760)	DOC1	217
	READ(1,100)VLD	DOC1	218
	IF(E7F(1)) 8,9	DOC1	219
	8 WRITE(6,765)	DOC1	220
	READ(1,100)EWBAT	DOC1	221
	IF(E7F(1)) 12,12	DOC1	222
	12 WRITE(6,770)	DOC1	223
	READ(1,100)EFBAT	DOC1	224
	IF(E7F(1)) 13,13	DOC1	225
	13 WRITE(6,773)	DOC1	226
	READ(1,100)WACOLL	DOC1	227
	IF(E7F(1)) 14,14	DOC1	228
	14 WRITE(6,786)	DOC1	229
	READ(1,100)EFCOLL	DOC1	230
	IF(E7F(1)) 15,15	DOC1	231
	15 WRITE(6,785)	DOC1	232
	READ(1,100)EFLUX	DOC1	233
C		DOC1	234
C	IF EFLUX INPUT IS 0., A NUCLEAR POWERED GLIMP IS REPRESENTED	DOC1	235
C		DOC1	236
	IF(E7F(1))16,16	DOC1	237
	16 WRITE(6,775)	DOC1	238
	READ(1,100)PWNUKE	DOC1	239
	IF(E7F(1))17,17	DOC1	240
	17 WRITE(6,780)	DOC1	241
	READ(1,100)PMDOT	DOC1	242
	IF(E7F(1))18,18	DOC1	243
	18 WRITE(6,781)	DOC1	244
	READ(1,100)WTFRACS	DOC1	245
	IF(E7F(1))19,19	DOC1	246
	19 WRITE(6,787)	DOC1	247
	READ(1,100)FHE	DOC1	248
	IF(E7F(1))20,20	DOC1	249
	20 WRITE(6,788)	DOC1	250
	READ(1,100)OFLPMIN	DOC1	251
	IF(E7F(1))21,21	DOC1	252
	21 WRITE(6,789)	DOC1	253
	READ(1,100)TSWIFT	DOC1	254
	IF(E7F(1))22,22	DOC1	255
	22 WRITE(6,790)	DOC1	256
	READ(1,100)PWTOP	DOC1	257
	IF(E7F(1))24,24	DOC1	258
	24 WRITE(6,791)	DOC1	259
	READ(1,100)PPYLD	DOC1	260
	IF(E7F(1))25,25	DOC1	261
	25 WRITE(6,792)	DOC1	262
	READ(1,100)WTPYLD	DOC1	263
	IF(E7F(1))68,68	DOC1	264
	68 WRITE(6,793)	DOC1	265
	READ(1,100)WPRDPT	DOC1	266
	IF(E7F(1))69,69	DOC1	267
	69 WRITE(6,922)	DOC1	268
	READ(1,100)SC1	DOC1	269
	IF(E7F(1))70,70	DOC1	270
	70 WRITE(6,923)	DOC1	271
	READ(1,100)SB1	DOC1	272
	IF(E7F(1))77,77	DOC1	273
	77 WRITE(6,924)	DOC1	274
	READ(1,100)VMAX	DOC1	275
	IF(E7F(1))7,7	DOC1	276
	7 WRITE(6,795)	DOC1	277
C		DOC1	278
C	*****	DOC1	279
C		DOC1	280
C	SELECTION OF A SINGLE PARAMETER TO VARY	DOC1	281
C		DOC1	282
C	*****	DOC1	283
	23 IF(CD.GE.81.)CD=.035	DOC1	284
	WRITE(6,119)	DOC1	285
	WRITE(6,120)	DOC1	286



10	WRITE(6,127)		
	PFAD(1,48)IELECT	00C1	287
	IF(F7F(1)) 10,11	00C1	288
11	WRITE(6,822)	00C1	289
	00 33 IMM=1.3	00C1	290
	WRITE(6,122)IMM	00C1	291
30	PFAD(1,100)E(IMM)	00C1	292
	00 02 IR=6.6	00C1	293
		00C1	294
	00 99 IMM=1.3	00C1	295
	IF(IELECT.FO.10)CD=E(IMM)	00C1	296
	IF(IELECT.FO.11)ALT=E(IMM)	00C1	297
	IF(IELECT.FO.12)ASPEED=E(IMM)	00C1	298
	IF(IELECT.FO.13)PWMOTOR=E(IMM)	00C1	299
	IF(IELECT.FO.14)EWRAE=E(IMM)	00C1	300
	IF(IELECT.FO.15)FFRAT=E(IMM)	00C1	301
	IF(IELECT.FO.16)EFCOLL=E(IMM)	00C1	302
	IF(IELECT.FO.17)WACOLL=E(IMM)	00C1	303
	IF(IELECT.FO.18)EFLUX=E(IMM)	00C1	304
	IF(IELECT.FO.19)FFPROP=E(IMM)	00C1	305
	IF(IELECT.FO.20)POFF=E(IMM)	00C1	306
	IF(IELECT.FO.21)FHE=E(IMM)	00C1	307
	IF(IELECT.FO.21)FAR=1.-FHE	00C1	308
	IF(IELECT.FO.22)DELPMIN=E(IMM)	00C1	309
	IF(IELECT.FO.23)TSHIFT=E(IMM)	00C1	310
	IF(IELECT.FO.24)WTFRACS=E(IMM)	00C1	311
	IF(IELECT.FO.25)PWTPP=E(IMM)	00C1	312
	IF(IELECT.FO.26)PPYLO=E(IMM)	00C1	313
	IF(IELECT.FO.27)WTPYLO=E(IMM)	00C1	314
	IF(IELECT.FO.28)WPRNPT=E(IMM)	00C1	315
	IF(IELECT.FO.29)SC1=E(IMM)	00C1	316
	IF(IELECT.FO.30)VMAX=E(IMM)	00C1	317
	IF(IELECT.FO.50)PWNUKE=E(IMM)	00C1	318
		00C1	319
C	CALCULATION OF AMBIENT TEMPERATURE	00C1	320
C		00C1	321
C	ALT=ALT/.3048	00C1	322
	IF(ALT.GE.0. .AND. ALT.LT.11.)T=289.15-(ALT*(289.15-216.65)/11.)	00C1	323
	IF(ALT.GE.11. .AND. ALT.LE.20.)T=216.65	00C1	324
	IF(ALT.GT.20. .AND. ALT.LT.32.)T=217.+((ALT-70.)*(229.-217.)/12.)	00C1	325
	IF(ALT.GE.32. .AND. ALT.LT.47.)T=229.+((ALT-32.)*(271.-229.)/15.)	00C1	326
	IF(ALT.GE.47. .AND. ALT.LE.52.)T=271.	00C1	327
	IF(ALT.GT.52. .AND. ALT.LT.61.)T=271.-((ALT-52.)*(271.-253.)/9.)	00C1	328
	IF(ALT.GE.61. .AND. ALT.LT.79.)T=253.-((ALT-61.)*(253.-181.)/18.)	00C1	329
	IF(ALT.GE.79.)T=181.	00C1	330
C	T IS AMBIENT TEMPERATURE(KELVIN)	00C1	331
C	T=T+TSHIFT	00C1	332
	ALT=ALT/.3048	00C1	333
		00C1	334
C	CALCULATION OF AMBIENT DENSITY AND PRESSURE	00C1	335
C		00C1	336
C	X=2.*((2.*ALT/AC)-1.)	00C1	337
	C(1)=1.	00C1	338
	COENS=0.	00C1	339
	CPRES=0.	00C1	340
	C(2)=X	00C1	341
	C(3)=(X**2.)-2.	00C1	342
		00C1	343
	00 33 IU=4,15	00C1	344
	C(IU)=(X*C(IU-1))-C(IU-2)	00C1	345
33	CONTINUE	00C1	346
	00 34 II=1,15	00C1	347
	COENS=COENS+(A(II)*C(II)/2.)	00C1	348
	CPRES=CPRES+(B(II)*C(II)/2.)	00C1	349
34	CONTINUE	00C1	350
		00C1	351
C	COENS IS AMBIENT DENSITY(SLUGS/FT/FT/FT)	00C1	352
C	DEFN=PHONOT*EXP(COENS)	00C1	353
	PPFSS=PNNT*EXP(CPRES)	00C1	354
		00C1	355
C	G=32.174-(ALT*(32.174-31.189)/AC2)	00C1	356
C	LINENO=LINENO+1	00C1	357
		00C1	358

C	*****	DOC1	359
C	*****	DOC1	360
C	ALIMP CONCEPT SIZING	DOC1	361
C	*****	DOC1	362
C	*****	DOC1	363
C	*****	DOC1	364
C	*****	DOC1	365
C	VOL IS BLIMP VOLUME(FT X FT X FT)	DOC1	366
C	VOL=10.00F+06	DOC1	367
C	DN 99 I=1.20	DOC1	368
C	VOL=VOL*(VOL/4.)	DOC1	369
C	EVOL=VOL*(1.F-06)	DOC1	370
C	VOLA=(VOL**0.667)	DOC1	371
C	DIAM IS BLIMP DIAMETER(FT)	DOC1	372
C	DIAM=((VOL*4.)/(PI*VLD*PC*PC))**0.333	DOC1	373
C	ARFF IS BLIMP PLANFORM AREA(FT X FT)	DOC1	374
C	ARFF=(DIAM*DIAM*VLD)*PC	DOC1	375
C	SURFACE IS BLIMP SURFACE AREA(FT X FT)	DOC1	376
C	SURFACE=PI*DIAM*PC*VLD*DIAM	DOC1	377
C	PMORFO IS MOTOR POWER PROVIDED AT AVERAGE AIRSPEED(W)	DOC1	378
C	PMORFO=CC1*CD*DENS*(ASPEED**3.)*(VOL**0.667)/(2.*EFFPROP)	DOC1	379
C	PMORFO1 IS MOTOR POWER PROVIDED AT MAXIMUM AIRSPEED(W)	DOC1	380
C	PMORFO1=CC1*CD*DENS*((VMAX)**3.)*(VOL**0.667)/(2.*EFFPROP)	DOC1	381
C	THRUST IS THRUST AT AVERAGE AIRSPEED(LBS)	DOC1	382
C	THRUST=CD*DENS*(ASPEED**2.)*(VOL**0.667)/(2.)	DOC1	383
C		DOC1	384
C		DOC1	385
C		DOC1	386
C		DOC1	387
C		DOC1	388
C		DOC1	389
C		DOC1	390
C		DOC1	391
C		DOC1	392
C			
C	THRUST1 IS THRUST AT MAXIMUM AIRSPEED(LBS)	DOC1	393
C	THRUST1=CD*DENS*((VMAX)**2.)*(VOL**0.667)/(2.)	DOC1	394
C		DOC1	395
C	ENERGY IS ENERGY PROVIDED BY RECTENNA AT AVERAGE AIRSPEED(W-H)	DOC1	396
C	ENERGY=((PMORFO/EFMOTOR)*PPYLD)*((24.-POFF)+(POFF/EFBAT))/EFPP	DOC1	397
C		DOC1	398
C	ENERGY1 IS ENERGY PROVIDED BY RECTENNA AT MAXIMUM AIRSPEED(W-H)	DOC1	399
C	ENERGY1=((PMORFO1/EFMOTOR)*PPYLD)*((24.-POFF)+(POFF/EFBAT))/EFPP	DOC1	400
C		DOC1	401
C	PCOLL IS POWER PROVIDED BY RECTENNA(W)	DOC1	402
C	PCOLL=ENERGY1/(24.-POFF)	DOC1	403
C		DOC1	404
C	*****	DOC1	405
C		DOC1	406
C	LIFT	DOC1	407
C	*****	DOC1	408
C	*****	DOC1	409
C	FAP IS FRACTION OF AIR IN BLIMP ENVELOPE	DOC1	410
C	FAP=1.-FHE	DOC1	411
C	FLIFTAR=FAR*GMOLAIR*(PRESS+DELPMIN)/((R*T*CB1)	DOC1	412
C	FLIFTHE=FHE*GMOLEHE*(PRESS+DELPMIN)/((R*T*CB1)	DOC1	413
C		DOC1	414
C		DOC1	415
C	FLIFT IS TOTAL BLIMP LIFT(LBS)	DOC1	416
C	FLIFT=VOL*DENS*G	DOC1	417
C	FLIFT=FLIFT*(1.0E-06)	DOC1	418
C		DOC1	419
C	*****	DOC1	420
C	*****	DOC1	421
C	WFIGHTS (LBS)	DOC1	422
C	*****	DOC1	423
C	*****	DOC1	424
C		DOC1	425
C	C1 PROVIDES FOR DESIRED WEIGHT FRACTION	DOC1	426
C	C1=WTFRACS/(1.-WTFRACS)	DOC1	427
C		DOC1	428
C	WTPP IS WEIGHT FOR POWER PROCESSING	DOC1	429
C	WTPP=((PPYLD/PWTPP)+(PMOREQ1/CPPI)	DOC1	430
C		DOC1	431
C	WTPRJP IS WEIGHT OF PROPELLER	DOC1	432
C	WTPRJP=WPROPT*THRUST1	DOC1	433
C		DOC1	434

C	WTMOTOR IS WEIGHT OF MOTOR AND GEAR BOX	DOC1	435
C	WTMOTOR=PMOREQ1/PMOTOR	DOC1	436
C	WTDISPG IS WEIGHT OF DISPLACED AIR	DOC1	437
C	WTDISPG=VOL*DENSG	DOC1	438
C	IF(EFLUX.LT.1.)G TO 51	DOC1	439
		DOC1	440
		DOC1	441
C	WTCOLL IS RECTENNA WEIGHT	DOC1	442
C	WTCOLL=(1.+SC1)*PCOLL+WACOLL/(EFLUX*EFCOLL)	DOC1	443
C	51 IF(EFLUX.LT.1.)WTCOLL=0.	DOC1	444
C	WTRAT IS WEIGHT OF BATTERY OR FUEL CELL	DOC1	445
C	WTRAT=(1.+SR1)*((PMOREQ/EFMOTOR)+PPYLD)*POFF/EBAT	DOC1	446
C		DOC1	447
C	WTGAS IS BLIMP ENVELOPE GAS WEIGHT	DOC1	448
C	WTGAS=VOL*G*(FLIFTAR+FLIFTHE)	DOC1	449
C		DOC1	450
C	WTNUKE IS WEIGHT OF NUCLEAR PROPULSION SYSTEM	DOC1	451
C	WTNUKE=PCOLL/PMNUKE	DOC1	452
C	IF(EFLUX.GT.1.)WTNUKE=0.	DOC1	453
C	IF(EFLUX.GT.1.)PMNUKE=0.	DOC1	454
C		DOC1	455
C	WEIGHT2=WTTP+WTMOTOR+WTCOLL+WTRAT+WTNUKE+WTPROP+WTPYLD	DOC1	456
C		DOC1	457
C	WTSTRT IS STRUCTURAL WEIGHT	DOC1	458
C	WTSTRT=WEIGHT2*C1	DOC1	459
C		DOC1	460
C	WEIGHT IS TOTAL BLIMP WEIGHT	DOC1	461
C	WEIGHT=WEIGHT2+WTSTRT+WTGAS	DOC1	462
C		DOC1	463
C		DOC1	464
C	*****	DOC1	465
C		DOC1	466
C	ACOLL IS AREA OF RECTENNA(FT X FT)	DOC1	467
C	ACOLL=WTCOLL/WACOLL	DOC1	468
C		DOC1	469
C	*****	DOC1	470
C	PAPAFTERS FOR PLOTTING	DOC1	471
C		DOC1	472
C	YPLNTJ=ENEGGY/(FLIFT*1000.)	DOC1	473
C	YPLNT(1)=ACOLL/AREF	DOC1	474
C	YPLNT(2)=(WTMOTOR+WTGAS+WTTP+WTPROP)/FLIFT	DOC1	475
C	YPLNT(3)=(WTSTRT+WTPYLD)/FLIFT	DOC1	476
C	IF(EFLUX.LT.1.)YPLNT(4)=WTNUKE/(FLIFT)	DOC1	477
C	IF(EFLUX.GT.1.)YPLNT(4)=WTCOLL/(FLIFT)	DOC1	478
C	YPLNT(5)=WTRAT/(FLIFT)	DOC1	479
C	YPLNT(6)=(FLIFT/WEIGHT)-1.	DOC1	480
C		DOC1	481
C		DOC1	482
C	99 WRTT(5,560)(INEND,EVOL,YPLNT(IR)	DOC1	483
C		DOC1	484
C	*****	DOC1	485
C	*****	DOC1	486
C		DOC1	487
C	OUTPJT	DOC1	488
C		DOC1	489
		DOC1	490
	ITT=ITT+1	DOC1	491
	WRITE(5,151)99999	DOC1	492
C		DOC1	493
	IF(IFLECT.EQ.10)CD=E(4)	DOC1	494
	IF(IFLECT.EQ.11)ALT=F(4)	DOC1	495
	IF(IFLECT.EQ.12)ASPEED=E(4)	DOC1	496
	IF(IFLECT.EQ.13)PMOTOR=E(4)	DOC1	497
	IF(IFLECT.EQ.14)EWRT=E(4)	DOC1	498
	IF(IFLECT.EQ.15)EFRAT=E(4)	DOC1	499
	IF(IFLECT.EQ.16)EFCOLL=E(4)	DOC1	500
	IF(IFLECT.EQ.17)WACOLL=E(4)	DOC1	501
	IF(IFLECT.EQ.18)EFLUX=E(4)	DOC1	502
	IF(IFLECT.EQ.19)EPROP=E(4)	DOC1	503
	IF(IFLECT.EQ.20)POFF=E(4)	DOC1	504
	IF(IFLECT.EQ.21)FHE=F(4)	DOC1	505
	IF(IFLECT.EQ.22)DELPMIN=E(4)	DOC1	506
	IF(IFLECT.EQ.23)TSHIFT=E(4)	DOC1	507
	IF(IFLECT.EQ.24)WTFRACS=E(4)	DOC1	508

C		DDC1	509
C	PLNT OUTPUT	DDC1	510
C	DD 4? IT=6.6	DDC1	511
	WRITE(5,152)4.1,1,1,1,0,1	DDC1	512
	WRITE(5,156)9999H,KA+0,KA+1,KA+2	DDC1	513
	KA=KA+3	DDC1	514
	WRITE(5,155)0,0,0	DDC1	515
	WRITE(5,155)7,7,7	DDC1	516
	WRITE(5,155)1,2,3	DDC1	517
C		DDC1	518
C	PLNT LABEL SPECIFICATION	DDC1	519
C	IF(IT.EQ.1) WRITE(5,800)	DDC1	520
	IF(IT.EQ.2) WRITE(5,801)	DDC1	521
	IF(IT.EQ.3) WRITE(5,802)	DDC1	522
	IF(IT.EQ.4.AND.EFLUX.LT.1.) WRITE(5,803)	DDC1	523
	IF(IT.EQ.4.AND.EFLUX.GT.1.) WRITE(5,804)	DDC1	524
	IF(IT.EQ.5) WRITE(5,805)	DDC1	525
	IF(IT.EQ.6) WRITE(5,805)	DDC1	526
C		DDC1	527
C	WRITE(5,192)CD,ASPEED,POFF,ALT	DDC1	528
	WRITE(5,194)EFPRDP,EWBAT,EFBAT,PWMOTOR	DDC1	529
	WRITE(5,196)PWNKX,WACOLL,EFCOLL,EFLUX	DDC1	530
C		DDC1	531
C	Y-AXIS GRID SCALE FACTOR	DDC1	532
C	IF(IT.EQ.1) WRITE(5,500)1.,0.,6.,1.,.20	DDC1	533
	IF(IT.EQ.2) WRITE(5,500)1.,0.,1.,1.,.05	DDC1	534
	IF(IT.EQ.3) WRITE(5,500)1.,0.,1.,1.,.05	DDC1	535
		DDC1	536
		DDC1	537
		DDC1	538
		DDC1	539
	IF(IT.EQ.4) WRITE(5,500)1.,0.,1.,1.,.05	DDC1	540
	IF(IT.EQ.5) WRITE(5,500)1.,0.,1.,1.,.05	DDC1	541
	IF(IT.EQ.6) WRITE(5,500)4.,-8.,8.,4.,.2	DDC1	542
C		DDC1	543
C	X-AXIS GRID SCALE FACTOR	DDC1	544
C	WRITE(5,500)4.,0.,8.,4.,.2	DDC1	545
C		DDC1	546
C	Y-AXIS LABEL	DDC1	547
C	WRITE(5,515)33.,?	DDC1	548
C		DDC1	549
C		DDC1	550
	IF(IT.EQ.1) WRITE(5,203)	DDC1	551
	IF(IT.EQ.2) WRITE(5,202)	DDC1	552
	IF(IT.EQ.3) WRITE(5,201)	DDC1	553
	IF(IT.EQ.4.AND.EFLUX.LT.1.) WRITE(5,200)	DDC1	554
	IF(IT.EQ.4.AND.EFLUX.GT.1.) WRITE(5,206)	DDC1	555
	IF(IT.EQ.5) WRITE(5,204)	DDC1	556
	IF(IT.EQ.6) WRITE(5,205)	DDC1	557
C		DDC1	558
C	X-AXIS LABEL	DDC1	559
C	WRITE(5,515)31.,?	DDC1	560
C	WRITE(5,535)	DDC1	561
		DDC1	562
C		DDC1	563
C	PREPARE FIGURE LEGEND	DDC1	564
C	IF(TELECT.EQ.10)WRITE(5,600)	DDC1	565
	IF(TELECT.EQ.11)WRITE(5,602)	DDC1	566
	IF(TELECT.EQ.12)WRITE(5,603)	DDC1	567
	IF(TELECT.EQ.13)WRITE(5,604)	DDC1	568
	IF(TELECT.EQ.14)WRITE(5,605)	DDC1	569
	IF(TELECT.EQ.15)WRITE(5,606)	DDC1	570
	IF(TELECT.EQ.16)WRITE(5,607)	DDC1	571
	IF(TELECT.EQ.17)WRITE(5,608)	DDC1	572
	IF(TELECT.EQ.18)WRITE(5,609)	DDC1	573
	IF(TELECT.EQ.19)WRITE(5,610)	DDC1	574
	IF(TELECT.EQ.20)WRITE(5,611)	DDC1	575
	IF(TELECT.EQ.21)WRITE(5,613)	DDC1	576
	IF(TELECT.EQ.22)WRITE(5,614)	DDC1	577
	IF(TELECT.EQ.23)WRITE(5,615)	DDC1	578
	IF(TELECT.EQ.24)WRITE(5,616)	DDC1	579
	IF(TELECT.EQ.25)WRITE(5,617)	DDC1	580
	IF(TELECT.EQ.26)WRITE(5,618)	DDC1	581
	IF(TELECT.EQ.27)WRITE(5,619)	DDC1	582
		DDC1	583
		DDC1	584

IF(ISELECT.EQ.28)WRITE(5,620)	00C1	585
IF(ISELECT.EQ.29)WRITE(5,621)	00C1	586
IF(ISELECT.EQ.30)WRITE(5,625)	00C1	587
IF(ISELECT.EQ.50)WRITE(5,622)	00C1	588
WRITE(5,601)E(1)	00C1	589
WRITE(5,601)E(2)	00C1	590
WRITE(5,601)E(3)	00C1	591
42 CONTINUE	00C1	592
GOTO 301	00C1	593
	00C1	594
*****	00C1	595
*****	00C1	596
FORMATS	00C1	597
	00C1	598
*****	00C1	599
48 FORMAT(I2)	00C1	600
52 FORMAT(45(1H-))	00C1	601
53 FORMAT(45(1H-))	00C1	602
13V, 30444 DATA PLOTTED VERSUS VOLUME	00C1	603
2/4*(1H-))	00C1	604
922 FORMAT(*COLLECTOR REDUNDANCY FRACTION (0.1)*)	00C1	605
923 FORMAT(*BATTERY REDUNDANCY FRACTION (0.0)*)	00C1	606
924 FORMAT(*MAXIMUM AIRSPEED, FT/S (140.))*)	00C1	607
54 FORMAT(*I AM PROGRAM GRAVES, DEVELOPED BY*/	00C1	608
1*FPMIF GRAVES AND STUDENTS TO AID IN THE*/	00C1	609
2*PARAMETRIC ANALYSIS OF SOLAR-, MICROWAVE-,*/	00C1	610
3*OR NUCLEAR-POWERED RLIMPS*)	00C1	611
540 FORMAT(I5,2F10.5)	00C1	612
151 FORMAT(I5)	00C1	613
152 FORMAT(7I5)	00C1	614
155 FORMAT(5X,4I5)	00C1	615
156 FORMAT(5I5)	00C1	616
192 FORMAT(9H\$1C\$00\$N*,F5.3,2X,*ASPEED=*,F5.2,2X,*POFF=*,F5.2,2X,	00C1	617
1*ALT=*,F5.2,2X)	00C1	618
194 FORMAT(*EFPROP=*,F4.2,2X,*EWBAT=*,F6.2,2X,*EFBAT=*,F4.2,2X,	00C1	619
1*PWWT=*,F6.2,2X)	00C1	620
196 FORMAT(*PWNUKE=*,F4.1,2X,*WACOLL=*,F5.2,2X,*EFCOLL=*,F4.2,2X,	00C1	621
1*FLUX=*,F5.0,2X,2H\$6)	00C1	622
200 FORMAT(*WNUCLEAR/TLIFT*)	00C1	623
201 FORMAT(*\$WSTRUCT-PAYLDS)/TLIFT*)	00C1	624
202 FORMAT(*WMISC/TLIFT*)	00C1	625
203 FORMAT(*ACOLL/ARFF*)	00C1	626
204 FORMAT(*WBATTERY/TLIFT*)	00C1	627
205 FORMAT(*E(XCESS LIFT FRACTION), \$(L/W\$)-1*)	00C1	628
206 FORMAT(*WCOLL/TLIFT*)	00C1	629
500 FORMAT(6F10.4)	00C1	630
515 FORMAT(I2,F7.4)	00C1	631
535 FORMAT(*V(NOLUME), V X 10\$U-6\$N, (FT)\$U3*)	00C1	632
550 FORMAT(5HCARDS)	00C1	633
600 FORMAT(*33H*,*D(PAG COEFFICIENT), C\$00\$N*)	00C1	634
601 FORMAT(*10H*,F10.3)	00C1	635
602 FORMAT(*23H*,*A(LTITUDE), 10\$U3\$N(FT)*)	00C1	636
603 FORMAT(*17H*,*A(IRSPEED, FT/S)*)	00C1	637
604 FORMAT(*22H*,*M(NTOR WEIGHT), W/(LR)*)	00C1	638
605 FORMAT(*26H*,*B(BATTERY WEIGHT), W-(4/LB)*)	00C1	639
606 FORMAT(*20H*,*R(ATTERY EFFICIENCY)*)	00C1	640
607 FORMAT(*21H*,*R(ECTENNA EFFICIENCY)*)	00C1	641
608 FORMAT(*29H*,*R(ECTENNA WEIGHT, LB/FT)\$U2\$N*)	00C1	642
609 FORMAT(*39H*,*I(NCIDENT MICROWAVE POWER), W/(FT)\$U2\$N*)	00C1	643
610 FORMAT(*22H*,*P(PPELLER EFFICIENCY)*)	00C1	644
611 FORMAT(*23H*,*E(ENERGY STORAGE, HOURS)*)	00C1	645
613 FORMAT(*21H*,*H(ELIUM GAS FRACTION)*)	00C1	646
614 FORMAT(*27H*,*S(SUPERPRESSURE, LB/FT)\$U2\$N*)	00C1	647
615 FORMAT(*13H*,*S(SUPERHEAT), K*)	00C1	648
616 FORMAT(*28H*,*S(TRUCTURAL WEIGHT FRACTION)*)	00C1	649
617 FORMAT(*33H*,*P(OWER PROCESSING WEIGHT), W/(LB)*)	00C1	650
618 FORMAT(*18H*,*P(AYLOAD POWER), W*)	00C1	651
619 FORMAT(*20H*,*P(AYLOAD WEIGHT, LB)*)	00C1	652
620 FORMAT(*32H*,*P(PPELLER WEIGHT, LB/LR-THRUST)*)	00C1	653
621 FORMAT(*30H*,*R(ECTENNA REDUNDANCY FRACTION)*)	00C1	654
622 FORMAT(*31H*,*N(UCLEAR SYSTEM WEIGHT), W/(LB)*)	00C1	655
625 FORMAT(*24H*,*M(AXIMUM AIRSPEED, FT/S)*)	00C1	656
701 FORMAT(*10H*,F10.3)	00C1	657
740 FORMAT(24HOPTION PACKAGE? (Y OR N))	00C1	658

750	FORMAT(A1)		
760	FORMAT(*VEHICLE LENGTH-TO-DIAMETER RATIO (5.0)*)	DDC1	659
765	FORMAT(*BATTERY ENERGY-TO-WEIGHT RATIO, WH/LB (15.3)*)	DDC1	660
770	FORMAT(*BATTERY OVERALL EFFICIENCY (.85)*)	DDC1	661
773	FORMAT(*COLLECTOR WEIGHT-TO-AREA RATIO, LB/FT/FT/(.08)*)	DDC1	662
775	FORMAT(*NUCLEAR SYSTEM POWER-TO-WEIGHT RATIO, W/LB (20.0)*)	DDC1	663
777	FORMAT(*POFF, HOURS (0.0)*)	DDC1	664
790	FORMAT(*MOTOR-GEAR POWER-TO-WEIGHT RATIO, W/LB (573.0)*)	DDC1	665
791	FORMAT(*STRUCTURE WEIGHT FRACTION, (.33)*)	DDC1	666
795	FORMAT(*AVERAGE ENERGY FLUX, W/FT/FT (37.1)*)	DDC1	667
796	FORMAT(*COLLECTOR EFFICIENCY (.80)*)	DDC1	668
797	FORMAT(*FRACTION OF HELIUM (.95)*)	DDC1	669
798	FORMAT(*MINIMUM SUPER PRESSURE, LB/FT/FT (5.2)*)	DDC1	670
799	FORMAT(*SUPERHEAT, K (0.1)*)	DDC1	671
799	FORMAT(*POWER PROCESSING POWER-TO-WEIGHT RATIO, W/LB (53.4)*)	DDC1	672
799	FORMAT(*PAYLOAD POWER, W (1000.1)*)	DDC1	673
799	FORMAT(*PAYLOAD WEIGHT, LB (100.1)*)	DDC1	674
799	FORMAT(*PROP WT-TO-STATIC THRUST RATIO, (.06)*)	DDC1	675
799	FORMAT(45(14-))	DDC1	676
801	FORMAT(3X,*MISCELLANEOUS SYSTEMS WEIGHT*)	DDC1	677
802	FORMAT(11X,*COLLECTOR AREA*)	DDC1	678
802	FORMAT(10X,*STRUCTURE-PAYLOAD WEIGHT*)	DDC1	679
803	FORMAT(8X,*NUCLEAR SYSTEM WEIGHT*)	DDC1	680
804	FORMAT(12X,*BATTERY WEIGHT*)	DDC1	681
805	FORMAT(12X,*VEHICLE WEIGHT*)	DDC1	682
806	FORMAT(10X,*COLLECTOR WEIGHT*)	DDC1	683
822	FORMAT(*ENTER 3 VALUES OF PARAMETER*)	DDC1	684
100	FORMAT(F10.3)	DDC1	685
		DDC1	686
102	FORMAT(4F20.5)		
110	FORMAT(*ALTITUDE, THOUSANDS OF FT (70.00)*)	DDC1	687
111	FORMAT(*AIRSPEED, FT/S (50.1)*)	DDC1	688
112	FORMAT(*DRAG COEFFICIENT(.035)*)	DDC1	689
113	FORMAT(*PARAMETER ??)	DDC1	690
113	FORMAT(*PROPELLER EFFICIENCY(.85)*)	DDC1	691
120	FORMAT(*10=CD*/11=ALT*/12=ASPEED*/13=PMOTOR*/	DDC1	692
	14=FWAT*/15=EFRA*/16=EFFCOLL*/17=WACOLL*/18=EFLUX*/	DDC1	693
	19=FFPROP*/20=POFF*/21=FHE*/22=DELPHIN*/	DDC1	694
	23=TSHIFT*/24=WTFRACS*/25=PHTRP*/26=PPYLD*/27=HTPYLD*/	DDC1	695
	28=WPDPOT*/29=REDUN(SC1)*/30=VMAX*/50=PHNUKE*/	DDC1	696
127	FORMAT(*ENTER ONE NUMBER ?*)	DDC1	697
127	FORMAT(*VALUE NUMBER *.11,* FOR PARAMETER*)	DDC1	698
900	FORMAT(*PLOT(FRAME) NUMBER*	DDC1	699
	1/*1-COLLECTOR AREA*/	DDC1	700
	2*2-MISCELLANEOUS SYSTEMS WEIGHT*/	DDC1	701
	3*3-STRUCTURE-PAYLOAD WEIGHT*/	DDC1	702
	4*4-COLLECTOR(NUCLEAR SYSTEM) WEIGHT*/	DDC1	703
	5*5-BATTERY WEIGHT*/6-VEHICLE WEIGHT*/	DDC1	704
2000	FORMAT(5F14.6)	DDC1	705
301	END	DDC1	706
		DDC1	707

## A.2 AIRPLANE

C	PROGRAM HEYSON (INPUT,OUTPUT,TAPE1=INPUT,TAPES,TAPE6=OUTPUT)	DOC	1
C	*****	DOC	2
C		DOC	3
C	PROGRAM HEYSON AIDS IN THE FEASIBILITY ANALYSIS OF	DOC	4
C	SOLAR-, MICROWAVE-, AND NUCLEAR-POWERED AIRPLANES	DOC	5
C		DOC	6
C	TAPE1 IS INPUT FROM INTERACTIVE TERMINAL	DOC	7
C	TAPE5 IS A PLOTTING PROGRAM INPUT TAPE	DOC	8
C	TAPE6 IS OUTPUT TO TERMINAL	DOC	9
C		DOC	10
C	*****	DOC	11
C		DOC	12
C	DIMENSION B(4),A(15),C(15),YPLT(6)	DOC	13
C	REWIND 5	DOC	14
C		DOC	15
C	RHO IS SEA LEVEL DENSITY(SLUGS/FT/FT)	DOC	16
C	RHO=.0023769	DOC	17
C		DOC	18
C	CC1 CONVERTS (FT-LB/S) TO W	DOC	19
C	CC1=1.355818	DOC	20
C		DOC	21
C	CPP IS PROPULSION POWER PROCESSING SPECIFIC POWER(W/LB)	DOC	22
C	CPP=250.	DOC	23
C		DOC	24
C	CHEBYSHEV A() VALUES--USED IN CALCULATING AMBIENT DENSITY	DOC	25
C		DOC	26
C	A(1)=-.10960632E+02	DOC	27
C	A(2)=-.55717132E+01	DOC	28
C	A(3)=-.99116555E-01	DOC	29
C	A(4)=-.61044847E-01	DOC	30
C	A(5)=-.14304157	DOC	31
C	A(6)=-.29492088E-02	DOC	32
C	A(7)=-.58789604E-02	DOC	33
C	A(8)=-.20421324E-02	DOC	34
C	A(9)=-.71033206E-02	DOC	35
C	A(10)=-.10314086E-01	DOC	36
C	A(11)=-.34100737E-02	DOC	37
C	A(12)=-.41764325E-02	DOC	38
C	A(13)=-.39151559E-02	DOC	39
C	A(14)=-.11227028E-02	DOC	40
C	A(15)=-.15751053E-02	DOC	41
C		DOC	42
C		DOC	43
C	WRITE(6,830)	DOC	44
C	WRITE(6,53)	DOC	45
C	WRITE(6,54)	DOC	46
C	WRITE(6,53)	DOC	47
C	WRITE(5,550)	DOC	48
C		DOC	49
C		DOC	50
C	N=0	DOC	51
C	C(1)=1.	DOC	52
C	CAL=262.467	DOC	53
C	B(4)=100000.12345678	DOC	54
C	*****	DOC	55
C		DOC	56
C	***** DEFAULT VALUES *****	DOC	57
C	DEFAULT VALUES ARE THOSE FOR A MICROWAVE-POWERED AIRPLANE	DOC	58
C		DOC	59
C		DOC	60
C	*****	DOC	61
C	CLMAX IS MAXIMUM LIFT COEFFICIENT	DOC	62
C	CLMAX=1.5	DOC	63
C		DOC	64
C	CDJ IS AIRPLANE PROFILE DRAG COEFFICIENT	DOC	65
C	CDJ=.010	DOC	66

C		DOC	67
C	ASPEED IS AVERAGE AIRSPEED(FT/S)	DOC	68
	ASPEED=140.0	DOC	69
C		DOC	70
C	VMAX IS MAXIMUM AIRSPEED(FT/S)	DOC	71
	VMAX=140.00	DOC	72
C		DOC	73
C	EFPROP IS PROPELLER EFFICIENCY	DOC	74
	EFPROP=.85	DOC	75
C		DOC	76
C	POFF IS NUMBER OF HOURS THAT FLIGHT OPERATIONS ARE	DOC	77
	MAINTAINED BY THE STORED ENERGY	DOC	78
	POFF=0.	DOC	79
C		DOC	80
C	WTFRACS IS STRUCTURE-TO-WEIGHT RATIO	DOC	81
	WTFRACS=.17	DOC	82
C		DOC	83
C	EWBAT IS BATTERY(ENERGY STORAGE DEVICE)	DOC	84
	ENERGY-TO-WEIGHT RATIO(W-H/LB)	DOC	85
	EWBAT=15.3	DOC	86
C		DOC	87
C	EFBAT IS BATTERY(ENERGY STORAGE DEVICE) EFFICIENCY	DOC	88
	EFBAT=.85	DOC	89
C		DOC	90
C	WACOLL IS RECTENNA(OR SOLAR CELL) WEIGHT-TO-AREA RATIO(LB/FT/FT)	DOC	91
	WACOLL=.04	DOC	92
C		DOC	93
C	PWMOTOR IS MOTOR-GEAR-BOX SYSTEM POWER-TO-WEIGHT RATIO(W/LB)	DOC	94
	PWMOTOR=573.	DOC	95
C		DOC	96
C	EFMOTOR IS MOTOR-GEAR-BOX SYSTEM EFFICIENCY	DOC	97
	EFMOTOR=.94	DOC	98
C			
C		DOC	99
C	EFLUX IS THE POWER-TO-AREA RATIO OF THE MICROWAVE BEAM	DOC	100
	(OR SUN'S RAYS) INCIDENT ON THE AIRPLANE(W/FT/FT/)	DOC	101
	EFLUX=37.0	DOC	102
C		DOC	103
C	EFCOLL IS THE RECTENNA(OR SOLAR CELL) EFFICIENCY	DOC	104
	EFCOLL=.80	DOC	105
C		DOC	106
C	ALT IS ALTITUDE(IN THOUSANDS OF FT)	DOC	107
	ALT=70.0	DOC	108
C		DOC	109
C	PPYLD IS PAYLOAD POWER(W)	DOC	110
	PPYLD=1000.	DOC	111
C		DOC	112
C	PWNUKE IS NUCLEAR SYSTEM POWER-TO-WEIGHT RATIO(W/LB)	DOC	113
	PWNUKE=15.	DOC	114
C		DOC	115
C	PI IS PI(THE MATHEMATICAL TERM)	DOC	116
	PI=3.14159	DOC	117
C		DOC	118
C	PWTPP IS POWER PROCESSING POWER-TO-WEIGHT RATIO(W/LB)	DOC	119
	PWTPP=53.4	DOC	120
C		DOC	121
C	EFPP IS POWER PROCESSING EFFICIENCY	DOC	122
	EFPP=.92	DOC	123
C		DOC	124
C	WPROPT IS PROPELLER WEIGHT-TO-THRUST RATIO(LB/LB-THRUST)	DOC	125
	WPROPT=.06	DOC	126
C		DOC	127
C	WTPYLD IS PAYLOAD WEIGHT(LBS)	DOC	128
	WTPYLD=100.	DOC	129
C		DOC	130
C	E IS OSWALD AIRPLANE EFFICIENCY FACTOR	DOC	131
	E=.85	DOC	132
C		DOC	133
C	AR IS AIRPLANE ASPECT RATIO	DOC	134
	AR=20.	DOC	135
C		DOC	136
C	SC1 IS RECTENNA(OR SOLAR CELL) REDUNDANCY FRACTION	DOC	137
	SC1=0.10	DOC	138
C		DOC	139
C	SB1 IS BATTERY(ENERGY STORAGE DEVICE) REDUNDANCY FRACTION	DOC	140
	SB1=0.0	DOC	141
C		DOC	142
C	SS1 IS STRUCTURAL WEIGHT-TO-WING AREA RATIO (LB/FT/FT)	DOC	143
	SS1=.4	DOC	144



C	*****	DOC	145
C		DOC	146
C		DOC	147
C	INTERACTIVE PROGRAM INPUT	DOC	148
C		DOC	149
C	*****	DOC	150
	1 CONTINUE	DOC	151
	WRITE(6,700)	DOC	152
	READ(1,50)CLMAX	DOC	153
C		DOC	154
C	IF CLMAX INPUT GREATER THAN 10., ALL DEFAULT VALUES ARE USED	DOC	155
C		DOC	156
	IF(EOF(1)) 2,2	DOC	157
	2 IF(CLMAX.GT.10.)GO TO 29	DOC	158
	WRITE(6,710)	DOC	159
	READ(1,50)CDD	DOC	160
	IF(EOF(1)) 3,3	DOC	161
	3 WRITE(6,720)	DOC	162
	READ(1,50)ASPEED	DOC	163
	IF(EOF(1)) 4,4	DOC	164
	4 WRITE(6,730)	DOC	165
	READ(1,50)POFF	DOC	166
	IF(EOF(1)) 5,5	DOC	167
	5 WRITE(6,740)	DOC	168
	READ(1,750)OPT	DOC	169
	IF(EOF(1))13,21	DOC	170
	21 IF(OPT.EQ.1HY) 6,13	DOC	171
	6 WRITE(6,53)	DOC	172
	WRITE(6,760)	DOC	173
	READ(1,50)EFPROP	DOC	174
	IF(EOF(1)) 8,8	DOC	175
	8 WRITE(6,765)	DOC	176
	READ(1,50)EWBAT	DOC	177
	IF(EOF(1)) 14,14	DOC	178
	14 WRITE(6,770)	DOC	179
	READ(1,50)EFBAT	DOC	180
	IF(EOF(1)) 9,9	DOC	181
	9 WRITE(6,780)	DOC	182
	READ(1,50)PW MOTOR	DOC	183
	IF(EOF(1)) 10,10	DOC	184
	10 WRITE(6,775)	DOC	185
	READ(1,50)WACOLL	DOC	186
	IF(EOF(1)) 11,11	DOC	187
	11 WRITE(6,790)	DOC	188
	READ(1,50)EFCOLL	DOC	189
	IF(EOF(1)) 12,12	DOC	190
	12 WRITE(6,785)	DOC	191
	READ(1,50)EFLUX	DOC	192
C		DOC	193
C	IF EFLUX INPUT IS 0.,A NUCLEAR POWERED AIRPLANE IS REPRESENTED	DOC	194
C		DOC	195
	IF(EOF(1)) 13,13	DOC	196
	13 WRITE(6,820)	DOC	197
	READ(1,50)ALT	DOC	198
	IF(EOF(1)) 66,66	DOC	199
	66 WRITE(6,840)	DOC	200
	READ(1,50)PWTPP	DOC	201
	IF(EOF(1))67,67	DOC	202
	67 WRITE(6,841)	DOC	203
	READ(1,50)PPYLD	DOC	204
	IF(EOF(1))68,68	DOC	205
	68 WRITE(6,842)	DOC	206
	READ(1,50)WTPYLD	DOC	207
	IF(EOF(1))69,69	DOC	208
	69 WRITE(6,843)	DOC	209
	READ(1,50)PWNUKE	DOC	210
	IF(EOF(1))70,70	DOC	211
	70 WRITE(6,844)	DOC	212
	READ(1,50)AR	DOC	213
	IF(EOF(1))81,81	DOC	214
	81 WRITE(6,922)	DOC	215
	READ(1,50)SC1	DOC	216
	IF(EOF(1))82,82	DOC	217
	82 WRITE(6,923)	DOC	218
	READ(1,50)S81	DOC	219
	IF(EOF(1))89,89	DOC	220

89	WRITE(6,927)	DOC	221
	READ(1,50)WTFRACS	DOC	222
	IF(EOF(1))93,93	DOC	223
93	WRITE(6,928)	DOC	224
	READ(1,50)SS1	DOC	225
	IF(EOF(1))91,91	DOC	226
91	WRITE(6,929)	DOC	227
	READ(1,50)E	DOC	228
	IF(EOF(1))88,88	DOC	229
88	WRITE(6,845)	DOC	230
	READ(1,50)VMAX	DOC	231
	WRITE(6,53)	DOC	232
	IF(EOF(1))15,15	DOC	233
C		DOC	234
C		DOC	235
C	*****	DOC	236
C	SELECTION OF A SINGLE PARAMETER TO VARY	DOC	237
C		DOC	238
C	*****	DOC	239
29	IF(CLMAX.GT.10.)CLMAX=1.5	DOC	240
15	CONTINUE	DOC	241
	WRITE(6,821)	DOC	242
	READ(1,40)IB	DOC	243
	IF(EOF(1))15,90	DOC	244
		DOC	245
90	WRITE(6,822)	DOC	246
	DO 49 IM=1,3	DOC	247
	WRITE(6,823)IM	DOC	248
92	READ(1,50)B(IM)	DOC	249
	IF(EOF(1))92,49	DOC	250
49	CONTINUE	DOC	251
C		DOC	252
	DO 41 IOU=6,6	DOC	253
	DO 41 IS=1,3	DOC	254
	IF(IB.EQ.10)CLMAX=B(IS)	DOC	255
	IF(IB.EQ.11)CDD=B(IS)	DOC	256
	IF(IB.EQ.12)ASPEED=B(IS)	DOC	257
	IF(IB.EQ.13)POFF=B(IS)	DOC	258
	IF(IB.EQ.14)EFPROP=B(IS)	DOC	259
	IF(IB.EQ.15)EWGAT=B(IS)	DOC	260
	IF(IB.EQ.16)EFGAT=B(IS)	DOC	261
	IF(IB.EQ.17)PHMOTOR=B(IS)	DOC	262
	IF(IB.EQ.18)WACOLL=B(IS)	DOC	263
	IF(IB.EQ.19)EFCOLL=B(IS)	DOC	264
	IF(IB.EQ.20)EFLUX=B(IS)	DOC	265
	IF(IB.EQ.21)ALT=B(IS)	DOC	266
	IF(IB.EQ.22)PHTPP=B(IS)	DOC	267
	IF(IB.EQ.23)PPYLD=B(IS)	DOC	268
	IF(IB.EQ.24)WTPYLD=B(IS)	DOC	269
	IF(IB.EQ.25)AR=B(IS)	DOC	270
	IF(IB.EQ.26)ISCL=B(IS)	DOC	271
	IF(IB.EQ.27)WTFRACS=B(IS)	DOC	272
	IF(IB.EQ.28)WPROPT=B(IS)	DOC	273
	IF(IB.EQ.29)VMAX=B(IS)	DOC	274
	IF(IB.EQ.30)SS1=B(IS)	DOC	275
	IF(IB.EQ.31)E=B(IS)	DOC	276
	IF(IB.EQ.50)PWHUKE=B(IS)	DOC	277
C		DOC	278
22	CONTINUE	DOC	279
	N=N+1	DOC	280
C		DOC	281
C	CALCULATION OF AMBIENT DENSITY	DOC	282
C		DOC	283
	X=2.*((2*ALT/CA1)-1.)	DOC	284
	RLN=0.	DOC	285
	C(2)=X	DOC	286
	C(3)=(X**2.)-2.	DOC	287
	DO 35 IZ=4,15	DOC	288
35	C(IZ)=(X*C(IZ-1))-C(IZ-2)	DOC	289
	DO 36 IV=1,15	DOC	290
36	RLN=RLN+(A(IV)*C(IV)/2.)	DOC	291
C		DOC	292
C	DENS IS AMBIENT DENSITY(SLUGS/FT/FT/FT)	DOC	293
	DENS=RHO*EXP(RLN)	DOC	294

C	*****	DOC	295
C	*****	DOC	296
C		DOC	297
C	AIRPLANE CONCEPT SIZING SCHEME	DOC	298
C		DOC	299
C	*****	DOC	300
C	*****	DOC	301
C	CL IS DESIGN CL FOR MINIMUM POWER OPERATION	DOC	302
C	CL=SQRT(3.*PI*AR*E+CDO)	DOC	303
C	IF(CL.GT.CLMAX)CL=CLMAX	DOC	304
C		DOC	305
C	CD IS CRUISE CD	DOC	306
C	CD=CDO+((CL**2.)/(PI*AR*E))	DOC	307
C		DOC	308
C	SREF IS WING PLANFORM AREA(FT X FT)	DOC	309
C	SREF=5.	DOC	310
C		DOC	311
C	DO 41 II=1.20	DOC	312
C	WTFRAC1=WTFRACS	DOC	313
C	SREF=1.5*SREF	DOC	314
C	56 C1=WTFRAC1/(1.-WTFRAC1)	DOC	315
C		DOC	316
C	PMOREQ IS MOTOR POWER AT CRUISE AIRSPEED(W)	DOC	317
C	PMOREQ=C1*CD*DENS*(ASPEED**3.)*SREF/(2.*EFPROP)	DOC	318
C		DOC	319
C	THRUST IS THRUST AT CRUISE AIRSPEED(LB)	DOC	320
C	THRUST=CD*DENS*(ASPEED**2.)*SREF/(2.)	DOC	321
C		DOC	322
C	PMOREQ1 IS MOTOR POWER AT MAXIMUM AIRSPEED(W)	DOC	323
C	PMOREQ1=C1*CD*DENS*((VMAX)**3.)*SREF/(2.*EFPROP)	DOC	324
C		DOC	325
C	THRUST1 IS THRUST AT MAXIMUM AIRSPEED(W)	DOC	326
C	THRUST1=CD*DENS*((VMAX)**2.)*SREF/(2.)	DOC	327
C		DOC	328
C	ELIFT IS DEVELOPED LIFT(LB)	DOC	329
C	ELIFT=CL*DENS*(ASPEED**2.)*SREF/2.	DOC	330
C		DOC	331
C	ENERGY IS ENERGY NEEDED AT CRUISE AIRSPEED(W-H)	DOC	332
C	ENERGY=((PMOREQ/EFMOTOR)+PPYLD)*(24.-POFF+(POFF/EFBAT))/EFPP	DOC	333
C		DOC	334
C	ENERGY1 IS ENERGY NEEDED AT MAXIMUM AIRSPEED(W-H)	DOC	335
C	ENERGY1=((PMOREQ1/EFMOTOR)+PPYLD)*(24.-POFF+(POFF/EFBAT))/EFPP	DOC	336
C		DOC	337
C	PCOLL IS POWER THAT RECTENNA MUST PROVIDE(W)	DOC	338
C	PCOLL=ENERGY1/(24.-POFF)	DOC	339
C		DOC	340
C	*****	DOC	341
C		DOC	342
C		DOC	343
C	WEIGHTS(LBS)	DOC	344
C	*****	DOC	345
C		DOC	346
C	WTMOT IS WEIGHT OF MOTOR AND GEAR BOX	DOC	347
C	WTMOT=PMOREQ1/PWMOTOR	DOC	348
C		DOC	349
C	WTPROP IS WEIGHT OF PROPELLER	DOC	350
C	WTPROP=WPROPT*THRUST1	DOC	351
C	IF(WTPROP.LT.2.0)WTPROP=2.0	DOC	352
C		DOC	353
C	WTPP IS POWER PROCESSING WEIGHT	DOC	354
C	WTPP=(PPYLD/PWTPP)+(PMOREQ1/CPP)	DOC	355
C	IF(EFLUX.LT.1.)GO TO 55	DOC	356
C		DOC	357
C	WTCOLL IS WEIGHT OF RECTENNA	DOC	358
C	WTCOLL=(1.+SC1)*(WACOLL*PCOLL)/(EFLUX*EFCOLL)	DOC	359
C	55 IF(EFLUX.LT.1.)WTCOLL=0.	DOC	360
C		DOC	361
C	WTBAT IS WEIGHT OF BATTERY OR FUEL CELL	DOC	362
C	WTBAT=(1.+S91)*((PMOREQ/EFMOTOR)+PPYLD)*POFF/EWBAT	DOC	363
C		DOC	364
C		DOC	365
C	WTNUKE IS WEIGHT OF NULEAR PROPULSION SYSTEM	DOC	366
C	WTNUKE=PCOLL/PWNUKE	DOC	367
C	IF(EFLUX.GT.1.)WTNUKE=0.	DOC	368
C	IF(EFLUX.GT.1.)PWNUKE=0.	DOC	369
C		DOC	370

	WTSTRT=0.	DOC	371
	WTOTHER=(WTPP+WTMOT+WTPYLD+WTSTRT)*(1.0E-03)	DOC	372
	WEIGHT2=WTMOT+WTCOLL+WTPP+WTBAT+WTPYLD+WTSTRT+WTNUKE	DOC	373
	1+WTPROP	DOC	374
C		DOC	375
C	WTSTRT IS STRUCTURAL WEIGHT	DOC	376
	WTSTRT=WEIGHT2*C1	DOC	377
C		DOC	378
C	TEST ASSURES THAT SS1 IS AT LEAST .4	DOC	379
	TEST=WTSTRT/SREF	DOC	380
	IF(TEST.LT.SS1)WTFRAC1=WTFRAC1+.005	DOC	381
	IF(TEST.LT.SS1)GOTO 56	DOC	382
C		DOC	383
C	WEIGHT IS TOTAL AIRPLANE WEIGHT	DOC	384
	WEIGHT=WEIGHT2+WTSTRT	DOC	385
C		DOC	386
C	*****	DOC	387
C		DOC	388
C	SCOLL IS AREA OF RECTENNA(FT X FT)	DOC	389
	SCOLL=WTCOLL/WACOLL	DOC	390
C		DOC	391
C	WNGLD IS WING LOADING(LB/(FT X FT))	DOC	392
	WNGLD=WEIGHT/SREF	DOC	393
C		DOC	394
C	ASpan IS WING SPAN(FT)	DOC	395
	ASpan=AR*SQRT(SREF/AR)	DOC	396
C		DOC	397
C	AREF IS WING PLANFORM AREA(FT X FT)	DOC	398
	AREF=SCOLL/SREF	DOC	399
C		DOC	400
C	*****	DOC	401
C		DOC	402
C	PARAMETERS FOR PLOTTING	DOC	403
C		DOC	404
C		DOC	405
C		DOC	406
	YPLOTH=(WTMOT/ELIFT)+(WTPP/ELIFT)	DOC	407
	YPLOT(1)=AREF	DOC	408
	YPLOT(2)=(WTPYLD/ELIFT)+YPLOTH	DOC	409
	YPLOT(3)=WTSTRT/ELIFT	DOC	410
	IF(EFLUX.LT.1.)YPLOT(4)=WTNUKE/ELIFT	DOC	411
	IF(EFLUX.GT.1.)YPLOT(4)=WTCOLL/ELIFT	DOC	412
	YPLOT(5)=WTBAT/ELIFT	DOC	413
	YPLOT(6)=(ELIFT/WEIGHT)-1.	DOC	414
	WRITE(5,100)N,ASpan,YPLOT(IQU)	DOC	415
41	CONTINUE	DOC	416
	WRITE(5,151)99999	DOC	417
C		DOC	418
C		DOC	419
C	*****	DOC	420
C	*****	DOC	421
C		DOC	422
C	PLOT OUTPUT	DOC	423
C		DOC	424
	IF(IB.EQ.10)CL=B(4)	DOC	425
	IF(IB.EQ.11)CD=B(4)	DOC	426
	IF(IB.EQ.12)ASPEED=B(4)	DOC	427
	IF(IB.EQ.13)POFF=B(4)	DOC	428
	IF(IB.EQ.14)EFPROP=B(4)	DOC	429
	IF(IB.EQ.15)EWBAT=B(4)	DOC	430
	IF(IB.EQ.16)EFBAT=B(4)	DOC	431
	IF(IB.EQ.17)PWMOTOR=B(4)	DOC	432
	IF(IB.EQ.18)WACOLL=B(4)	DOC	433
	IF(IB.EQ.19)EFCOLL=B(4)	DOC	434
	IF(IB.EQ.20)EFLUX=B(4)	DOC	435
	IF(IB.EQ.21)ALT=B(4)	DOC	436
	IF(IB.EQ.22)PWTPP=B(4)	DOC	437
	IF(IB.EQ.23)PPYLD=B(4)	DOC	438
	IF(IB.EQ.24)WTPYLD=B(4)	DOC	439
	IF(IB.EQ.25)AR=B(4)	DOC	440
	IF(IB.EQ.50)PWNUKE=B(4)	DOC	441

C			DOC	442
C	DO 42 IT=6,6		DOC	443
	KA=1		DOC	444
	WRITE(5,152)4,1,1,1,1,0,1		DOC	445
	WRITE(5,156)99998,KA+0,KA+1,KA+2		DOC	446
	KA=KA+3		DOC	447
	WRITE(5,155)0,0,0		DOC	448
	WRITE(5,155)7,7,7		DOC	449
	WRITE(5,155)1,2,3		DOC	450
C			DOC	451
C	PLOT TITLE SPECIFICATION		DOC	452
C			DOC	453
	IF(IT.EQ.1) WRITE(5,203)		DOC	454
	IF(IT.EQ.2) WRITE(5,204)		DOC	455
	IF(IT.EQ.3) WRITE(5,202)		DOC	456
	IF(IT.EQ.4.AND.EFLUX.GT.1.) WRITE(5,200)		DOC	457
	IF(IT.EQ.4.AND.EFLUX.LT.1.)WRITE(5,206)		DOC	458
	IF(IT.EQ.5) WRITE(5,201)		DOC	459
	WRITE(5,190)CL,CD,ASPEED,POFF,ALT		DOC	460
	IF(IT.EQ.6)WRITE(5,205)		DOC	461
	WRITE(5,192)EFPROP,EWBAT,EFBAT,PWMOTOR		DOC	462
	WRITE(5,194)PWNUKE,WACOLL,EFCOLL,EFLUX,AR		DOC	463
C			DOC	464
C	Y-AXIS GRID SCALE FACTOR		DOC	465
C			DOC	466
	IF(IT.EQ.1) WRITE(5,500)1.,0.,6.,1.,.20		DOC	467
	IF(IT.EQ.2) WRITE(5,500).1,0.,1.,.1.,.05		DOC	468
	IF(IT.EQ.3) WRITE(5,500).1,0.,1.,.1.,.05		DOC	469
	IF(IT.EQ.4) WRITE(5,500).1,0.,1.,.1.,.05		DOC	470
	IF(IT.EQ.5) WRITE(5,500).1,0.,1.,.1.,.05		DOC	471
	IF(IT.EQ.6) WRITE(5,500).4,-.8,.8,.4,.2		DOC	472
C			DOC	473
C	X-AXIS GRID SCALE FACTOR		DOC	474
C			DOC	475
	WRITE(5,500)200.,0.,400.,200.,100.		DOC	476
C			DOC	477
C	Y-AXIS LABEL		DOC	478
C			DOC	479
	WRITE(5,515)35.,.2		DOC	480
	IF(IT.EQ.1) WRITE(5,803)		DOC	481
	IF(IT.EQ.2) WRITE(5,804)		DOC	482
	IF(IT.EQ.3) WRITE(5,802)		DOC	483
	IF(IT.EQ.4.AND.EFLUX.GT.1.) WRITE(5,800)		DOC	484
	IF(IT.EQ.4.AND.EFLUX.LT.1.)WRITE(5,806)		DOC	485
	IF(IT.EQ.5) WRITE(5,801)		DOC	486
	IF(IT.EQ.6) WRITE(5,805)		DOC	487
C			DOC	488
C	X-AXIS LABEL		DOC	489
			DOC	490
C			DOC	491
	WRITE(5,515)18.,.2		DOC	492
	WRITE(5,535)		DOC	493
C			DOC	494
C	PREPARE FIGURE LEDGEND		DOC	495
C			DOC	496
	IF(IB.EQ.10)WRITE(5,602)		DOC	497
	IF(IB.EQ.11)WRITE(5,600)		DOC	498
	IF(IB.EQ.12)WRITE(5,603)		DOC	499
	IF(IB.EQ.13)WRITE(5,604)		DOC	500
	IF(IB.EQ.14)WRITE(5,605)		DOC	501
	IF(IB.EQ.15)WRITE(5,606)		DOC	502
	IF(IB.EQ.16)WRITE(5,607)		DOC	503
	IF(IB.EQ.17)WRITE(5,608)		DOC	504
	IF(IB.EQ.18)WRITE(5,609)		DOC	505
	IF(IB.EQ.19)WRITE(5,610)		DOC	506
	IF(IB.EQ.20)WRITE(5,611)		DOC	507
	IF(IB.EQ.21)WRITE(5,612)		DOC	508
	IF(IB.EQ.22)WRITE(5,613)		DOC	509
	IF(IB.EQ.23)WRITE(5,614)		DOC	510
	IF(IB.EQ.24)WRITE(5,615)		DOC	511
	IF(IB.EQ.25)WRITE(5,616)		DOC	512
	IF(IB.EQ.26)WRITE(5,617)		DOC	513
	IF(IB.EQ.27)WRITE(5,618)		DOC	514
	IF(IB.EQ.28)WRITE(5,619)		DOC	515
	IF(IB.EQ.29)WRITE(5,621)		DOC	516
	IF(IB.EQ.30)WRITE(5,622)		DOC	517
	IF(IB.EQ.31)WRITE(5,623)		DOC	518
	IF(IB.EQ.50)WRITE(5,620)		DOC	519
			DOC	520

	WRITE(5,601)0(1)		
	WRITE(5,601)0(2)	DOC	521
	WRITE(5,601)0(3)	DOC	522
42	CONTINUE	DOC	523
C	*****	DOC	524
C		DOC	525
C	FORMATS	DOC	526
C	*****	DOC	527
C		DOC	528
C		DOC	529
C		DOC	530
	48 FORMAT(I2)	DOC	531
	50 FORMAT(F10.5)	DOC	532
	51 FORMAT(4F10.5)	DOC	533
	52 FORMAT(7F10.5)	DOC	534
	53 FORMAT(45H-----)	DOC	535
	54 FORMAT(3X,*ALL DATA PLOTTED VERSUS WING SPAN*)	DOC	536
	100 FORMAT(I5,2F10.5)	DOC	537
	150 FORMAT(I1)	DOC	538
	151 FORMAT(I5)	DOC	539
	152 FORMAT(7I5)	DOC	540
	155 FORMAT(5X,4I5)	DOC	541
	156 FORMAT(5I5)	DOC	542
	190 FORMAT(9H1CSDLSN=F4.2,2X,7HCSDDSN=F4.3,2X,2HV=F5.1,2X,51POFF=	DOC	543
	1F5.2,2X,2HM=F5.2)	DOC	544
	192 FORMAT(*EFPROP=F4.2,2X,*EWBAT=F5.1,2X,*EFBAT=F4.2,2X,	DOC	545
	1*PWMDT=F5.1)	DOC	546
	194 FORMAT(*PWNUKE=F4.1,2X,*WACOLL=F5.2,2X,*EFCOLL=F4.2,2X,	DOC	547
	1*EFLUX=F5.3,2X,*AR=F4.1,2H56)	DOC	548
	20J FORMAT(8X,*RECTENNA WEIGHT*)	DOC	549
	201 FORMAT(8X,*BATTERY WEIGHT*)	DOC	550
	202 FORMAT(7X,*STRUCTURE WEIGHT*)	DOC	551
	204 FORMAT(5X,*MISCELLANEOUS SYSTEMS WEIGHT*)	DOC	552
	203 FORMAT(8X,*RECTENNA AREA*)	DOC	553
	205 FORMAT(8X,*VEHICLE WEIGHT*)	DOC	554
	206 FORMAT(5X,*NUCLEAR SYSTEM WEIGHT*)	DOC	555
	222 FORMAT(F20.1)	DOC	556
	500 FORMAT(6F10.5)	DOC	557
	515 FORMAT(I2,F7.4)	DOC	558
	530 FORMAT(*WCOLL/TLIFT*)	DOC	559
	535 FORMAT(18H(WING SPAN, B, FT))	DOC	560
	540 FORMAT(I2,F10.5)	DOC	561
	550 FORMAT(5HCARDS)	DOC	562
	600 FORMAT(*35H*,*D(RAG COEFFICIENT), CSD,DSN*)	DOC	563
	601 FORMAT(*10H*,F10.3)	DOC	564
	602 FORMAT(*38H*,*H(MAXIMUM LIFT COEFFICIENT), CSDL,MAXSN*)	DOC	565
	603 FORMAT(*17H*,*A(IRSPEED, FT/S)*)	DOC	566
	604 FORMAT(*23H*,*E(ENERGY STORAGE, HOURS)*)	DOC	567
	605 FORMAT(*22H*,*P(POPELLER EFFICIENCY)*)	DOC	568
	606 FORMAT(*26H*,*B(ATTERY WEIGHT), W-(H/LB)*)	DOC	569
	607 FORMAT(*20H*,*B(ATTERY EFFICIENCY)*)	DOC	570
	608 FORMAT(*22H*,*H(MOTOR WEIGHT), W/(LB)*)	DOC	571
	609 FORMAT(*27H*,*R(ECTENNA HEIGHT, LB/FT)2SN*)	DOC	572
	610 FORMAT(*21H*,*R(ECTENNA EFFICIENCY)*)	DOC	573
	611 FORMAT(*39H*,*I(NCIDENT MICROWAVE POWER), W/(FT)2U2SN*)	DOC	574
	612 FORMAT(*25H*,*A(ALTITUDE), 1050-35H (FT)*)	DOC	575
	613 FORMAT(*33H*,*P(OWER PROCESSING HEIGHT), W/(LB)*)	DOC	576
	614 FORMAT(*10H*,*P(AYLOAD POWER), W*)	DOC	577
	615 FORMAT(*20H*,*P(AYLOAD WEIGHT, LB)*)	DOC	578
	616 FORMAT(*13H*,*A(SPECT RATIO)*)	DOC	579
	617 FORMAT(*20H*,*R(ECTENNA REDUNDANCY FRACTION)*)	DOC	580
	618 FORMAT(*28H*,*S(TRUCTURAL WEIGHT FRACTION)*)	DOC	581
	619 FORMAT(*25H*,*P(POPELLER HEIGHT, LB/LB)*)	DOC	582
	620 FORMAT(*31H*,*N(UCLEAR SYSTEM WEIGHT), W/(LB)*)	DOC	583
	621 FORMAT(*24H*,*M(AXIMUM AIRSPEED, FT/S)*)	DOC	584
	622 FORMAT(*51H*,*S(TRUCTURAL WEIGHT-TO-WING AREA RATIO, LBS/FT2U2SN)*)	DOC	585
	1)	DOC	586
	623 FORMAT(*30H*,*D(SWALD'S AIRPLANE EFFICIENCY)*)	DOC	587
	700 FORMAT(*CLMAX (1.5)*)	DOC	588

710	FORMAT(*CD,0 (.010)*)	DOC	589
720	FORMAT(*AIRSPEED, FT/S(140.0)*)	DOC	590
730	FORMAT(*BATTERY OPERATIONS, HOURS(0.0)*)	DOC	591
740	FORMAT(24HOPTION PACKAGE? (Y OR N))	DOC	592
750	FORMAT(A1)	DOC	593
760	FORMAT(*PROPELLER EFFICIENCY (.85)*)	DOC	594
765	FORMAT(45HBATTERY ENERGY-TO-WEIGHT RATIO, W-H/LB (15.3))	DOC	595
770	FORMAT(33HBATTERY OVERALL EFFICIENCY (.85))	DOC	596
775	FORMAT(*RECTENNA WEIGHT-TO-AREA RATIO, LB/FT/FT(.04)*)	DOC	597
780	FORMAT(*MOTOR-GEAR POWER-TO-WEIGHT RATIO, W/LB (573.0)*)	DOC	598
785	FORMAT(*AVERAGE ENERGY FLUX, W/FT/FT (37.)*)	DOC	599
790	FORMAT(*RECTENNA EFFICIENCY (.80)*)	DOC	600
800	FORMAT(*WCOLL/TLIFT*)	DOC	601
801	FORMAT(*WBATTERY/TLIFT*)	DOC	602
802	FORMAT(*WSTRUCTURE/TLIFT*)	DOC	603
804	FORMAT(*WMISCELLANEOUS/TLIFT*)	DOC	604
803	FORMAT(*SCOLL/SREF*)	DOC	605
805	FORMAT(*EXCESS LIFT FRACTION), S(L/W5)-1*)	DOC	606
806	FORMAT(*WNUCLEAR/TLIFT*)	DOC	607
820	FORMAT(*ALTITUDE, THOUSANDS OF FT (70.00)*)	DOC	608
821	FORMAT(*PARAMETER 7*/10--CLMAX*/11--CD,0*/12--AIRSPEED*/	DOC	609
	1*13--BATTERY HOURS*/14--PROP EFFICIENCY*/15--BATTERY WEIGHT*/	DOC	610
	2*16--BATTERY EFFICIENCY*/17--MOTOR WEIGHT*/18--RECTENNA WEIGHT*/	DOC	611
	3*19--RECTENNA EFFICIENCY*/20--INCIDENT POWER*/21--ALTITUDE*/	DOC	612
	7*22--POWER PROCESSING WEIGHT*/23--PAYLOAD POWER*/	DOC	613
	4*24--PAYLOAD WEIGHT*/25--ASPECT RATIO*/26--RECTENNA REDUNDANCY*/	DOC	614
	5*27--STRUCTURAL WEIGHT FRACTION*/28--PROP WEIGHT*/	DOC	615
	6*29--MAXIMUM AIRSPEED*/30--STRUCTURE WT-TO-WING AREA*/	DOC	616
	7*31--OSWALD'S AIRPLANE EFFICIENCY*/50--NUCLEAR SYSTEM WEIGHT*/	DOC	617
	8/*ENTER 1 NUMBER*)	DOC	618
822	FORMAT(*ENTER 3 VALUES OF PARAMETER*)	DOC	619
823	FORMAT(*VALUE*,1X,11,1X,*OF PARAMETER*)	DOC	620
825	FORMAT(12)	DOC	621
826	FORMAT(*ALT*,12)	DOC	622
827	FORMAT(*DENS*,F20.10)	DOC	623
828	FORMAT(* /*PLOT(FRAME) NO.*/ * /*	DOC	624
	1*1--RECTENNA AREA*/	DOC	625
	2*2--MISCELLANEOUS SYSTEMS WEIGHT*/	DOC	626
	3*3--STRUCTURE WEIGHT*/4--RECTENNA(NUCLEAR SYSTEM) WEIGHT*/	DOC	627
	4*5--BATTERY WEIGHT*/6--VEHICLE WEIGHT/* *)	DOC	628
830	FORMAT(* /*I AM PROGRAM HEYSON, DEVELOPED BY */	DOC	629
	1*ERNIE GRAVES AND STUDENTS TO AID IN THE*/	DOC	630
	2*ANALYSIS OF SOLAR-, MICROWAVE-, AND NUCLEAR-*/	DOC	631
	3*POWERED AIRPLANE CONCEPTS/* *)	DOC	632
840	FORMAT(*POWER PROCESSING POWER-TO-WT RATIO, W/LB(53.4)*)	DOC	633
841	FORMAT(*PAYLOAD POWER, W(1000.0)*)	DOC	634
842	FORMAT(*PAYLOAD WEIGHT, LB(100.)*)	DOC	635
843	FORMAT(*NUCLEAR SYSTEM POWER-TO-WT RATIO, W/LB(15.0)*)	DOC	636
844	FORMAT(*VEHICLE ASPECT RATIO, (20.0)*)	DOC	637
845	FORMAT(*MAXIMUM AIRSPEED, FT/S(140.)*)	DOC	638
922	FORMAT(*RECTENNA REDUNDANCY FRACTION (0.10)*)	DOC	639
923	FORMAT(*BATTERY REDUNDANCY FRACTION (0.0)*)	DOC	640
927	FORMAT(*STRUCTURAL WEIGHT FRACTION (.17)*)	DOC	641
928	FORMAT(*STRUCTURAL WEIGHT-TO-WING AREA RATIO, LB/FT/FT (.43)*)	DOC	642
929	FORMAT(*OSWALD'S AIRPLANE EFFICIENCY FACTOR (.85)*)	DOC	643
99	END	DOC	644

## APPENDIX B

### LIST OF CONSULTANTS

#### B.1 Solar Power Technology

1. Albeck, James  
Spectrolab, Inc.  
Sylmar, CA
2. Baraona, Cosmo  
Space Photovoltaic Branch  
NASA/Lewis Research Center  
Cleveland, OH
3. Brandhorst, Jr., Dr. Henry W.  
Space Photovoltaic Branch  
NASA/Lewis Research Center  
Cleveland, OH
4. Conway, Dr. Edmund J.  
Space Technology Branch  
NASA/Langley Research Center  
Hampton, VA
5. Giuliano, Michael N.  
Solarex Corporation  
Rockville, MD
6. Harrison, Edwin F.  
Mission & Operations Branch  
NASA/Langley Research Center  
Hampton, VA
7. Kamath, Dr. G. Sanjiv  
Hughes Research Laboratory  
Malibu, CA
8. Randolph, Dr. Lynwood  
NASA Headquarters  
Washington, DC
9. Walker, Gilbert H.  
Space Technology Branch  
NASA/Langley Research Center  
Hampton, VA



## B.2 Microwave Power Technology

1. Brown, William C.  
Raytheon Company  
Waltham, MA
2. Dickinson, Richard M.  
Jet Propulsion Laboratory  
Pasadena, CA
3. Triner, James E.  
Applied Physics Branch  
NASA/Lewis Research Center  
Cleveland, OH

## B.3 Alternate Power Technologies

### B.3.1 Nuclear Power

1. Buden, David  
Los Alamos Scientific Laboratory  
Los Alamos, NM
2. Mullin, Jerry  
NASA Headquarters  
Washington, DC

## B.4 Flight Systems Technologies

### B.4.1 Energy Storage Systems

#### B.4.1.1 Batteries

1. Ambruse, Dr. Judith  
NASA Headquarters  
Washington, DC
2. Bragg, Bobby J.  
Power Generation Branch  
NASA/Johnson Space Center  
Houston, TX
3. Chilenskas, Albert  
Argonne National Laboratory  
Chicago, IL
4. Fordyce, Dr. Stewart J.  
Solar & Electrochemistry Division  
NASA/Lewis Research Center  
Cleveland, OH

5. Reid, Dr. Margaret A.  
Electrochemistry Branch  
NASA/Lewis Research Center  
Cleveland, OH

#### B.4.1.2 Fuel Cells

1. Bell, David II  
Life Sciences Experiments Program Office  
NASA/Johnson Space Center  
Houston, TX
2. McBryar, Hoyt  
Power Generation Branch  
NASA/Johnson Space Center  
Houston, TX
3. Stedman, Jay K.  
United Technologies Corporation  
South Windsor, CT

#### B.4.1.3 Flywheels

1. Jarvinen, Dr. Philip  
Massachusetts Institute of Technology  
Cambridge, MA
2. Keckler, Claude R.  
Spacecraft Controls Branch  
NASA/Langley Research Center
3. Kulkarni, Dr. S. V.  
Lawrence Livermore Laboratory  
Livermore, CA
4. Millner, Dr. Alan R.  
Tri-Solar, Inc.  
Bedford, MA
5. Studer, Philip A.  
Electromechanical Branch  
NASA/Goddard Space Center  
Greenbelt, MD

#### B.4.2 Electric Motors

1. Boucher, R. J.  
Astro-Flight, Inc.  
Venice, CA

2. Sawyer, Bert  
Delco Electronics  
Santa Barbara, CA

B.4.3 Power Processing

1. Slifer, Luther W.  
Space Power Applications Branch  
NASA/Goddard Space Center  
Greenbelt, MD

B.5 Aerodynamics

1. Liebeck, Dr. Robert  
McDonnell-Douglas Aircraft Company  
Sunnyvale, CA
2. Miley, Dr. Stanley T.  
Texas A & M University  
Houston, TX
3. Mueller, Dr. Thomas J.  
University of Notre Dame  
Notre Dame, IN
4. Phillips, William H.  
Distinguished Research Associate  
Langley Research Center  
Hampton, VA
5. Somers, Dan M.  
Airfoil Research Group  
Langley Research Center  
Hampton, VA
6. Turrizianni, R. Victor  
Kentron International, Inc.  
Hampton, VA

B.6 Systems Integration

1. Heyson, Harry H.  
Vehicle Integration Branch  
NASA/Langley Research Center  
Hampton, VA

2. Mayer, Norman J.  
NASA Headquarters  
Washington, DC
3. Morgan, W. Ray  
Aero-Vironment, Inc.  
Sihi Valley, CA
4. Morris, Charles E. K., Jr.  
Vehicle Integration Branch  
NASA/Langley Research Center  
Hampton, VA
5. Schwenk, F. Carl  
NASA Headquarters  
Washington, DC
6. Youngblood, James W.  
Systems & Experiments Branch  
NASA/Langley Research Center  
Hampton, VA

B.7 Societal Constraints

1. Ficklen, Carter B.  
Environmental Health Services  
NASA/Langley Research Center  
Hampton, VA
2. Hearth, Dr. Donald P.  
Director  
NASA/Langley Research Center  
Hampton, VA



1. Report No. NASA TM-84508		2. Government Accession No.		3. Recipient's Catalog No.	
4. Title and Subtitle  THE FEASIBILITY OF A HIGH-ALTITUDE AIRCRAFT PLATFORM WITH CONSIDERATION OF TECHNOLOGICAL AND SOCIETAL CON- STRAINTS				5. Report Date June 1982	
				6. Performing Organization Code 533-01-43-08	
7. Author(s)  Ernauld B. Graves				8. Performing Organization Report No.	
9. Performing Organization Name and Address  NASA Langley Research Center Hampton, VA 23665				10. Work Unit No.	
				11. Contract or Grant No.	
12. Sponsoring Agency Name and Address  National Aeronautics and Space Administration Washington, DC 20546				13. Type of Report and Period Covered Technical Memorandum	
				14. Sponsoring Agency Code	
15. Supplementary Notes  Submitted to the School of Engineering and the Faculty of the Graduate School of the University of Kansas in partial fulfillment of the requirement for the degree of Doctor of Engineering					
16. Abstract  This study has been conducted to determine the feasibility of remotely-piloted air- craft to perform year-around missions over the continental United States at an altitude of 70,000 feet. Technologies anticipated to be available within the 1985 to 1990 time period were used in analyzing both blimp- and airplane-type vehicles employing solar- voltaic, microwave, or nuclear propulsion systems. A payload weighing 100 pounds and requiring 1000 watts of continuous power was assumed for analysis purposes.  The study results indicate that a solar-powered aircraft requires more solar cell area than is available on conventional aircraft configurations if designed for the short days and high wind speeds associated with the winter season. A conventionally shaped blimp that uses solar power appears feasible if maximum airspeed is limited to about 100 ft/s. No viable airplane configuration that uses solar power and designed to with- stand the winter environment could be found. Both a conventionally shaped blimp and airplane appear feasible using microwave power. Nuclear powered aircraft of these type may also be feasible.  Societal attitudes toward the use of solar power in high altitude aircraft appear favorable. The use of microwave power for this purpose may be controversial, even though the ground station required would transmit power at levels comparable to exist- ing satellite communications stations. The use of nuclear power for aircraft propulsion does not appear to be acceptable to society.					
17. Key Words (Suggested by Author(s)) High altitude aircraft      Nuclear power High altitude platforms      Blimps High altitude missions      Sailplanes Solar power Microwave power			18. Distribution Statement  Unclassified - Unlimited  SUBJECT CATEGORY - 05		
19. Security Classif. (of this report) Unclassified		20. Security Classif. (of this page) Unclassified		21. No. of Pages 252	
				22. Price A12	



